frontiers | Research Topics

Integrating nature-based solutions for land degradation neutrality and deriving co-benefits

Edited by
Ting Hua, Paulo Pereira, Yang Yu, Miguel Inácio and Yi Han

Published in
Frontiers in Plant Science

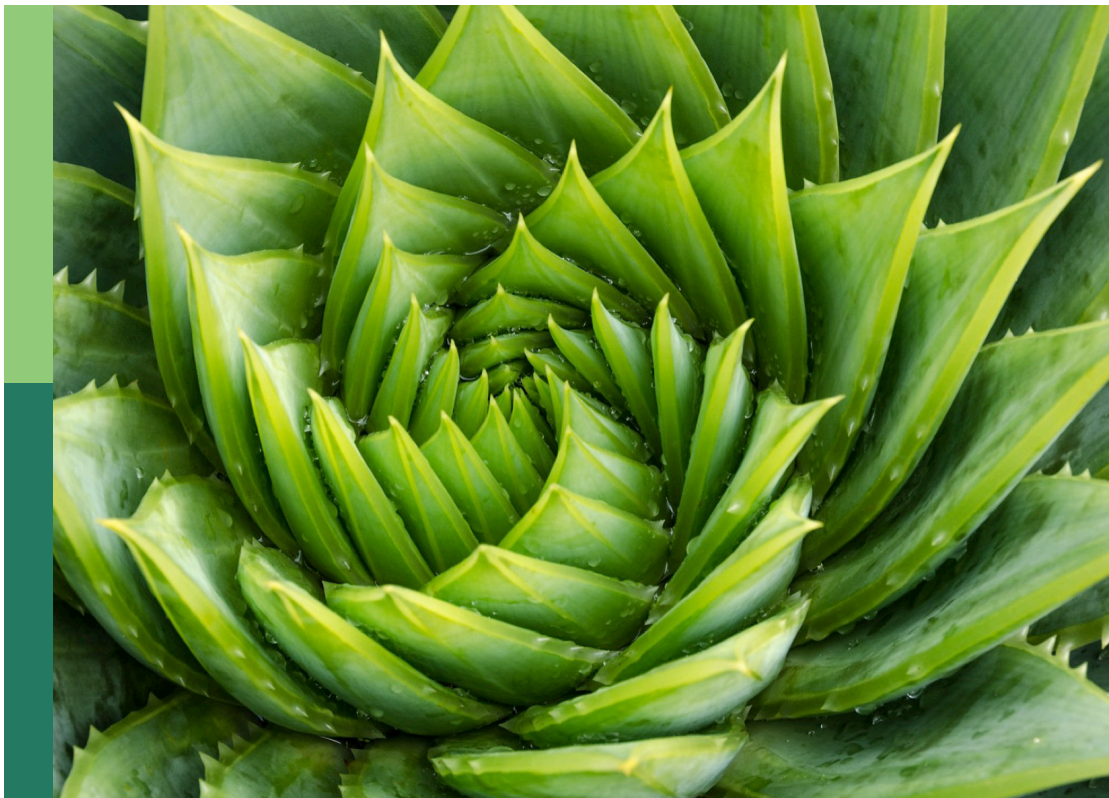

ISSN 1664-8714
ISBN 978-2-8325-7500-0
DOI 10.3389/978-2-8325-7500-0

Generative AI statement
Any alternative text (Alt text) provided alongside figures in the articles in this ebook has been generated by Frontiers with the support of artificial intelligence and reasonable efforts have been made to ensure accuracy, including review by the authors wherever possible. If you identify any issues, please contact us.

About Frontiers

Frontiers is more than just an open access publisher of scholarly articles: it is a pioneering approach to the world of academia, radically improving the way scholarly research is managed. The grand vision of Frontiers is a world where all people have an equal opportunity to seek, share and generate knowledge. Frontiers provides immediate and permanent online open access to all its publications, but this alone is not enough to realize our grand goals.

Frontiers journal series

The Frontiers journal series is a multi-tier and interdisciplinary set of open-access, online journals, promising a paradigm shift from the current review, selection and dissemination processes in academic publishing. All Frontiers journals are driven by researchers for researchers; therefore, they constitute a service to the scholarly community. At the same time, the *Frontiers journal series* operates on a revolutionary invention, the tiered publishing system, initially addressing specific communities of scholars, and gradually climbing up to broader public understanding, thus serving the interests of the lay society, too.

Dedication to quality

Each Frontiers article is a landmark of the highest quality, thanks to genuinely collaborative interactions between authors and review editors, who include some of the world's best academicians. Research must be certified by peers before entering a stream of knowledge that may eventually reach the public - and shape society; therefore, Frontiers only applies the most rigorous and unbiased reviews. Frontiers revolutionizes research publishing by freely delivering the most outstanding research, evaluated with no bias from both the academic and social point of view. By applying the most advanced information technologies, Frontiers is catapulting scholarly publishing into a new generation.

What are Frontiers Research Topics?

Frontiers Research Topics are very popular trademarks of the *Frontiers journals series*: they are collections of at least ten articles, all centered on a particular subject. With their unique mix of varied contributions from Original Research to Review Articles, Frontiers Research Topics unify the most influential researchers, the latest key findings and historical advances in a hot research area.

Find out more on how to host your own Frontiers Research Topic or contribute to one as an author by contacting the Frontiers editorial office: frontiersin.org/about/contact

Integrating nature-based solutions for land degradation neutrality and deriving co-benefits

Topic editors

Ting Hua — Norwegian University of Science and Technology, Norway
Paulo Pereira — Mykolas Romeris University, Lithuania
Yang Yu — Beijing Forestry University, China
Miguel Inácio — Mykolas Romeris University, Lithuania
Yi Han — Jiangxi Normal University, China

Citation

Hua, T., Pereira, P., Yu, Y., Inácio, M., Han, Y., eds. (2026). *Integrating nature-based solutions for land degradation neutrality and deriving co-benefits*.
Lausanne: Frontiers Media SA. doi: 10.3389/978-2-8325-7500-0

Table of contents

frontiers | Frontiers in Plant Science

TYPE Editorial
PUBLISHED 29 January 2026
DOI 10.3389/fpls.2026.1766472

OPEN ACCESS

EDITED AND REVIEWED BY
Lucian Copolovici,
Aurel Vlaicu University of Arad, Romania

*CORRESPONDENCE
Ting Hua
huatingcn@126.com

RECEIVED 12 December 2025
REVISED 13 January 2026
ACCEPTED 13 January 2026
PUBLISHED 29 January 2026

CITATION
Hua T, Han Y, Yu Y, Inácio M and Pereira P (2026) Editorial: Integrating nature-based solutions for land degradation neutrality and deriving co-benefits.
Front. Plant Sci. 17:1766472.
doi: 10.3389/fpls.2026.1766472

Editorial: Integrating nature-based solutions for land degradation neutrality and deriving co-benefits

Ting Hua[1]*, Yi Han[2], Yang Yu[3,4], Miguel Inácio[5] and Paulo Pereira[5]

[1]Industrial Ecology Programme, Department for Energy and Process Engineering, Norwegian University of Science and Technology, Trondheim, Norway, [2]Key Laboratory of Poyang Lake Wetland and Watershed Research (Ministry of Education), School of Geography and Environment, Jiangxi Normal University, Nanchang, China, [3]School of Soil and Water Conservation, Beijing Forestry University, Beijing, China, [4]Department of Agricultural Sciences, Institute of Agronomy, University of Natural Resources and Life Sciences, Vienna, Austria, [5]Environmental Management Research Laboratory, Mykolas Romeris University, Vilnius, Lithuania

KEYWORDS

climate change, ecological restoration, ecosystem service, land degradation neutrality (LDN), nature-based solution

Editorial on the Research Topic
Integrating nature-based solutions for land degradation neutrality and deriving co-benefits

Land degradation remains one of the most significant challenges of the 21st century, undermining ecosystem integrity, agricultural productivity, biodiversity, and human well-being (Prăvălie, 2021). Global economic losses associated with land degradation, arising from declines in multiple ecosystem services, could total 6.3–10.6 trillion US dollars annually (UNCCD, 2017). In response to growing policy momentum and scientific consensus, Land Degradation Neutrality (LDN) has gained prominence as a unifying global objective to achieve 'zero net land degradation' (UNCCD, 2015). In parallel, Nature-based Solutions (NbS), actions that protect, restore, and sustainably manage natural or modified ecosystems, have attracted increasing attention as a practical approach toward LDN, while delivering substantial environmental and social co-benefits (IUCN, 2016). However, the effectiveness of NbS is shaped by complex interactions among intervention types, biophysical conditions, climate, and management practices, resulting in substantial heterogeneity in ecosystem service provision across different contexts (Griscom et al., 2017; Seddon et al., 2020). Multidisciplinary approaches and governance perspectives could strengthen both micro- and macro-level understanding of how NbS can most effectively support LDN and other co-benefits (Griscom et al., 2017; Seddon et al., 2020). Against this backdrop, this Research Topic of *Frontiers in Plant Science* features 11 papers that span forests, grasslands, croplands, coastal ecosystems, and urban landscapes. Collectively, they demonstrate the potential of NbS to mitigate and reverse land degradation, while

navigating complex interactions among climate change, hydrological processes, soil dynamics, and social constraints.

Diagnosing degradation risks and climate pressures as a foundation for NbS

Several papers in this Research Topic provided critical diagnostics that help shape effective NbS strategies to mitigate degradation risks and guide restoration efforts. Rui et al. quantified the joint effects of climate change and human activities on grassland growth in Xinjiang, showing that vegetation greening is mainly attributable to a warming, humidifying climate. In contrast, local plant loss is more strongly associated with human pressures such as overgrazing and urbanisation. Hai et al. investigated the mechanisms by which precipitation frequency and amplitude influence forest growth in Northeast China, identified degradation hotspots in areas with high-frequency but low-amplitude fluctuations, and provided key climate-ecological insights for NbS-informed forest management. Zhu et al. compared multiple deep soil moisture profiles on the Loess Plateau and demonstrated that long-term artificial planting can substantially deplete deep soil water relative to farmland and native grassland, highlighting the hydrological trade-offs of restoration in water-scarce regions.

In cropland landscapes, Liao et al. mapped cultivated land degradation in southern China and disentangled the relative contributions of natural factors and management interventions (e.g., straw incorporation, fertilisation). The authors then translate these diagnostics into targeted restoration options, including deep-rooted crops, crop rotations and straw incorporation. In rapidly urbanising regions, Liu et al. analysed invasive alien plant species distributions across urban green spaces, rural areas and croplands, showing that native plant diversity and socio-economic conditions jointly shape invasion patterns and underscoring the need for differentiated NbS approaches in urban and peri-urban landscapes. Together, these studies highlight robust diagnostics of degradation and associated abiotic and biotic pressures to guide the design of NbS and support avoiding unintended consequences.

NbS for enhancing ecosystem functioning and services in diverse environments

A second group of contributions focused on how NbS interventions can stabilise ecosystem functioning and enhance ecosystem multifunctionality, such as soil quality and carbon stocks. In an ecologically vulnerable region of the Taihang Mountains, Zhang et al. demonstrated, across 72 sites, that land-use transition (from barren hills to cropland to pear orchards) combined with intercropping (ryegrass and winter rape) can substantially increase soil carbon and nutrient levels. That is because cover crops and root systems increase carbon input, optimise soil structure, and form a nutrient-carbon pool synergy. On the Qinghai–Tibet Plateau, Li et al. investigated long-term cultivation of Kentucky bluegrass as both a restoration intervention and alternative forage species, improving soil fertility and microbial community structure over time, thereby informing sustainable management practices to support soil health and ecosystem stabilisation.

Complementing these soil-focused studies, Xue et al. found that simulated warming and litter removal in alpine grassland generate opposite above- and below-ground responses. Warming reduces vegetation cover and above-ground multifunctionality while enhancing below-ground functions. In contrast, litter removal partly buffers the warming-induced declines. Zhan et al.extended ecological process understanding to management by developing zoning-based adaptive strategies for Tibetan Plateau grasslands using the "quality–pressure–resilience" framework. Their approach delineates zones for protection, selective enhancement and active intervention, thereby providing an illustrative roadmap for conserving and restoring alpine grassland.

Beyond terrestrial systems, this Research Topic also expands the NbS focus to coastal ecosystems. Marletta et al. evaluated the use of different growth promoters in seagrass (*Cymodocea nodosa*) restoration, comparing synthetic plant growth regulators with plant growth-promoting bacteria in controlled aquarium experiments. This study showed that applying plant growth-promoting bacteria markedly improves survival and vegetative propagation, whereas synthetic hormones provide only limited additional benefits. Collectively, these studies demonstrate the diverse mechanisms through which NbS can reinforce ecosystem functioning and multifunctionality in both terrestrial and coastal environments, delivering actionable evidence to support more resilient management.

Social and biophysical constraints on scaling NbS

Finally, the Topic included contributions that reflect on the multiple biophysical and social constraints for NbS deployment. Zha and Zhang synthesised diverse empirical evidence on the mitigation and adaptation benefits of agroforestry, while emphasising that biophysical and social constraints strongly shape both its deployment and performance. Their perspective aligns with recent research pointing to constraints on NbS deployment, posed by biodiversity conservation and water scarcity (Gvein et al., 2023); the influences of carbon pricing on NbS economic feasibility (Lu et al., 2022); and competition with demands for food, timber, and bioenergy production (Fuhrman et al., 2020). Overcoming these challenges will require coordinated, multi-level engagement

involving farm-level practitioners, policymakers, and a broad set of stakeholders (Pereira and Zhao, 2025).

Concluding remarks

Together, these papers in this Research Topic provide practical evidence on when, where and how NbS can support long-term benefits across the land-water-climate-people nexus. Such insights are particularly timely, as decision-makers urgently need to understand the role that NbS can play in advancing LDN and limiting further global temperature increases. These papers also highlight the necessity of multidisciplinary approaches—spanning ecology, remote sensing, agronomy, economics, and the social sciences—to design effective and context-appropriate interventions. Future research will need to build on this foundation by integrating long-term monitoring, co-designed interventions with local stakeholders, and comparative analyses across regions and ecosystem types, so that NbS can more reliably support progress toward LDN and broader co-benefits.

Author contributions

TH: Writing – original draft, Writing – review & editing. YH: Writing – review & editing. YY: Writing – review & editing. MI: Writing – review & editing. PP: Writing – review & editing.

Funding

The author(s) declared financial support was received for this work and/or its publication. YY was supported by the National Natural Science Foundation of China (No. 42377331).

Conflict of interest

The author(s) declared that this work was conducted in the absence of any commercial or financial relationships that could be construed as a potential conflict of interest.

The author(s) declared that they were an editorial board member of Frontiers, at the time of submission. This had no impact on the peer review process and the final decision.

Generative AI statement

The author(s) declared that generative AI was used in the creation of this manuscript. ChatGPT 5.1 was used exclusively to improve clarity and language quality, while all scientific content, analyses, and interpretations were developed entirely by the authors.

Any alternative text (alt text) provided alongside figures in this article has been generated by Frontiers with the support of artificial intelligence and reasonable efforts have been made to ensure accuracy, including review by the authors wherever possible. If you identify any issues, please contact us.

Publisher's note

References

Fuhrman, J., McJeon, H., Patel, P., Doney, S., Shobe, M., and Clarens, A. (2020). Food–energy–water implications of negative emissions technologies in a +1.5 °C future. *Nat. Clim. Change* 10, 920–927. doi: 10.1038/s41558-020-0876-z

Griscom, B., Adams, J., Ellis, P., Houghton, R., Lomax, G., Miteva, D., et al. (2017). Natural climate solutions. *Proc. Natl. Acad. Sci. U.S.A.* 114, 11645–11650. doi: 10.1073/pnas.1710465114

Gvein, M., Hu, X., Næss, J., Watanabe, M., Cavalett, O., Malbranque, M., et al. (2023). Potential of land-based climate change mitigation strategies on abandoned cropland. *Commun. Earth Environ.* 4, 39. doi: 10.1038/s43247-023-00696-7

IUCN (2016). *Nature-based Solutions for societal challenges: Policy brief* (Gland: International Union for Conservation of Nature).

Lu, N., Tian, H., Fu, B., Yu, H., Piao, S., Chen, S., et al. (2022). Biophysical and economic constraints on China's natural climate solutions. *Nat. Clim. Change* 12, 847–853. doi: 10.1038/s41558-022-01432-3

Pereira, P., and Zhao, W. (2025). Geography and geographical knowledge contribute decisively to all Sustainable Development Goals targets. *Geogr. Sustain.* 2025, 100267. doi: 10.1016/j.geosus.2025.100267

Prăvălie, R. (2021). Exploring the multiple land degradation pathways across the planet. *Earth-Sci. Rev.* 220, 103689. doi: 10.1016/j.earscirev.2021.103689

Seddon, N., Chausson, A., Berry, P., Girardin, C., Smith, A., and Turner, B. (2020). Understanding the value and limits of nature-based solutions to climate change and other global challenges. *Philos. Trans. R. Soc B* 375, 20190120. doi: 10.1098/rstb.2019.0120

UNCCD (2015). *Land degradation neutrality: resilience at the land degradation neutrality target setting programme* (Bonn: United Nations Convention to Combat Desertification).

UNCCD (2017). *Global land outlook. 1st Edn* (Bonn: United Nations Convention to Combat Desertification (UNCCD) Secretariat).

frontiers | Frontiers in Plant Science

TYPE Original Research
PUBLISHED 22 January 2025
DOI 10.3389/fpls.2024.1497248

OPEN ACCESS

EDITED BY
Ting Hua,
Norwegian University of Science and Technology, Norway

REVIEWED BY
Zhenchao Zhang,
Qingdao Agricultural University, China
Qian Zhang,
Nanjing Tech University, China

*CORRESPONDENCE
Ying Wang
mfacewang@njxzc.edu.cn

RECEIVED 16 September 2024
ACCEPTED 30 December 2024
PUBLISHED 22 January 2025

CITATION
Rui H, Luo B, Wang Y, Zhu L and Zhu Q (2025) Quantitative impacts of climate change and human activities on grassland growth in Xinjiang, China.
Front. Plant Sci. 15:1497248.
doi: 10.3389/fpls.2024.1497248

Quantitative impacts of climate change and human activities on grassland growth in Xinjiang, China

Hanyi Rui[1], Beier Luo[2], Ying Wang[3]*, Lin Zhu[1] and Qinyuan Zhu[1]

[1]Nanjing Institute of Environmental Sciences, Ministry of Ecology and Environment, Nanjing, China, [2]College of Geography and Remote Sensing, Hohai University, Nanjing, China, [3]School of Tourism and Social Management, Nanjing Xiaozhuang University, Nanjing, China

Grassland is an important vegetation type in Xinjiang, China, playing a crucial role in the terrestrial carbon cycle. Previous studies have shown that both climate change and human activities significantly impact grassland growth. However, research quantifying the contributions of these two factors to grassland changes is still not thorough enough. This study utilized remote sensing data, i.e., Normalized Difference Vegetation Index (NDVI), to analyze the spatial trends of grassland changes from 1982 to 2015, and the correlation between NDVI and climate factors. Then, relative contributions of climate change and human activities to grassland changes were explored across Xinjiang. The results indicated that there was a significant spatial heterogeneity in the interannual variations of NDVI in the study area, showing an overall increasing trend (covering 62.5% of the study area). This was mainly attributed to the warming and humidifying trend of Xinjiang's climate in recent decades, where increased precipitation and rising temperatures promoted grassland growth. The main regions with increased NDVI included the western part of Changji Hui Autonomous Prefecture, the southern part of Tacheng Prefecture, and the northwestern part of the Tarim Basin; while the areas with decreased NDVI were mainly located in the western part of the study area, e.g., the Ili River basin, and the Tekes River basin. Compared to precipitation, NDVI showed a stronger correlation with temperature, which was related to temperature promoting organic matter decomposition and enhancing vegetation nutrient utilization efficiency. NDVI was negatively correlated with VPD, mainly due to the effects of transpiration and surface evaporation. In terms of grassland growth, climate change (52%) contributed as much as human activity (48%). For the grassland reduction, human activities played a larger role. Overall, in mountainous and flat areas, human activities contributed more (64.29%) than climate change (35.71%), including activities such as grazing and urbanization.

KEYWORDS

grassland, climate change, human activities, Xinjiang, NDVI

1 Introduction

Grassland is an important component of the terrestrial ecosystem in our country, with functions such as sand fixation, dust prevention, water conservation, climate regulation, and playing a key role in biodiversity conservation and carbon sink function maintenance (Xu et al., 2022). Climate change and human activities are the main driving factors for changes in terrestrial ecosystems (Zhang et al., 2024), which have always been the focus of fields such as ecology (Zheng et al., 2019). Climate change includes temperature, precipitation, and vapor pressure deficit (VPD) (Yuan et al., 2019). Among them, temperature and precipitation are the dominant factors affecting processes such as seed germination and seedling growth, and have important impacts on vegetation distribution and carbon balance (Xu et al., 2019, 2016). VPD is defined as the difference between saturated water vapor pressure and actual water vapor pressure at a specific temperature, and is an important driving factor for plant demand for atmospheric water (Rawson et al., 1977). The impact of human activities on grasslands has also been widely studied (Hilker et al., 2013; Li et al., 2017). For example, the "settled pastoralists project" and the "national grazing ban and grassland restoration project" have improved the grassland areas in Xinjiang, China, but overgrazing has led to grassland degradation in the Ili River Valley and Tacheng area (Yang et al., 2014). Accurately assessing the impact of climate change and human activities on grassland ecosystems will help the government formulate ecological protection policies and provide theoretical basis for grassland management, utilization, and protection.

Normalized Difference Vegetation Index (NDVI) has been widely used in vegetation remote sensing (Defries and Townshend, 1994; Detsch et al., 2016; Huang et al., 2010), gradually maturing in the analysis of vegetation growth, yield estimation, and land desertification research, becoming an important tool for analyzing changes in land surface cover and their response to climate change and human activities (Li and He, 2009; Jiang et al., 2021; Li et al., 2022). NDVI is sensitive to global climate change, especially in arid and semi-arid areas where it exhibits high sensitivity to precipitation (Eklundh, 1998; Piao et al., 2004, 2003). Human activities also have a strong impact on NDVI (Hilker et al., 2013).

Currently, many scholars have conducted extensive research on the factors of climate change and human activities inducing NDVI changes using remote sensing methods, but further research is needed to quantify the contributions of climate change and human activities to vegetation changes (Sun et al., 2015; Wang et al., 2015; Xie et al., 2016). Residual analysis is a common quantitative analysis method that quantifies the contribution of climate change by establishing an equation between NDVI and climate factors (Li et al., 2017; Wang et al., 2015). This method has achieved good results in distinguishing and quantifying the climatic and anthropogenic impacts on vegetation dynamics in the central and northern regions of China and the Yulin region in northwest China (Sun et al., 2015; Jiang et al., 2017).

Xinjiang Uygur Autonomous Region is a hotspot for global climate change research. Grasslands, as an important vegetation type, play a crucial role in maintaining ecological balance and ensuring the region's climate and economic health. Considering the impact of climate change and human activities on grasslands, this study takes Xinjiang's grasslands as the research object, using the GIMMS NDVI3g dataset, GLASS-GLC dataset, and Vegetation Continuous Fields (VCF) time series data to analyze the changing trends of Xinjiang's grasslands, elucidate the driving factors of grasslands and their correlations, and explore the quantitative contributions of climate change and human activities to grasslands. This will contribute to the rational utilization of grassland resources in Xinjiang and the protection of the ecological environment, while providing a scientific basis for understanding vegetation evolution and predicting the changing characteristics of vegetation under climate and human influences.

2 Materials

2.1 Study area

Xinjiang Uygur Autonomous Region is located between 73°40′ to 96°18′ east longitude and 34°25′ to 48°10′ north latitude. It is the largest provincial-level administrative region in China with a total area of approximately 1.6649 million square kilometers, accounting for one-sixth of China's land area. It is a region with diverse and harsh environments (Zhang and Zhang, 2023). The Altai Mountains are in the north, while the Kunlun Mountains, Altun Mountains, and Tianshan Mountains are in the south. The Tianshan Mountains run through the central part, forming the Tarim Basin in the south and the Junggar Basin in the north.

Xinjiang is located deep inland, surrounded by high mountains on all sides, far from the ocean, which limits the arrival of maritime air currents and forms a distinct temperate continental climate. Under this climate condition, Xinjiang experiences large temperature variations, significant day-night temperature differences, abundant sunshine, low precipitation, and a dry climate. In Xinjiang, grasslands serve as an important vegetation type, playing a crucial role in ecosystem services such as soil and water conservation, and climate regulation. However, occurrences of drought and overgrazing have negative impacts on Xinjiang's ecosystems. Therefore, analyzing the changes in Xinjiang's grasslands and their driving factors is of great significance for studying global and regional changes.

The study area consists of pixels of grassland that appeared at least once from 1981 to 2015 (OOGP) (referred to below), mainly distributed in regions above 40° north latitude, located near the Tianshan Mountains and Altai Mountains, on the edge of the Gurbantünggüt Desert, and the western edge of the Taklimakan Desert (Figure 1). The study area covers the main distribution areas of grasslands in Xinjiang, reflecting the interannual variation trends of grasslands in Xinjiang.

2.2 GIMMS 3g NDVI dataset

The vegetation index is an indicator that reflects the relative abundance and activity of green vegetation through quantified

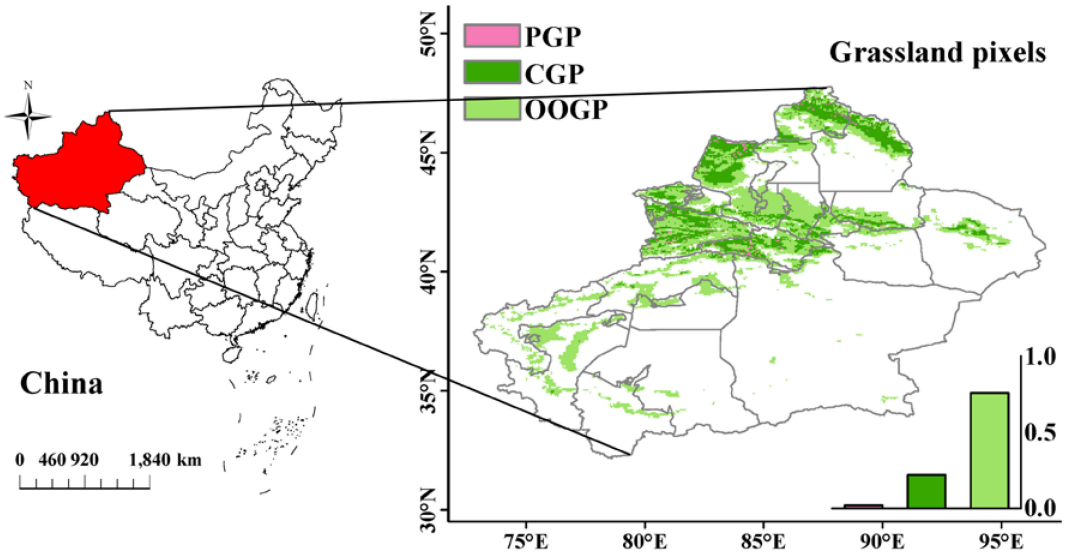

FIGURE 1
Grassland pixel over the Xinjiang from 1981 to 2015.The colors represent three types of grassland pixels. Light green pixels represent pixels where grassland has appeared at least once from 1981 to 2015 (OOGP), pink pixels represent approximated pure grassland pixels (PGP), and dark green pixels represent pixels that have always been grassland (CGP). The frequency histogram displaying the areal proportions (%) of corresponding regions is inset.

radiation values. It is commonly used to describe the physiological status, green biomass, and productivity of vegetation in a study area, and is highly sensitive to vegetation growth (Tucker et al., 1986). The GIMMS NDVI3g.V1 dataset (https://ecocast.arc.nasa.gov/data/pub/gimms/3g.v1/) is a long time series of NDVI data obtained by the Advanced Very High Resolution Radiometer (AVHRR) sensor from NOAA. This dataset is global in scope, covering the time range from 1981 to 2015, with a spatial resolution of 1/12° and a temporal resolution of 15 days. This is the NDVI data product with the longest time span currently, widely used in long-term vegetation change studies in different regions. Compared to early AVHRR products, GIMMS NDVI3g has higher accuracy and is less affected by factors such as atmospheric water vapor and volcanic eruptions, hence it has been widely applied in research. Previous studies suggested that the GIMMS NDVI data performed well in detections of grass changes across Xinjiang, China (Liu et al., 2018; Du et al., 2015; Yao et al., 2018).

2.3 GLASS-GLC dataset

The GLASS-GLC dataset (https://doi.pangaea.de/10.1594/PANGAEA.913496) records the annual dynamic changes in global land cover from 1982 to 2015 for the first time at a resolution of 5 kilometers. This dataset is generated using the latest version of GLASS CDRs and the Google Earth Engine (GEE) platform. Compared to earlier global land cover products, GLASS-GLC has higher consistency, more details, longer temporal coverage, and more detailed categories. It includes seven categories such as cropland, forest, grassland, shrubland, tundra, barren land, ice, and snow, with an average overall accuracy of 82.81% over 34 years. GLASS-GLC is suitable for long-term analysis of land cover changes, application in Earth system modeling, and promoting research on vegetation dynamics (Liu et al., 2020).

Based on GLASS-GLC data, this article obtained the annual land cover types in Xinjiang from 1982 to 2015. By comparing the land cover types of each pixel over 34 years, it identified pixels where the land cover type has always been grassland (CGP) and pixels where grassland has appeared at least once in the 34 years (OOGP).

2.4 Climatic data

The climate data used in this study includes near-surface air temperature (°C), surface precipitation rate (mm h^{-1}), near-surface air pressure (Pa), and near-surface specific humidity. These data are sourced from the China Meteorological Forcing Dataset (CMFD, https://poles.tpdc.ac.cn/zh-hans/data/8028b944-daaa-4511-8769-965612652c49/) (1979-2018). The CMFD is produced by integrating conventional meteorological observation data from the China Meteorological Administration with existing international Princeton reanalysis data, GLDAS data, GEWEX-SRB radiation data, and TRMM precipitation data as background fields. The data is in NETCDF format, with a temporal resolution of 3 hours and a horizontal spatial resolution of 0.1°. Compared to internationally published reanalysis data, CMFD has higher spatiotemporal resolution, more comprehensive integration of ground observation data, continuous time coverage, and stable quality. Therefore, it exhibits superior performance in regional climate research and is one of the most widely used climate datasets in China (He et al., 2020).

The formula for calculating VPD (vapor pressure deficit) based on climate data is as follows:

$$q = 0.622\frac{e}{P} \quad (1)$$

$$P_S = 610.78exp\left[\frac{17.269T}{237.3 + T}\right] \quad (2)$$

$$VPD = P_S - e \quad (3)$$

In the formula, q represents specific humidity, p represents air pressure, e represents actual water vapor pressure, P_S represents saturated water vapor pressure, T represents temperature, and VPD represents atmospheric vapor pressure deficit (Singh et al., 2002).

3 Methods

3.1 Statistical analysis

Maximum Value Composition (MVC) is commonly used for synthesizing satellite images with revisit cycles to reduce or eliminate the impact of clouds, weather, or other factors on the data (Huete et al., 2002). By processing NDVI data using the MVC method, NDVI raster images at the annual scale of Xinjiang from 1981 to 2015 can be obtained. At the pixel scale, using a simple linear regression method, the annual variation rate of NDVI from 1981 to 2015 can be calculated to depict its temporal trend and change intensity (Gao et al., 2022). This method comprehensively considers the NDVI data of each year within the study period, and the calculation formula is as follows:

$$\theta_{slope} = \frac{n \times \sum_{i=1}^{n}(i \times NDVI_i) - \left(\sum_{i=1}^{n} i\right) \times \left(\sum_{i=1}^{n} NDVI_i\right)}{n \times \sum_{i=1}^{n} i^2 - \left(\sum_{i=1}^{n} i\right)^2} \quad (4)$$

In the formula, n represents the length of the study period (NDVI data in this study is from 1981 to 2015, n=35); i is the serial number of the study year, with 1981 corresponding to i=1, and so on, up to 2015 corresponding to i=35; $NDVI_i$ represents the NDVI value in year i of the study period; θ_{slope} is the interannual change rate of NDVI. If $\theta_{slope} > 0$, NDVI shows an increasing trend, if $\theta_{slope} < 0$, NDVI shows a decreasing trend.

In order to quantify the relationship between NDVI and temperature, precipitation, and VPD, this study uses Pearson correlation analysis to calculate the single correlation coefficients of NDVI with temperature, precipitation, and VPD at the pixel scale. The calculation formula is as follows:

$$R_{xy} = \frac{\sum_{i=1}^{n}[(x_i - \bar{x})(y_i - \bar{y})]}{\sqrt{\sum_{i=1}^{n}(x_i - \bar{x})^2 \sum_{i=1}^{n}(y_i - \bar{y})^2}} \quad (5)$$

In the formula, R_{xy} represents the correlation coefficient; x_i is the NDVI for the i-th year; y_i is the temperature, precipitation, and VPD for the i-th year; $\bar{x}$ is the mean value of NDVI during the study period; $\bar{y}$ is the mean value of temperature, precipitation, and VPD during the study period. When $|R_{xy}|>0.8$, it is highly correlated; $0.5< |R_{xy}|<0.8$ is moderately correlated; $0.3< |R_{xy}|<0.5$ is weakly correlated; generally, $|R_{xy}|<0.3$ is uncorrelated (Chen et al., 2023).

The partial correlation coefficients between NDVI and concurrent temperature, precipitation, VPD, assuming two variables remain constant, the relationship between NDVI and the other variable is calculated as follows:

$$R_{xy\times z} = \frac{R_{xy} - R_{xz}R_{yz}}{\sqrt{(1 - R_{xz}^2)(1 - R_{xz}^2)}} \quad (6)$$

In the formula, $R_{xy\times z}$ represents the partial correlation coefficient between x and y under the assumption that variable z remains unchanged, and so on.

In order to analyze the fluctuation pattern of vegetation coverage, this study adopted the coefficient of variation method (Milich and Weiss, 2000). The calculation formula is as follows:

$$CV_{NDVI} = \frac{\sigma_{NDVI}}{\overline{NDVI}} \quad (7)$$

In the formula, CV_{NDVI} refers to the coefficient of variation of NDVI values at a certain time sequence. σ represents standard deviation, and $\overline{NDVI}$ represents the mean, used to evaluate the stability of NDVI in the time series. A larger CV_{NDVI} value indicates a more dispersed data distribution, greater fluctuation, and unstable time series; conversely, a smaller value indicates a more concentrated data distribution and a relatively stable time series.

Using the F test to determine the significance of interannual variation rate, the formula is as follows:

$$F = K \times \frac{(n-2)}{M} \quad (8)$$

Among them, K and M are the regression sum of squares and residual sum of squares respectively, with n being the total number of years, which is 35.

3.2 Vegetated area of interest

This study aims to establish a purely climate-induced grassland NDVI model using approximated pure grassland pixels (Zhou et al., 2022). For each pixel, this study ignores areas with sparse or non-existent grassland vegetation (areas with annual average NDVI less than 0.1) (de Jong et al., 2011; Weiss et al., 2010). The model is then applied to the entire study area, specifically to pixels where grassland has appeared at least once (OOGP). Finally, the NDVIc derived from the model (the NDVI values influenced by climate change) is subtracted from the observed NDVI data (NDVIo) to obtain the NDVI values influenced by human activities (NDVIh), studying the impact of Climate Change (Cc) and Human Activities (Ha) on grassland vegetation in the study area. The detailed methodology framework of this study is shown in the figure below.

Step 1: Extract approximated pure grassland pixels (PGP) (Figure 2). Based on the GLASS-GLC dataset and vegetation continuous field (VCF) time series data, a method for extracting approximated PGP was developed by combining grassland pixels (CGP) and coefficient of variation (CV) from 1982 to 2015. CV is the ratio of the standard deviation to the mean of the VCF time series at each pixel, widely used as an indicator to measure the degree of fluctuation, distinguishing grassland pixels affected by climate from those not affected by climate. Therefore, it can be assumed that pure grassland pixels are only influenced by climate change.

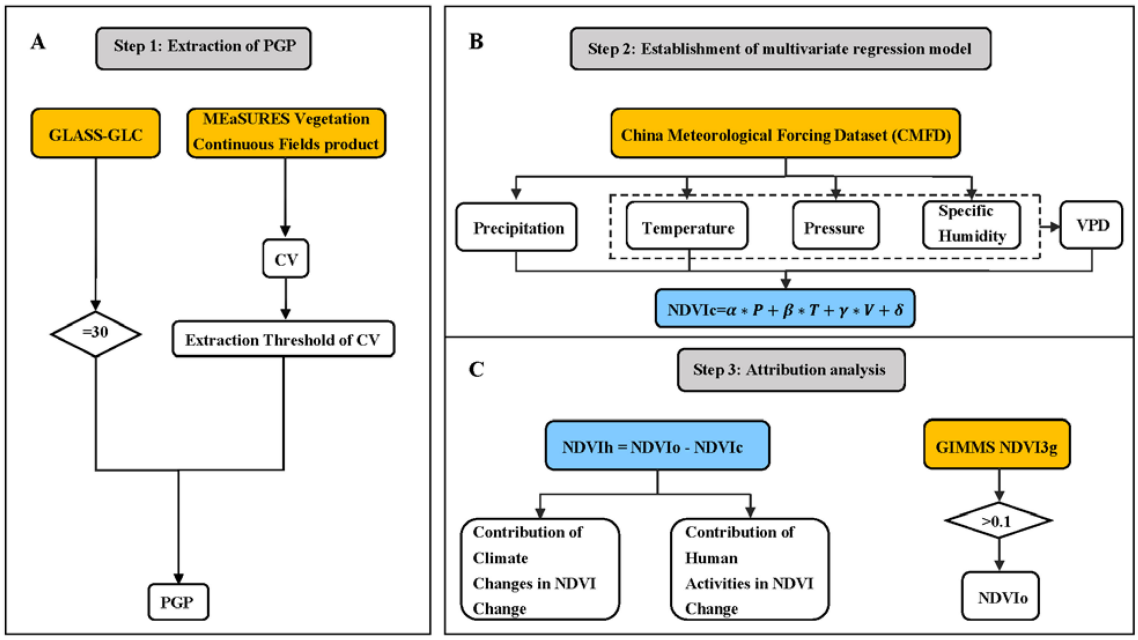

FIGURE 2
Step 1: Extraction of approximated pure grassland pixels (PGP) **(A)**. Initially, grassland pixels with a value of 30 were extracted from the GLASS-GLC dataset to obtain pixels that were consistently grassland from 1981 to 2015 (Constant Grassland Pixels, CGP). Then, the CV (Coefficient of Variation) values of the CGP were calculated using VCF data, and approximated PGP were identified based on a specified threshold. Step 2: NDVIc was calculated using a multiple regression equation based on precipitation, temperature, and VPD **(B)**. Step 3: In the GIMMS NDVI3g dataset, data greater than 0.1 were considered as observed NDVI (NDVIo). NDVIh represents the difference between NDVIo and NDVIc **(C)**.

Step 2: Establish a multiple regression model (Figure 2). Based on the selected PGP, import four climate variables from CMFD: precipitation, near-surface air temperature, surface air pressure, and near-surface air specific humidity. VPD is calculated from temperature, pressure, and specific humidity (Singh et al., 2002). Establish a multiple regression model between NDVI and climate variables (precipitation, temperature, and VPD). Based on this, the NDVIc of each pixel was simulated. Where NDVIc represents climatic grassland; P, T, V represent annual average precipitation, temperature, and VPD, with units in mm, ℃, and hPa respectively; α, β, γ represent the regression coefficients of multiple linear regression; δ is the error term.

Step 3: Calculate the impact of human activities on grasslands (Figure 2). Based on GIMMS NDVI3g data, obtain observed NDVI (NDVIo). The difference between NDVIc and NDVIo is the residual (NDVIh), indicating the response of grasslands to human activities. Quantitatively analyze the impact of climate change and human activities on grasslands in Xinjiang.

According to the above method, over the past 35 years, the grassland pixel (CGP) has mainly been distributed above 43°N (Figure 1). Because the smaller the CV value, the more stable it is. Among the pixels that have always been grassland, the CV values range from 0.6% to 28%. Sorting the CV values from small to large, the 5th percentile is chosen as the threshold (Zhou et al., 2022). Therefore, approximated PGP with CV values less than 4% are selected for modeling (Figure 1). Compared to the model based on CGP, the NDVIc obtained from the multiple linear regression model based on PGP (i.e., NDVI induced by Cc) can better reflect the impact of climate on grassland NDVI.

According to the indicators provided in the literature, the correlation coefficient (CC) of the model is 0.496, the bias (BIAS) is -1.2%, and the root mean square error (RMSE) is 0.185 (Mentaschi et al., 2013). Therefore, it can be considered that the model is reasonable and reliable in the study area, and can be used to distinguish the impact of human activities (Ha) and climate change (Cc) on NDVI during the study period. Further analysis revealed that if modeling is done on the same modeling pixel without considering VPD, the CC is 0.475, BIAS is -0.836%, and RMSE is 0.132. If modeling is done using pixels where grassland has appeared at least once in 35 years and considering VPD factors, the CC is 0.6, BIAS is 1.0141e-06, and RMSE is 0.0708; if VPD factors are not considered, the CC is 0.49, BIAS is 2.9364e-06, and RMSE is 0.077. Overall, the model considering VPD factors performs better in terms of correlation and error, making it more suitable for distinguishing the effects of different factors on NDVI during the study period.

3.3 Quantitative evaluations

Usually, we use correlation coefficient (CC), relative bias (Bias), and root mean square error (RMSE) to verify the accuracy of the model. The changing trends of NDVIc, NDVIh, and NDVIo are obtained at the pixel scale to determine the spatial distribution and impact of Cc and Ha on grasslands in the study area. Based on these trends, six response patterns of NDVI to Cc and Ha were further determined along with their contribution rates (Supplementary Table 1) (Zhou et al., 2022; Guo et al., 2021).

Using the partial correlation analysis method, the partial correlation coefficients between NDVIo and various meteorological factors are used to identify the impact of each Cc factor on grassland changes (Supplementary Table 2) (Zhou et al., 2022). The contribution rates of each driving factor are gradually stripped away in various scenarios.

4 Results

4.1 Spatiotemporal patterns of grassland changes

Supplementary Figure 1 shows the fluctuation status of NDVI in Xinjiang from 1981 to 2015, categorizing the fluctuation status of NDVI into five levels. Among them, 8% of pixels are in a low fluctuation state, 66% of pixels are in a relatively low fluctuation state, with low fluctuation areas mainly located in the Taklimakan Desert, Kumtag Desert, and eastern Xinjiang; 4% of pixels show a higher fluctuation state (0.2> CV_{NDVI} >=0.15), and 3% of pixels show a high fluctuation state (CV_{NDVI} >=0.2). Specifically, areas with higher fluctuations are mainly located in the Tianshan Mountains, Altai Mountains, and Kunlun Mountains, while other regions have lower NDVI fluctuations.

Figure 3 shows the spatial variation trend of NDVI. From 1981 to 2015, the interannual regression coefficient distribution of NDVI in the study area ranged from -0.004 to 0.012/a. Among them, 62.5% of the regions showed an increasing trend in NDVI, indicating that NDVI gradually increased over time, while the remaining 37.5% of the regions exhibited a decreasing trend, meaning that NDVI gradually decreased over time, mainly concentrated in the western part of the study area, including the Ili River and Tekes River basins. Supplementary Figure 2 shows that 50% of the study area's pixel NDVI trend passed the significance test, with significant increases and decreases in NDVI distributed across the entire study area. Specifically, 36% of the regions showed a significant increasing trend in NDVI ($P<0.05$), with the distribution range highly overlapping with the areas where NDVI trend >0.001 in Figure 3; 14% of the regions exhibited a significant decreasing trend in NDVI, mainly located in the central and western parts of the study area. Generally, there was a significant spatial heterogeneity in the interannual variations of NDVI in the study area, showing an overall increasing trend.

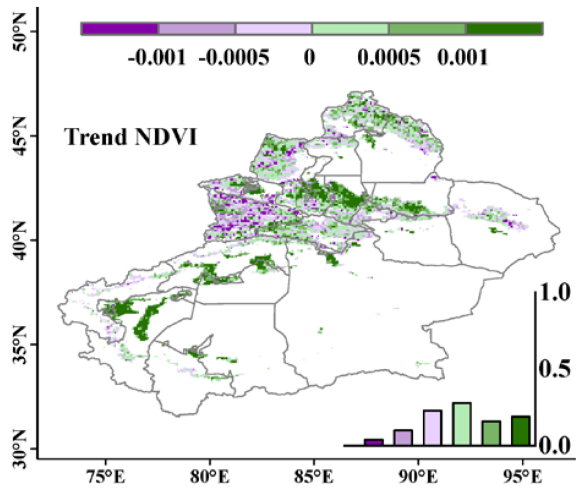

FIGURE 3
Spatial distribution of the interannual variation trend of NDVI in the study area from 1981 to 2015.The frequency histogram displaying the areal proportions (%) of corresponding coefficients is inset.

4.2 Correlations between NDVI and climate variables

Using precipitation, temperature, and VPD as control variables, the correlation coefficient and partial correlation coefficient between NDVI and precipitation, temperature, and VPD were calculated. Supplementary Figure 3 show the spatial distribution of the correlation coefficients between NDVI and precipitation, temperature, and VPD. The main relationship between NDVI and precipitation is positive ($r>0$), meaning that NDVI increases with increasing precipitation. The highest correlation coefficient is 0.76, the lowest is -0.62, with 29% of the study area pixels being significant. 78% of the pixels in the study area show a positive correlation, with the majority having correlation coefficients less than 0.3, mainly distributed in mountainous areas. Similarly, the dominant relationship between NDVI and temperature is positive, meaning that NDVI increases with rising temperatures. The highest correlation coefficient is 0.78, while the lowest is -0.72. 25% of the pixels in the study area show significant performance, with 69% exhibiting a positive correlation, mostly falling within the range of 0 to 0.3. 31% of the pixels show a negative correlation, indicating that NDVI decreases as temperature rises, generally exceeding -0.3, mainly concentrated in the Tacheng region. As for VPD, the number of pixels showing positive and negative correlations with NDVI is roughly equal, with the highest correlation coefficient being 0.78 and the lowest being -0.81. 30% of the pixels show significant correlation. Among these, 57% exhibit a negative correlation, where the trend of NDVI and VPD changes oppositely, primarily distributed in the western part of the study area, the central part of the Tianshan Mountains, and the southern part of the Altai Mountains. 43% of the pixels show a positive correlation, where the trend of NDVI and VPD changes in the same direction, with 64% of the pixels falling within the range of -0.3 to 0.3 overall.

In addition, the partial correlation coefficient is used to measure the relationship between NDVI and precipitation, temperature, and VPD. Figure 4 shows the spatial distribution of the corresponding partial correlation coefficients. The partial correlation coefficient between NDVI and precipitation ranges from -0.67 to 0.81, indicating a positive correlation in the study area, accounting for 69% of the area. The partial correlation coefficient between NDVI and temperature ranges from -0.59 to 0.82, showing a positive correlation, accounting for 83%. As for VPD, the minimum partial correlation coefficient is -0.85, and the maximum is 0.79, indicating a negative correlation between NDVI and VPD, accounting for 73% of the area. Overall, NDVI showed a stronger correlation with

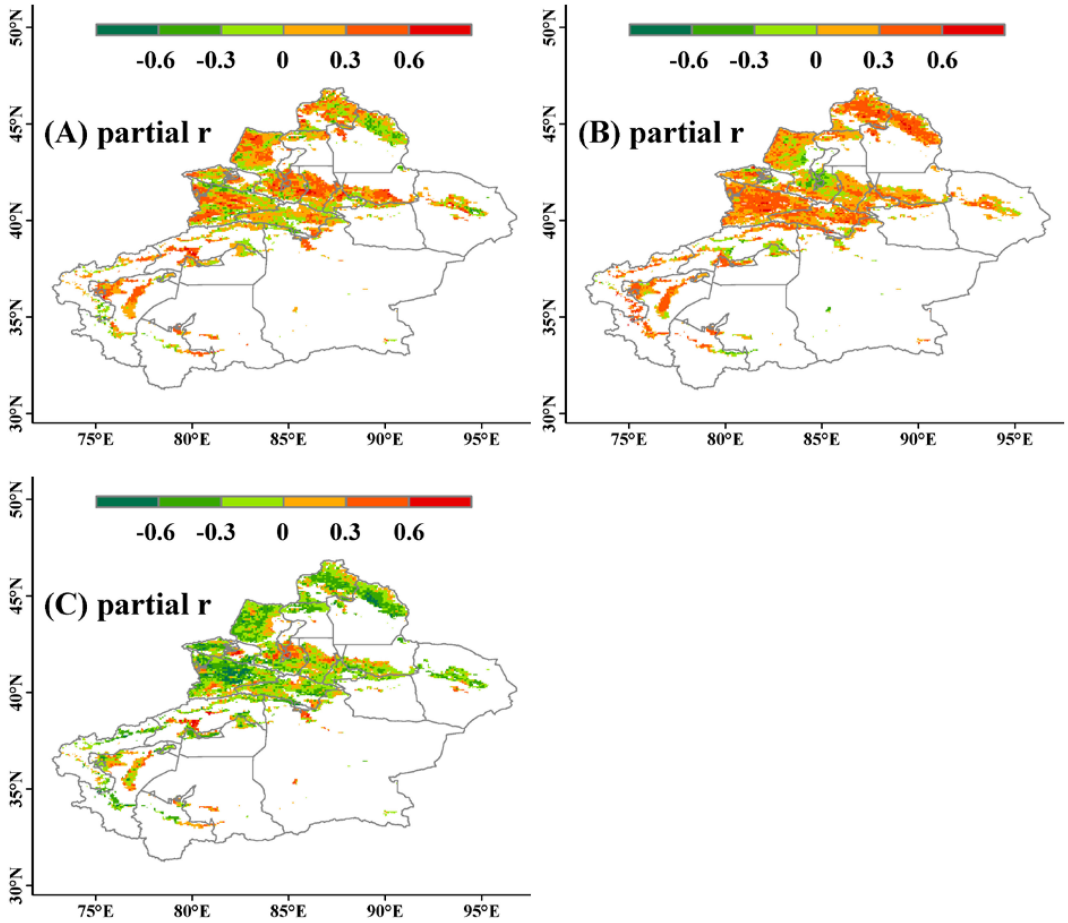

FIGURE 4
Spatial distribution of partial correlation coefficients between NDVI and climate variables. **(A–C)** represent the partial correlation coefficients between NDVI and precipitation, temperature, and VPD, respectively.

temperature compared to precipitation, and was negatively correlated with VPD.

4.3 Attributions of grassland changes

By establishing the grassland NDVI model, the values and spatial distribution of NDVIc and NDVIh in the study area from 1981 to 2015 were calculated. Figure 5 shows the spatial distribution of the changing trends of NDVIc and NDVIh. NDVIc overall shows a gradually increasing trend over time, accounting for 77.7% of the study area, mainly distributed in the southern Tianshan Mountains and northern Altai Mountains; the remaining 22.3% of pixels show a decreasing trend year by year, with the declining areas evenly distributed within the study area. In contrast to NDVIc, NDVIh exhibits a widespread decreasing trend, covering 60% of the study area. The remaining 40% of pixels show an increasing trend year by year, mainly distributed in the western part of Changji Hui Autonomous Prefecture, downstream of the Yarkant River, and near Kashgar City.

This study identified six response patterns of grassland NDVI to climate change and human activities through the interannual variation trends of NDVIc, NDVIo, and NDVIh. The spatial results are shown in Figure 6. In terms of grassland growth, the promotion effects of climate change-induced pattern (Cc), human activities-induced pattern (Ha), and climate change combined with human activities-induced pattern (Cc-Ha) on grasslands account for 37%, 28%, and 35% of the increased area, respectively. In terms of grassland reduction, it is mainly influenced by human activities (Ha), accounting for 85% of the reduced area. Other patterns Cc and Cc-Ha account for 5% and 10% of the reduced area, mainly distributed near the Tekes River and Ili River. The entire study area is dominated by an increase in grassland NDVI, accounting for 62.5% of the area. The remaining 37.5% of pixel grassland growth is inhibited, leading to a decrease in grassland NDVI, with grassland NDVI responding most significantly to pattern Ha, accounting for 32% of the study area. Overall, climate change contributed as much as human activity in terms of grassland growth, while the later one played a larger role for the grassland reduction.

4.4 Contributions of Cc and Ha to grassland changes

According to Supplementary Table 2, the contribution rates of climate change (Cc) and human activities (Ha) to grassland changes are obtained. Figure 7 shows the spatial distribution of the contributions.

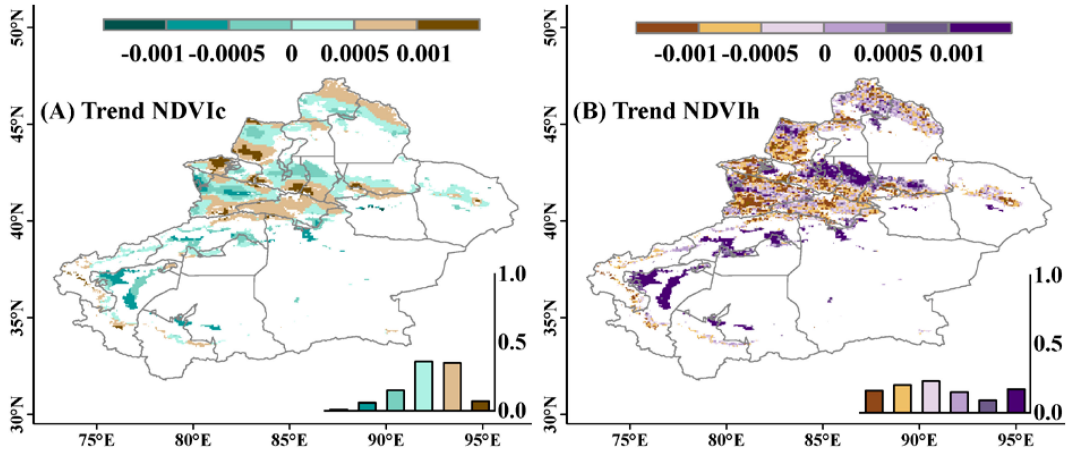

FIGURE 5
Spatial distribution of the interannual variation trends in grassland NDVI in Xinjiang from 1981 to 2015. **(A, B)** reflect the variation trends of NDVIc and NDVIh, respectively. The frequency histogram displaying the areal proportions (%) of corresponding coefficients is inset.

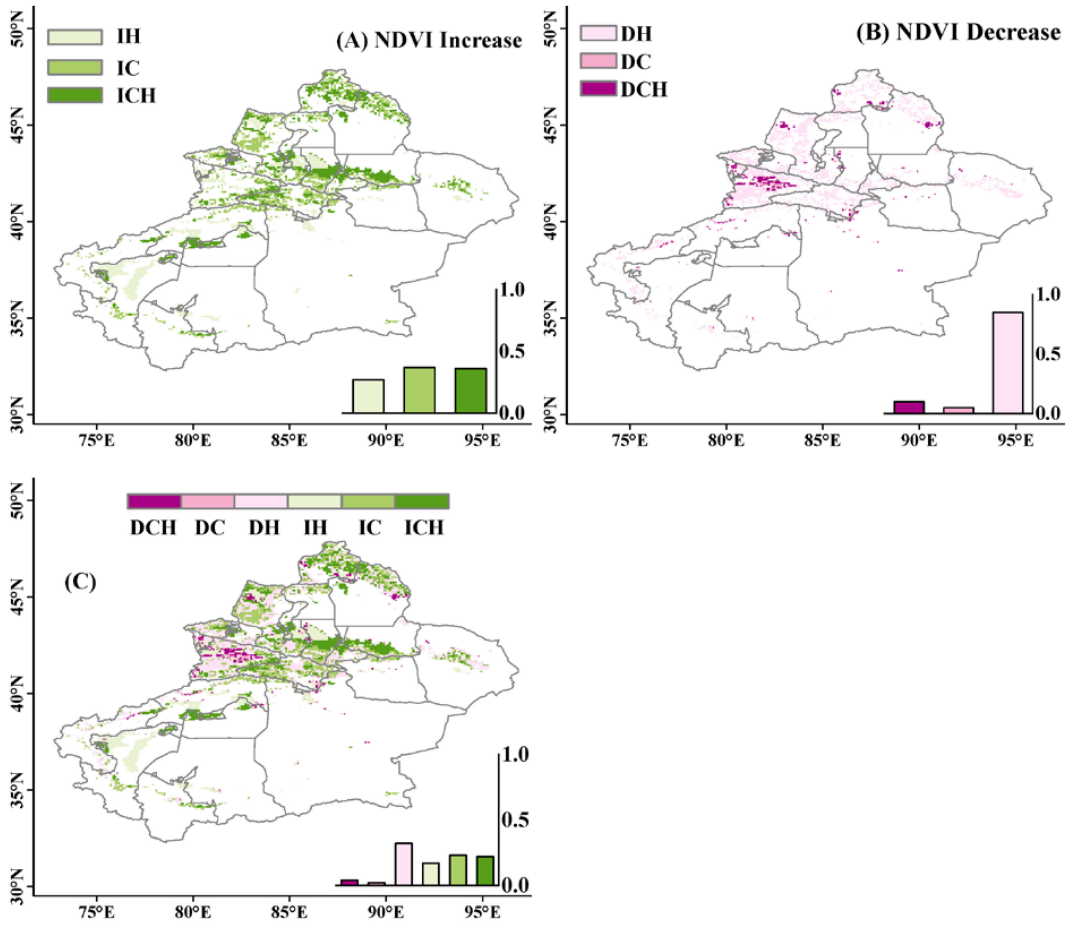

FIGURE 6
Spatial distribution of grassland NDVI response patterns. **(A–C)** reflect the overall situation of NDVI decrease, increase, and total change, respectively. In these panels, IH, IC, and ICH represent grassland increase caused by human activities, climate change, and the combined effect of climate change and human activities, respectively; DH, DC, and DCH represent grassland decrease caused by human activities, climate change, and the combined effect of climate change and human activities, respectively. The frequency histogram displaying the areal proportions (%) of corresponding regions is inset.

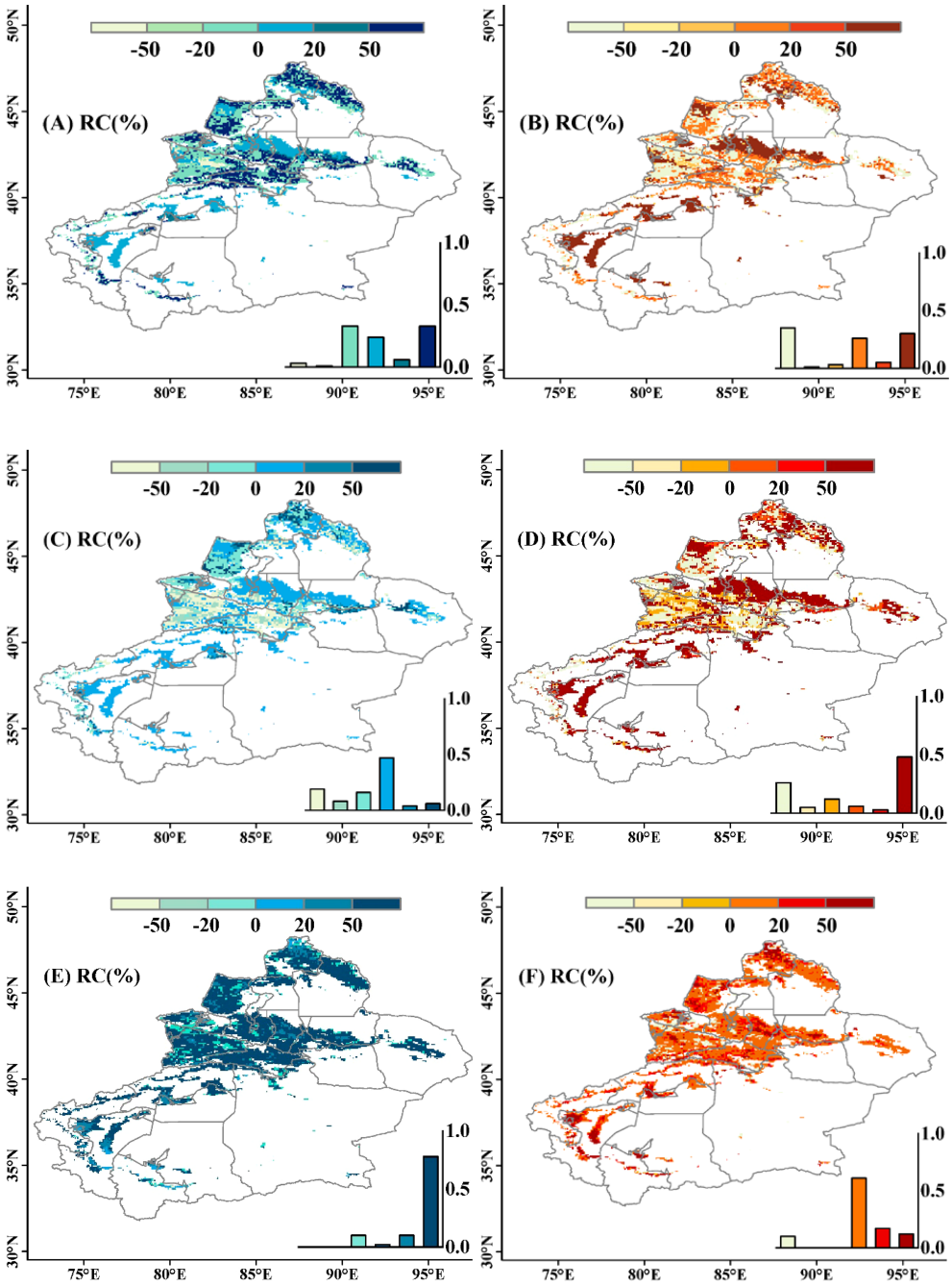

FIGURE 7
Spatial distribution of the relative contribution of climate change (left panels) and human activities (right panels) to interannual variation in grassland NDVI in Xinjiang during 1981-2015 **(A, B)**, 1981-2000 **(C, D)** and 2001-2015 **(E, F)**. A positive contribution rate indicates a trend of grassland increase, while a negative contribution rate indicates a trend of grassland decrease. The frequency histogram displaying the areal proportions (%) of corresponding coefficients is inset.

The results indicate that form 1981-2015, climate change mainly affects 32% of pixels, where grassland changes show an increasing trend, meaning that the contribution rate of Cc is greater than Ha, promoting grassland growth. The main contribution area of Cc to grassland decrease is small, accounting for 3%, mainly concentrated in the Ili River Basin. For human activities, in both cases of grassland growth and decrease, the number of pixels making the main contribution is roughly the same. 29% of pixels contribute to grassland growth, with Ha's contribution rate greater than Cc, indicating a growth trend in grassland; while pixels contributing mainly to grassland decrease account for 35%. Overall, Cc and Ha contribute 35.71% and 64.29% respectively to the total amount of grassland changes during the entire study period (Figures 7A, B). It should be noted that the contributions of climatic variables and human activities to grassland changes varied with time, because of enhanced climate changes and developments of the projects and policies. Hence, a temporal difference of the

contributions was further explored before and after the 2000 year. The results showed that the positive contributions of climate change obviously enhanced from 80s-90s to 20s-21s (Figure 7C, E). The main contributing area (relative contribution > 50%) accounted for 78% of the study area after the 2000 year. Meanwhile, the negative contributions of human activities also reduced from 80s-90s to 20s-21s, especially in the areas with Ha< 50% (Figure 7D, F). The positive Ha is widespread across the study area after 2000, but most of them had a low contribution of between 0 and 20%.

Based on the partial correlation coefficients of temperature, precipitation, VPD with NDVI and their identification criteria (Supplementary Table 2), the spatial patterns of driving factors were plotted as shown in Figure 8. In the case of grassland growth, the range of the combined impact of temperature and precipitation (TP) is greater than other climatic variables, accounting for 32% of the study area, mainly distributed in the Tianshan Mountains, northern part of the Kaidu River, near the Ili River, downstream of the Yarkant River, and around Kashgar City; followed by the composite pattern of temperature, precipitation, and VPD (TPV), accounting for 12%. For grasslands showing a decreasing trend, they are mainly driven by precipitation and VPD (PV), accounting for 18% of the study area, concentrated in the southern part of the Bortala Mongol Autonomous Prefecture. In general, human activities contributed more than climate change, including grazing and urbanization, in mountainous and flat areas.

5 Discussion

5.1 Spatiotemporal patterns of NDVI, NDVIc, and NDVIh

Based on the fluctuation status of NDVI, the results of this study show that the NDVI in the research area mainly remains in a low fluctuation state and a relatively low fluctuation state, indicating that from 1981 to 2015, the fluctuation degree was low, data distribution was concentrated, time series were stable, and reliability was high. This helps to improve the accuracy and effectiveness of data analysis, as well as the credibility and interpretability in practical applications. Precipitation in Xinjiang is generally low, and the arid and semi-arid climate suppresses vegetation growth, resulting in sparse vegetation cover, low and relatively stable NDVI values (Liu et al., 2016). The fluctuation status in the Tianshan Mountains and Altai Mountains is higher due to sufficient moisture and higher temperatures in these areas, which extend the vegetation growth period, leading to more luxuriant vegetation during the growing season, with greater fluctuations between the maximum and minimum NDVI values (Liu et al., 2016).

50% of the research area pixel NDVI change trend was tested for significance, indicating a large magnitude of data change and strong reliability. The entire research area exhibits spatial heterogeneity in NDVI, showing an overall upward trend. The areas with increasing NDVI mainly include the western part of Changji Hui Autonomous Prefecture, the southern part of Tacheng Prefecture, and the northwestern part of the Tarim Basin, accounting for 62.5% of the research area. The decreasing areas are mainly distributed in the western part of the research area, as well as the Ili River and Tekes River basins, accounting for 37.5% of the research area. This is mainly attributed to the warming and humidifying trend of the climate in Xinjiang in recent years, where increased precipitation and rising temperatures have promoted grassland growth (Li et al., 2018; Zhang et al., 2021; Yao et al., 2018). Research by Zhang et al. (2018) on the dynamic response of grassland to climate change and human activities in Xinjiang shows that the grasslands in the Ili River Valley are experiencing a degradation trend, similar to the results of this study (Zhang et al., 2018). Furthermore, it indicates that the degraded grassland area is gradually spreading towards the western part of the Tianshan Mountains in terms of spatial distribution. Additionally, the

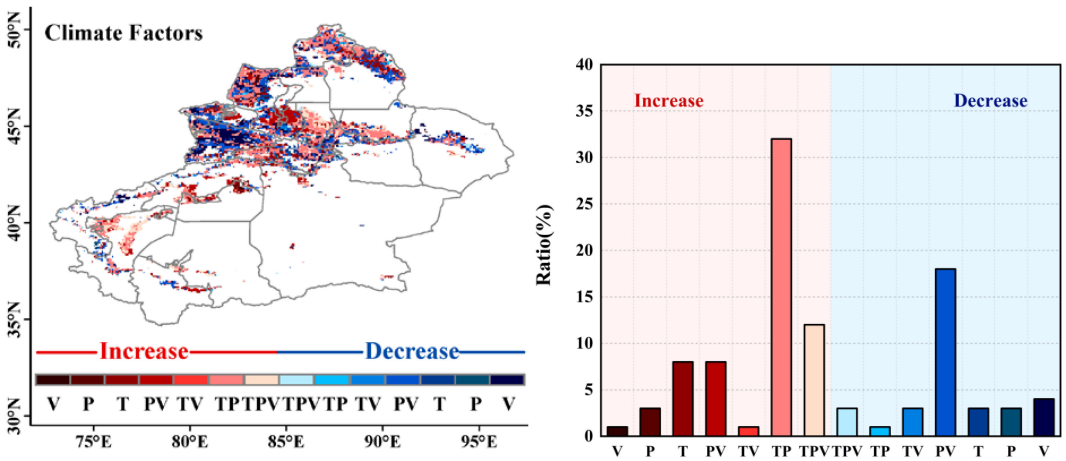

FIGURE 8
Spatial distribution of climatic drivers of grassland NDVI and frequency histogram of area proportions. The red colors indicate an increasing trend, and the blue colors indicate a decreasing trend. (P-V) represents the combined effect of precipitation and VPD, (T-V) represents temperature and VPD, (T-P) represents temperature and precipitation, and (T-P-V) represents the combined effect of temperature, precipitation, and VPD.

turning-point has been detected for the NDVI series over the study area. It shows that the increasing trend of NDVI changed after the year of 2000. However, there was a little difference between the slopes before and after the turning point, and thereby it was not considered in the present work.

Through the grassland NDVI model, the spatiotemporal patterns of NDVIc (NDVI affected by climate change) and NDVIh (NDVI affected by human activities) in the study area were analyzed. The results show that NDVIc generally increases over time, indicating a growing role of climate change in promoting grassland growth year by year, accounting for 77.7% of the study area, with 41.7% of pixels greater than 0.0005/a. The growth areas mainly include the Tianshan Mountains, Altai Mountains, Irtysh River Basin, Tacheng area, and Bortala Mongol Autonomous Prefecture. This may be related to climate change and topographical fluctuations in Xinjiang: on the one hand, there has been a trend of warming and increased humidity in Xinjiang in recent years (Wang et al., 2020), with increased precipitation and thereby soil moisture helping meet the water needs of grassland growth, rising temperatures promoting grassland photosynthesis, improving photosynthetic efficiency, and thus enhancing grassland growth; on the other hand, the closer to mountainous areas or the larger the mountains, the greater the trend of increasing annual precipitation, as moist air forced to rise when passing through mountains leads to cooling with altitude, making water vapor in the air more likely to condense into precipitation, promoting grassland around mountainous and basin areas, thereby improving degradation (Yao et al., 2022).

In contrast to NDVIc, NDVIh mainly shows a decreasing trend, indicating that human activities are increasingly inhibiting grassland growth year by year, accounting for 60% of the study area. About 37% of the pixels have a decrease rate of less than -0.0005/a, which is lower than the increase rate of NDVIc. The remaining 40% of pixels show an increasing trend. The areas where NDVIh is increasing year by year are mainly distributed in the western part of Changji Hui Autonomous Prefecture, downstream of Yarkant River, Aksu City, Xinhe City, Korla City, and near Kashgar City. This is related to land use changes, conservation and restoration projects, and water resource management: human activities have led to changes in land use, such as an increase in parks, green spaces, or protected areas; at the same time, irrigation systems or other water projects have a restorative effect on the ecological environment, promoting grassland growth.

5.2 Effects of climatic variables to grass growth

In order to eliminate the influence of other variables, partial correlation coefficients were used to measure the relationship between NDVI and precipitation, temperature, and VPD. The results show that compared to the correlation coefficient, in the study area, NDVI is mainly positively correlated with precipitation. That is, in areas with higher precipitation, the NDVI values are also higher, accounting for a relatively low proportion of 69%, with a distribution range roughly the same, mainly distributed in mountainous areas. Moreover, the number of pixels showing a negative correlation in the southern part of the mountains increases, indicating that moisture conditions are an important factor affecting the variation of grassland NDVI, as soil moisture is one of the essential resources for plant photosynthesis and growth, and an increase in soil moisture leads to an increase in NDVI values (Liang et al., 2015). It should be noted that NDVI is calculated from the reflectance values of the near-infrared and red visible light bands, with the near-infrared band being a strong absorption region for water bodies. When precipitation causes significant changes in soil moisture content, the NDVI values decrease. Therefore, in some areas, there is a negative correlation between NDVI and precipitation (Li et al., 2011).

NDVI is mainly positively correlated with temperature, accounting for 83%, slightly higher than the correlation coefficient of 69%, and the correlation strength is stronger than that with precipitation. The number of negatively correlated pixels in the western part of Tacheng region is smaller, mainly located in its southern part. Specifically, it reflects the sensitivity of vegetation activity in mid-high latitude zones to heat factors: on the one hand, most areas in the study area belong to arid or semi-arid climates, with relatively low precipitation. Under such climatic conditions, the impact of temperature on vegetation growth is more significant than that of precipitation, promoting organic matter decomposition and improving the effectiveness of vegetation nutrient utilization; on the other hand, the increase in temperature leads to the evaporation of soil moisture in water-rich areas, maintaining high air humidity, improving local microclimates, and increasing NDVI (Huang et al., 2022).

For VPD, unlike the correlation coefficient, it is mainly negatively correlated with NDVI. That is, NDVI increases as VPD decreases and decreases as VPD increases, accounting for 73%, much higher than the correlation coefficient of 57%. Moreover, the number of pixels showing a negative correlation in the southern Altai Mountains and the Tianshan Mountains has significantly increased. The reason is that when VPD is low, the air is humid, which can suppress transpiration and surface evaporation, beneficial for soil moisture retention and organic matter accumulation (Huang et al., 2022), thereby promoting grassland growth. In regions where NDVI is positively correlated with VPD, high VPD is usually associated with clear and dry weather conditions, meaning sufficient sunlight and suitable temperatures. Compared to the inhibitory effect of VPD, these weather conditions have a stronger promoting effect on plant growth.

In summary, the changes in precipitation, temperature, and VPD are closely related to the variation of NDVI in the study area. Considering the individual impacts of precipitation, temperature, and VPD, NDVI is mainly positively correlated with precipitation and temperature, and negatively correlated with VPD. Among them, the region where NDVI is positively correlated with temperature has a larger area and a stronger relationship, indicating that temperature has a greater impact on the vegetation coverage of grasslands in the study area.

For the same pixel, the partial correlation coefficient and the correlation coefficient show different relationships, indicating that there are complex composite relationships between NDVI and

precipitation, temperature, and VPD. After controlling for other variables, the direct relationship between NDVI and the remaining variables may exhibit an opposite trend. To further explore the impact of climate variables on grassland NDVI changes, identify the individual and composite contributions of climate variables, and generate spatial pattern maps of driving factors. The results indicate that grasslands in the study area are more influenced by the combined effects of multiple climate variables than by the effects of a single climate variable. Combining the contribution rates of climate variables to grassland changes (Figure 7), it is mainly found that Cc promotes grassland recovery. In terms of individual climate variables, the influencing factors from largest to smallest are temperature, VPD, and precipitation, meaning that temperature has a greater impact on grassland changes, which is consistent with the above conclusion.

In regions where there is a growing trend in grassland, the main factor is the combined influence of temperature and precipitation (TP). That is, the composite pattern of temperature and precipitation is the main factor for grassland improvement, as grass growth depends on both water and temperature, and neither can be lacking.

In areas showing a decreasing trend in grassland, the main influence is from the combined effects of precipitation and VPD (PV), meaning that the composite pattern of precipitation and VPD has the most significant driving effect on grassland degradation. As most parts of Xinjiang are in arid or semi-arid climates with low annual precipitation, high VPD indicates strong air absorption capacity for moisture, leading to rapid evaporation of soil moisture and exacerbating water stress in grasslands.

5.3 Relative contributions to grassland changes

Based on the spatial distribution map of six response modes to climate change and human activities based on grassland NDVI, it can be seen that for grassland growth, it is influenced by both climate change and human activities, with a relatively equal degree of impact. The contributions of climate change and human activities are 52% and 48%, respectively. Regions with higher contributions from climate change are mainly distributed in the Altai Mountains, western Tacheng area, Kaidu River Basin, as well as the junction of Turpan City and Changji Hui Autonomous Prefecture; regions with higher contributions from human activities are located in the northern part of the Tianshan Mountains, western Tarim Basin, and the northern part. Grassland growth on the edge of the Tarim Basin and the southern edge of the Junggar Basin mainly benefits from human activities. The sand control and desertification control projects implemented after the National Sand Control Conference in 1991, including the construction of a sand control system with shrubs and grasses and measures such as fencing and enclosure of desert grasslands, have improved soil quality, provided suitable growth environments, and promoted grassland growth. The ecological governance project around the Tarim Basin launched in 2009 and the sand control and desertification control project in the Junggar Basin further accelerated the recovery of grasslands. In addition, the settlement project for herdsmen implemented in 1986, the national grazing ban and grassland restoration project in 2002, the grassland ecological compensation incentive mechanism in 2011, all played a role in promoting grassland growth (Cai et al., 2022).

Human activities (Ha) are the main driving factor for the reduction of grasslands, such as urban expansion, mining, grazing, and agricultural activities, which inhibit grass growth, leading to a decrease in biomass, and they also occupy the largest area of the entire study area (32%). In this study, the main cause of grassland degradation and desertification is grazing (Yang et al., 2014). The Altai Mountains, Tacheng region, and Ili River Valley are regions with high grazing rates in Xinjiang (Huang et al., 2018), so they are also concentrated areas where human activities lead to a decrease in NDVI. Notably, our present approach could technologically distinguish the contributions of the climatic variables and non-climatic variables to the variations of NDVI over the grasslands. However, it is difficult to identify what kind of human activities dominates contribution without corresponding driving data. Hence, we tried to investigate the relationship between the contribution of human activities and the grazing intensity obtained from a recently released data (Wang et al., 2024). We found that the negative contributions were quite consistent with the increasing grazing intensity across the study area. In contrast, the positive contributions were mainly associated to the reducing grazing. This generally support our results and infer.

Based on the results of the relative contributions of climate change and human activities to grassland NDVI changes, it is shown that human activities contribute more (64.29%) to grassland changes than climate change (35.71%). These results are generally consistent with the previous studies which investigated grassland dynamics in response to climate change and human activities in Xinjiang or the (semi-) arid areas of China (Zhang et al., 2018; Yang et al., 2017; Xue et al., 2023). This is because the study area is mainly composed of mountains, river basins, and oases. For mountainous areas, due to the complex and varied terrain in mountainous regions, as well as significant differences in climate and human environment between the southern and northern slopes, grasslands are more driven by non-climatic factors than climatic factors (Zhang et al., 2018). In river basins and oasis areas, due to the fact that the river valleys and areas around oases are the main grazing and pasture areas, human activities are significant, so human activities contribute more to grassland changes (Huang et al., 2022).

5.4 Uncertainties and further studies

Although the aims were generally achieved, there remain some limitations in our work. First, the GIMMS dataset offers a spatially continuous and long temporal span NDVI data, its spatial resolution is relatively coarse, which may impact the detections of vegetation growth to some extent. Remotely sensed data with a higher spatial resolution would be needed for a finer analysis. Second, the relative contributions of climate change and human activities were quantified, while the approach adopted in this study

is still an empirical-based statistical analysis. Finally, it could not identify what kind of human activities dominates the contribution. A robust casual analysis or model simulation may be helpful to crack these nuts.

6 Conclusions

This article systematically studied the spatiotemporal patterns and fluctuation status of grasslands in Xinjiang from 1981 to 2015, revealing the correlation between NDVI and precipitation, temperature, and VPD. By combining six response modes of NDVI changes, it quantitatively analyzed the contributions of climate change and human activities to grassland changes. The study found that the NDVI of Xinjiang grasslands exhibits spatial heterogeneity, with an overall upward trend. This is mainly attributed to the warming and humidifying trend of Xinjiang's climate in recent years, where increased precipitation and higher temperatures have promoted grass growth. The regions with increasing NDVI are mainly concentrated in the western part of Changji Hui Autonomous Prefecture, the southern part of Tacheng area, and the northwestern part of the Tarim Basin; while the decreasing areas are mainly distributed in the western part of the study area, the Ili River, and the Tekes River basin. Further analysis shows that temperature and precipitation (TP) have the most significant impact on grassland growth, while precipitation and VPD (PV) have the greatest impact on grassland reduction. For grassland growth, the contributions of climate change and human activities are roughly equivalent; however, for grassland reduction, the influence of human activities is more pronounced. Overall, in mountainous and flat areas, human activities have a greater contribution to grassland changes than climate change. Therefore, when predicting future trends in grassland ecosystem changes, it is necessary to consider the quantitative impacts of both climate change and human activities simultaneously.

Data availability statement

The original contributions presented in the study are included in the article/Supplementary Material. Further inquiries can be directed to the corresponding author.

Author contributions

HR: Formal analysis, Funding acquisition, Methodology, Writing – original draft. BL: Formal analysis, Methodology, Software, Writing – review & editing. YW: Conceptualization, Funding acquisition, Resources, Supervision, Writing – review & editing. LZ: Writing – review & editing. QZ: Writing – review & editing.

Funding

The author(s) declare that financial support was received for the research, authorship, and/or publication of this article. This research was funded by the General Project of Philosophy and Social Science Research in Jiangsu Universities, grant number 2024SJYB0409; the Scientific research project of Nanjing Xiaozhuang University, grant number 2023NXY11; and Environmental Impact Assessment Project for Wastewater Treatment and Discharge Engineering of Korla Fiber Company of Xinjiang Zhongtai Textile Group.

Conflict of interest

This study received funding from Korla Fiber Company of Xinjiang Zhongtai Textile Group, which were involved with the collection of data.

Publisher's note

Supplementary material

The Supplementary Material for this article can be found online at: https://www.frontiersin.org/articles/10.3389/fpls.2024.1497248/full#supplementary-material

References

Cai, Y., Zhang, F., and Duan, P. (2022). Vegetation cover changes in China induced by ecological restoration-protection projects and land-use changes from 2000 to 2020. *Catena* 217, 106530. doi: 10.1016/j.catena.2022.106530

Chen, C. B., Li, G. Y., and Peng, J. (2023). Spatio-temporal characteristics of Xinjiang grassland NDVI and its response to climate change from 1981 to 2018. *Acta Ecol. Sin.* 43, 1537–1552. doi: 10.5846/stxb202201260251

Defries, R., and Townshend, J. (1994). NDVI-derived land cover classification at a global scales. *Int. J. Remote Sens.* 15, 3567–3586. doi: 10.1080/01431169408954345

de Jong, R., de Bruin, S., and de Wait, A. (2011). Analysis of monotonic greening and browning trends from global NDVI time-series. *Remote Sens. Environ.* 115, 692–702. doi: 10.1016/j.rse.2010.10.011

Detsch, F., Otte, I., Appelhans, T., Hemp, A., and Nauss, T. (2016). Seasonal and long-term vegetation dynamics from 1-km GIMMS-based NDVI time series at Mt. Kilimanjaro, Tanzania. *Remote Sens. Environ.* 178, 70–83. doi: 10.1016/j.rse.2016.03.007

Du, J., Shu, J., Yin, J., Yuan, X., Jiaerheng, A., Xiong, S., et al. (2015). Analysis on spatio-temporal trends and drivers in vegetation growth during recent decades in Xinjiang, China. *Int. J. Appl. Earth Obs. Geoinf.* 38, 216–228. doi: 10.1016/j.jag.2015.01.006

Eklundh, L. (1998). Estimating relations between AVHRR NDVI and rainfall in East Africa at 10-day and monthly time scales. *Int. J. Remote Sens.* 19, 563–570. doi: 10.1080/014311698216198

Gao, W. D., Zheng, C., Liu, X. H., Lu, Y. D., Chen, Y. F., Wei, Y., et al. (2022). NDVI-based vegetation dynamics and their responses to climate change and human activities from 1982 to 2020: A case study in the Mu Us Sandy Land, China. *Ecol. Indic.* 137, 108745. doi: 10.1016/j.ecolind.2022.108745

Guo, E., Wang, Y., Wang, C., Sun, Z., Bao, Y., Mandula, N., et al. (2021). NDVI indicates long-term dynamics of vegetation and its driving forces from climatic and anthropogenic factors in Mongolian plateau. *Remote Sens.* 13, 688. doi: 10.3390/rs13040688

He, J., Yang, K., Tang, W., Lu, H., Qin, J., Chen, Y., et al. (2020). The fist high-resolution meteorological forcing dataset for land process studies over China. *Sci. Data* 7, 25. doi: 10.1038/s41597-020-0369-y

Hilker, T., Natsagdorj, E., Waring, R. H., Lyapustin, A., and Wang, Y. (2013). Satellite observed widespread decline in Mongolian grasslands largely due to overgrazing. *Global Change Biol.* 20, 418–428. doi: 10.1111/gcb.12365

Huang, X., Luo, G., and Ye, F. P. (2018). Effects of grazing on net primary productivity, evapotranspiration and water use efficiency in the grasslands of Xinjiang, China. *J. Arid. Land* 4, 1–13. doi: 10.1007/s40333-018-0093-z

Huang, H. B., Xu, H. L., and Lin, T. (2022). Spatio-temporal variation characteristics of NDVI and its response to climate change in the Altay region of Xinjiang from 2001 to 2020. *Acta Ecol. Sin.* 42, 2798–2809. doi: 10.5846/stxb202107021768

Huang, Q., Zhang, L., Wu, W., and Li, D. (2010). "MODIS-NDVI-Based crop growth monitoring in China Agriculture Remote Sensing Monitoring System," in *2010 IITA International Conference on Geoscience and Remote Sensing* (Beijing: Institute of Electrical and Electronics Engineers, China, Qingdao). doi: 10.1109/IITA-GRS.2010.5603948

Huete, A., Didan, K., Miura, T., Rodriguez, E. P., Gao, X., and Ferreira, L. G. (2002). Overview of the radiometric and biophysical performance of the MODIS vegetation indices. *Remote Sens. Environ.* 83, 195–213. doi: 10.1016/S0034-4257(02)00096-2

Jiang, L. L., Gu, L. J., and Bao, A. M. (2017). Vegetation dynamics and responses to climate change and human activities in Central Asia. *Sci. Total Environ.* 599-600, 967–980. doi: 10.1016/j.scitotenv.2017.05.012

Jiang, L. G., Liu, Y., and Wu, S. (2021). Analyzing ecological environment change and associated driving factors in China based on NDVI time series data. *Ecol. Indic.* 129, 107933. doi: 10.1016/j.ecolind.2021.107933

Li, Y. G., and He, D. M. (2009). The spatial and temporal variation of NDVI and its relationships to the climatic factors in Red River Basin. *J. Mountain Sci.* 27, 333–340.

Li, H. X., Liu, G. H., and Fu, B. J. (2011). Response of vegetation to climate change and human activity based on NDVI in the Three-River Headwaters region. *Acta Ecol. Sin.* 19, 5495–5504.

Li, J., Peng, S., and Li, Z. (2017). Detecting and attributing vegetation changes on China's Loess Plateau. *Agric. For. Meteorol.* 247, 260–270. doi: 10.1016/j.agrformet.2017.08.005

Li, C., Wang, R. H., Ning, H. S., and Luo, Q. H. (2018). Characteristics of meteorological drought pattern and risk analysis for maize production in Xinjiang, Northwest China. *Theor. Appl. Climatol.* 133, 1269–1278. doi: 10.1007/s00704-017-2259-6

Li, F., Zhou, W. Z., and Shao, Z. L. (2022). Effects of ecological projects on vegetation in the Three Gorges Area of Chongqing, China. *J. Mountain Sci.* 19, 121–135. doi: 10.1007/s11629-021-6768-5

Liang, S., Yi, Q., and Liu, J. (2015). Vegetation dynamics and responses to recent climate change in Xinjiang using leaf area index as an indicator. *Ecol. Indic.* 58, 64–76. doi: 10.1016/j.ecolind.2015.05.036

Liu, H., Gong, P., Wang, J., Clinton, N., Bai, Y. Q., and Liang, S. L. (2020). Annual dynamics of global land cover and its long-term changes from 1982 to 2015. *Earth Syst. Sci. Data* 12, 1217–1243. doi: 10.5194/essd-12-1217-2020

Liu, Y., Li, L., Chen, X., Zhang, R., and Yang, J. (2018). Temporal-spatial variations and influencing factors of vegetation cover in Xinjiang from 1982 to 2013 based on GIMMS-NDVI3g. *Global Planet. Change* 169, 145–155. doi: 10.1016/j.gloplacha.2018.06.005

Liu, Y., Li, C. Z., and Liu, Z. H. (2016). Assessment of spatio-temporal variations in vegetation cover in Xinjiang from 1982 to 2013 based on GIMMS-NDVI. *Acta Ecol. Sin.* 36, 6198–6208. doi: 10.5846/stxb201506071149

Mentaschi, L., Besio, G., Cassola, F., and Mazzino, A. (2013). Problems in RMSE-based wave model validations. *Ocean Modell.* 72, 53–58. doi: 10.1016/j.ocemod.2013.08.003

Milich, L., and Weiss, E. (2000). GAC NDVI interannual coefficient of variation (CoV) images: ground truth sampling of the Sahel along north-south transects. *Int. J. Remote Sens.* 21, 235–260. doi: 10.1080/014311600210812

Piao, S., Fang, J., Ji, W., Guo, Q., Ke, J., Tao, S., et al. (2004). Variation in a satellite-based vegetation index in relation to climate in China. *J. Veg. Sci.* 15, 219–226. doi: 10.1658/1100-9233(2004)015[0219:VIASVI]2.0.CO;2

Piao, S., Fang, J., and Zhou, L. (2003). Interannual variations of monthly and seasonal normalized difference vegetation index (NDVI) in China from 1982 to 1999. *J. Geophys. Res.: Atmos.* 108, 4401–4413. doi: 10.1029/2002JD002848

Rawson, H. M., Begg, J. E., and Woodward, R. G. (1977). The effect of atmospheric humidity on photosynthesis, transpiration and water use efficiency of leaves of several plant species. *Planta* 134, 5–10. doi: 10.1007/BF00390086

Singh, A. K., Singh, H., Singh, S. P., and Sawhney, R. L. (2002). Numerical calculation of psychrometric properties on a calculator. *Build. Environ.* 37, 415–419. doi: 10.1016/S0360-1323(01)00032-4

Sun, Y. L., Yang, Y. L., and Zhang, L. (2015). The relative roles of climate variations and human activities in vegetation change in North China. *Phys. Chem. Earth.* 87-88, 67–78. doi: 10.1016/j.pce.2015.09.017

Tucker, C. J., Fung, I. Y., Keeling, C. D., and Gammon, R. H. (1986). Relationship between atmospheric CO2 variations and a satellite-derived vegetation index. *Nature* 319, 195–199. doi: 10.1038/319195a0

Wang, D., Peng, Q., Li, X., Zhang, W., Xia, X., Qin, Z., et al. (2024). A long-term high-resolution dataset of grasslands grazing intensity in China. *Sci. Data* 11, 1194. doi: 10.1038/s41597-024-04045-x

Wang, J., Wang, K., Zhang, M., and Zhang, C. (2015). Impacts of climate change and human activities on vegetation cover in hilly southern China. *Ecol. Eng.* 81, 451–461. doi: 10.1016/j.ecoleng.2015.04.022

Wang, Q., Zhai, P. M., and Qin, D. H. (2020). New perspectives on 'warming-wetting' trend in Xinjiang, China. *Adv. Clim. Change Res.* 11, 252–260. doi: 10.1016/j.accre.2020.09.004

Weiss, E., Marsh, S. E., and Pfirman, E. S. (2010). Application of NOAA-AVHRR NDVI timeseries data to assess changes in Saudi Arabia's rangelands. *Int. J. Remote Sens.* 22, 1005–1027. doi: 10.1080/014311601300074540

Xie, B., Jia, X., Qin, Z., Shen, J., and Chang, Q. (2016). Vegetation dynamics and climate change on the Loess Plateau, China: 1982-2011. *Reg. Environ. Change* 16, 1–12. doi: 10.1007/s10113-015-0881-3

Xu, Y. J., Dong, K., Jiang, M., Liu, Y. L., He, L. Y., Wang, J. L., et al. (2022). Soil moisture and species richness interactively affect multiple ecosystem functions in a microcosm experiment of simulated shrub encroached grasslands. *Sci. Total Environ.* 803, 149950. doi: 10.1016/j.scitotenv.2021.149950

Xu, X. J., Du, H. Q., Fan, W. L., Hu, J. G., Mao, F. J., and Dong, H. (2019). Long-term trend in vegetation gross primary production, phenology and their relationships inferred from the FLUXNET data. *J. Environ. Manage.* 246, 605–616. doi: 10.1016/j.jenvman.2019.06.023

Xu, Y. F., Yang, J., and Chen, Y. N. (2016). NDVI-based vegetation responses to climate change in an arid area of China. *Theor. Appl. Climatol.* 126, 213–222. doi: 10.1007/s00704-015-1572-1

Xue, Y., Liang, H., Ma, Y., Xue, G., and He, J. (2023). The impacts of climate and human activities on grassland productivity variation in China. *Remote Sens.* 15, 3864. doi: 10.3390/rs15153864e

Yang, H. F., Mu, S. J., and Li, J. L. (2014). Effects of ecological restoration projects on land use and land cover change and its influences on territorial NPP in Xinjiang, China. *Catena* 115, 85–95. doi: 10.1016/j.catena.2013.11.020

Yang, H., Yao, L., Wang, Y., and Li, J. (2017). Relative contribution of climate change and human activities to vegetation degradation and restoration in North Xinjiang, China. *Rangeland J.* 39, 289–302. doi: 10.1071/RJ16069

Yao, J. Q., Chen, Y. L., Guan, X. F., Zhao, Y., and Chen, J. (2022). Recent climate and hydrological changes in a mountain-basin system in Xinjiang, China. *Earth Sci. Rev.* 226, 103957. doi: 10.1016/j.earscirev.2022.103957

Yao, J. Q., Chen, Y. N., Zhao, Y., Mao, W. Y., Xu, X. B., Liu, Y., et al. (2018). Response of vegetation NDVI to climatic extremes in the arid region of Central Asia: a case study in Xinjiang, China. *Theor. Appl. Climatol.* 131, 1503–1515. doi: 10.1007/s00704-017-2058-0

Yuan, W., Zheng, Y., Piao, S., and Ciais, P. (2019). Increased atmospheric vapor pressure deficit reduces global vegetation growth. *Sci. Adv.* 5, 1396. doi: 10.1126/sciadv.aax1396

Zhang, R., Liang, T., Guo, J., Xie, H., Feng, Q., and Aimaiti, Y. (2018). Grassland dynamics in response to climate change and human activities in Xinjiang from 2000 to 2014. *Sci. Rep.* 8, 2888. doi: 10.1038/s41598-018-21089-3

Zhang, T. K., Wang, J. B., Ye, H., Lai, W. Q., and Zhang, X. J. (2024). Vulnerability of alpine ecosystems and its response to climate change and human activities. *Acta Ecol. Sin.* 44, 154–170. doi: 10.20103/j.stxb.202212143591

Zhang, Q., Yang, J. H., Wang, W., Ma, P. L., Lu, G. Y., Liu, H. P., et al. (2021). Climatic warming and humidification in the arid region of northwest China: multi-scale characteristics and impacts on ecological vegetation. *J. Meteorolog. Res.* 35, 113–127. doi: 10.1007/s13351-021-0105-3

Zhang, C. L., and Zhang, J. H. (2023). Landscape genomics reveals adaptive divergence of indigenous sheep in different ecological environments of Xinjiang, China. *Sci. Total Environ.* 904, 166698. doi: 10.1016/j.scitotenv.2023.166698

Zheng, K., Wei, J. Z., Pei, J. Y., Cheng, H., Zhang, X. L., and Huang, F. Q. (2019). Impacts of climate change and human activities on grassland vegetation variation in the Chinese Loess Plateau. *Sci. Total Environ.* 660, 236–244. doi: 10.1016/j.scitotenv.2019.01.022

Zhou, Z., Jin, J., Yong, B., and Yu, L. (2022). Quantifying the influences of climate change and human activities on the grassland in the Southwest Transboundary Basin, China. *J. Environ. Manage.* 319, 115612. doi: 10.1016/j.jenvman.2022.115612

frontiers | Frontiers in Plant Science

TYPE Original Research
PUBLISHED 19 February 2025
DOI 10.3389/fpls.2025.1533855

OPEN ACCESS

EDITED BY
Ting Hua,
Norwegian University of Science and Technology, Norway

REVIEWED BY
Jian Zhang,
China University of Mining and Technology, China
He Li,
Institute of Geographic Sciences and Natural Resources Research, Chinese Academy of Sciences (CAS), China

*CORRESPONDENCE
Yingcong Ye
yycdayu@126.com

RECEIVED 25 November 2024
ACCEPTED 27 January 2025
PUBLISHED 19 February 2025

CITATION
Liao Y, Yu Z, Kuang L, Jiang Y, Yu C, Li W, Liu M, Guo X and Ye Y (2025) Analysis of cultivated land degradation in southern China: diagnostics, drivers, and restoration solutions. *Front. Plant Sci.* 16:1533855. doi: 10.3389/fpls.2025.1533855

Analysis of cultivated land degradation in southern China: diagnostics, drivers, and restoration solutions

Yanqing Liao[1,2], Zhihong Yu[1,2], Lihua Kuang[1,2], Yefeng Jiang[1,2], Chenxi Yu[1,2], Weifeng Li[1,2], Ming Liu[3], Xi Guo[1,2] and Yingcong Ye[1,2]*

[1]Jiangxi Agricultural University, Jiangxi Province Key Laboratory of Arable Land Improvement and Quality Enhancement, Nanchang, China, [2]Technology Innovation Center for Land Spatial Ecological Unprotection and Restoration in Great Lakes Basin, Ministry of Natural Resources (MNR), Nanchang, China, [3]Institute of Soil Science, Chinese Academy of Sciences, Nanjing, China

Introduction: Cultivated land quality degradation is a critical challenge to food security, requiring effective nature-based restoration strategies based on comprehensive assessments of land quality. However, existing methods are often costly, limited in scope, and fail to capture the multidimensional complexity of the degradation processes.

Methods: This study integrated vegetation indices, topographic data, and soil physical and chemical properties to construct a model for identifying cultivated land degradation. Remote sensing indices were calculated using Google Earth Engine, enabling large-scale spatial analysis. Machine learning, combined with SHapley Additive exPlanations (SHAP), was employed to explore the driving factors of degradation.

Results: The results indicate that 11.86% of cultivated land in Yugan County is degraded, primarily in the central plain and riparian zones, driven by both natural factors (precipitation, temperature) and anthropogenic factors (straw incorporation, fertilization management). Soil erosion was concentrated in southern hills and near rivers, fertility decline occurred in the central plain, and soil acidification was evenly distributed with generally low degradation levels.

Discussion: Based on these findings, vegetation-based restoration solutions, including deep-rooted crops, crop rotation and intercropping, and straw incorporation, are proposed to address different types of cultivated land quality degradation and support sustainable land management.

KEYWORDS

cultivated land quality degradation, remote sensing indices, SHAP, Yugan County, nature-based solutions

1 Introduction

The escalating issue of cultivated-land degradation threatens food security and ecosystem stability (Nguyen et al., 2023). According to the Food and Agriculture Organization of the United Nations, approximately one-third of the world's land faces degradation, primarily due to climate change, over-farming, and irrational land use, leading to soil erosion, nutrient loss, and reduced organic matter, which endanger global food production and ecosystem health (FAO, 2022). If these trends continue, 840 million people will face hunger globally by 2030 and the risk of food supply instability will increase (FAO, 2021). In China, cultivated land quality degradation poses significant threat to national food security, particularly in the southern regions (Fan et al., 2023). Declining soil fertility, nutrient loss, soil erosion, and heavy metal pollution are prevalent issues driven by excessive chemical fertilizer use, monoculture cropping, and intensified soil erosion and water loss (Wang et al., 2020; He et al., 2024). These practices accelerate soil structural damage and reduce biodiversity, further undermining land productivity (Zhang et al., 2021b). As a typical agricultural area in southern China, Poyang Lake exemplifies these challenges, with soil degradation exacerbated by extreme weather events linked to climate change. Problems such as soil erosion, fertility decline, and heavy metal contamination have far-reaching implications for agricultural productivity and ecosystem resilience (Li et al., 2021b). Additionally, urbanization and industrialization intensify resource competition, compounding the degradation of cultivated land (Zheng et al., 2019; Su et al., 2024). Immediate, region-specific protection and restoration measures are essential to mitigate these threats and promote sustainable land management.

Nature-based solutions (NbS) are sustainable approaches that emulate or enhance natural processes to address environmental, social, and economic challenges (Keesstra et al., 2018). NbS emphasize the conservation, restoration, and sustainable management of ecosystems to deliver diverse ecological services, addressing contemporary environmental issues while laying the foundation for future ecological resilience (Cohen-Shacham et al., 2016; Prăvălie et al., 2024). In the context of cultivated land degradation, NbS offer promising strategies for restoring cultivated land quality through vegetation restoration, soil management, and agroecological practices (Sharma et al., 2024). These solutions are vital for mitigating land degradation, enhancing soil fertility, improving water retention, and fostering biodiversity in agricultural settings (Intergovernmental Panel on Climate, C, 2019; Debele et al., 2023). For cultivated land degradation, vegetation restoration not only holds significant importance for ecological rehabilitation in degraded lands but also demonstrates considerable economic benefits, environmental advantages, and operational feasibility (Miralles-Wilhelm, 2021). Moreover, the restoration process enhances biodiversity, improves microclimate conditions, and substantially increases regional ecosystem service provisioning (Sušnik et al., 2022). These benefits are achieved through reduced soil erosion, improved water retention capacity, and enhanced carbon sequestration, providing a critical pathway to achieving ecosystem sustainability (Lal, 2020; Blanco-Canqui, 2024). However, to devise effective restoration strategies for mitigating or reversing cultivated land degradation, the primary challenge is to scientifically identify and assess the types and severity of cultivated land degradation.

Despite its importance, accurately determining the state of land degradation and its driving factors remains a significant challenge. cultivated land degradation exhibits complex spatiotemporal characteristics at a global scale (He et al., 2024). Traditional large-scale, generalized assessments of cultivated land degradation are often costly and fail to support the refined and multidimensional demands of cultivated land management. Incorporating prior knowledge is therefore critical for identifying cultivated land degradation and formulating effective restoration strategies. Vegetation, as an essential indicator of ecosystem health, reflects changes in land conditions (Gaitán et al., 2013). Remote sensing techniques, such as calculating the Ratio Vegetation Index (RVI), Normalized Difference Vegetation Index (NDVI), and Difference Vegetation Index (DVI), have proven effective in identifying areas of soil stress due to their high precision, temporal efficiency, and extensive coverage (Han and Song, 2019). These methods provide a reliable foundation for precise soil sampling and analysis, enabling a deeper understanding of the extent of cultivated land degradation and informing targeted restoration measures (Yan et al., 2021). Furthermore, the complexity of cultivated land degradation processes is exacerbated by the dual influences of climate change and human activities (He et al., 2024). While traditional linear analysis methods can reveal associations between natural conditions, socioeconomic factors, and soil quality, they struggle to capture the nonlinear responses of cultivated land quality to environmental changes (Zhang et al., 2024a). Machine learning (ML) methods address this limitation, yet challenges remain regarding the interpretability of their results (Hussain et al., 2023). SHapley Additive exPlanations (SHAP), a game-theory-based analytical approach, provides a solution by offering a quantifiable and intuitive framework to explain complex ML model outputs (Han et al., 2024). By calculating each feature's contribution to model predictions, SHAP facilitates the interpretation of model results and enhances transparency in identifying the driving factors behind cultivated land degradation.

Therefore, this study aimed to 1) construct a cultivated land quality degradation diagnosis model for multiple cultivated land quality degradation types by integrating a remote sensing index and the physical and chemical properties of topsoil, enabling quantitative degradation assessment across regions; 2) analyze the cultivated land quality degradation driving factors based on machine learning and SHapley Additive exPlanations (SHAP); and 3) propose vegetation-based cultivated land restoration solutions tailored to different types and levels of cultivated land degradation.

2 Materials and methods

2.1 Study area

The study area is located in Yugan County, Shangrao City, Jiangxi Province (Figure 1). It has a total area of 2,350.36 km^2 and spans from 28°21'36″ to 29°03'24″ N and 116°13'48″ to 116°54'24″ E (Figure 1). It is under the jurisdiction of 9 towns and 11 townships, with a total of

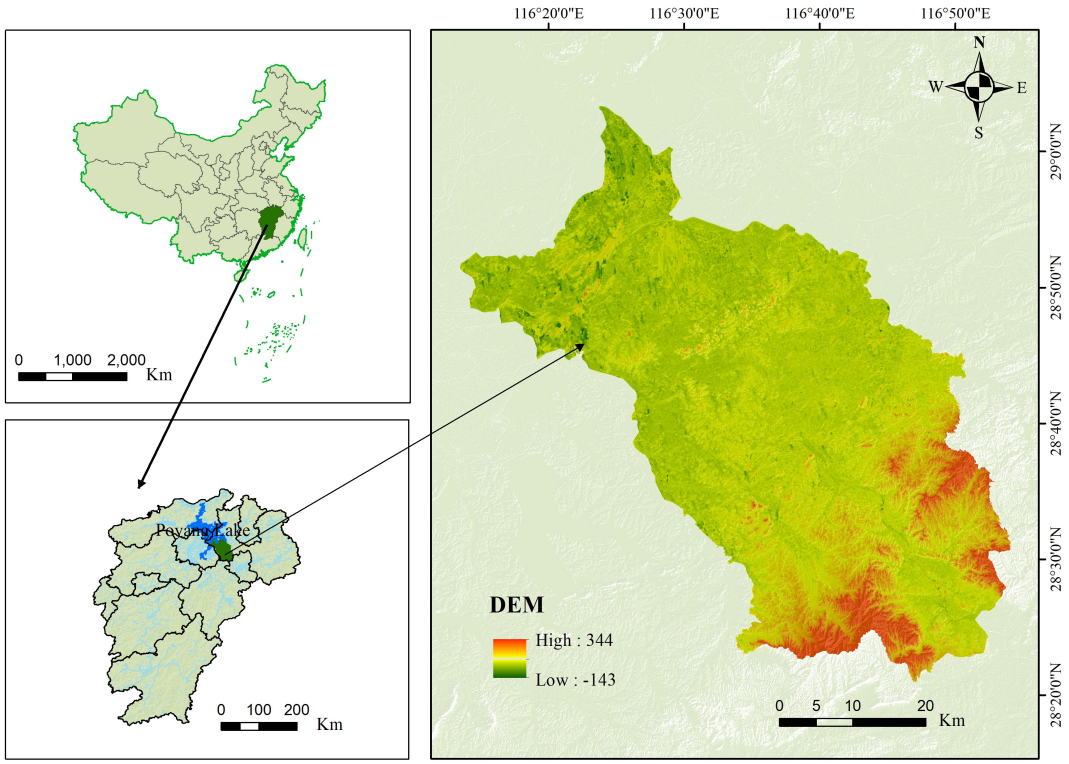

FIGURE 1
Location of the study area.

372 village committees. The topography of the city is dominated by low hills and lakeside plains with high terrain in the southeast and low terrain in the northwest. It belongs to a subtropical humid monsoon climate, with an average annual precipitation of 1,548 to 1,692 mm, average annual temperature of 15.4°C to 19.5°C, and frost-free period of 240 to 300 days. Land use mainly consists of arable land and forest land, with arable land accounting for 37.44% of the total area and forest land constituting 19% (Figure 2). Rice is the main grain crop, accounting for more than 90% of the total grain production. The soil types are dominated by rice and red soils and vegetation by broad-leaved and coniferous forests. The concentration of cultivated land and gentle slopes in the region make it ideal for studying cropland degradation.

Yugan County represents the typical ecological and agricultural conditions of the Poyang Lake region, characterized by the concentration of cultivated land, gentle slopes, and proximity to the lake's dynamic water system. Its location within the Poyang Lake basin makes it a hotspot for understanding the interactions between land use, water resource dynamics, and soil degradation. The area is subject to significant land degradation pressures, including soil acidification, soil fertility decline, soil erosion, and soil physical structure degradation, driven by intensive agricultural practices, heavy fertilizer use, and terrain features conducive to runoff and nutrient loss. These issues mirror broader degradation trends across the Poyang Lake region, making Yugan County a critical case for studying the mechanisms and drivers of farmland degradation. Moreover, its role as a major agricultural producer in the region highlights the broader environmental and socio-economic implications of land degradation, such as the risks of reduced crop yields, water eutrophication, and downstream ecological impacts, underscoring its representative significance in regional and national agricultural studies.

2.2 Dataset

The data sources covered a wide range of aspects and provided solid support for scientific analysis (Table 1).

The topsoil physical and chemical data, including soil organic matter content, pH value, total nitrogen content, and bulk density, along with fertilizer application amount, and straw return amount data were obtained from the Soil Testing and Formula Fertilization Dataset of Yugan County for 2012 and 2019.

Land use data, obtained from the Third National Land Survey of China for 2019 were incorporated to map the spatial distribution of land use types.

Remote sensing data, including Landsat 7 images, were obtained from the Google Earth Engine platform and ASTER GDEM V2 data were provided by the Geospatial Data Cloud (http://www.gscloud.cn/).

Socioeconomic data were obtained from population data from ORNL LandScan Viewer and The China GDP Spatial Distribution Kilometer Grid Dataset - Data from the Registration and Publishing System for Resource and Environmental Science Data (Xu, 2017).

For climate data, 1-km-resolution precipitation and temperature data were provided by the National Tibetan Plateau/Third Pole

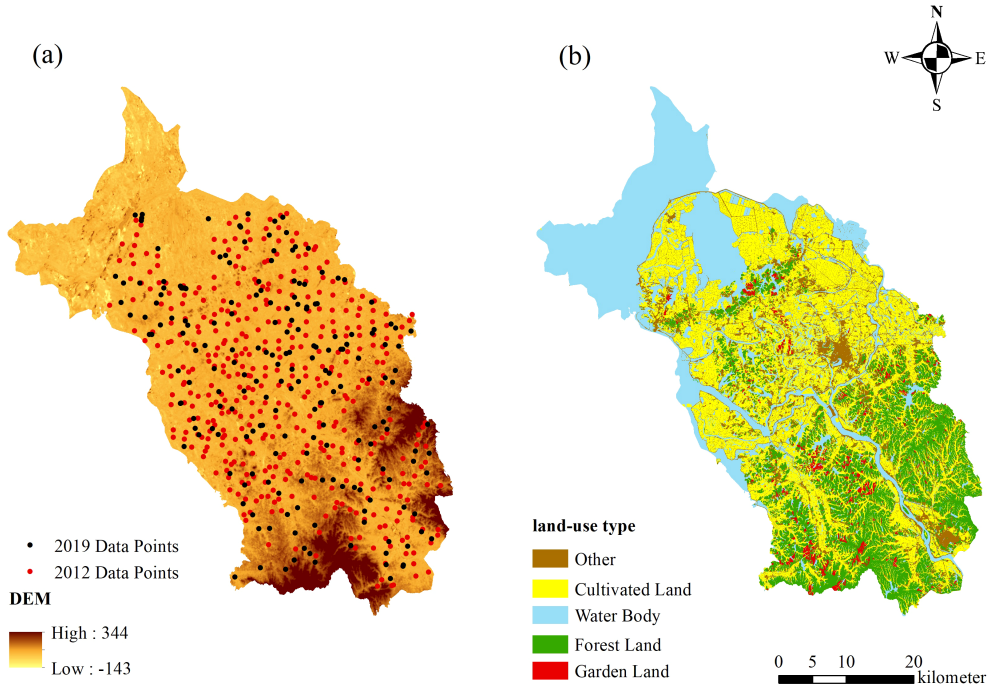

FIGURE 2
Spatial distribution of sampling sites and land use categories in the study area.

Environment Data Center (Peng, 2024) and 1-km resolution month-by-month mean temperature dataset (1901–2023) by the National Tibetan Plateau Data Center (Peng, 2019) was used.

2.3 Diagnostic model of degree of integrated cultivated land quality degradation

Based on the Cultivated Land Quality Grade Standard (GB/T33469-2016) and relevant documents issued by the Ministry of Agriculture and Rural Affairs, the grading standards for the physicochemical properties of the cultivated land in the study area were determined through comprehensive consideration (Table 2). Following the approach proposed by Tang et al. (2023), which emphasizes the integration of natural condition assessments and quality factor thresholds, we adopted a refined method for evaluating cultivated land quality. Specifically, we incorporated their equation for determining quality grades to ensure consistency and accuracy in assessing the degradation thresholds of cultivated land. Cultivated land quality grade was assessed using the 2019 Third National Land Survey Cultivated Land Map as the evaluation unit. The five indicators, including slope, soil organic matter content, soil total nitrogen content, soil pH, and bulk weight, were categorized into four grades based on their respective thresholds. The cultivated land quality grade of each evaluation unit was determined by the cumulative scoring of these indicators in accordance with the method outlined in Equation 1, derived and adapted from the formula used by Tang et al. (2023). This approach allows for a comprehensive evaluation of the degradation and quality status of cultivated land while aligning with region-specific thresholds for sustainable land management.

Equation 1 and its detailed parameters are elaborated to align with the methodology proposed in Tang et al. (2023), ensuring a robust framework for cultivated land quality assessment.

$$Grade\begin{cases} 1, if\ 0 \le n_{i2}+n_{i3} \le 1, n_{i4}=0, \sum_{j=1}^{4} n_{ij}=5 \\ 2, if\ 2 \le n_{i2}+n_{i3} \le 3, n_{i4}=0, \sum_{j=1}^{4} n_{ij}=5 \\ 3, if\ 4 \le n_{i2}+n_{i3} \le 5, n_{i4}=0, \sum_{j=1}^{4} n_{ij}=5\ or\ n_{i4}=1, \sum_{j=1}^{4} n_{ij}=5 \\ 4, if\ 2 \le n_{i4} \le 5, \sum_{j=1}^{4} n_{ij}=5 \end{cases} \quad (1)$$

where grade is the quality indicator for cultivated land quality evaluation, n is the number of indicators, i respect the ith evaluation unit, and j is the indicator grade. i is taken as 1,2,3…n and j is taken as 1,2,3,4.

The level of degradation of cultivated land quality was determined using the grade of the two-year cultivated land quality evaluation, calculated using Equation 2.

$$Grade(d) = Grade12 - Grade19 \quad (2)$$

TABLE 1 Sources of data used in the study.

Typology	Name	Source
Vector data	Soil sample data	Yugan County Soil Testing and Formula fertilization Dataset
	Landmark data	2019 Third National Land Survey Cultivated Land
Remote sensing data	Landsat 7 imagery	Google Earth Engine (GEE) https://developers.google.com/earth-engine/datasets/catalog/landsat-7
	ASTER GDEM V2	Geospatial Data Cloud https://www.gscloud.cn/sources/accessdata
	NASA DEM	EARTH DATA https://earthdata.nasa.gov/esds/competitive-programs/measures/nasadem
Socioeconomic data	Population density	ORNL LandScan Viewer - Oak Ridge National Laboratory: https://landscan.ornl.gov
	Gross domestic product	Registration and Publishing System for Resource and Environmental Science Data (Xu, 2017)
Climate data	Mean annual precipitation	1-km monthly precipitation dataset for China (1901–2023). National Tibetan Plateau/Third Pole Environment Data Center (Peng, 2024)
	Mean annual temperature	China 1-km resolution month-by-month mean temperature dataset (1901–2023). National Tibetan Plateau Data Center (Peng, 2019)
Fertilizer management data	Fertilization data	Yugan County Soil Testing and Formulation Dataset
	Straw return data	Yugan County Soil Testing and Formulation Dataset

The above data in ArcGIS 10.8.1 unified coordinate system.

where Grade(d) is the degradation grade of arable land, Grade12 is the quality grade of arable land in 2012, and Grade19 is the quality grade of arable land in 2019; a positive number represents an increase in grade, that is, no degradation, and a negative number represents a decrease in grade, that is, degradation.

The type of degradation was categorized into four grades: no degradation (the evaluation grade remained unchanged or increased), slight degradation (the grade decreased by one level), moderate degradation (the grade decreased by two levels), and severe degradation (the grade decreased by three levels or more).

2.4 Diagnostic model of the degree of single type degradation of cultivated land quality

2.4.1 Soil acidification

Soil acidification refers to the process of soil pH reduction owing to the accumulation of acidic substances, leading to the deterioration of soil physicochemical properties, which in turn affects plant growth and ecosystem functioning (Yadav et al., 2020). The Ratio Vegetation Index (RVI) is a remotely sensed ratio vegetation index that can accurately reflect the degree and spatial distribution of soil degradation (He et al., 2020). The main degradation factors affect soil health and vegetation on the soil surface, leading to changes in RVI. A past study found that RVI reflected soil acidification conditions in southern hilly areas (Bouslihim et al., 2024). Therefore, this study used the GEE cloud-computing platform to perform the band-ratio operation (Equation 3) on remote sensing images and extracted the RVI to indicate the degree of acidification of the soil. RVI was calculated as follows:

$$RVI = \frac{NIR}{RED} \tag{3}$$

where *NIR* is the reflectance in the near infrared band and *RED* is the reflectance in the red band.

The change in RVI was significantly correlated with the change in soil pH ($P<0.01$). We first screened cultivated lands with decreasing RVI and then determined the degree of soil acidification based on the change in pH level.

2.4.2 Soil fertility decline

Soil fertility decline is the process by which the ability of the soil to supply fertilizer and support plant growth declines because of nutrient depletion, particularly total nitrogen, or a reduction in organic matter (Kimetu et al., 2008). Organic matter improves the soil structure, promotes water infiltration and root growth, and provides plants with the necessary nutrients to enhance their water and fertilizer retention capacity and resistance. While nitrogen, as an essential element for plant growth, directly affects nitrogen uptake, utilization, and crop yield (Nguemezi et al., 2020). There was a strong positive correlation between the organic matter and total nitrogen contents($P<0.01$); therefore, the organic matter content was chosen as the main soil fertility evaluation index. Normalized Difference Vegetation Index (NDVI) indirectly characterizes soil fertility by reflecting vegetation cover and effectively predicting soil organic carbon content (Zhang et al., 2019). NDVI was calculated as follows:

$$NDVI = \frac{NIR-RED}{NIR+RED} \tag{4}$$

NDVI was significantly positively ($P<0.01$) correlated with soil organic matter and total nitrogen ($P<0.01$); therefore we chose the area with a declining NDVI tendency and determined the degree of soil fertility decline through changes in soil organic matter content levels.

TABLE 2 Classification criteria for evaluation indicators of arable land.

	Category	First class	Second class	Third class	Fourth class
SOM (g/kg)	Dryland	≥20	15~20	10~15	<10
	Paddy field	≥30	25~30	15~25	<15
TN (g/kg)	Dryland	≥20	15~20	10~15	<10
	Paddy field	≥30	25~30	15~25	<15
pH	Dryland	>=6.0	5.5~6.0	4.5~5.5	<4.5
	Paddy field	>=5.5	5.0~5.5	4.5~5.0	<4.5
BD	Dryland	1.00~1.25	1.25~1.35, 0.90~1.00	1.35~1.45	≥1.45, <0.90
	Paddy field				
SLOPE	Dryland	<=5°	5°~8°	8°~18°	>18°
	Paddy field				

2.4.3 Soil erosion

Soil erosion refers to the erosion of the top layer of soil caused by rainfall, surface runoff, wind erosion, or irrational land use, which manifests as soil loss, an increase in the sand content of rivers, a decrease in land fertility, and ecosystem degradation (Morgan, 2005). The factors related to soil erosion on cultivated land include slope, water flow, and fertility. Slope is an important factor for measuring the steepness of a terrain, with the greater the slope, the greater the risk of soil erosion (Mei et al., 2024). Soil moisture status is a key indicator for assessing the quality of cultivated land, and the Differential Vegetation Index (DVI) can effectively reflect the regional soil moisture content (Wang et al., 2021). DVI was calculated as follows:

$$DVI = NIR - RED \quad (5)$$

There was a significant correlation (P<0.01) between DVI, slope, and organic matter. Based on the soil sampling protocol of this study and previous research findings, we selected cultivated land with slopes greater than 5° that showed a increasing tend in DVI and assessed the degree of soil erosion by examining the changes in soil organic matter content (Mei et al., 2024).

2.4.4 Soil physical structure degradation

Soil physical structure degradation is the process of disruption of the soil aggregate structure, reduction in porosity, and increase in compactness, resulting in the deterioration of water permeability, aeration, and root growth conditions (Hillel, 1998). Bulk density is the mass per unit volume of soil, usually expressed in grams per cubic centimeter or grams per liter (Ferreras et al., 2000). Bulk density reflects the structure and compactness of the soil and has an important influence on soil fertility and aeration. High volumetric weights indicate dense soils with impeded root growth, poor water permeability, and limited gas exchange, all of which affect crop growth (McLenaghen et al., 2017). In contrast, low bulkiness may indicate loose soil with smoother root growth and good water permeability, which favors gas exchange but may also lead to water and nutrient loss (García-Orenes et al., 2005; Omuto, 2008). The higher the soil bulk weight, the lower the soil water content, and the tighter the soil (Fernández-Ugalde et al., 2009). In this study, changes in DVI were significantly negatively correlated with changes in soil bulk density (P<0.01); therefore, these factors were combined to determine the degree of degradation of the soil physical structure. In this study, we selected cultivated land with a DVI declining tendency and then determined the degree of fertility decline via the changes in their soil bulkiness levels.

The types of degradation were categorized into four classes: no degradation (no change or increase in the evaluation rating), slight degradation (one level down), moderate degradation (two levels down), and severe degradation (three levels down).

2.5 Random forest model

Random forest (RF) is a widely used integrated learning method for classification and regression tasks, proposed by Breiman and Cutler in 2001. The core idea is to improve the overall accuracy and robustness of the model by constructing multiple mutually independent decision trees and synthesizing the prediction results for each tree (Sheykhmousa et al., 2020; Smith and Wang, 2020). The construction of decision trees by randomly selecting features and data subsets greatly improves the resistance of the model to overfitting and performs well in dealing with high-dimensional data, noisy data, and nonlinear relationships (Jain and Jana, 2023). RF has been widely used in remote sensing image classification and for predicting forest degradation (Gong et al., 2018; Zhou et al., 2023). In this study, the RF model was implemented using the Scikit-learn library for Python 3.11.4. Environmental variables such as topography and climate were selected as inputs, and a spatial distribution map of soil attributes with spatial information was generated by training the model.

The optimal parameters of the model were configured as follows: number of estimation trees (n_estimators) = 300, maximum tree depth (max_depth) = 30, and maximum number of features (max_features) = 1.0. 10-fold cross-validation was used during the model training process and the random seeds of both the training and test datasets were set to 30 to ensure the stability and reproducibility of the results.

2.6 Light gradient boosting machine modeling with SHAP

SHAP is a game theory-based analytical method for interpreting the output of complex machine learning models (Huang et al., 2023a). By calculating the contribution of each feature to the model predictions, SHAP provides an intuitive and quantifiable framework for model interpretation. Its core is based on the Shapley value, an assignment method derived from cooperative game theory that measures the impact of each feature on model predictions fairly, thus providing a solid theoretical foundation for the interpretation of complex models (Han et al., 2024). In recent years, SHAP has been widely used in biomedicine, environmental monitoring, and other fields to help decision-makers better understand the importance of features and their impacts on the final results by explaining the prediction mechanism of machine learning models (Zhang et al., 2023a; Du et al., 2024). The contribution rate of each characteristic variable to the target variable, represented by the Shapley value, can be calculated using the following formula.

$$\varphi_i(v) = \frac{1}{|K|!}\sum_{R}[v(S_R^i \cup) - v(S_R^i)] \quad (6)$$

Where φi represents the Shapley value for feature i, S_R^i is the subset of features preceding i in a permutation R, |K| is the total number of features, and $v(S_R^i)$ denotes the predictive contribution of subset S_R^i. The Shapley value quantifies the average marginal contribution of feature iii across all possible feature subsets.

Light Gradient Boosting Machine (LightGBM) is an efficient machine learning algorithm based on gradient boosting designed for processing large-scale data and high-dimensional features (Wei et al., 2021). Its core innovation lies in the leafwise growth strategy, which generates a deeper tree structure and improves the prediction accuracy of the model by prioritizing the leaf nodes with the largest error reduction during expansion. In addition, LightGBM discretizes features using a histogram-based algorithm, which significantly reduces memory occupation and computational cost and improves training efficiency (Wang et al., 2023a). Compared to traditional gradient boosting models, LightGBM can efficiently handle sparse data and large-scale datasets while maintaining good prediction performance and scalability (Lokker et al., 2024).

This study employs LightGBM and SHAP to identify the importance of multiple factors and explore the primary drivers of cultivated land quality degradation. Eleven factors from five aspects of topography, climate, location, socioeconomics, and agricultural management were selected that may affect cultivated land quality degradation, including *Digital Elevation Model (DEM), Slope Direction (ASPECT), Slope Gradient (SLOPE), Mean Annual Precipitation (MAP), Mean Annual Temperature (MAT), Distance to the Rivers (Dist. Rivers), Distance to the Rodes(Dist. Roads), Population Density (POP), Gross Domestic Product (GDP), Straw Return Rate (SRR), Fertilizer Application Rate (FAR)*. This comprehensive selection ensures that various dimensions influencing land quality, such as physical environment, climatic conditions, accessibility, human activity, and agricultural practices, are represented in the model.

The integration of these factors into the LightGBM model, combined with the interpretative power of SHAP, enables a robust analysis of the underlying mechanisms and key contributors to farmland degradation in the study area.

3 Results

3.1 Analysis of the integrated cultivated land quality degradation

Using the cultivated land quality degradation type identification model and degradation degree evaluation method, this study presents a comparative table of the degradation degree of each degradation type in the study area during the decade (Table 3). The overall health of cultivated land quality degradation in the study area was good, with only approximately 11.86% showing signs of degradation, of which lightly degraded cultivated land accounted for 11.81% of the total cultivated land, with very little moderate degradation and no heavily

TABLE 3 Levels of cultivated land quality degradation.

Degradation type		No degradation	Slight degradation	Moderate degradation	Severe degradation	Total degradation
All types	Area (km^2)	783.0586	104.9531	0.3884	0	105.3416
	Percentage (%)	88.1426	11.8137	0.0437	0	11.8574
soil acidification	Area (km^2)	853.5768	34.3451	0.4783	0	34.8234
	Percentage (%)	96.0802	3.8659	0.0538	0	3.9198
fertility decline	Area (km^2)	643.6857	226.9326	17.7661	0.0158	244.7145
	Percentage (%)	72.4545	25.5440	1.9998	0.0018	27.5455
soil erosion	Area (km^2)	887.2728	0.8959	0.2306	0.0008	1.1274
	Percentage (%)	99.8731	0.1008	0.0260	0.0001	0.1269
Physical structural degradation	Area (km^2)	888.1472	0.2530	0	0	0.2530
	Percentage (%)	99.9715	0.0285	0	0	0.0285

degraded cultivated land. To visualize the spatial distribution of the degree of degradation of the overall quality of cultivated land in Yugan County, we measured the degree of degradation in each township and constructed a spatial distribution map (Figure 3). Degradation was mainly concentrated in the central and western plains and along the rivers in the southern hilly areas, whereas the degradation degree of the northern lakeshore plain was the least significant.

3.2 Analysis of each degradation form of the cultivated land quality

Soil acidification accounted for 3.92% of the total cultivated land area, primarily at the slight degradation level (3.87%), followed by moderate degradation (less than 0.1%) (Table 3). Fertility decline made up 27.55% of the total cultivated land quality degradation, predominantly light degradation, which accounted for 25.54% of the total cultivated land area. Moderate degradation represented 2% of the total cultivated land area, significantly higher than other types of degradation, while heavy degradation was observed in only 0.002% of the plots. Soil erosion contributed to 0.03% of total cultivated land quality degradation, mostly slight degradation, with almost no moderate or severe degradation. Lastly, physical structure degradation accounted for 0.13% of the total cultivated land quality degradation, with no cases of moderate or severe degradation. Taken together, most of the degradation types predominantly resulted in slight degradation, especially soil acidification and soil physical structure degradation. However, the proportion of moderate degradation of fertility decline and soil erosion was relatively high, which needs to be studied further. Heavy degradation is rare and occurs only during fertility declines and soil erosion.

To visualize the spatial distribution of different types of cultivated land quality degradation and their degree of degradation in Yugan County, we measured the degradation types and degree of degradation in each township and drew corresponding spatial distribution maps (Figure 4). The results showed that the spatial differentiation pattern of cultivated land quality degradation presented obvious regional differences. Soil acidification was widely distributed throughout the county, with a lower degree of acidification in the northern lakeshore plain area, whereas acidification is more severe in the central and southern hilly areas, especially in the central area, where acidified cultivated land is more concentrated (Figure 4A). In contrast, fertility decline has the widest impact and is particularly problematic in the central, river, and lake littoral areas (Figure 4B). Soil erosion was mainly concentrated in the southern hilly areas and along rivers and lakes.

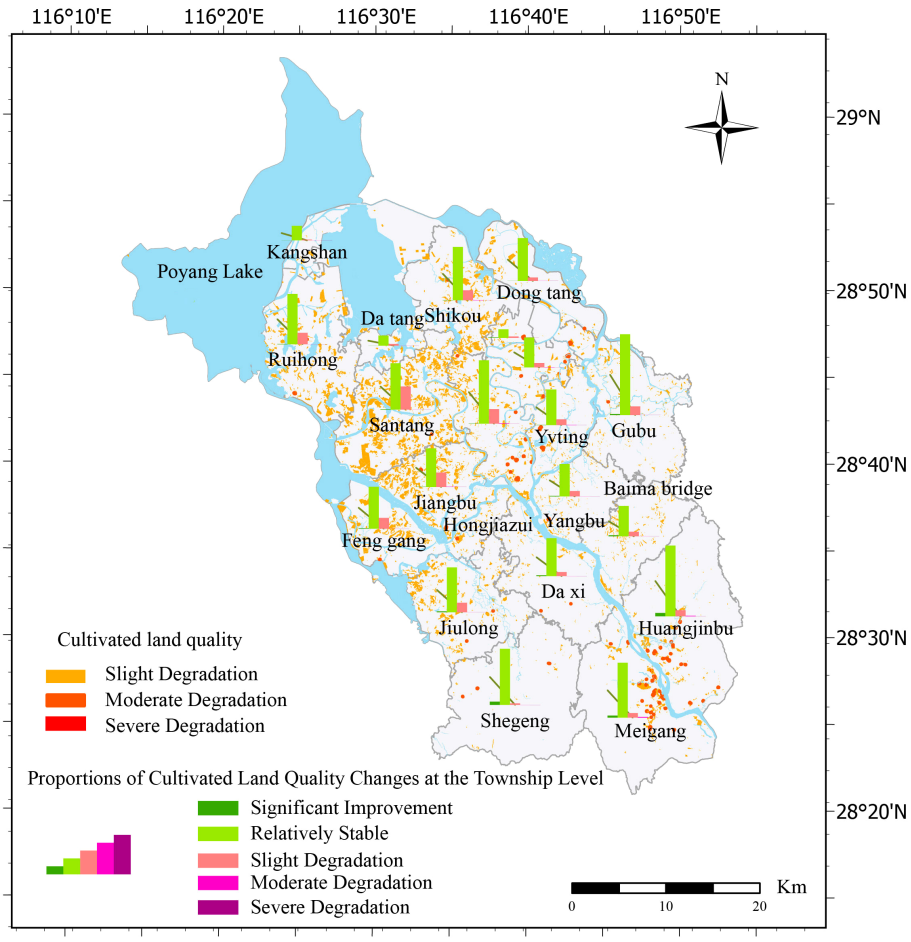

FIGURE 3
Spatial patterns of integrated cultivated land quality degradation.

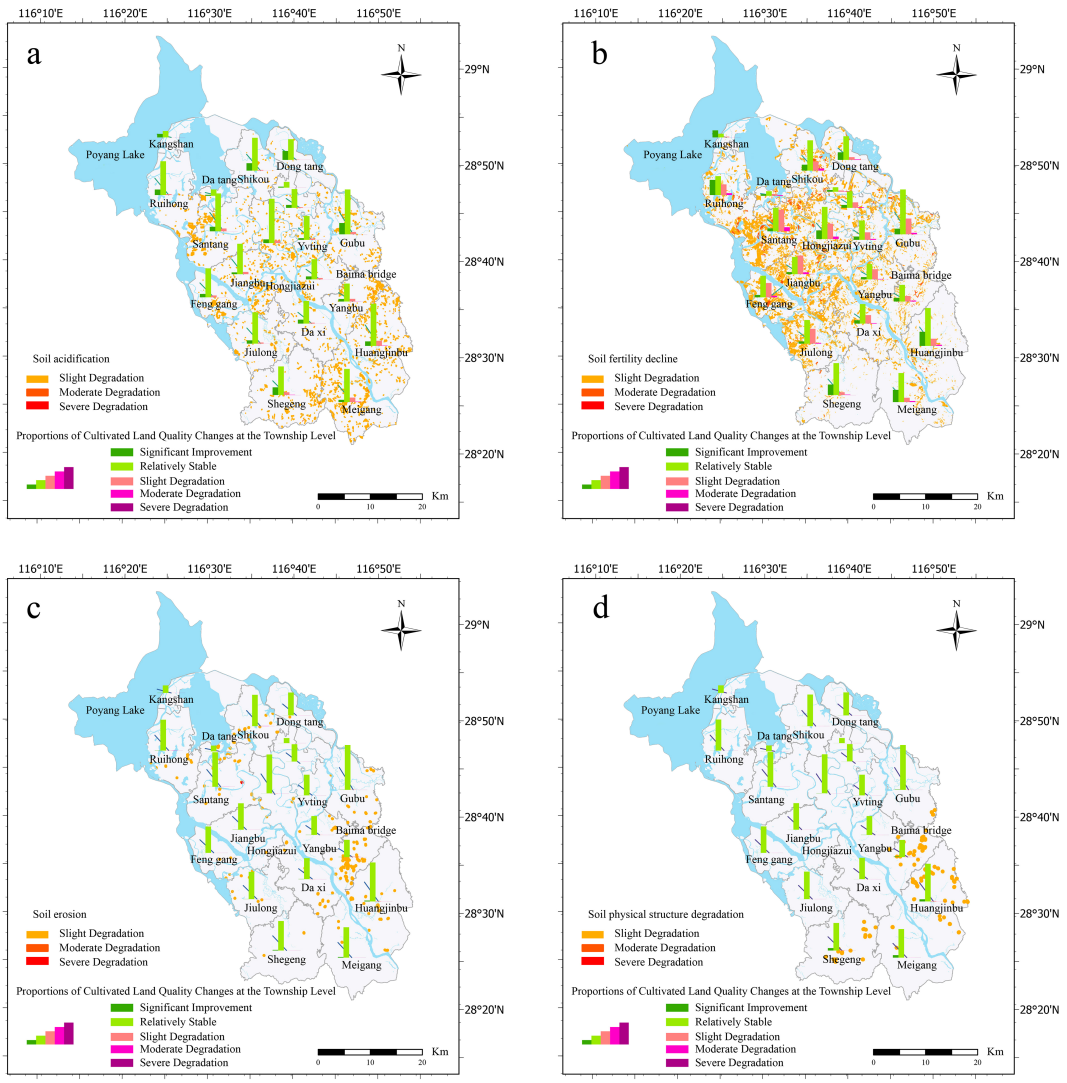

FIGURE 4
Spatial patterns of degradation levels categorized by degradation types **(A)** soil acidification, **(B)** soil fertility decline, **(C)** soil erosion, and **(D)** soil physical structure degradation.

Although the overall distribution was small, it had significant impacts in localized areas (Figure 4C). In contrast, the area of soil erosion was limited, and the degree of degradation was relatively mild. The physical structure of the soil was degraded to the least extent and was mainly distributed in the southern hilly area, with a relatively scattered and limited range (Figure 4D). Comprehensive analysis showed that fertility decline in the central part and soil acidification in the south were the most prominent problems, whereas the impacts of soil erosion and physical structure degradation were more localized.

3.3 Drivers influencing the cultivated land quality degradation

In this study, 11 factors influencing the degradation of cultivated land quality were systematically selected, encompassing five dimensions: topography, climate, geographic location, socio-economic conditions, and agricultural management practices. After the VIF test (VIF < 5) for the 11 factors, it was confirmed that there was no multicollinearity problem for these independent variables. On this basis, the influence characteristics of each driving variable on the degradation of comprehensive quality of cultivated land and different cultivated land quality degradation types were analyzed by the SHAP value interpretive method, and the results are shown in Figure 5 and Figure 6. The target variable for this study is the score for a particular type of degradation, where an increase in the score indicates mitigation of degradation and vice versa. For example, an increase in the soil acidification score mitigates acidification, whereas a decrease in the score intensifies acidification.

By analyzing the SHAP values, this study revealed the main factors influencing the degradation of each type of cultivated land. Overall, MAP and agricultural management factors had significant effects on the different types of degradation but the drivers of each degradation type differed. For soil acidification, MAP was the most important mitigating factor, and its increase significantly reduced the

10.3389/fpls.2025.1533855

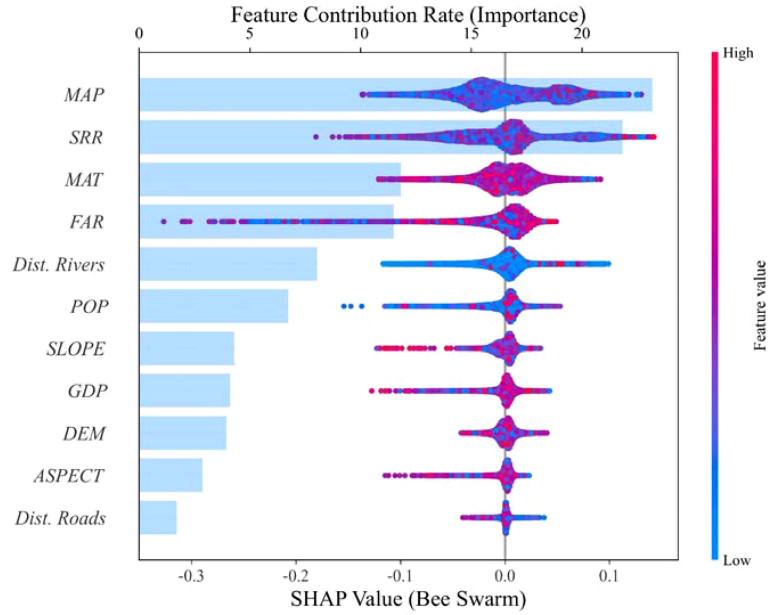

FIGURE 5
Importance ranking of impact factors based on LGB-SHAP mode.

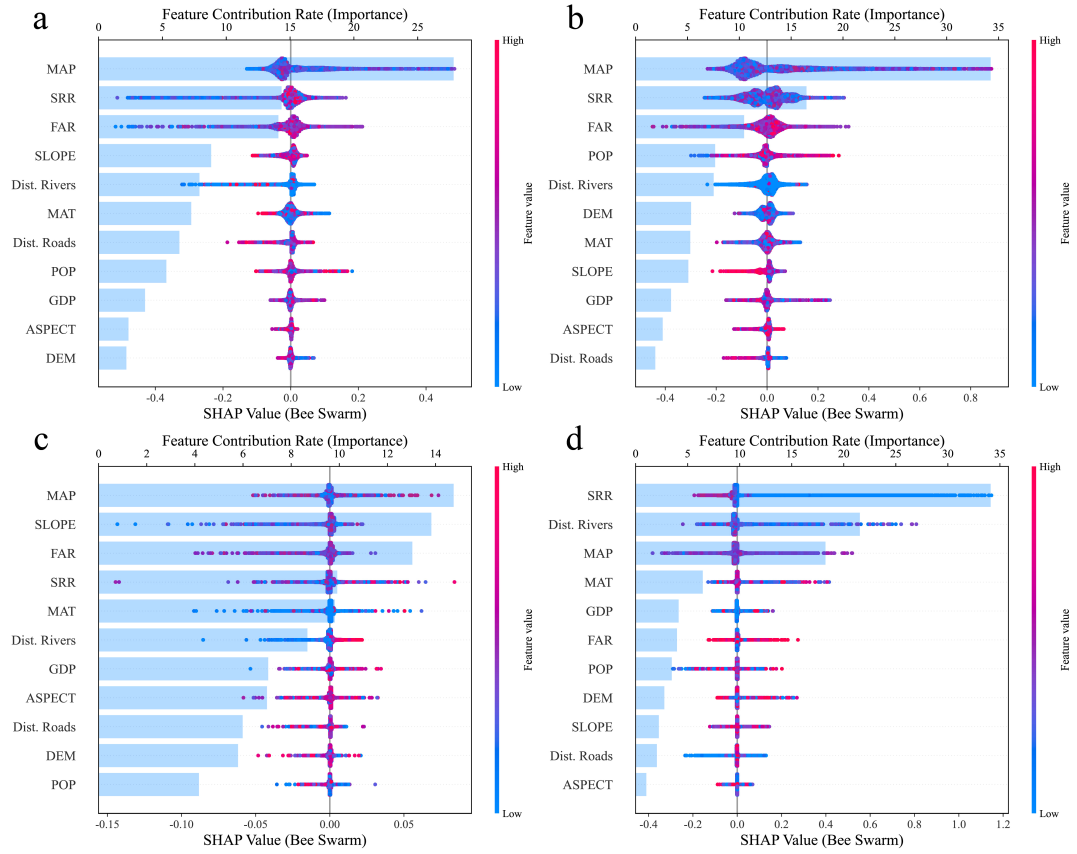

FIGURE 6
Importance ranking of impact factors for different degradation types based on the LGB-SHAP model **(A)** spatial distribution of soil acidification, **(B)** spatial distribution of soil fertility decline, **(C)** spatial distribution of soil erosion, and **(D)** spatial distribution of soil physical structure degradation.

acidification risk, whereas the excessive application of fertilizers exacerbated the acidification process. The fertility decline was mainly driven by precipitation and straw return rate, both of which increased to help mitigate the fertility decline, whereas excessive fertilizer application exacerbated this problem. Soil erosion was mainly affected by slope, with larger slopes exacerbating erosion; however, appropriate increases in annual precipitation and rational fertilizer use helped to mitigate it. The degradation of the soil physical structure was more mitigated by the straw return rate; however, it tended to be exacerbated in areas with greater slopes and the degradation was more pronounced farther away from the river. Changes in the overall cultivated land quality were also positively correlated with precipitation and straw return rate but excessive fertilizer application negatively affected the overall quality.

4 Discussion

4.1 Tendency of cultivated land quality degradation

This study indicates that cultivated land in the Poyang Lake area is facing a series of degradation risks, including soil acidification, soil fertility decline, soil erosion and soil physical structure degradation, a finding that is consistent with existing research. For example, Zeng et al. conducted a spatial assessment of farmland soil pollution across China, revealing similar degradation trends in other regions, such as a decline in soil fertility and the accumulation of heavy metals, which may lead to significant ecological and health risks (Zeng et al., 2019). In the Poyang Lake area, the long-term application of chemical fertilizers has led to a decline in soil organic matter content, looser and less stable soil structure, and fertility decline (Liu et al., 2023). Excessive use of nitrogen and phosphorus fertilizers breaks the acid-base balance of the soil, which affects the healthy growth of the crops and increases the risk of soil acidification (Huang et al., 2012). Intensive land use in areas with high precipitation and complex terrain has led to the destruction of vegetation and degradation of the soil physical structure, triggering serious soil erosion and nutrient loss (Yuan et al., 2016; Zhang et al., 2021b). These issues are further corroborated by Zeng et al., who highlighted the widespread challenges of soil fertility decline and contamination across China (Zeng et al., 2019). If these issues are not addressed, they could lead to a series of environmental and socio-economic problems, including water eutrophication (Cai et al., 2017), acid rain, and a decline in crop yields (Zhang et al., 2021a), which would severely impact both the environment and local livelihoods. This study further highlights that the most prominent risk in the region is the degradation of arable land fertility, which poses a significant threat to sustainable agriculture. Given the urgency of this issue, it is critical to implement nature-based solutions (NbS) and other adaptive management strategies to mitigate the negative impacts and restore soil health.

4.2 Drivers influencing cultivated land quality degradation

The mean annual precipitation, straw return rate, and fertilizer application rate exhibited important effects on various types of cultivated land quality degradation. High precipitation exacerbates soil erosion, especially on slopes or in areas where soil and water conservation measures have not been implemented. Precipitation in the Poyang Lake Basin is concentrated during the rainy season and its complex topography makes precipitation-induced erosion a serious problem (Chen et al., 2020). Under excessive precipitation, topsoil is easily washed away, leading to the loss of soil organic matter and nutrients, a gradual decline in soil fertility, and destruction of the physical structure of the soil, making it loose and unstable (Zhan et al., 2023). In addition, precipitation affects the acid-base balance of the soil and can exacerbate soil acidification, especially under the condition of long-term application of nitrogen fertilizer (Guo et al., 2018). Higher precipitation increases the risk of nutrient loss, especially soluble nutrients, such as nitrogen and phosphorus, which are more likely to be leached by rainfall into groundwater or discharged into river systems, weakening soil fertility (Siddique et al., 2020). In terms of soil structure, excessive precipitation leads to the dispersion of soil particles, weakening the water-holding and carrying capacity of the soil, making it more susceptible to erosion, and thus accelerating the degradation of the physical structure of the soil (Jin et al., 2021).

Straw returning can increase soil organic matter content, improve soil structure, and alleviate soil acidification (Hu et al., 2023b). Straw returning strengthens the carbon and nitrogen cycles and increases soil microbial activity, thus enhancing the water and fertilizer retention capacity of the soil and reducing the risk of soil erosion (Shi et al., 2022). In addition, straw returning can reduce the dependence on chemical fertilizers and the associated problems stemming from their overuse, including increased soil degradation (Wang et al., 2023b) and acidification and decreased soil fertility (Islam et al., 2023).

Runoff and leaching transport excess fertilizer nutrients into water bodies, aggravating eutrophication and pollution problems (Zhang et al., 2021a). To address overfertilization, fertilizer management strategies such as soil testing and formulation have been developed. Precise fertilization plans can reduce the waste of chemical fertilizers and alleviate soil acidification and water pollution (Smith and Siciliano, 2015). Appropriate farmland management practices, such as the combination of straw return and rotational cropping systems, can also significantly improve soil health and promote the sustainable use of arable land (Zhang et al., 2024b).

This study found that the effect of river distance on the degradation of soil physical structure in the Poyang Lake area was particularly significant, supporting the results of past studies (Yuan et al., 2016; Li et al., 2021a). Simultaneously, population growth had a significant effect on the fertility decline of arable land, which was observed in past studies (Bao et al., 2021; Liu et al., 2021).

4.3 NbS measures for addressing the degradation of cultivated land quality

Vegetation-based cultivated land restoration solutions offer ecologically friendly and economically feasible strategies for addressing cultivated land degradation by optimizing vegetation selection and management (Feng et al., 2022). These solutions leverage the ecological functions and regulatory capacities of vegetation to effectively mitigate various types of soil degradation (Seddon et al., 2020). In the Poyang Lake region, such approaches have shown significant potential and effectiveness in tackling key challenges, including soil acidification, soil fertility decline, soil erosion, and soil structural degradation (Zhang et al., 2023b).

Soil acidification, the prominent degradation issue in the Poyang Lake region, often results from prolonged fertilizer use and acid rain. In this context, Cerda et al. (Spain) found that planting acid-tolerant species and employing vegetative cover are essential for mitigating soil acidification. For example, in acidic soils, *Lolium perenne* and *Trifolium repens* improve soil microbial activity and enhance buffering capacity through root exudates (Cerdà et al., 2022). Furthermore, straw incorporation has proven to be a highly effective strategy for neutralizing acidic soils. Research shows that applying 6–10 tons of straw per hectare significantly raises soil pH and increases the availability of calcium and magnesium ions. This method chemically balances soil acidity through the release of organic carbon and carbonate ions during straw decomposition (Chen et al., 2023). Such integrated vegetation management strategies provide a scientific foundation for the sustainable development of agriculture in the region.

Cultivated land fertility decline, largely caused by long-term monocropping and nutrient overexploitation, remains a critical issue. A typical approach is to plant cover crops, such as legumes like *Medicago sativa* and *Trifolium repens*, which, by forming symbiotic relationships with rhizobia, significantly increase soil nitrogen content and improve microbial activity in the soil (Lal, 2022). Furthermore, implementing crop rotation and intercropping systems, such as alternating leguminous crops with cereal crops, effectively alleviates nutrient depletion caused by monoculture practices and promotes nutrient cycling (Zhang et al., 2016). Studies in the Poyang Lake region indicate that incorporating 6–10 tons of straw per hectare, combined with moderate nitrogen fertilization (30–50 kg/ha), can substantially increase soil organic matter and enzyme activity, thereby enhancing nutrient availability. This practice releases significant amounts of nutrients during straw decomposition while optimizing microbial community structure, effectively restoring soil fertility (Lin et al., 2017; Hu et al., 2023a).

Soil erosion presents a major challenge for sloped cultivated lands in the Poyang Lake region, particularly during the rainy season. Vegetative buffer strips, an essential vegetation-based solution, effectively reduce surface runoff and soil erosion. The research conducted in the Poyang Lake region showed that using vegetative buffer strips with species such as *Salix* spp. and *Phragmites australis* along sloped cultivated lands not only reduces sediment loss but also contributes to stabilizing soil structure (Huang et al., 2023b). Similarly, straw mulching has proven highly effective in preventing soil erosion. Studies reveal that applying 6–8 tons of straw per hectare can reduce soil erosion rates by 35%–50% (Xing et al., 2023). In southern China, deep-rooted plants such as *Medicago sativa* significantly improve soil infiltration and stability, reduce erosion and enhance water retention and utilization efficiency (Xie et al., 2022). Additionally, *Robinia pseudoacacia*, used as a biological barrier, provides effective runoff interception and enhances soil stability on sloped lands through its deep-root system and dense canopy (Pan et al., 2024).

Soil physical structural degradation, characterized by compaction, reduced porosity, and poor aeration, significantly impairs root growth and water circulation. In the Poyang Lake region, planting deep-rooted crops like *Brassica napus* and *Beta vulgaris* effectively addresses these issues. The deep roots of these crops penetrate compacted layers, improving aggregate stability and enhancing soil aeration and water retention (Zhang et al., 2014). Additionally, incorporating biochar derived from straw into the soil has emerged as an innovative solution. This practice not only increases soil porosity and water retention but also creates favorable habitats for microorganisms, further enhancing soil ecological functionality (Xu et al., 2021). These solutions provide a scientific pathway for restoring heavily degraded cultivated land in the Poyang Lake region while underscoring the critical role of vegetation in soil health management.

In conclusion, vegetation-based natural solutions fundamentally improve soil health and ecosystem service capacity through scientific vegetation management (Qiu et al., 2024). From employing cover crops to enhance fertility to utilizing deep-rooted plants and straw incorporation technologies to improve soil structure, these strategies highlight the central role of vegetation in mitigating cultivated land degradation. Additionally, straw incorporation, as a circular utilization of vegetative resources, demonstrates comprehensive benefits in enhancing soil fertility, alleviating acidification, and stabilizing soil structure. Moving forward, integrating digital agriculture technologies and region-specific management strategies will be crucial for optimizing these solutions and achieving greater ecological and economic benefits.

4.4 Study limitations

While this study advanced the understanding of cultivated land quality degradation risks and drivers in the Poyang Lake area, there were some limitations. First, although the use of LightGBM and SHAP improved the accuracy to a certain extent, these models have limitations in capturing complex nonlinear relationships and may fail to comprehensively reflect all potential influencing factors. In addition, key variables, such as socioeconomic factors, were not fully incorporated into the analytical framework, which may have led to the limited comprehensiveness of some of the findings. Furthermore, the data and indicators used in this study may have some measurement errors, and the accuracy of the soil's physical and chemical properties may have been affected by differences in local monitoring methods. Therefore, future studies should consider expanding the scope of data collection, incorporating more variables, and exploring different analytical models to

comprehensively reveal the complex mechanisms of cultivated land quality degradation.

5 Conclusions

This study analyzed cultivated land quality degradation in Yugan County, examining the spatial distribution characteristics of different degradation types and their driving factors using remote sensing, GIS technologies, LightGBM, and SHAP. The results revealed significant spatial differences in cultivated land return degradation, with fertility decline being particularly serious. The mean annual precipitation, straw return rate, and chemical fertilizer application rate were the main driving factors of cultivated land quality degradation. The degree of soil acidification was higher in the central and southern hilly areas and lower in the northern lakeshore plains. Fertility decline was especially obvious in the central area and along the rivers and lakes, soil erosion was mainly concentrated in the southern hilly areas with larger slopes, and soil physical structure degradation was concentrated in the southern hilly areas but with a fragmented distribution and relatively small influence.

This study not only reveals the spatial pattern of cultivated land quality degradation in Yugan County but also provides a scientific foundation for understanding the primary drivers of different types of degradation. These findings offer valuable guidance for the development of regional strategies for cultivated land unprotection and degradation management, particularly in addressing acidification and fertility decline in the central and southern parts of Yugan County to promote the sustainable development of regional agriculture.

Data availability statement

The original contributions presented in the study are included in the article/supplementary material. Further inquiries can be directed to the corresponding author.

Author contributions

YL: Formal analysis, Supervision, Writing – original draft, Writing – review & editing. ZY: Data curation, Writing – original draft, Formal analysis. LK: Funding acquisition, Methodology, Software, Writing – review & editing. YJ: Supervision, Writing – review & editing, Methodology. CY: Methodology, Writing – review & editing, Resources, Software. WL: Investigation, Supervision, Validation, Writing – review & editing. ML: Writing – review & editing, Funding acquisition, Methodology. XG: Writing – review & editing, Conceptualization, Investigation, Resources. YY: Conceptualization, Writing – review & editing, Funding acquisition, Supervision, Writing – original draft.

Funding

The author(s) declare financial support was received for the research, authorship, and/or publication of this article. This research received funding from the National Agricultural Science and Technology Major Project (Grant No. NK2022180101), Jiangxi Province Social Science “14th Five-Year Plan” (2024) Fund Project (Grant No. 24GL36), the National Key R&D Program of China (Grant No.2023YFD1900300).

Conflict of interest

The authors declare that the research was conducted in the absence of any commercial or financial relationships that could be construed as a potential conflict of interest.

Generative AI statement

The author(s) declare that no Generative AI was used in the creation of this manuscript.

Publisher’s note

References

Bao, B., Jiang, A., Jin, S., and Zhang, R. (2021). The evolution and influencing factors of Total factor productivity of grain production environment: evidence from Poyang Lake Basin, China. *Land* 10, 606. doi: 10.3390/LAND10060606

Blanco-Canqui, H. (2024). Assessing the potential of nature-based solutions for restoring soil ecosystem services in croplands. *Sci. Total. Environ.* 897, 164525. doi: 10.1016/j.scitotenv.2024.164525

Bouslihim, Y., John, K., Miftah, A., Azmi, R., Aboutayeb, R., Bouasria, A., et al. (2024). The effect of covariates on Soil Organic Matter and pH variability: a digital soil mapping approach using random forest model. *Ann. GIS.* 30, 215–232. doi: 10.1080/19475683.2024.2309868

Cai, S., Shi, H., Pan, X., Liu, F., Cui, Y., and Xie, H. (2017). Integrating ecological restoration of agricultural non-point source pollution in poyang lake basin in China. *Water* 9 (10), 745–760. doi: 10.3390/w9100745

Cerdà, A., Franch-Pardo, I., Novara, A., Sannigrahi, S., and Rodrigo-Comino, J. (2022). Examining the effectiveness of catch crops as a nature-based solution to mitigate surface soil and water losses as an environmental regional concern. *Earth Syst Environ.* 6 (1), 29–44. doi: 10.1007/s41748-021-00284-9

Chen, X., Liang, Z., and Zhang, L. (2020). Effects of soil and water conservation measures on runoff and sediment yield in red soil slope farmland under natural rainfall. *Sustainability* 12, 3417. doi: 10.3390/su12083417

Chen, S., Zhang, G., and Wang, C. (2023). Effects of straw-incorporation rate on runoff and erosion on sloping cropland of black soil region. *Agricult. Ecosyst. Environ.* 346, 108901. doi: 10.1016/j.agee.2023.108901

Cohen-Shacham, E., Walters, G., Janzen, C., and Maginnis, S. (2016). *Nature-based Solutions to Address Global Societal Challenges* (Gland, Switzerland: IUCN).

Debele, S. E., Leo, L. S., Kumar, P., Sahani, J., Young, S., and Soulis, E. D. (2023). Nature-based solutions can help reduce the impact of natural hazards: A global analysis of NBS case studies. *Sci. Total. Environ.* 858, 159233. doi: 10.1016/j.scitotenv.2023.165824

Du, H., Yang, Q., Ge, A., Zhao, C., Ma, Y., and Wang, S. (2024). Explainable machine learning models for early gastric cancer diagnosis. *Sci. Rep.* 14, 17457. doi: 10.1038/s41598-024-67892-z

Fan, Y., Jin, X., Gan, L., Yang, Q., Wang, L., Lyu, L., et al. (2023). Exploring an integrated framework for "dynamic-mechanism-clustering" of multiple cultivated land functions in the Yangtze River Delta region. *Appl. Geogr.* 159, 103061. doi: 10.1016/j.apgeog.2023.103061

FAO (2021). *The State of Food Security and Nutrition in the World 2021*. (Rome, Italy: Food and Agriculture Organization of the United Nations).

FAO (2022). *The State of the World's Land and Water Resources for Food and Agriculture*. (Rome, Italy: Food and Agriculture Organization of the United Nations).

Feng, J., Xu, Q., and Zhang, T. (2022). Evaluating the effects of vegetation and wetland restoration on soil erosion control. *Ecol. Indic.* 135, 108564. doi: 10.1016/j.ecolind.2022.108564

Fernández-Ugalde, O., Virto, I., Bescansa, P., Imaz, M. J., Enrique, A., and Karlen, D. L. (2009). No-tillage improvement of soil physical quality in calcareous, degradation-prone, semiarid soils. *Soil Tillage. Res.* 106, 29–35. doi: 10.1016/j.still.2009.09.012

Ferreras, L. A., Costa, J. L., Garcia, F. O., and Pecorari, C. (2000). Effect of no-tillage on some soil physical properties of a structural degraded Petrocalcic Paleudoll of the southern "Pampa" of Argentina. *Soil Tillage. Res.* 54, 31–39. doi: 10.1016/S0167-1987(99)00102-6

Gaitán, J. J., Bran, D., Oliva, G., Ciari, G., Nakamatsu, V., and Salomone, J. (2013). Evaluating the performance of multiple remote sensing indices to predict the spatial variability of ecosystem structure and functioning in Patagonian steppes. *Ecol. Indic.* 26, 108–117. doi: 10.1016/j.ecolind.2013.05.007

García-Orenes, F., Guerrero, C., Mataix-Solera, J., Navarro-Pedre, O. J., Gómez, I., and Mataix-Beneyto, (2005). Factors controlling the aggregate stability and bulk density in two different degraded soils amended with biosolids. *Soil Tillage. Res.* 82, 65–76. doi: 10.1016/j.still.2004.06.004

Gong, H., Sun, Y., Shu, X., and Huang, B. (2018). Use of random forests regression for predicting IRI of asphalt pavements. *Construction. Building. Mater.* 189, 890–897. doi: 10.1016/j.conbuildmat.2018.09.017

Guo, X., Li, H., and Yu, H. (2018). Drivers of spatio-temporal changes in paddy soil pH in Jiangxi Province, China from 1980 to 2010. *Sci. Rep.* 8, 20873. doi: 10.1038/s41598-018-20873-5

Han, J. W., Kim, T., Lee, S., Kang, T., and Im, J. K. (2024). Machine learning and explainable AI for chlorophyll-a prediction in Namhan River Watershed, South Korea. *Ecol. Indic.* 166, 112361. doi: 10.1016/j.ecolind.2024.112361

Han, X., and Song, Y. (2019). Using GIS and multi-temporal remote sensing data to assess soil erosion and salinization. *Environ. Sci. Technol.* 53, 3581. doi: 10.1021/acs.est.9b00312

He, Q., Li Liu, D., Wang, B., Wang, Z., Cowie, A., Simmons, A., et al. (2024). A food-energy-water-carbon nexus framework informs region-specific optimal strategies for agricultural sustainability. *Resources. Conserv. Recycling.* 203, 107428. doi: 10.1016/j.resconrec.2024.107428

He, L., Zhang, Q., Chen, F., Tang, F., Wang, F., and Liang, K. (2020). The trade-offs and synergies of ecosystem services in Jiulianshan National Nature Reserve in Jiangxi Province, China. *Forests* 11, 1203. doi: 10.3390/f11070732

Hillel, D. (1998). *Environmental Soil Physics* (San Diego, CA: Academic Press).

Hu, B., Ni, H., Xie, M., Li, H., Wen, Y., and Chen, S. (2023a). Mapping soil organic matter and identifying potential controls in the farmland of Southern China. *Land. Degradation. Dev.* 34, 25–36. doi: 10.1002/ldr.4858

Hu, B., Xie, M., Li, H., He, R., Zhou, Y., Jiang, Y., et al. (2023b). Climate and soil management factors control spatio-temporal variation of soil nutrients and soil organic matter in the farmland of Jiangxi Province in South China. *J. Soils. Sediments.* 23, 2373–2395. doi: 10.1007/s11368-023-03471-5

Huang, X., Li, Y., Lin, H., Wen, X., Liu, J., Yuan, Z., et al. (2023b). Flooding dominates soil microbial carbon and phosphorus limitations in Poyang Lake wetland, China. *CATENA* 232, 107468. doi: 10.1016/j.catena.2023.107468

Huang, L., Shao, Q., and Liu, J. (2012). Forest restoration to achieve both ecological and economic progress, Poyang Lake basin, China. *Ecol. Eng.* 44, 53–60. doi: 10.1016/j.ecoleng.2012.03.007

Huang, W., Suominen, H., Liu, T., Rice, G., Salomon, C., and Barnard, A. (2023a). Explainable discovery of disease biomarkers: The case of ovarian cancer to illustrate the best practice in machine learning and Shapley analysis. *J. Biomed. Inf.* 141, 104365. doi: 10.1016/j.jbi.2023.104365

Hussain, S., Raza, A., Abdo, H. G., Mubeen, M., and Tariq, A. (2023). Relation of land surface temperature with different vegetation indices using multi-temporal remote sensing data in Sahiwal region, Pakistan. *Geosci. Lett.* 10, 87–97. doi: 10.1186/s40562-023-00287-6

Intergovernmental Panel on Climate, C (2019). *Climate Change and Land: An IPCC Special Report on Climate Change, Desertification, Land Degradation, Sustainable Land Management, Food Security, and Greenhouse Gas Fluxes in Terrestrial Ecosystems*. (Geneva, Switzerland: IPCC).

Islam, M. U., Jiang, F., Halder, M., Liu, S., and Peng, X. (2023). Impact of straw return combined with different fertilizations on soil organic carbon stock in upland wheat and maize croplands in China: A meta-analysis. *Crop Environ.* 2, 233–241. doi: 10.1016/j.crope.2023.10.003

Jain, N., and Jana, P. K. (2023). LRF: A logically randomized forest algorithm for classification and regression problems. *Expert Syst. Appl.* 213, 119225. doi: 10.1016/j.eswa.2022.119225

Jin, Q., Peñuelas, J., Sardans, J., Romero, E., Chen, S., Liu, X., et al. (2021). Changes in soil carbon, nitrogen, and phosphorus contents, storages, and stoichiometry during land degradation in jasmine croplands in subtropical China. *Exp. Agric.* 57, 113–125. doi: 10.1017/S0014479721000089

Keesstra, S., Nunes, J., Novara, A., Finger, D., Avelar, D., Kalantari, Z., et al. (2018). The superior effect of nature-based solutions in land management for enhancing ecosystem services. *Sci. Total. Environ.* 610–611, 997–1009. doi: 10.1016/j.scitotenv.2017.08.077

Kimetu, J. M., Lehmann, J., Ngoze, S. O., Mugendi, D. N., Kinyangi, J. M., Riha, S., et al. (2008). Reversibility of soil productivity decline with organic matter of differing quality along a degradation gradient. *Ecosystems* 11, 726–739. doi: 10.1007/S10021-008-9154-Z

Lal, R. (2020). Carbon sequestration in agricultural ecosystems. *J. Soil Water Conserv.* 75, 38A–40A. doi: 10.2489/jswc.75.2.38A

Lal, R. (2022). Nature-based solutions of soil management and agriculture. *J. Soil Water Conserv.* 77, 23A. doi: 10.2489/jswc.2022.0204A

Li, Q., Lai, G., and Devlin, A. T. (2021a). A review on the driving forces of water decline and its impacts on the environment in Poyang Lake, China. *J. Water Climate Change* 12, 1370–1391. doi: 10.2166/WCC.2020.216

Li, X., Zhang, L., and Liu, J. (2021b). Climate change and its impact on soil erosion in the poyang lake region: A case study. *J. Environ. Manage.* 281, 111888. doi: 10.1016/j.jenvman.2020.111888

Lin, S., Wang, S., Si, Y., Yang, W., Zhu, S., and Ni, W. (2017). Variations in eco-enzymatic stoichiometric and microbial characteristics in paddy soil as affected by long-term integrated organic-inorganic fertilization. *PloS One* 12, e0189908. doi: 10.1371/journal.pone.0189908

Liu, S., Sun, Y., Liu, Y., and Wang, F. (2021). Effects of landscape features on the roadside soil heavy metal distribution in a tropical area in southwest China. *Appl. Sci.* 11, 1408. doi: 10.3390/app11041408

Liu, S., Zhang, W., and Chen, J. (2023). Soil health challenges and opportunities in the red soil regions of southern China. *J. Cleaner. Production.* 387, 137659. doi: 10.1016/j.jclepro.2023.137659

Lokker, C., Abdelkader, W., Bagheri, E., Parrish, R., Cotoi, C., Navarro, T., et al. (2024). Boosting efficiency in a clinical literature surveillance system with LightGBM. *PloS Digital. Health* 3, e0000299. doi: 10.1371/journal.pdig.0000299

McLenaghen, R., Malcolm, B., Cameron, K., Di, H., and McLaren, R. (2017). Improvement of degraded soil physical conditions following the establishment of permanent pasture. *Comput. Electron. Agric.* 60, 287–297. doi: 10.1080/00288233.2017.1334668

Mei, S., Tong, T., Zhang, S., Ying, C., Tang, M., Zhang, M., et al. (2024). Optimization study of soil organic matter mapping model in complex terrain areas: A case study of mingguang city, China. *Sustainability* 16, 4312. doi: 10.3390/su16104312

Miralles-Wilhelm, F. (2021). *Nature-based solutions in agriculture: Sustainable management and conservation of land, water, and biodiversity* (Cham, Switzerland: Springer).

Morgan, R. P. C. (2005). *Soil Erosion and Conservation* (Oxford, UK: Wiley-Blackwell).

Nguemezi, C., Tematio, P., Yemefack, M., Tsozue, D., and Silatsa, T. B. F. (2020). Soil quality and soil fertility status in major soil groups at the Tombel area, South-West Cameroon. *Heliyon* 6 (2), e03432. doi: 10.1016/j.heliyon.2020.e03432

Nguyen, T. T., Grote, U., Neubacher, F., Do, M. H., and Paudel, G. P. (2023). Security risks from climate change and environmental degradation: Implications for sustainable land use transformation in the Global South. *Curr. Opin. Environ. Sustainabil.* 63, 101322. doi: 10.1016/j.cosust.2023.101322

Omuto, C. (2008). Assessment of soil physical degradation in Eastern Kenya by use of a sequential soil testing protocol. *Agric. Ecosyst. Environ.* 128, 199–211. doi: 10.1016/j.agee.2008.06.006

Pan, L., Shi, D., Jiang, G., and Xu, Y. (2024). Management measures on soil nutrients and stoichiometric characteristics for sloping farmland under erosive environments. *Soil Tillage. Res.* 245, 104338. doi: 10.1016/j.still.2024.104338

Peng, S. (2019). *1-km monthly mean temperature dataset for China, (1901-2021)* (Beijing, China: Ecological Data Center of Sanjiangyuan National Park). doi: 10.11888/Meteoro.tpdc.270961

Peng, S. (2024). *1-km monthly precipitation dataset for China, (1901-2023)* (Beijing, China: National Tibetan Plateau Data Center). doi: 10.5281/zenodo.3114194

Prăvălie, R., Borrelli, P., and Panagos, P. (2024). A unifying modelling of multiple land degradation pathways in Europe. *Nat. Commun.* 15 (1), 3862–3875. doi: 10.1038/s41467-024-48252-x

Qiu, T., Shi, Y., Penuelas, J., Liu, J., Cui, Q., Sardans, J., et al. (2024). Optimizing cover crop practices as a sustainable solution for global agroecosystem services. *Nat. Commun.* 15 (1), 10617–10632. doi: 10.1038/s41467-024-54536-z

Seddon, N., Chausson, A., and Berry, P. (2020). Nature-based solutions: A powerful means of mitigating and adapting to climate change. *Nat. Climate Change* 10, 590. doi: 10.1038/s41558-020-0802-8

Sharma, N., Khan, M. A., Dubey, P., Pandey, C. N., Kumar, S., and Jain, V. (2024). Soil carbon storage and greenhouse gas fluxes in forested and grassland ecosystems of Gujarat undergoing anthropogenic and climatic disturbances. *EGU General Assembly 2024*, Vienna, Austria, EGU24–19605. doi: 10.5194/egusphere-egu24-19605

Sheykhmousa, M., Mahdianpari, M., Ghanbari, H., Mohammadimanesh, F., Ghamisi, P., and Homayouni, S. (2020). Support vector machine versus random forest for remote sensing image classification: A meta-analysis and systematic review. *IEEE J. Selected. Topics. Appl. Earth Observ. Remote Sens.* 13, 6308–6325. doi: 10.1109/JSTARS.2020.3026724

Shi, Y., Zhang, Q., Liu, X., Jing, X., Shi, C., and Zheng, L. (2022). Organic manure input and straw cover improved the community structure of nitrogen cycle function microorganism driven by water erosion. *Int. Soil Water Conserv. Res.* 10, 129–142. doi: 10.1016/j.iswcr.2021.03.005

Siddique, M. N. E. A., De Bruyn, L. L., and Guppy, C. N. (2020). Temporal variations of soil organic carbon and pH at landscape scale and the implications for cropping intensity in rice-based cropping systems. *Agronomy* 11, 59. doi: 10.3390/agronomy11010059

Smith, L. E. D., and Siciliano, G. (2015). A comprehensive review of constraints to improved management of fertilizers in China and mitigation of diffuse water pollution from agriculture. *Agricult. Ecosyst. Environ.* 209, 15–25. doi: 10.1016/j.agee.2015.01.010

Smith, J., and Wang, Y. (2020). An evaluation of guided regularized random forest for classification and regression tasks in remote sensing. *J. Appl. Geospatial. Inf.* 55, 102–115. doi: 10.1016/j.jag.2020.102051

Su, H., Liu, F., Zhang, H., Ma, X., and Sun, A. J. S. (2024). Progress and Prospects of non-grain production of cultivated land in China. *Sustainability* 16, 3517. doi: 10.3390/su16093517

Sušnik, J., Masia, S., Kravčík, M., Pokorný, J., and Hesslerová, P. (2022). Costs and benefits of landscape-based water retention measures as nature-based solutions to mitigating climate impacts in eastern Germany, Czech Republic, and Slovakia. *Land. Degradation. Dev.* 33 (16), 3074–3087. doi: 10.1002/ldr.4373

Tang, H., Niu, Z., Cheng, F., Niu, J., Zhang, L., Guo, M., et al. (2023). Can we prevent irreversible decline? A comprehensive analysis of natural conditions and quality factor thresholds of cultivated land in China. *Land* 12 (9), 1669–1685. doi: 10.3390/land12091669

Wang, Y., Liang, B., Bao, H., Chen, Q., Cao, Y., and He, Y. (2023b). Potential of crop straw incorporation for replacing chemical fertilizer and reducing nutrient loss in Sichuan Province, China. *Environ. pollut.* 313, 120739. doi: 10.1016/j.envpol.2023.120739

Wang, M., Shen, K., Tai, C., Zhang, Q., Yang, Z., and Guo, C. (2023a). Research on fault diagnosis system for belt conveyor based on internet of things and the LightGBM model. *PloS One* 18, e0277352. doi: 10.1371/journal.pone.0277352

Wang, Y., Zhou, L., and Li, X. (2020). Impact of soil degradation on agricultural productivity and food security in southern China. *Agric. Syst.* 179, 103028. doi: 10.1016/j.agsy.2020.103028

Wang, S., Zhou, M., Zhuang, Q., and Guo, L. (2021). Prediction potential of remote sensing-related variables in the topsoil organic carbon density of liaohekou coastal wetlands, northeast China. *Sustainability* 13, 4106. doi: 10.3390/rs13204106

Wei, J., Li, Z., Pinker, R. T., Wang, J., Sun, L., Xue, W., et al. (2021). Himawari-8-derived diurnal variations in ground-level PM 2.5 pollution across China using the fast space-time Light Gradient Boosting Machine (LightGBM). *Atmospheric. Chem. Phys.* 21, 7863–7880. doi: 10.5194/acp-2020-1277

Xie, Z., Shah, F., and Zhou, C. (2022). Combining rice straw biochar with leguminous cover crop as green manure and mineral fertilizer enhances soil microbial biomass and rice yield in south China. *Front. Plant Sci.* 13. doi: 10.3389/fpls.2022.778738

Xing, S., Zhang, G., Wang, C., Chen, S., Zhang, N., Li, L., et al. (2023). Effects of straw incorporation on soil erosion resistance along a land degradation gradient in the black soil region of China. *Catena* 229, 107194. doi: 10.1016/j.catena.2023.107365

Xu, X. (2017). China GDP Spatial Distribution Kilometer Grid Dataset. Available online at: http://www.resdc.cn/DOI.

Xu, J., Wang, X., Liu, J., Xiong, L., Xu, L., and Hu, C. (2021). The influence of water regime on cadmium uptake by Artemisia: A dominant vegetation in Poyang Lake wetland. *J. Environ. Manage.* 297, 113258. doi: 10.1016/j.jenvman.2021.113258

Yadav, D. S., Jaiswal, B., Gautam, M., and Agrawal, M. (2020). "Soil acidification and its impact on plants," in *Plant responses to soil acidification* (Cham, Switzerland: Springer).

Yan, K., Gao, S., Chi, H., Qi, J., Song, W., Tong, K., et al. (2021). Evaluation of the vegetation-index-based dimidiate pixel model for fractional vegetation cover estimation. *IEEE Trans. Geosci. Remote Sens.* 60 (1), 1–14. doi: 10.1109/TGRS.2020.3048493

Yuan, L., Yang, G., Zhang, Q., and Li, H. (2016). Soil erosion assessment of the poyang lake basin, China: using USLE, GIS and remote sensing. *J. Remote Sens. GIS.* 5 (3), 168. doi: 10.4172/2469-4134.1000168

Zeng, S., Ma, J., Yang, Y., Zhang, S., Liu, G.-J., and Chen, F. (2019). Spatial assessment of farmland soil pollution and its potential human health risks in China. *Sci. Total. Environ.* 687, 642–653. doi: 10.1016/j.scitotenv.2019.05.291

Zhan, M., Wu, Q., Zhan, L., and Xin, J. (2023). Change in extreme precipitation events: Exposure and vulnerability in the Poyang Lake Basin, China. *Front. Earth Sci.* 11. doi: 10.3389/feart.2023.1125837

Zhang, P., Chen, X., Wei, T., Yang, Z., Jia, Z., Yang, B., et al. (2016). Effects of straw incorporation on the soil nutrient contents, enzyme activities, and crop yield in a semiarid region of China. *Soil Tillage. Res.* 160, 65–72. doi: 10.1016/j.still.2016.02.006

Zhang, Y., Guo, L., Chen, Y., Shi, T., Luo, M., Ju, Q., et al. (2019). Prediction of soil organic carbon based on Landsat 8 monthly NDVI data for the Jianghan Plain in Hubei Province, China. *Remote Sens.* 11, 1683. doi: 10.3390/rs11141683

Zhang, Q., Xiao, M., Singh, V.P., and Wang, Y. (2016). Spatiotemporal variations of temperature and precipitation extremes in the Poyang Lake basin, China. *Theor Appl Climatol.* 124, 855–864. doi: 10.1007/s00704-015-1470-6

Zhang, B., Salem, F. K. A., Hayes, M. J., Smith, K. H., Tadesse, T., and Wardlow, B. D. (2023a). Explainable machine learning for the prediction and assessment of complex drought impacts. *Sci. Total. Environ.* 898, 165509. doi: 10.1016/j.scitotenv.2023.165509

Zhang, C., Su, G., and Li, X. (2021a). Nutrient runoff and its impact on Poyang Lake's eutrophication. *Water* 15, 3304. doi: 10.3390/w15183304

Zhang, L., Wei, D., and Chen, M. (2023b). Strategies for reducing soil erosion in sloping areas through ecological approaches. *J. Environ. Manage.* 319, 115676. doi: 10.1016/j.jenvman.2023.115676

Zhang, P., Wei, T., Jia, Z., and Chen, X. (2014). Soil aggregate and crop yield changes with different rates of straw incorporation in semiarid areas of northwest China. *Geoderma* 230, 41–49. doi: 10.1016/j.geoderma.2014.11.002

Zhang, Y., Wu, J., Liang, L., Li, M., Huang, Z., and Zhou, P. (2024). Dynamic monitoring of grassland vegetation degradation based on multi-source data. In *Proceedings of the 2024 12th International Conference on Agro-Geoinformatics (Agro-Geoinformatics)*, 1–6. doi: 10.1109/Agro-Geoinformatics262780.2024.10661035

Zhang, Z., Zhao, Z., Tian, M., Jiang, D., Qiu, Z., and Miao, X. (2024b). Crop rotation shapes the fungal rather than bacterial community for enhanced straw degradation. *SSRN. Electronic. J.* doi: 10.2139/ssrn.4727924

Zheng, Y., Zhang, X., and Li, J. (2019). Urbanization and its impact on agricultural land use in the Poyang Lake region. *Landscape Urban. Plann.* 189, 165–173. doi: 10.1016/j.landurbplan.2019.04.009

Zhou, Z., Qiu, C., and Zhang, Y. (2023). A comparative analysis of linear regression, neural networks and random forest regression for predicting air ozone employing soft sensor models. *Sci. Rep.* 13, 22420. doi: 10.1038/s41598-023-49899-0

frontiers | Frontiers in Plant Science

TYPE Original Research
PUBLISHED 12 March 2025
DOI 10.3389/fpls.2025.1518721

OPEN ACCESS

EDITED BY
Jingxue Zhao,
Lanzhou University, China

REVIEWED BY
Fuhong Miao,
Qingdao Agricultural University, China
Jialuo Yu,
Chinese Academy of Sciences (CAS), China

*CORRESPONDENCE
Shurong Zhang
srzhang@bnu.edu.cn

RECEIVED 28 October 2024
ACCEPTED 21 February 2025
PUBLISHED 12 March 2025

CITATION
Zhan T, Zhang S and Zhao W (2025) Adaptive management for alpine grassland of the Tibetan Plateau based on a multi-criteria assessment. *Front. Plant Sci.* 16:1518721. doi: 10.3389/fpls.2025.1518721

Adaptive management for alpine grassland of the Tibetan Plateau based on a multi-criteria assessment

Tianyu Zhan[1,2], Shurong Zhang[1,2*] and Wenwu Zhao[1,2]

[1]State Key Laboratory of Earth Surface Processes and Resource Ecology, Faculty of Geographical Science, Beijing Normal University, Beijing, China, [2]Institute of Land Surface System and Sustainable Development, Faculty of Geographical Science, Beijing Normal University, Beijing, China

With the increasing threats of global climate change and human activities to terrestrial ecosystems, understanding the quality of alpine grassland ecosystems and their influencing factors is fundamental for effective ecosystem management and improving human well-being. However, current adaptive management plans for alpine grasslands based on multi-criteria assessment are limited. This study utilized field investigations at 77 sampling points, drone remote sensing, and satellite remote sensing data to construct an alpine grassland quality index based on vegetation and soil indicators, and assess the ecosystem's resilience and pressure. The assessment revealed that the alpine grasslands of the Tibetan Plateau were classified into five zones, indicating significant differences in quality and pressure levels. Key findings showed that the High-Quality Pressure Zone comprise 41.88% of the area of alpine meadow and 31.89% of alpine steppe, while the Quality Improvement-Limitation Zone account for 21.14% and 35.8% of the respective areas. The study recommends graded protection and recovery strategies for alpine grasslands based on quality levels: prioritizing high-quality grasslands, implementing dynamic monitoring and enhancement for moderate-quality grasslands, and applying artificial interventions and suitable species for low-quality grasslands. This research underscores the importance of zoning-based adaptive strategies for sustainable ecosystem management and provides valuable insights for effective management and protection of alpine grasslands in the Tibetan Plateau.

KEYWORDS

adaptive management, zone, multi-criteria, alpine grassland, Tibetan Plateau

1 Introduction

Climate change (Gao et al., 2014) and grazing activities (Lu et al., 2017) are significant driving forces influencing alpine grassland ecosystems, especially in high-altitude regions where sensitivity and vulnerability are heightened (Li et al., 2020b; Wang et al., 2024a). These impacts have led to substantial declines in grassland quality, exacerbating

biodiversity loss (Li et al., 2018b), soil erosion (Li et al., 2019), and reduced carbon sequestration capacity (Wang et al., 2023), representing a pressing global environmental challenge (Dong et al., 2020). In addition to their ecological functions, alpine grasslands play important societal roles, such as supporting grazing and providing livelihoods for local communities (Wang et al., 2024b). Therefore, systematic ecosystem restoration and conservation measures are crucial to enhancing the quality of alpine grasslands (Harzé et al., 2018). This is not merely a local ecological concern but a vital component of global ecological health.

Traditional management paradigms for alpine grasslands primarily focus on static objectives, often guided by a single indicator, such as forage yield (Loucougaray et al., 2015) or vegetation biomass (Jäger et al., 2020), and lack comprehensive consideration of the dynamic changes within the ecosystem (Dong et al., 2022). While this approach may effectively enhance short-term productivity, it frequently overlooks the complexity and diversity of the ecosystem (Chapin et al., 2010), leading to resource overexploitation and ecological imbalance (Zhou et al., 2023). In light of the complexities associated with changes in alpine grassland quality, a singular management strategy is clearly inadequate. Researchers have proposed the adoption of a multi-criteria comprehensive assessment approach to better understand and address the dynamic changes in alpine grassland ecosystems (Villoslada et al., 2018; Grilli et al., 2017). Therefore, the restoration and conservation of alpine grassland quality require two key decision-making foundations: (1) the current state of alpine grassland quality; and (2) the external pressures faced by alpine grasslands (such as climate change and grazing activities) and its resilience.

In response to the increasing complexity and challenges faced by alpine grasslands, resilience theory has provided a new perspective for managing these fragile ecosystems (Yang et al., 2022; Ji et al., 2024). Adaptive management, as a key application of resilience theory, provides a dynamic and responsive framework for conservation and restoration efforts (Stoffels et al., 2024; Garmestani et al., 2023). This approach emphasizes the unique characteristics and evolving conditions of alpine grasslands, allowing for continuous adjustments to management strategies (Wang et al., 2022). Addressing the ongoing pressures from climate change and intensive grazing requires a more comprehensive and environment-specific management framework (Shang et al., 2014). While various restoration techniques, such as fertilization (Jiang et al., 2013), reseeding (Tian et al., 2023), and grazing exclusion (Sun et al., 2020), have been applied in the alpine grassland ecosystems of the Tibetan Plateau, these methods often face challenges. Natural recovery processes remain sluggish (Zhen et al., 2018), and artificial restoration approaches can be technically demanding and resource-intensive (Dong et al., 2015). Furthermore, the short-term benefits of these interventions are limited, with uncertainties surrounding their long-term efficacy and sustainability (Sun et al., 2024; Zhu et al., 2023). Therefore, it is imperative to develop a context-specific management framework that integrates restoration techniques into a coherent strategy, tailored to the unique environmental conditions of alpine grasslands. The significant spatial heterogeneity of alpine grassland ecosystems across different regions further limits the effectiveness of generic management practices, which often fail to adapt to diverse environmental conditions (Wang et al., 2020). A more integrated management framework is essential—one that addresses the distinct types of alpine grasslands while incorporating their current ecological status, external pressures, and intrinsic resilience.

To address these challenges, adaptive zoning management has emerged as a promising regional planning method (Wang et al., 2022). This approach involves implementing tailored regulatory measures for different spatial areas, acknowledging the unique ecological functions and characteristics of each zone (Jiang et al., 2024). For instance, China's ecological protection red lines classify regions according to the significance of their ecological functions into ecological red line zones and both important and generally important ecological functional areas (Bai et al., 2018). Different zones have varying ecological protection policies. Recent studies on grassland adaptive zoning demonstrate that it is essential to fully consider the impacts of climate change and human activities, highlighting the necessity of effective management strategies (Wang et al., 2022). By recognizing and responding to the inherent variability among alpine grasslands, zoning adaptive management can facilitate more effective conservation strategies that cater to local ecological dynamics.

The TP serves as a vital ecological security barrier in China, playing a critical role in maintaining regional and global environmental stability (Liu et al., 2021). Understanding the current quality, resilience, and external pressures of alpine grassland ecosystems is essential for implementing adaptive management practices tailored to different zones, thereby ensuring the sustainable development of these environments (Huber et al., 2013). This study aims to address the aforementioned challenges by (1) integrating quantitative assessments of alpine grassland quality, resilience, and external pressures to support planning and decision-making, and (2) providing zoning-based conservation and restoration strategies specific to alpine grasslands.

2 Materials and methods

2.1 Study area

Our sampling sites covered the TP, primarily including regions in Tibet, Qinghai Province, and northwestern Sichuan Province (Supplementary Figure S1). Within an altitude range of 3000 to 5000 meters, a grassland transect approximately 5000 kilometers long was sampled for vegetation and soil across the main grasslands of the TP. The transect sample plots were natural zonal grasslands, including alpine meadow (AM) and alpine steppe (AS). A total of 77

Abbreviations: TP, Tibetan Plateau; AM, alpine meadow; AS, alpine steppe; GQI, Grassland Quality Index; LQZ, Low-Quality Zone; QILZ, Quality Improvement-Limited Zone; QRPZ, Quality Restoration Potential Zone; HQSZ, High-Quality Stable Zone; HQPZ, High-Quality Pressure Zone.

sample plots were collected from the alpine grasslands, including 49 AM plots and 28 AS plots (Supplementary Figure S1).

2.2 Date collection

2.2.1 Field data

Field surveys were conducted during the peak vegetation growth periods of 2021 and 2022 (i.e., between July and August) in various alpine grasslands on the TP, with priority given to areas with uniform vegetation distribution. Sample plots were chosen based on a stratified random sampling method to ensure representativeness across the different vegetation types within the study area. In each selected sample plot, three large quadrats of 30×30 meters were established to record detailed plot attributes. To assess the structure and functional characteristics of the vegetation community, 0.5×0.5m subplots were randomly located within each quadrat. At each site, aboveground biomass was obtained by clipping all vegetation within the selected subplots at ground level using scissors. Soil samples were collected using a soil auger with a diameter of 5 cm at depths of 0-10 cm, 10-20 cm, and 20-30 cm. To minimize the risk of mold in plant samples, species identification and preliminary drying of all samples were completed within 48 hours after collection for subsequent laboratory analysis. Roots were washed free of soil residues with clean water, then dried in an oven at 65°C for about 48 hours until a constant weight was achieved to determine belowground biomass. Plant diversity indices, including the Shannon-Wiener index, Simpson's index, and Pielou's index, were calculated using standard methods. Soil bulk density and moisture content were measured using the ring knife method and drying method, respectively. Specifically, soil samples obtained by the ring knife method were first weighed fresh, then dried in an oven at 105°C for 24 hours until a constant weight was reached. Soil organic carbon content was determined using the potassium dichromate oxidation-external heating method, total nitrogen content was measured by the sulfuric acid-hydrogen peroxide digestion-semi-micro Kjeldahl method (Standard NY/T 2419-2013), and total phosphorus content was determined by the sulfuric acid-hydrogen peroxide digestion-molybdenum antimony anti-colorimetry method (Standard DB37/T 1625-2010). Soil available nitrogen was measured by the alkali-hydrolyzed diffusion method, available phosphorus by the molybdenum antimony anti-colorimetry method, and soil pH was determined using a portable soil tester (TDR 100, Spectrum Technologies Inc., Chicago, USA).

2.2.2 UAV remote sensing

The multispectral remote sensing images used in this study were acquired by the DJI Phantom 4 Multispectral drone (DJI-P4M, DJI Technology Co., Ltd., Shenzhen, China). The DJI-P4M is equipped with an integrated multispectral imaging system, which includes one visible light sensor and five multispectral sensors. These sensors cover three visible light bands, one red-edge band, and one near-infrared band. The central wavelengths of the imaging bands are as follows: blue band (450nm ± 16nm), green band (560nm ± 16nm), red band (650nm ± 16nm), red-edge band (730nm ± 16nm), and near-infrared band (840nm ± 26nm). Each sensor has a resolution of 2 megapixels and uses the same global shutter. The entire system is mounted on a 3-axis gimbal. Before data collection, gray card photographs were taken for radiometric calibration, with data collection scheduled between 12:00 and 16:00 to ensure optimal lighting conditions. For calibration and validation of the UAV data, three 50 cm × 50 cm PVC plates with black and white crisscross lines were utilized as positioning plates, evenly laid on the ground in each landscape. The center point of each PVC plate was designated as the image control point, allowing for the accurate recording of latitude and longitude information. To enhance data validity, flight path planning was completed using DJI GS PRO software. The flight area was set to 200m × 200m, with forward and side overlap rates of 90% and 70%, respectively. Data collection was conducted at a flight altitude of 100m with a nadir view angle of 90°.

The raw UAV aerial survey image data were processed indoors to produce usable product data. Initially, the raw images were manually inspected to remove invalid images taken during takeoff and landing. The valid flight data were then processed using Agisoft Photoscan software for stitching and calibration to generate orthomosaic images. The actual sample plot size was 50cm × 50cm, and the spatial resolution of the UAV multispectral images was 3.1cm. Three small sample plots were used to represent a larger plot, and the raster data corresponding to the larger plot were statistically analyzed. Vegetation indices were extracted from the data points by clipping the corresponding large plots. Vegetation indices (VIs) are common and effective indicators in remote sensing ecological studies (Glenn et al., 2008; Xue and Su, 2017). This study utilized five multispectral bands, namely blue, green, red, red-edge, and near-infrared (NIR). Numerous vegetation indices based on these multispectral bands have been constructed and widely used. These indices have proven effective in monitoring plant growth and ecosystem characteristics. In this study, 42 vegetation indices, incorporating the B, G, R, RE, and NIR bands, were selected for the inversion of alpine grassland quality at the landscape scale (Supplementary Table S2).

2.2.3 Remote sensing data

The products selected for the inversion of regional alpine grassland quality include NDVI (Normalized Difference Vegetation Index), EVI (Enhanced Vegetation Index), and LAI (Leaf Area Index). The NDVI data, representing vegetation greenness characteristics, were derived from the MODIS Terra MOD13A1 16-day composite data with a resolution of 500 m. The LAI data, representing vegetation cover characteristics, were obtained from the MODIS Terra MOD15A2H product, which provides 8-day composite data with a 500 m spatial resolution. The EVI, indicative of vegetation productivity, was derived from the MODIS Terra MOD13A1 product, which offers 16-day composite data with a 500 m spatial resolution, covering the time frame of August 2021, corresponding to the sampling and UAV aerial photography period.

Vegetation type data were sourced from the 1:1,000,000 scale China Vegetation Type Map provided by the Resource and

Environment Science and Data Center (RESDC) of the Chinese Academy of Sciences (http://www.resdc.cn). Using the vector boundary of the TP, vegetation type data were clipped from the region. By aggregating and extracting similar vegetation types, the spatial distribution ranges of AM and AS on the TP were classified. Air temperature and precipitation data for the growing season (May-September) from January 2001 to December 2020 were selected for this study. These data were sourced from the ERA5-Land dataset. The ERA5-Land data have a temporal resolution of 1 hour and a spatial resolution of 0.1° (Dee et al., 2011). The grazing data were collected from the National Tibetan Plateau Data Center (Liu, 2023). The spatial resolution was 1 km and the temporal resolution was year.

2.3 Data analysis

2.3.1 Grassland quality assessment

In this study, data from field transects were utilized to select 14 vegetation and soil indicators. Principal Component Analysis (PCA) was employed to filter these indicators, subsequently constructing the plot-scale alpine Grassland Quality Index (GQI). The GQI was developed at three scales: plot, landscape, and regional. By using UAV-based multispectral vegetation indices as an intermediary, field survey data of grassland ecosystem communities were integrated with remote sensing ecological parameters. Through statistical analysis and model computation, relationships between parameters across multiple scales were established, thereby enabling the assessment of the GQI at the regional scale.

2.3.1.1 Plot-scale grassland quality index

To quantitatively assess the ecosystem quality of AM and AS, this study adopted a dual methodological framework that combines data on grassland vegetation and soil attributes. First, key indicators that reflect grassland quality were selected through (PCA), including biomass, vegetation cover, diversity, soil organic carbon, total nitrogen, total phosphorus, and soil moisture. These indicators were chosen because they are essential for understanding the health, productivity, and resilience of grassland ecosystems. By integrating these critical factors, we can better assess the overall grassland quality. After selecting the key indicators, a comprehensive GQI was constructed. The GQI integrates multiple ecological indicators into a single index, simplifying the assessment process and providing an intuitive measure of grassland quality. The construction of the GQI involves standardizing each key indicator and assigning corresponding coefficients based on their weights in the PCA to ensure that the contribution of each indicator to the final index is proportionate to its importance in representing grassland quality (Supplementary Table S1).

2.3.1.2 Landscape-scale grassland quality index

To define GQI at the landscape scale, this study employed 42 vegetation indices derived from UAV multispectral imagery as independent variables (Supplementary Table S2), with the plot-scale GQI serving as the dependent variable. A stepwise regression analysis was performed to establish the relationship between the plot-scale GQI and the UAV-derived vegetation indices (Supplementary Table S3). The significance of each variable was assessed using a Random Forest model (Supplementary Figure S2), leading to the formulation of a robust regression relationship for the GQI based on multispectral vegetation indices (Supplementary Table S4).

Multivariate Stepwise Regression (MSR) was utilized to identify the most significant predictors among the selected vegetation indices, involving the iterative addition and removal of variables based on their statistical significance, thus optimizing the model to retain only those variables that substantially explain the variability in grassland quality (Supplementary Table S4). The criteria for variable inclusion and exclusion were based on the Akaike Information Criterion (Ghani and Ahmad, 2010). Building on the insights gained from the stepwise regression, we implemented a Random Forest (RF) model to refine the selection of key vegetation indices (Supplementary Figure S1). The RF algorithm aggregates predictions from multiple decision trees constructed during training, thereby enhancing predictive accuracy and mitigating overfitting. This approach excels in managing the complex interactions between predictor variables (Rigatti, 2017).

To validate the landscape-scale GQI model, seventy percent of the sampling data was designated as the training set, while thirty percent was utilized as the testing set. The model's accuracy was assessed using the coefficient of determination (R^2). The observed values corresponded to the plot-scale GQI, and the predicted values represented the landscape-scale GQI (Supplementary Figure S3).

2.3.1.3 Regional-scale grassland quality index

At the regional scale, the landscape-scale GQI served as the ground truth for further inversion of the regional-scale GQI. Using the GQI as the dependent variable, and NDVI, EVI, and LAI as independent variables, a Partial Least Squares Regression (PLSR) model was constructed (Supplementary Table S5). PLSR combines the advantages of PCA, Canonical Correlation Analysis (CCA), and Multiple Linear Regression (MLR). While PLSR and PCA aim to extract maximum information reflecting data variation, PCA focuses solely on one matrix of independent variables. In contrast, PLSR simultaneously considers the correlations between independent and dependent variables, thereby enhancing predictive capabilities (Geladi and Kowalski, 1986). Overall, the PLSR algorithm effectively mitigates collinearity among variables and optimizes the use of spectral information, resulting in improved modeling accuracy and estimation outcomes (Geladi and Kowalski, 1986). To evaluate the performance of the regional-scale model, leave-one-out cross-validation (LOOCV) was implemented (Supplementary Figure S4) (Kearns and Ron, 1997). The GQI of AM and AS on the TP is categorized into high-quality (HQ), moderate-quality (MQ), and low-quality (LQ) areas based on natural breakpoints.

2.3.2 Resilience assessment

Grassland resilience refers to the ability of grassland ecosystems to recover to their original state after disturbance (Gunderson,

2000). In this study, grassland resilience primarily considers the response of vegetation growth to the rate of climate change. T The methods and data used to assess ecosystem resilience are derived from traditional approaches (Yao et al., 2021), with optimizations made to the linear regression model (Li et al., 2018a). The model can be represented as follows:

$$LAI_t = a*tem_t + b*pre_t + c*LAI_{t-1} + k \quad (1)$$

Where LAI_t, tem_t, pre_t represent the *LAI*, temperature, and precipitation sequences at time *t*, respectively, and LAI_{t-1} denotes the *LAI* value at time *t-1*. The coefficients *a*, *b*, and *c* correspond to temperature, precipitation, and *LAI* from the previous month, with *k* as the regression error. The coefficients a, b, and c were derived through a multiple linear regression analysis, using historical data of LAI, temperature, and precipitation. To ensure comparability and eliminate bias due to differing units, these coefficients are normalized using min-max standardization, transforming their values to a range between 0 and 1.Additionally, using the coefficients *a* and *b* from Equation 1, Equation 2 calculates the sensitivity of the ecosystem to climate variability (Seddon et al., 2016):

$$SI = a*sens(\text{tem}) + b*\text{sens}(\text{pre}) \quad (2)$$

In this context, *SI* represents the sensitivity index, while *sens(tem)* and *sens(pre)* denote the ecosystem's sensitivity to temperature and precipitation changes, quantified through the residuals obtained from linear fits of vegetation variation against temperature and precipitation changes (Seddon et al., 2016). According to Equation 3, we utilize coefficient c to evaluate the recovery capacity of the ecosystem following climate disturbances, indicating that a smaller c value corresponds to stronger recovery capability:

$$RI = 1 - c \quad (3)$$

RI refers to the resilience index of the alpine grassland ecosystem. The resilience of AM and AS on the TP is categorized into high-resilience (HR), moderate-resilience (MR), and low-resilience (LR) areas based on natural breakpoints.

2.3.3 Pressure assessment

Pressure factors, such as grazing, precipitation, and temperature, play a critical role in the protection and restoration of alpine grasslands. In this study, pressure factors were determined by standardizing the grazing, precipitation, and temperature data and then aggregating them. To effectively assess the pressure gradients in different regions, the natural breaks method was employed to categorize the pressure factors of the AM and AS on the TP into high-pressure (HP), moderate-pressure (MP), and low-pressure (LP)areas.

2.4 Zoning basis

Based on the ecological characteristics of the alpine grassland ecosystems on the TP, this study established adaptive zoning management for alpine meadows and alpine steppes. The zoning criteria were based on the natural break method, utilizing key indicators and methodologies derived from vegetation and soil attributes at the plot scale, alongside spatial assessments of grassland quality at the regional scale. The analysis primarily focused on three critical dimensions: grassland quality, resilience, and pressure factors. Using the layers derived from these three individual indicators, the study employed analytical methods such as threshold segmentation and overlay calculations to identify five distinct zone types: Low-Quality Zone (LQZ), Quality Improvement-Limited Zone (QILZ), Quality Restoration Potential Zone (QRPZ), High-Quality Stable Zone (HQSZ), and High-Quality Pressure Zone (HQPZ) (Table 1).

3 Results

3.1 Classification of alpine grassland quality, resilience and pressure

The distribution of grassland quality in the AM of the TP from 2001 to 2020 exhibits significant spatial heterogeneity. LQ meadows, MQ meadows, and HQ meadows account for 33.58%, 34.48%, and 31.93%, respectively. The spatial distribution characteristics show a decreasing trend in the quality of AM from southeast to northwest. In contrast, the spatial distribution characteristics of grassland quality in the AS are markedly different from those in the AM. LQ steppes, MQ steppes, and HQ steppes comprise 3.72%, 40.71%, and 55.57%, respectively. Notably, the quality of AS demonstrates the highest values in the Qiangtang Nature Reserve, with lower quality observed in densely populated areas near Xining and Lhasa (Figure 1). Areas of LR, MR and HR in the AM make up 34.34%, 30.33%, and 35.33%, respectively. Areas of LR, MR and HR in the AS account for 24.48%, 25.70%, and 49.82%, respectively. The resilience overall shows a decreasing trend from north to south: the northern region exhibits the strongest resilience, particularly in the central area of the Qiangtang Nature Reserve (Figure 2). Areas of LP, MP and HP in the AM consist of 31.63%, 34.07%, and 34.29%, respectively. In the AS, areas of LP, MP and HP make up 32.66%, 33.72%, and 33.62%, respectively. HP areas are primarily concentrated in regions with intense human activities, such as Lhasa, Xining, and northern Sichuan, whereas LP areas are mainly distributed within nature reserves (Figure 3).

TABLE 1 Zoning based on grassland quality, resilience, and pressure.

Zone Names	Zoning Basis
Low-Quality Zone (LQZ)	Low quality grassland
Quality Improvement-Limited Zone (QILZ)	Low to moderate resilience grasslands in moderate quality
Quality Restoration Potential Zone (QRPZ)	High resilience grasslands in moderate quality
High-Quality Stable Zone (HQSZ)	Low pressure grasslands in high quality
High-Quality Pressure Zone (HQPZ)	Moderate to high pressure grasslands in high quality

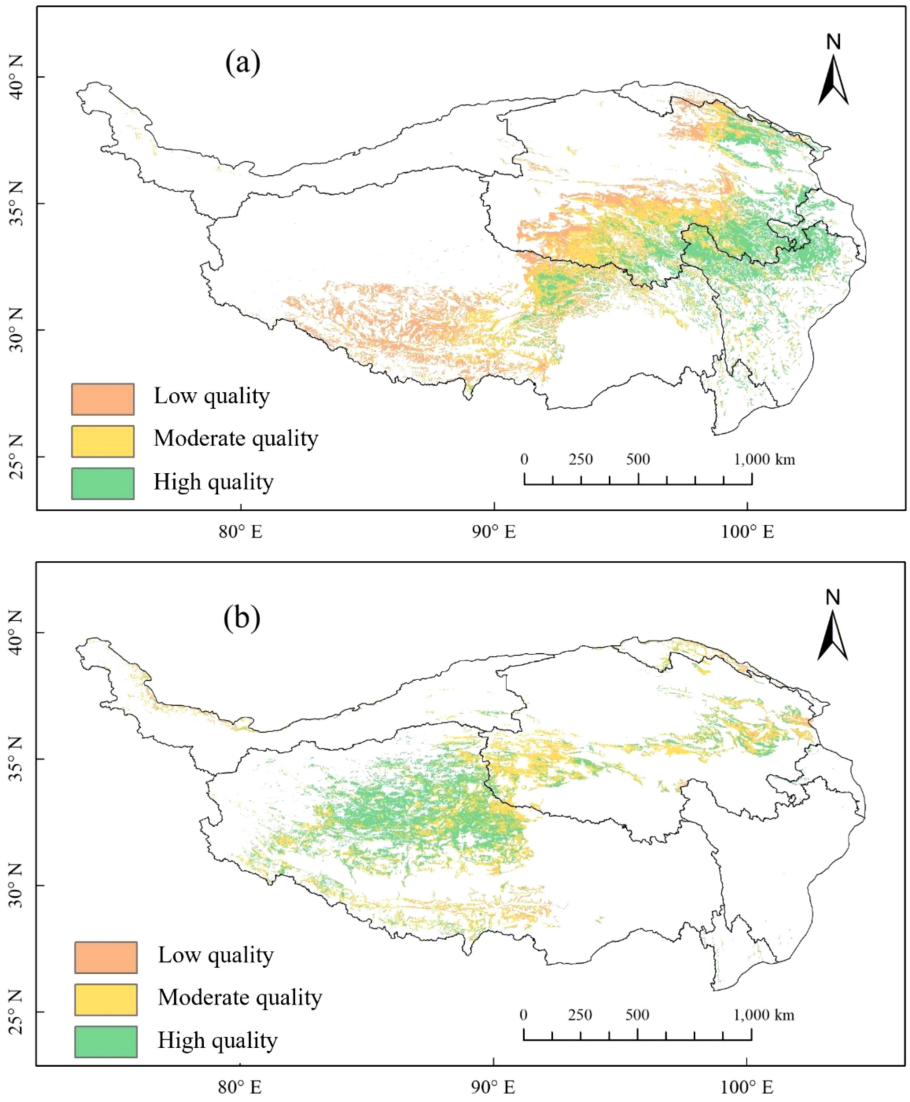

FIGURE 1
Spatial pattern of alpine grassland quality in Tibetan Plateau from 2001-2020: **(a)** alpine meadows; **(b)** alpine steppes.

3.2 Adaptive zoning management of alpine grassland

Based on the dimensions of grassland quality, resilience, and pressure, five distinct zonations were identified for the AM and AS on the TP. For the AM, LQZ account for 24.26%, QILZ account for 21.14%, QRPZ comprise 4.83%, HQSZ make up 7.89%, and HQPZ represent 41.88%. In the case of the AS, LQZ constitute 4.74%, QIlZ make up 35.80%, QRPZ account for 13.39%, HQSZ comprise 14.18%, and HQPZ cover 31.89% (Figure 4). In terms of spatial distribution, QILZ in the AM are mainly found in the Sanjiangyuan region. HQSZ and HQPZ are concentrated in the Qilian Mountain alpine basin. In the AS, HQSZ and HQPZ are primarily located in the Qiangtang Nature Reserve, while the QILZ and QRPZ are spread across the Ali Mountain desert, Qiangtang Nature Reserve, and the Kunlun Mountains.

4 Discussion

The zoning results of this study are consistent with existing research on the spatial heterogeneity of alpine grasslands on the Tibetan Plateau. For instance, previous studies have also emphasized the significant differences in ecological characteristics across different regions (Sun et al., 2023; Li et al., 2020a). This consistency highlights the robustness and applicability of our framework in a broader ecological context. Additionally, the zoning results provide a comprehensive basis for grassland protection and restoration, facilitating a deeper understanding of the patterns and processes governing alpine grassland ecosystems. Based on the zoning results of alpine grasslands, this study proposes a framework of "high-quality protection—moderate-quality enhancement—low-quality restoration," which holds significant value in the protection and restoration of alpine grasslands

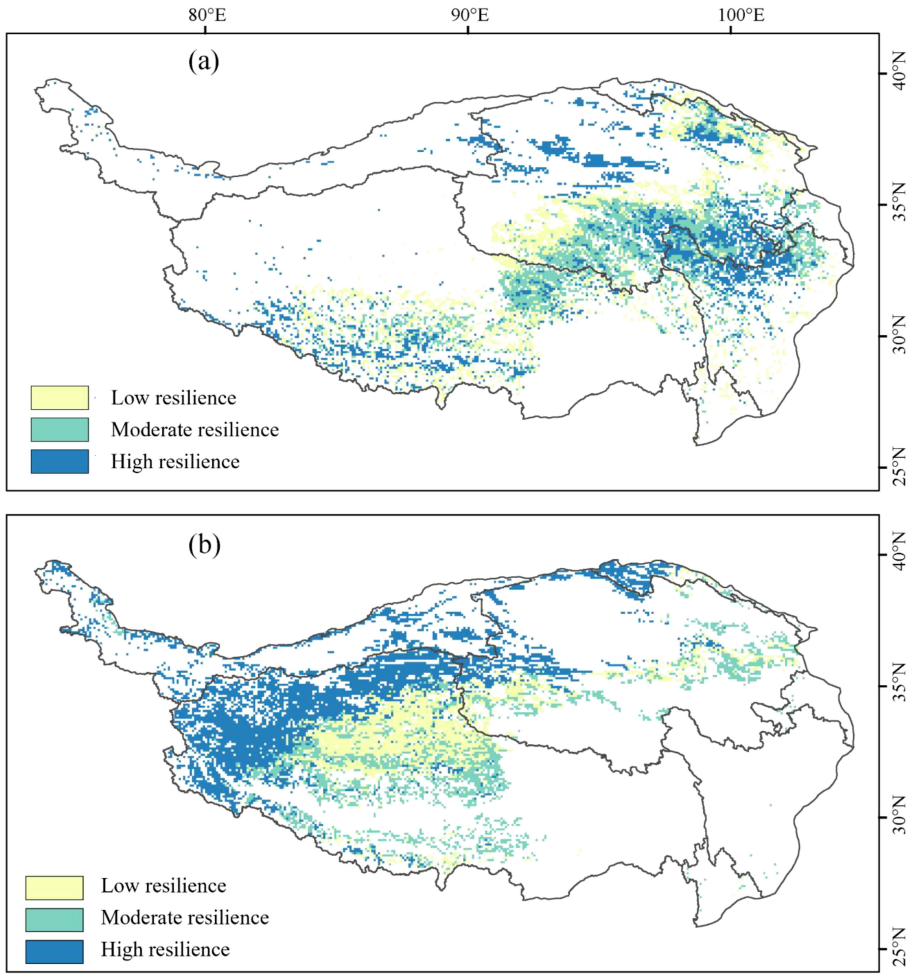

FIGURE 2
Spatial pattern of alpine grassland resilience in Tibetan Plateau from 2001-2020: **(a)** alpine meadows; **(b)** alpine steppes.

(Figure 5). The research findings indicate significant differences in spatial distribution, degradation risks, and more among various quality grades of alpine grasslands (Figure 1), providing theoretical support and guidance for subsequent protection and restoration strategies. Therefore, this study proposes pathways for the protection and restoration of alpine grasslands from the perspective of different quality grades.

Regarding the protection of HQ grasslands, the findings highlight the crucial need to establish ecological fragile zones and nature reserves (Ma and Yang, 2023), with a focus on preserving pristine, uninhabited grasslands. Given the inherent vulnerability and irreparability of grassland ecosystems (Niu et al., 2022), protective measures should adhere to principles of respecting nature and prioritizing conservation, while assessments of the comprehensive value of economic, environmental, and resource aspects, as well as potential ecological negative impacts, are essential during development and utilization phases. Furthermore, science-based grassland protection plans should be formulated based on locational conditions and resource endowments. In particular, for HQSZ, it is crucial to maintain the current state. For HQPZ, vigilance against degradation risks from disruptive factors is necessary, along with the implementation of improved grazing policies to ensure sustainable development.

In terms of MQ grassland enhancement, the research indicates that implementing a dynamic, multifaceted monitoring framework is necessary, employing various methods and scales to advance integrated monitoring and assessment of alpine grassland ecosystems (Akiyama and Kawamura, 2007). Measures for enhancing moderate-quality grasslands should align with natural principles, leveraging Nature-Based Solutions to harness natural recovery benefits and reduce restoration costs. In QRPZ, natural restoration should be prioritized through measures such as natural diffusion, moderate enclosure, soil and water conservation, and maintaining biodiversity. Moreover, the significance of artificial restoration should also be acknowledged. In QILZ, supplementary interventions such as ecological substrate improvement, artificial planting, and localized irrigation are necessary. This study emphasizes the importance of plant species selection and pastoral community involvement in the success of natural recovery processes, asserting that success should not only be measured through vegetation recovery but also by assessing whether the original attributes and structures of the ecosystem have been

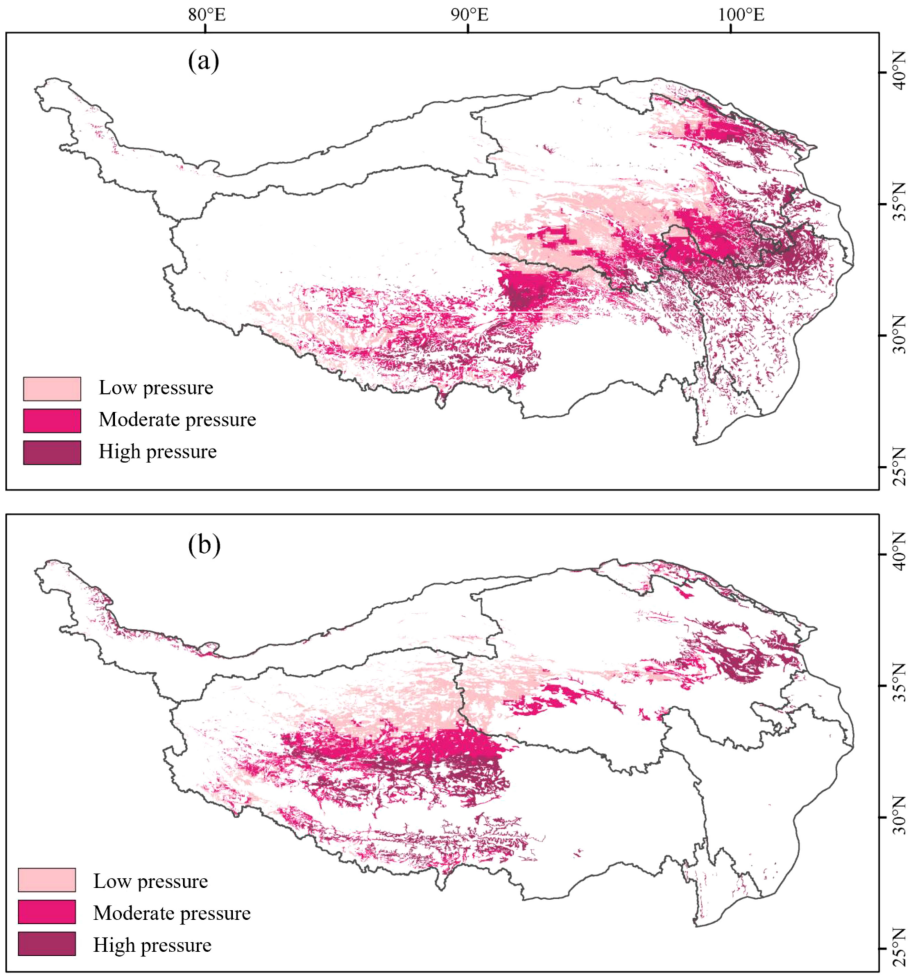

FIGURE 3
Spatial pattern of alpine grassland pressure in Tibetan Plateau from 2001-2020: **(a)** alpine meadows; **(b)** alpine steppes.

restored, thereby fostering natural recovery and achieving a positive feedback loop (Nilsson et al., 2016).

In the context of LQ grassland restoration, referencing HQ grasslands is crucial. The restoration of LQ grasslands should involve cultivating suitable forage species, promoting forage demonstration projects, and developing long-term management plans. When selecting grass species, priorities should be given to those with strong adaptability, drought resistance, and cold tolerance, such as sand *alfafa* and wild barley, to improve vegetation recovery capacity (Porqueddu et al., 2016). Forage demonstration projects can enhance pastoral community engagement and awareness by establishing model sites, implementing windbreaks, and providing various technical training. This study provides specific implementation plans for the restoration of low-quality grasslands, highlighting the synergistic effects of multiple factors as essential for successful restoration. Continuous monitoring, evaluation, and policy support, alongside risk management strategies and ecological service payment mechanisms, are vital for ensuring the long-term effectiveness and sustainable development of grassland restoration. Furthermore, fostering interdepartmental cooperation can ensure information sharing and strategic coordination, optimizing grassland resource management and promoting comprehensive recovery and steady development of grassland ecosystems.

The zoning framework proposed in this study offers a structured approach to managing changes in grassland quality by considering the resilience and pressures of different regions, while adapting to varying environmental conditions. However, the limitations of this framework must also be acknowledged. It relies on current quality assessments, which may not fully capture the temporal ecological dynamics induced by ongoing climate change and anthropogenic pressures. Furthermore, although the framework is adaptive, it has not fully integrated ecological initiatives such as natural grassland protection, grazing reduction, the establishment of Qiangtang National Park, and relocations from extremely high-altitude areas. Thus, future efforts require continuous policy adjustments and localized implementation strategies. Adaptive zoning is closely aligned with Nature-Based Solutions, leveraging natural processes and ecosystem restoration to achieve ecological balance. Through strategic zoning policies that prioritize natural recovery alongside moderate human interventions, this study addresses the degradation of alpine grasslands and contributes to sustainable grassland management practices.

10.3389/fpls.2025.1518721

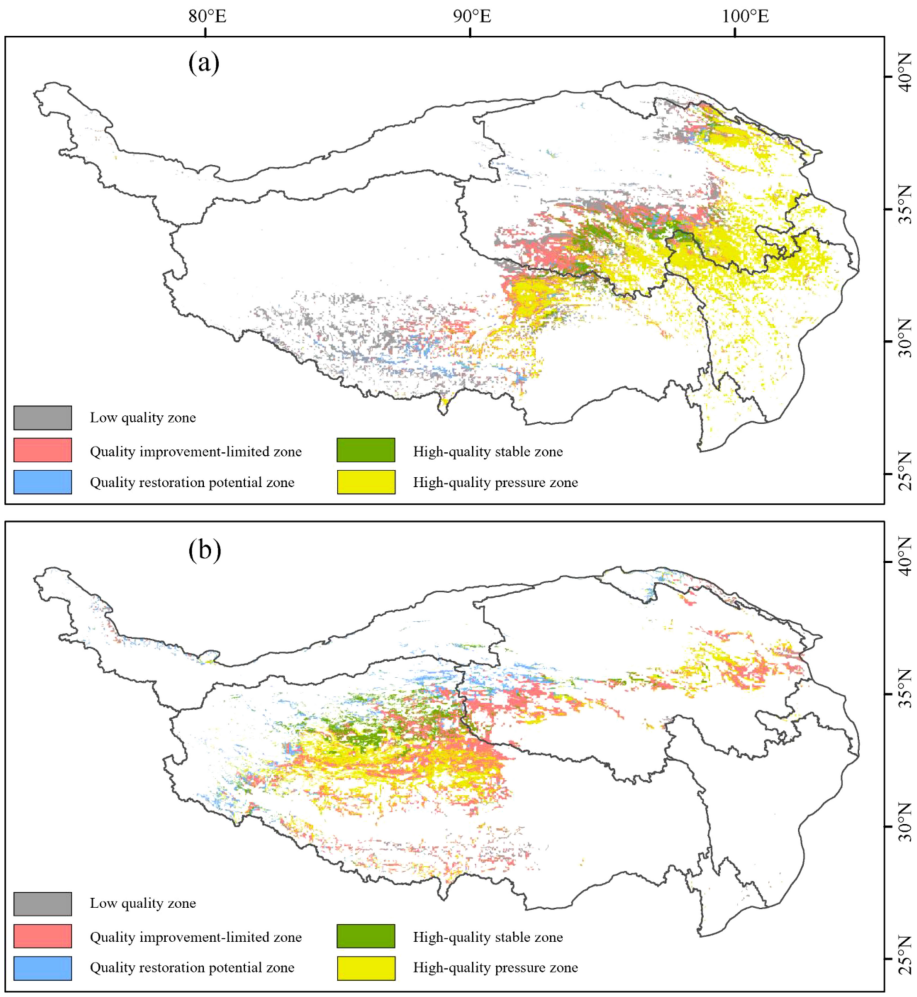

FIGURE 4
Spatial pattern of alpine grassland zoning in Tibetan Plateau: **(a)** alpine meadows; **(b)** alpine steppes.

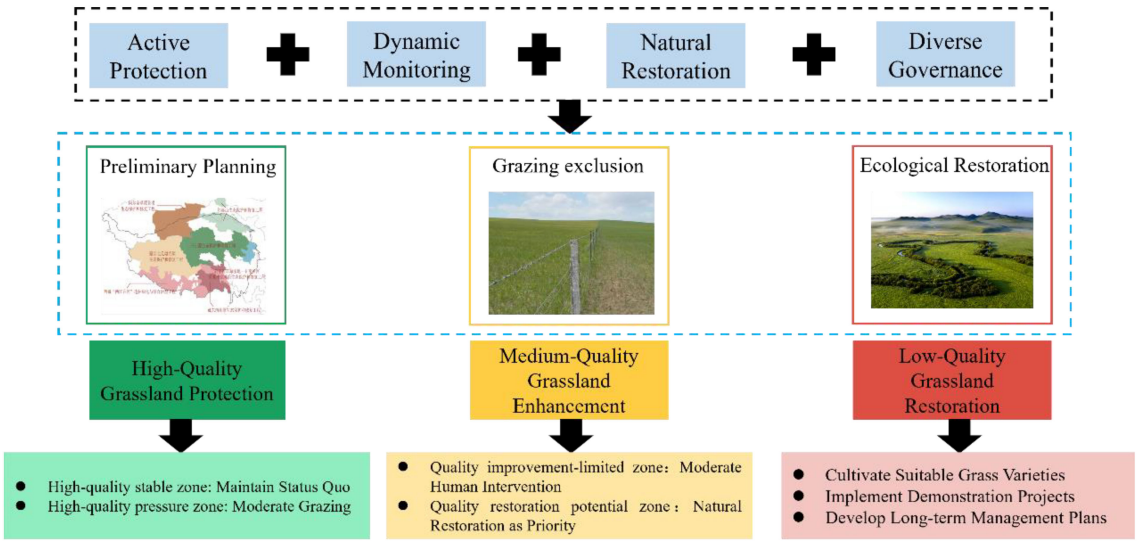

FIGURE 5
Implementation pathways for the protection and restoration of alpine grassland.

5 Conclusion

This study provides a systematic assessment and analysis of the quality, resilience, and pressures of alpine grassland ecosystems, emphasizing the critical role of adaptive zoning management in the protection and restoration of alpine grassland quality. By constructing the alpine grassland quality and evaluating its resilience and pressures, we revealed the spatial heterogeneity of alpine grasslands and proposed specific practical adaptive zoning management strategies tailored for different ecological regions. The results indicate that priority should be given to the protection of high-quality grasslands to prevent ecological degradation. For moderate-quality grasslands, we recommend the implementation of dynamic enhancement measures that promote natural recovery and improve ecological functions. The restoration of low-quality grasslands requires a targeted approach focusing on the introduction of suitable plant species and the establishment of long-term management mechanisms supported by local communities. By clarifying the characteristics and needs of different grassland qualities, this study provides new insights into adaptive management, offering scientific evidence and implementation pathways for the sustainable management of alpine grasslands in the Tibetan Plateau. This aims to effectively address increasingly complex ecological challenges and ensure regional ecological security.

Data availability statement

The data analyzed in this study is subject to the following licenses/restrictions: The data that support the findings of this study are available from the corresponding author upon reasonable request. Requests to access these datasets should be directed to Shurong Zhang srzhang@bnu.edu.cn.

Author contributions

TZ: Writing – original draft, Writing – review & editing. SZ: Data curation, Writing – review & editing, Funding acquisition, Supervision. WZ: Data curation, Writing – original draft, Writing – review & editing, Funding acquisition, Supervision.

Funding

The author(s) declare that financial support was received for the research and/or publication of this article. This research was funded by the National Natural Science Foundation of China (No. 41991232) and the Second Tibetan Plateau Scientific Expedition and Research Program (2019QZKK0405).

Conflict of interest

The authors declare that the research was conducted in the absence of any commercial or financial relationships that could be construed as a potential conflict of interest.

Generative AI statement

The author(s) declare that no Generative AI was used in the creation of this manuscript.

Publisher's note

Supplementary material

The Supplementary Material for this article can be found online at: https://www.frontiersin.org/articles/10.3389/fpls.2025.1518721/full#supplementary-material

References

Akiyama, T., and Kawamura, K. (2007). Grassland degradation in China: methods of monitoring, management and restoration. *Grassland Sci.* 53, 1–17. doi: 10.1111/j.1744-697X.2007.00073.x

Bai, Y., Wong, C. P., Jiang, B., Hughes, A. C., Wang, M., and Wang, Q. (2018). Developing China's Ecological Redline Policy using ecosystem services assessments for land use planning. *Nat. Commun.* 9, 3034. doi: 10.1038/s41467-018-05306-1

Chapin, F. S., Carpenter, S. R., Kofinas, G. P., Folke, C., Abel, N., Clark, W. C., et al. (2010). Ecosystem stewardship: sustainability strategies for a rapidly changing planet. *Trends Ecol. Evol.* 25, 241–249. doi: 10.1016/j.tree.2009.10.008

Dee, D. P., Uppala, S. M., Simmons, A. J., Berrisford, P., Poli, P., Kobayashi, S., et al. (2011). The ERA-Interim reanalysis: Configuration and performance of the data assimilation system. *Q. J. R. meteorological Soc.* 137, 553–597. doi: 10.1002/qj.v137.656

Dong, S., Shang, Z., Gao, J., and Boone, R. B. (2020). Enhancing sustainability of grassland ecosystems through ecological restoration and grazing management in an era of climate change on Qinghai-Tibetan Plateau. *Agriculture Ecosyst. Environ.* 287, 106684. doi: 10.1016/j.agee.2019.106684

Dong, S., Shang, Z., Gao, J., and Boone, R. (2022). Enhancing the ecological services of the Qinghai-Tibetan Plateau's grasslands through sustainable restoration and management in era of global change. *Agriculture Ecosyst. Environ.* 326, 107756. doi: 10.1016/j.agee.2021.107756

Dong, S., Wang, X., Liu, S., Li, Y., Su, X., Wen, L., et al. (2015). Reproductive responses of alpine plants to grassland degradation and artificial restoration in the Qinghai–Tibetan Plateau. *Grass Forage Sci.* 70, 229–238. doi: 10.1111/gfs.2015.70.issue-2

Gao, J.-G., Zhang, Y.-L., Liu, L.-S., and Wang, Z.-F. (2014). Climate change as the major driver of alpine grasslands expansion and contraction: A case study in the Mt. Qomolangma (Everest) National Nature Preserve, southern Tibetan Plateau. *Quaternary Int.* 336, 108–116. doi: 10.1016/j.quaint.2013.09.035

Garmestani, A., Allen, C. R., Angeler, D. G., Gunderson, L., and Ruhl, J. (2023). Multiscale adaptive management of social–ecological systems. *BioScience* 73, 800–807. doi: 10.1093/biosci/biad096

Geladi, P., and Kowalski, B. R. (1986). Partial least-squares regression: a tutorial. *Analytica chimica Acta* 185, 1–17. doi: 10.1016/0003-2670(86)80028-9

Ghani, I. M. M., and Ahmad, S. (2010). Stepwise multiple regression method to forecast fish landing. *Procedia-Social Behav. Sci.* 8, 549–554. doi: 10.1016/j.sbspro.2010.12.076

Glenn, E. P., Huete, A. R., Nagler, P. L., and Nelson, S. G. (2008). Relationship between remotely-sensed vegetation indices, canopy attributes and plant physiological processes: What vegetation indices can and cannot tell us about the landscape. *Sensors* 8, 2136–2160. doi: 10.3390/s8042136

Grilli, G., De Meo, I., Garegnani, G., and Paletto, A. (2017). A multi-criteria framework to assess the sustainability of renewable energy development in the Alps. *J. Environ. Plann. Manage.* 60, 1276–1295. doi: 10.1080/09640568.2016.1216398

Gunderson, L. H. (2000). Ecological resilience—in theory and application. *Annu. Rev. Ecol. systematics* 31, 425–439. doi: 10.1146/annurev.ecolsys.31.1.425

Harzé, M., Monty, A., Boisson, S., Pitz, C., Hermann, J. M., Kollmann, J., et al. (2018). Towards a population approach for evaluating grassland restoration—a systematic review. *Restor. Ecol.* 26, 227–234. doi: 10.1111/rec.12663

Huber, R., Rigling, A., Bebi, P., Brand, F. S., Briner, S., Buttler, A., et al. (2013). Sustainable land use in mountain regions under global change: synthesis across scales and disciplines. *Ecol. Soc.* 18, 18. doi: 10.5751/ES-05499-180336

Jäger, H., Peratoner, G., Tappeiner, U., and Tasser, E. (2020). Grassland biomass balance in the European Alps: current and future ecosystem service perspectives. *Ecosystem Serv.* 45, 101163. doi: 10.1016/j.ecoser.2020.101163

Ji, Z., Zou, S., Zhang, W., Song, F., Yuan, T., and Xu, B. (2024). Optimizing zoning for ecological management in alpine region by combining ecosystem service supply and demand with ecosystem resilience. *J. Environ. Manage.* 365, 121508. doi: 10.1016/j.jenvman.2024.121508

Jiang, F., Song, P., Gu, H., Zhang, J., Xu, B., Li, B., et al. (2024). New shortcut for boundary delimitation and functional zoning of national parks based on keystone species in China: A case study of kunlun mountains national park. *Ecol. Indic.* 159, 111675. doi: 10.1016/j.ecolind.2024.111675

Jiang, J., Zong, N., Song, M., Shi, P., Ma, W., Fu, G., et al. (2013). Responses of ecosystem respiration and its components to fertilization in an alpine meadow on the Tibetan Plateau. *Eur. J. Soil Biol.* 56, 101–106. doi: 10.1016/j.ejsobi.2013.03.001

Kearns, M., and Ron, D. (1997). "Algorithmic stability and sanity-check bounds for leave-one-out cross-validation," in *Proceedings of the Tenth Annual Conference on Computational Learning Theory—COLT'97*, Nashville, TN, USA, 6–9 July 1997. (New York, NY, USA: ACM Press), 152–162.

Li, C., de Jong, R., Schmid, B., Wulf, H., and Schaepman, M. E. (2020a). Changes in grassland cover and in its spatial heterogeneity indicate degradation on the Qinghai-Tibetan Plateau. *Ecol. Indic.* 119, 106641. doi: 10.1016/j.ecolind.2020.106641

Li, Y., Li, J., Are, K. S., Huang, Z., Yu, H., and Zhang, Q. (2019). Livestock grazing significantly accelerates soil erosion more than climate change in Qinghai-Tibet Plateau: Evidenced from 137Cs and 210Pbex measurements. *Agriculture Ecosyst. Environ.* 285, 106643. doi: 10.1016/j.agee.2019.106643

Li, W., Li, X., Zhao, Y., Zheng, S., and Bai, Y. (2018b). Ecosystem structure, functioning and stability under climate change and grazing in grasslands: current status and future prospects. *Curr. Opin. Environ. Sustainability* 33, 124–135. doi: 10.1016/j.cosust.2018.05.008

Li, D., Wu, S., Liu, L., Zhang, Y., and Li, S. (2018a). Vulnerability of the global terrestrial ecosystems to climate change. *Global Change Biol.* 24, 4095–4106. doi: 10.1111/gcb.2018.24.issue-9

Li, M., Zhang, X., He, Y., Niu, B., and Wu, J. (2020b). Assessment of the vulnerability of alpine grasslands on the Qinghai-Tibetan Plateau. *PeerJ* 8, e8513. doi: 10.7717/peerj.8513

Liu, Y. (2023). *County-level data on livestock stocks and herds on the Tibetan Plateau 2000-2019. ed. C. National Tibetan Plateau Data* (Beijing, China: National Tibetan Plateau Data Center).

Liu, W.-H., Zheng, J.-W., Wang, Z.-R., Li, R., and Wu, T.-H. (2021). A bibliometric review of ecological research on the Qinghai–Tibet Plateau 1990–2019. *Ecol. Inf.* 64, 101337. doi: 10.1016/j.ecoinf.2021.101337

Loucougaray, G., Dobremez, L., Gos, P., Pauthenet, Y., Nettier, B., and Lavorel, S. (2015). Assessing the effects of grassland management on forage production and environmental quality to identify paths to ecological intensification in mountain grasslands. *Environ. Manage.* 56, 1039–1052. doi: 10.1007/s00267-015-0550-9

Lu, X., Kelsey, K. C., Yan, Y., Sun, J., Wang, X., Cheng, G., et al. (2017). Effects of grazing on ecosystem structure and function of alpine grasslands in Qinghai–Tibetan Plateau: A synthesis. *Ecosphere* 8, e01656. doi: 10.1002/ecs2.2017.8.issue-1

Ma, Y., and Yang, Z. (2023). Ecological protection status and protection countermeasures of qinghai-tibet plateau. *Br. J. Biol. Stud.* 3, 01–07. doi: 10.32996/bjbs.2023.3.1.1

Nilsson, C., Aradottir, A. L., Hagen, D., Halldórsson, G., Høegh, K., Mitchell, R. J., et al. (2016). Evaluating the process of ecological restoration. *Ecol. Soc.* 21, 41. doi: 10.5751/ES-08289-210141

Niu, D., Wang, L., Qiao, F., and Li, W. (2022). Analysis of landscape characteristics and influencing factors of residential areas on the qinghai–tibet plateau: A case study of Tibet, China. *Int. J. Environ. Res. Public Health* 19, 14951. doi: 10.3390/ijerph192214951

Porqueddu, C., Ates, S., Louhaichi, M., Kyriazopoulos, A. P., Moreno, G., del Pozo, A., et al. (2016). Grasslands in 'Old World'and 'New World'Mediterranean-climate zones: past trends, current status and future research priorities. *Grass Forage Sci.* 71, 1–35. doi: 10.1111/gfs.2016.71.issue-1

Rigatti, S. J. (2017). Random forest. *J. Insurance Med.* 47, 31–39. doi: 10.17849/insm-47-01-31-39.1

Seddon, A. W., Macias-Fauria, M., Long, P. R., Benz, D., and Willis, K. J. (2016). Sensitivity of global terrestrial ecosystems to climate variability. *Nature* 531, 229–232. doi: 10.1038/nature16986

Shang, Z., Gibb, M., Leiber, F., Ismail, M., Ding, L., Guo, X., et al. (2014). The sustainable development of grassland-livestock systems on the Tibetan plateau: problems, strategies and prospects. *Rangeland J.* 36, 267–296. doi: 10.1071/RJ14008

Stoffels, R. J., Booker, D. J., Franklin, P. A., and Holmes, R. (2024). Monitoring for the adaptive management of rivers. *J. Environ. Manage.* 351, 119787. doi: 10.1016/j.jenvman.2023.119787

Sun, J., Liu, M., Fu, B., Kemp, D., Zhao, W., Liu, G., et al. (2020). Reconsidering the efficiency of grazing exclusion using fences on the Tibetan Plateau. *Sci. Bull.* 65, 1405–1414. doi: 10.1016/j.scib.2020.04.035

Sun, Y., Liu, S., Liu, C., Sun, J., Liu, Y., and Wang, F. (2023). Interactive response and spatial heterogeneity of alpine grassland biodiversity to soil, topography, climate, and human factors on the Qinghai-Tibet Plateau. *Land Degradation Dev.* 34, 4488–4502. doi: 10.1002/ldr.v34.15

Sun, J., Wang, Y., Lee, T. M., Nie, X., Wang, T., Liang, E., et al. (2024). Nature-based Solutions can help restore degraded grasslands and increase carbon sequestration in the Tibetan Plateau. *Commun. Earth Environ.* 5, 154. doi: 10.1038/s43247-024-01330-w

Tian, L., Yang, W., Ji-Shi, A., Ma, Y., Zhao, W., Chen, Y., et al. (2023). Artificial reseeding improves multiple ecosystem functions in an alpine sandy meadow of the eastern Tibetan Plateau. *Land Degradation Dev.* 34, 2052–2060. doi: 10.1002/ldr.v34.7

Villoslada, M., Vinogradovs, I., Ruskule, A., Veidemane, K., Nikodemus, O., Kasparinskis, R., et al. (2018). A multitiered approach for grassland ecosystem services mapping and assessment: The Viva Grass tool. *One Ecosystem* 3, e25380. doi: 10.3897/oneeco.3.e25380

Wang, Y., Liu, Y., Chen, P., Song, J., and Fu, B. (2024a). Interannual precipitation variability dominates the growth of alpine grassland above-ground biomass at high elevations on the Tibetan Plateau. *Sci. Total Environ.* 931, 172745. doi: 10.1016/j.scitotenv.2024.172745

Wang, Y., Liu, Y., Ding, J., Chen, P., Zhan, T., Yao, Y., et al. (2024b). Impact of functional groups on aboveground biomass in alpine grassland communities. *Prog. Phys. Geography: Earth Environ.* 48, 698–715. doi: 10.1177/03091333241280095

Wang, Y., Lv, W., Xue, K., Wang, S., Zhang, L., Hu, R., et al. (2022). Grassland changes and adaptive management on the Qinghai–Tibetan Plateau. *Nat. Rev. Earth Environ.* 3, 668–683. doi: 10.1038/s43017-022-00330-8

Wang, Y., Sun, Y., Chang, S., Wang, Z., Fu, H., Zhang, W., et al. (2020). Restoration practices affect alpine meadow ecosystem coupling and functions. *Rangeland Ecol. Manage.* 73, 441–451. doi: 10.1016/j.rama.2020.01.004

Wang, Y., Xiao, J., Ma, Y., Ding, J., Chen, X., Ding, Z., et al. (2023). Persistent and enhanced carbon sequestration capacity of alpine grasslands on Earth's Third Pole. *Sci. Adv.* 9, eade6875. doi: 10.1126/sciadv.ade6875

Xue, J., and Su, B. (2017). Significant remote sensing vegetation indices: A review of developments and applications. *J. sensors* 2017 (1), 1353691. doi: 10.1155/2017/1353691

Yang, Y., Sun, Y., Niu, B., Feng, Y., Han, F., and Li, M. (2022). Increasing connections among temporal invariability, resistance and resilience of alpine grasslands on the Tibetan Plateau. *Front. Plant Sci.* 13, 1026731. doi: 10.3389/fpls.2022.1026731

Yao, Y., Liu, Y., Wang, Y., and Fu, B. (2021). Greater increases in China's dryland ecosystem vulnerability in drier conditions than in wetter conditions. *J. Environ. Manage.* 291, 112689. doi: 10.1016/j.jenvman.2021.112689

Zhen, L., Du, B., Wei, Y., Xiao, Y., and Sheng, W. (2018). Assessing the effects of ecological restoration approaches in the alpine rangelands of the Qinghai-Tibetan Plateau. *Environ. Res. Lett.* 13, 095005. doi: 10.1088/1748-9326/aada51

Zhou, H., Yang, X., Zhou, C., Shao, X., Shi, Z., Li, H., et al. (2023). Alpine grassland degradation and its restoration in the Qinghai–Tibet plateau. *Grasses* 2, 31–46. doi: 10.3390/grasses2010004

Zhu, Q., Chen, H., Peng, C., Liu, J., Piao, S., He, J.-S., et al. (2023). An early warning signal for grassland degradation on the Qinghai-Tibetan Plateau. *Nat. Commun.* 14, 6406. doi: 10.1038/s41467-023-42099-4

frontiers | Frontiers in Plant Science

TYPE Original Research
PUBLISHED 21 March 2025
DOI 10.3389/fpls.2025.1539457

OPEN ACCESS

EDITED BY
Yi Han,
Jiangxi Normal University, China

REVIEWED BY
Cuiping Zhang,
Qingdao Agricultural University, China
Yang Zhou,
North China Electric Power University, China

*CORRESPONDENCE
Yanpeng Zhu
zhuyp@craes.org.cn

RECEIVED 04 December 2024
ACCEPTED 24 February 2025
PUBLISHED 21 March 2025

CITATION
Liu Y, Ren Y, Zhang H, Qiu D and Zhu Y (2025) Characteristics of invasive alien plants in different urban areas: the case of Kunshan City, Jiangsu Province, China. *Front. Plant Sci.* 16:1539457. doi: 10.3389/fpls.2025.1539457

Characteristics of invasive alien plants in different urban areas: the case of Kunshan City, Jiangsu Province, China

Yubing Liu[1,2], Yueheng Ren[1,2], Hua Zhang[1,2], Dongdong Qiu[1,2] and Yanpeng Zhu[1,2]*

[1]State Key Laboratory of Environmental Criteria and Risk Assessment, Chinese Research Academy of Environmental Sciences, Beijing, China, [2]State Environmental Protection Key Laboratory of Regional Eco-process and Function Assessment, Chinese Research Academy of Environmental Sciences, Beijing, China

As globalization progresses, the threat of invasive alien plants to ecosystems is becoming increasingly prominent, and the negative effects of these plants on human health and socioeconomics are gradually increasing with the development of cities; thus, concern about the problem of invasive alien plants in cities is gradually increasing. In this context, we analyzed the differences in the distribution characteristics of invasive alien plants in urban green space, countryside and farmland in Kunshan city, which is located in the Yangtze River Delta region, an area characterized by rapid urbanization. Additionally, the relations between local plant diversity and the intensity of human activities on invasive alien plants were explored. The following results were obtained: (1) There are 38 species of invasive plants in Kunshan, among which 9 species, such as *Alternanthera philoxeroides* and *Erigeron canadensis*, are distributed in all kinds of urban areas. There are no endemic invasive plants in the urban green space; however, *Amaranthus blitum* and eight other species are distributed only in the countryside, and seven species, such as *Bidens pilosa*, are found only in farmland areas. (2) In different urban areas, native plant species and phylogenetic diversity vary in their resistance to invasive alien plants. Compared with those in other areas, the coverage and importance values of alien invasive plants in the urban countryside significantly decreased with increasing quantity of native plant species and phylogenetic diversity. (3) GDP per capita, the proportion of built-up land and road density were the main factors affecting the distribution of invasive alien plants, but there were differences in the influence of human activities in different urban areas. The importance values of invasive alien plants increased significantly with increasing population density and GDP per capita in the countryside, but there was no such trend in urban green space or farmland areas. Overall, these findings suggest that urban planning and landscape management strategies should target the management of invasive alien plants based on the characteristics in different urban areas to maintain the stability and sustainability of urban ecosystems.

KEYWORDS

invasive alien plants, urban ecology, species diversity, phylogenetic diversity, sustainable development

1 Introduction

With the acceleration of global urbanization, the structure and function of urban ecosystems are constantly changing (Wang et al., 2020; Holzmann et al., 2023; Román-Palacios and Wiens, 2020). Urban expansion and land use changes have led to the destruction or replacement of native natural vegetation, resulting in the fragmentation of urban habitats and declining biodiversity (Walsh et al., 2016), and artificially disrupted habitats can have different degrees of restriction on native species, whereas invasive alien plants can adapt in these areas (Liu et al., 2021); moreover, invasive alien plants are more capable of coping with environmental changes than are native plants, for example, some studies have shown that invasive alien species are better able to adapt to global climate change than native species are (Jia et al., 2016; Herben et al., 2004) and that invasive alien plants can quickly enter artificially disrupted habitats to compete with native species for survival space by utilizing their strong reproductive ability to adapt to these environments (Bradley et al., 2010; Valladares et al., 2015).

The proliferation of invasive alien plants in urban areas not only affects the survival of native plants but also profoundly affects the local ecological environment and human life (Potgieter et al., 2022; Seebens et al., 2020). Studies have shown that invasive plants have obvious preferences for different land uses in urban environments (Godefroid and Ricotta, 2018), their distribution in urban environments is spatially variable (Štajerová et al., 2017), and the ecological heterogeneity of urban landscapes can drive significant changes in the invasion process of invasive plants (Wang et al., 2019). Therefore, it is important to understand the distribution patterns of invasive plants in heterogeneous urban environments and explore the impact mechanisms of invasive plants in different urban areas, which can provide a basis for decision-making and the scientific management of biological invasions.

In 1958, Charles Elton, a British ecologist, proposed the "diversity-invasibility hypothesis", which states that the higher the species diversity of native communities is, the stronger the resistance to the invasion of exotic plants and the lower the probability of successful invasion of exotic plants (Erickson and Elton, 1960). This may be because the greater the species diversity is, the more complex the interactions between species in the plant community and the greater their ability to resist invasion by exotic plants (Beaury et al., 2020). Additionally, the abundance, variety, and composition of native species can affect invasion by exotic plants (Levine, 2000; Dukes, 2001; Levine et al., 2004; Pearson et al., 2018). In addition to species diversity, some studies have suggested that the phylogenetic diversity of plants in native communities is closely related to the successful invasion of exotic plants (Li et al., 2015; Feng and Kleunen, 2016; Malecore et al., 2019; Fridley et al., 2007). One study showed that phylogenetic diversity buffers the extent of invasion by exotic trees (Delavaux et al., 2023). When native communities have high phylogenetic diversity, their species tend to display well-established patterns and strong adaptations in terms of resource utilization, ecological niche occupancy, and ecological functions (Kraft et al., 2011); this complexity and adaptability may enable native communities to compete more effectively with invasive alien plants for resources and thus inhibit the invasion and spread of alien species (Catford et al., 2009).

The results of several studies of urban invasive alien plants globally indicate that urbanization has had a significant effect on the species, distribution and invasion mechanism of invasive alien plants (Yang et al., 2009). For example, land use changes during urbanization (e.g., the construction of urban green spaces and landscape gardens) may unintentionally introduce exotic plants. Moreover, high-use transportation and logistics networks in cities, as well as night-time light pollution caused by the addition of streetlights during urbanization, facilitate the spread of exotic plants and promote the invasion of some exotic plants (Speißer et al., 2021; Liu et al., 2022; Murphy et al., 2022). Warmer climates, an abundant nutrient supply and few natural enemies in urban artificial environments are also conducive to the growth and reproduction of invasive alien plants (Li et al., 2005).

There have been few studies of the distribution patterns and invasion mechanisms of alien invasive plants in different urban areas. Therefore, in this study, Kunshan city, which is located in the Yangtze River Delta region and has experienced rapid urbanization and economic development, is selected as the research area, and the alien invasive plants in Kunshan city are selected as the research objects. On the basis of systematic vegetation surveys, we analyzed the composition and distribution characteristics of alien invasive plants in different urban areas and explored the relationships between the species diversity and phylogenetic diversity of native plants and alien invasive plants. Moreover, we identified the important factors affecting the invasion of invasive plants, with the aim of providing a scientific basis and suggestions for ecological protection, urban planning and biodiversity maintenance.

2 Materials and methods

2.1 Study area

Kunshan (120°48′21″-121°09′04″E, 31°06′34″-31°32′36″N) is located in the Taihu Lake Plain of the Yangtze River Delta. The total area of the city is 931 km^2, of which the water area accounts for 23.1%. The terrain is flat, with an overall hilly plain landscape. Since the 1990s, economic and social development has rapidly occurred in Kunshan, and by 2020, the urban area expanded by six times that in 1990, with the built-up area accounting for approximately 45% of the total area. Between 2010 and 2020, the resident population increased by 27.21%, and the GDP doubled. Via data reviews and onsite surveys, the number of invasive alien plant species was determined, and many of these species were found to be very harmful to the local environment.

2.2 Sample survey and data collection

The invasive alien plant survey points were selected considering various factors, such as the urban ecosystem, degree and type of anthropogenic interference, land use type, and level of road traffic.

Finally, we selected three areas with different degrees of urbanization, namely, urban green space, countryside and farmland, for the survey. In July 2022, we systematically surveyed each sample plot via a combination of sample surveys and visual evaluation methods. At each sampling point, we set up a 10 m × 10 m tree sample, and four 1 m × 1 m herbaceous samples were obtained near the top of each tree sample. We recorded the name, number of trees, cover and height of the plant species in each layer of the tree–shrub–grass systems at each sample location at the time of the survey, and each plant was labelled to indicate if it was cultivated or not cultivated and whether it was an invasive alien species or not. Invasive alien plants were identified according to the China Invasive Alien Species Information System (https://www.iplant.cn/ias/) and the Chinese List of Invasive and Naturalized Plants 2023 Edition (https://www.cvh.ac.cn/iapc/). After comparison and labelling, we identified 93 sampling sites with invasive alien plants that were randomly distributed in different urban areas of Kunshan (Figure 1).

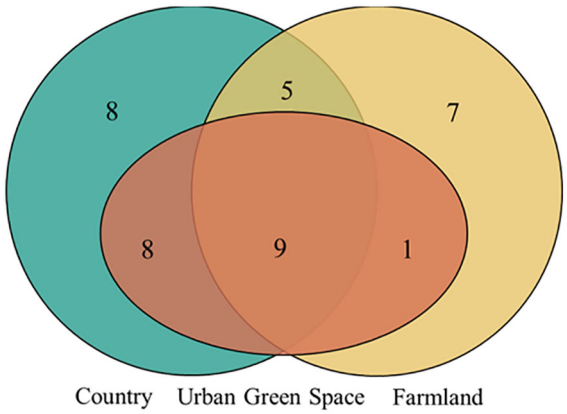

FIGURE 2
Venn diagram of the distribution of invasive alien plants in different urban areas. Orange represents urban greenspace, green represents countryside, and yellow represents farmland. The overlap of the three represents the distribution of 9 invasive plants in the three urban areas; the overlap of orange and green represents the distribution of 8 invasive plants in urban greenspace and countryside, the overlap of orange and yellow represents the distribution of 1 invasive plant in urban greenspace and farmland, the overlap of green and yellow represents the distribution of 5 invasive plants in countryside and farmland; only green represents the distribution of 8 invasive plants only in the countryside, and only yellow represents the distribution of 7 invasive plants only in the farmland.

2.3 Data acquisition and analysis

2.3.1 Selection of indicators

According to different invasion mechanisms, we selected invasive alien plant richness (S_I), invasive alien plant coverage (IC), and invasive alien plant abundance importance value (IIV) as the indices to assess invasive alien plants. S_I was expressed as the number of species of invasive alien plants in the sample, and IC was expressed as the total coverage of all invasive alien plants in the sample.

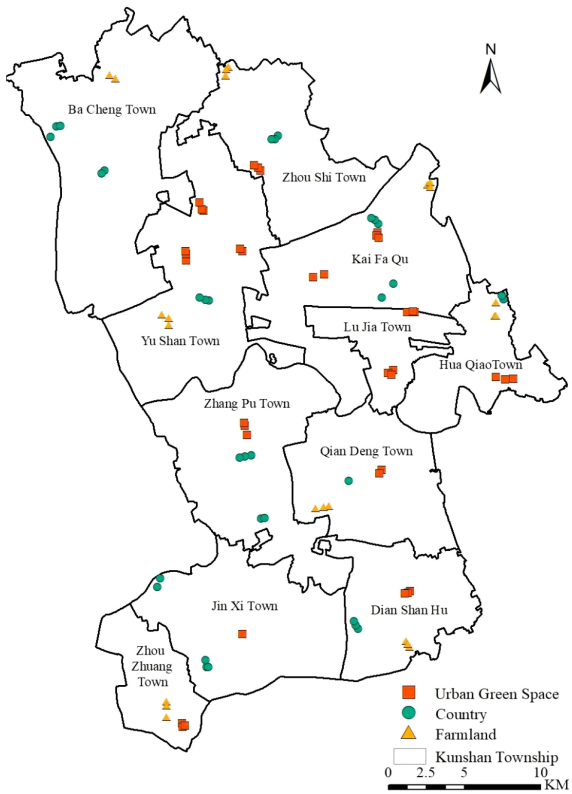

FIGURE 1
Sample Distribution of Invasive Alien Plants in Kunshan City.

We selected native plant species richness (S_N), native plant species Shannon diversity (H_N), and native plant species phylogenetic diversity (PD) as native plant indicators. The population density (POPD), GDP per capita (GDPP), built-up land area share (BUI), and road network share (ROA) were selected as urbanization environment indicators. The relationships between each indicator and the indices at the sampling sites were analyzed.

The source of population data and GDPP was the Kunshan 2020 Statistical Yearbook. The source of land use data was the 2020 land use vector data provided by the Resource Environment Science and Data Center (https://www.resdc.cn/) of the Institute of Geographic Sciences and Resources, Chinese Academy of Sciences, with an accuracy of 30 meters. The source of the road data was Open Street Map (OSM). A circle with a radius of 500 m with a sampling point as the center was created, and the density of the road network and the percentage of built-up land area in the circular area were calculated.

2.3.2 Methods of data processing

The importance value indicates the relative importance of a plant species in a community, and IIV of each sample site was calculated as follows: importance value = (relative abundance + relative cover + relative frequency)/3.

We used the Keping Ma method at each sample site to calculate the abundance of native plants (S_N) and the Shannon–Wiener index of

diversity (H_N) of native plants (Ma and Liu, 1994). The spectral diversity (PD) of the native plants was calculated at each sample site (Faith, 1992).

The construction land share was calculated via the following formula:

$$BUI = \frac{\sum_{i=1}^{S} s_i}{S},$$

where *BUI* is the road density index in the study area; s_i is the area of different construction sites in terms of land use in square kilometers (km^2); and *S* is the total area of the study area in square kilometers (km^2).

The road density index was calculated via the following formula:

$$ROA = \frac{\sum_{i=1}^{5} l_i}{S},$$

where *ROA* is the road density index in the study area; l_i is the length of different grades of roads in kilometers (km); and *S* is the total area of the study area in square kilometers (km^2).

One-way ANOVA and Duncan tests were used to examine the differences in the richness, cover and importance values of invasive alien plants in different urban areas. Redundancy analysis (RDA) was used to explore the relationships between native plant diversity and the importance values of alien invasive plants, and a Monte Carlo replacement test of the analysis results was performed. Linear fitting analysis was used to explore the relationships between native plant species diversity and phylogenetic diversity and invasive alien plant abundance, cover, and importance values in different urban areas. Redundancy analysis (RDA) was used to explore the relationships between environmental factors and the importance values of alien invasive plants, and a Monte Carlo replacement test of the analysis results was performed. Linear regression analysis was subsequently used to explore the relationships between environmental factors and in the index values of alien invasive plants in different urban areas.

The data indices were calculated and analyzed in R, the Venn Diagram package was used for compositional analysis of invasive alien plants, the vegan package for species diversity calculations and RDA analyses, the picnate package for phylogenetic diversity calculations, and the ggplot2, ggpubr packages for mapping analyses.

3 Results

3.1 Composition of invasive alien plants in Kunshan

We recorded a total of 302 plant species in our surveys, belonging to 91 families and 236 genera, among which 38 species of invasive plants spanned 13 families and 30 genera. Among the sample points, those containing invasive plants accounted for 87.74% of all sample points, indicating that the invasive plant problem in Kunshan is serious. There were 18 species of invasive alien plants in urban green areas, 30 species of invasive alien plants in the countryside, and 22 species of invasive alien plants in farmland areas. In terms of invasive grade, according to the national invasive grade classification of the "China Invasive Alien Plant List" (Ma and Li, 2018), there are 7 species with the invasive grade 1 in urban green areas, 8 species of invasive grade 1 in the countryside, and 9 species of invasive grade 1 in farmland areas. In terms of origin, most invasive alien plants in urban green spaces, countryside areas and farmlands originated from America, with 16, 22 and 16 species, respectively. In terms of life forms, there were 10 species of invasive annuals in urban green spaces, 17 species of invasive annuals in the countryside, and 18 species of invasive annuals in farmland areas.

Among all the invasive alien plants surveyed (Figure 2), nine species were distributed in urban green spaces, countryside areas and farmland areas, namely, *Euphorbia maculata*, *Bidens frondosa*, *Amaranthus retroflexus*, *Solidago canadensis*, *Sonchus oleraceus*, *Alternanthera philoxeroides*, *Erigeron canadensis*, *Erigeron annuus*, and *Symphyotrichum subulatum*. Eight invasive alien plants were distributed only in the countryside, namely, *Amaranthus blitum*, *Amaranthus tricolour*, *Melilotus officinalis*, *Cosmos bipinnatus*, *Oxalis corymbosa*, *Coreopsis basalis*, *Amorpha fruticose*, and *Gaura lindheimeri*. Seven invasive alien plants were distributed only in farmland areas, namely, *Bidens pilosa*, *Ricinus communis*, *Abutilon theophrasti*, *Oxybasis glauca*, *Physalis angulate*, *Sonchus asper*, and *Gaillardia pulchella*.

3.2 Characteristics of invasive alien plants in different urban areas

The results of one-way ANOVA (Figure 3) revealed that alien invasive plant richness (F=6.791, P=0.002), alien invasive plant cover (F=7.584, P<0.001), and the alien invasive plant importance value (F=7.606, P<001) differed significantly. The results of multiple comparisons indicated that alien invasive plant richness, cover, and importance value were significantly greater in the countryside than in the urban green space. The abundance and importance value of invasive alien plants in farmland areas were significantly greater than those in urban green spaces, and the abundance, cover and importance value of invasive alien plants in the countryside and farmland areas were not significantly different.

3.3 Impact of native plant diversity on invasive alien plants in different urban areas

On the basis of the DCA results (axis length<4.0), RDA was selected to rank and analyze the exotic invasive plant importance values and native plant diversity data in different urban areas. The results of the RDA showed that S_N and PD contributed mainly to RDA axis 1 and that H contributed mainly to RDA axis 2 (Figure 4), with the first principal component explaining 36.78% of the variation and the second principal component explaining 34.1%; the two axes together encompassed the contribution of 70.88% of all

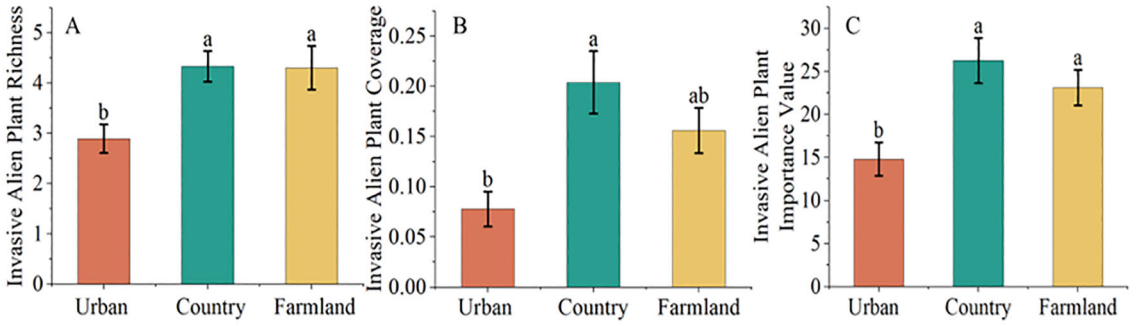

FIGURE 3
Differences in invasive alien plant richness **(A)**, coverage **(B)**, and importance value **(C)** across different urban areas. The data are the means ± SEs. Different lowercase letters indicate significant differences according to Duncan's test (P<0.05).

the variables. As shown in the figure, the results of the RDA indicate a positive correlation between S for countryside invasive alien plant importance values and H for farmland invasive alien plant importance values.

The results of the Monte Carlo replacement test revealed that S, H, and PD are all native plant-related factors that influence the importance values of invasive alien plants (Table 1).

The analysis of the results revealed (Figure 5) that in the countryside, the cover of invasive alien plants (R^2 = 0.247, P=0.003) and the importance values of invasive alien plants (R^2 = 0.206, P=0.008) significantly decreased with increasing richness of native plants. There was no significant trend in the Shannon diversity index of native plants or invasive alien plants. As the diversity index of the native plant spectrum increased, the cover of invasive alien plants (R^2 = 0.293, P=0.001) and the importance values of invasive alien plants (R^2 = 0.241, P=0.004) significantly decreased. Areas of native plants with high phylogenetic diversity (PD) display a negative relationship with the abundance of exotic invasive plants. The relations between native plant richness, the Shannon's diversity index of native plants, and phylogenetic diversity and invasive alien plants were all significant in urban green spaces and farmland areas.

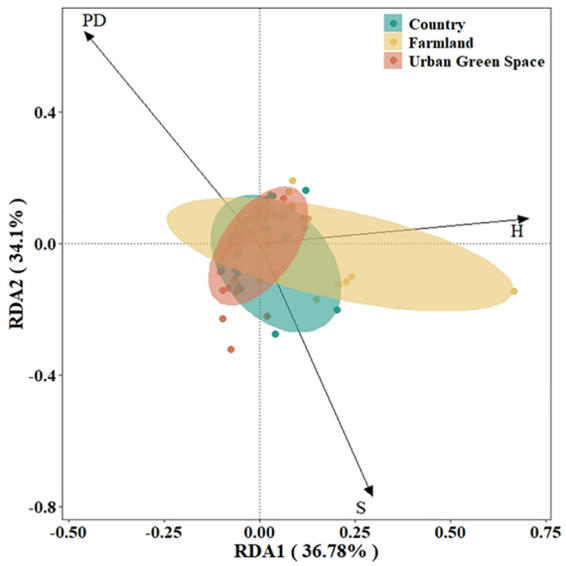

FIGURE 4
RDA rankings of importance values of invasive alien plant and native plant diversity in Kunshan city, China. S for native plant richness, H for native plant Shannon diversity, PD for native plant phylogenetic diversity.

3.4 Environmental impacts of invasive alien plants in different urban areas

On the basis of the DCA results (axis length<4.0), RDA was selected to rank and analyze the importance values of alien invasive plants in different urban areas. The confidence ellipses for urban green space and the countryside were relatively small, indicating high consistency among the samples, whereas the confidence ellipse for agricultural land was larger, indicating greater internal variability. The results of the RDA showed that ROA and GDPP mainly contribute to RDA axis 1 and that BUI and POPD mainly contribute to RDA axis 2 (Figure 6). The first principal component explains 36.84% of the variation, and the second principal component explains 27.96%; the two axes together encompass the contribution of 64.80% of all the variables. The results of the RDA indicate the strong influence of the environmental factor GDPP on the importance values of green spaces and the countryside in urban areas.

The results of the Monte Carlo replacement test revealed that the GDPP, BUI and ROA are variables correlated with the distribution of alien invasive plants (Table 2), and the importance

TABLE 1 Importance values of invasive alien plants and the results of native plant diversity replacement tests in Kunshan.

	R^2	P	
S	0.1445	0.001	***
H	0.2043	0.001	***
PD	0.1601	0.002	**

*** means P<0.001, there is a highly statistically significant difference; ** means P<0.01, statistically significant difference.

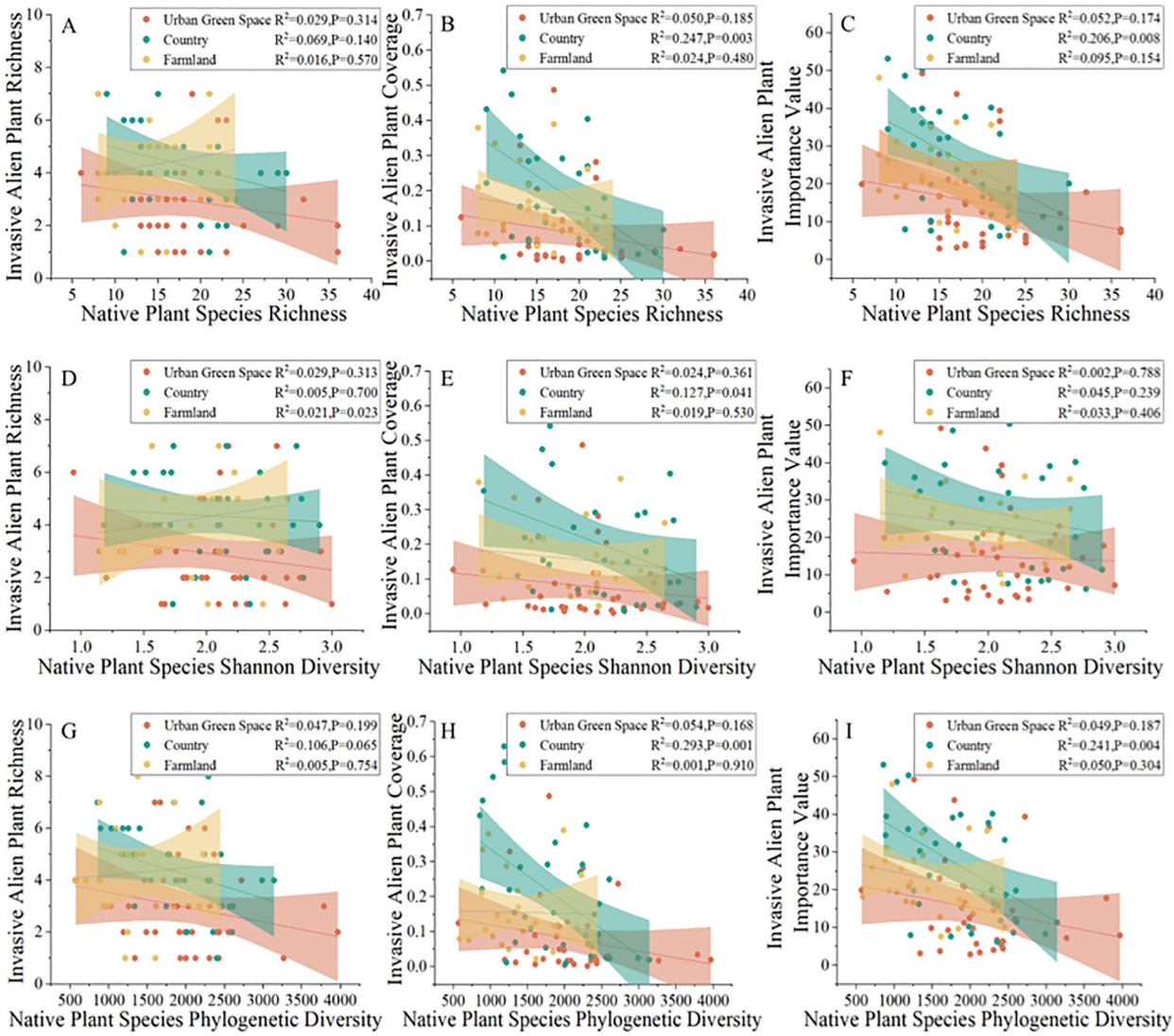

FIGURE 5
Relations between the native plant richness **(A-C)**, Shannon's diversity index **(D-F)**, phylogenetic diversity index **(G-I)** and invasive alien plant richness, coverage and importance values in different urban areas.

values of alien invasive plants in Kunshan city are highly significantly correlated with the BUI and ROA (P<0.01) and significantly correlated with the GDPP (P<0.05).

A linear regression analysis of the importance values of alien invasive plants in different urban areas with respect to environmental factors was conducted, and the results are shown in Figure 7; notably, in the countryside, the importance values of alien invasive plants (R^2 = 0.126, P=0.043; R^2 = 0.148, P=0.027) significantly increased with increasing POPD and GDPP, which indicated that in the countryside, POPD and GDPP are the main factors related to alien plant invasion.

TABLE 2 Importance values of invasive alien plants and the environmental factor replacement test results in Kunshan.

	R^2	P	
POPD	0.0716	0.057	
GDPP	0.0808	0.027	*
BUI	0.1293	0.009	**
ROA	0.2418	0.001	***

*** means P<0.001, there is a highly statistically significant difference; ** means P<0.01, statistically significant difference; * means P<0.05, fhere is a difference.

4 Discussion

4.1 Characteristics of invasive alien plants in different urban areas

Among the 38 species of invasive alien plants investigated in this study, 18 species were in urban green spaces, 30 species were in the countryside, and 22 species were in farmland areas. In terms of origin, the most invasive alien plants in urban green spaces, countryside

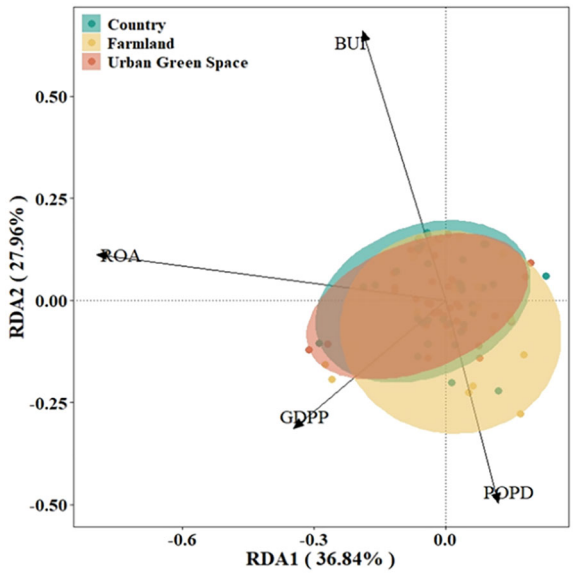

FIGURE 6
RDA rankings of the importance values of invasive alien plants on the basis of environmental factor data in Kunshan city, China. POPD for population density, GDPP for per capita GDP, BUI for built-up land area share, and ROA for road network share.

areas and farmland areas originated from America, with 16, 22 and 16 species, respectively; the results of this study were the same as those of studies on the status of invasive alien plants in Zhanjiang (Duan et al., 2022). In terms of life type, annual herbaceous plants accounted for the largest proportion of sampled invasive species; these plants are characterized by a short growth cycle and high adaptability (Xi et al., 2021), with 10, 17, and 18 species, respectively. In different urban areas of Kunshan, there were 9, 13, and 11 species of Asteraceae, as previously indicated in a survey of alien invasive plants in the built-up areas of Shenzhen (Li et al., 2024), with Asteraceae being the most abundant alien invasive plant (Qiang and Ma, 2022). Among all the investigated alien invasive plants, nine species were distributed in urban green areas, the countryside and farmland areas, and invasive class I species accounted for the largest proportion of the nine species, indicating that the invasive ability of alien plants is widely distributed.

The distribution of invasive alien plants in different urban areas is characterized by species differentiation and a structure with notable spatial variability. In this study, the abundance, cover, and importance values of invasive alien plants were lowest in the urban green space; the abundance, cover, and importance values of invasive alien plants in the countryside were significantly greater than those in the urban green space; and the abundance and importance values of invasive alien plants in the farmland were significantly greater than those in the urban green space. As previously noted in an invasive alien plant study in Beijing, the diversity of invasive alien herbaceous plants increased as the urbanization gradient decreased, and the richness of invasive alien plants in parks in the urban core area was lower than that in adjacent areas and the suburbs because environmental factors are the main factors affecting the distribution of invasive plants in remote areas of the city, whereas human activities are the main factors affecting the distribution of invasive plants in highly urbanized areas (Zhang, 2014; Zhao et al., 2022). The results are influenced by the significant differences in the ecological conditions and human activity patterns in different urban areas. In urban green spaces, the influence of environmental factors is lower, and the influence of human activities is greater. Plants in urban green spaces are usually artificially maintained and managed on a regular basis to prevent the growth of invasive plants, protect native vegetation and maintain an ecological balance; in turn, the vegetation species and distribution in green spaces are relatively stable. For example, in one study, management priority criteria were developed for invasive plants in the city of Cape Town to ensure the stabilization of the urban environment (Potgieter et al., 2018). Management practices and the management intensity have a greater impact on invasive alien plants than do other factors. Invasive alien plants that are able to stably survive in urban green spaces have the ability to adapt to the environment of the urban green space, and only those that are adapted to high levels of disturbance and are able to survive with limited resources are able to survive for a long period in urban green spaces (Munné-Bosch and Santos, 2024). In the countryside, the influence of environmental factors is greater than that in other areas, and the influence of human activities is smaller. Due to the lower level of human interference, the environment is more natural and the ecosystem is generally well established; therefore, it is easy for exotic plants to grow and spread in these areas. The ecological environment in the countryside is comparatively complex and includes diverse habitats and ecological niches in the community; therefore, it can accommodate different types of invasive alien plants. A study of the distribution of invasive plants in the urban and rural areas of Cape Town showed that the countryside can accommodate both urban invasive alien plants introduced as horticultural ornamental plants and alien invasive plants from farmland areas (Afonso et al., 2020).

4.2 The resistance of native plants in areas with different diversity levels to invasive alien plants varies across urban areas

Resistance to invasive alien plants varies with native plant diversity in different urban areas, with resistance to invasive alien plants gradually increasing with increasing native plant diversity in relatively more natural countryside areas, but this trend does not occur in urban green spaces or agricultural areas. The diversity-invasiveness hypothesis suggests that the greater the diversity of native plants is, the greater the resistance to alien invasions (Erickson and Elton, 1960). In urban green spaces and agricultural areas, the results of this study are inconsistent with the diversity-invasiveness hypothesis. In the countryside, the results of this study are consistent with the diversity-invasiveness hypothesis. The results of the present study are similar to those of a study based on data from native plant communities, in which species and phylogenetic diversity differed at different stages of invasion in response to alien plant invasions, suggesting that the biotic resistance hypothesis may be stage dependent, a result that is also supported by the findings of the present study (Guo et al., 2024).

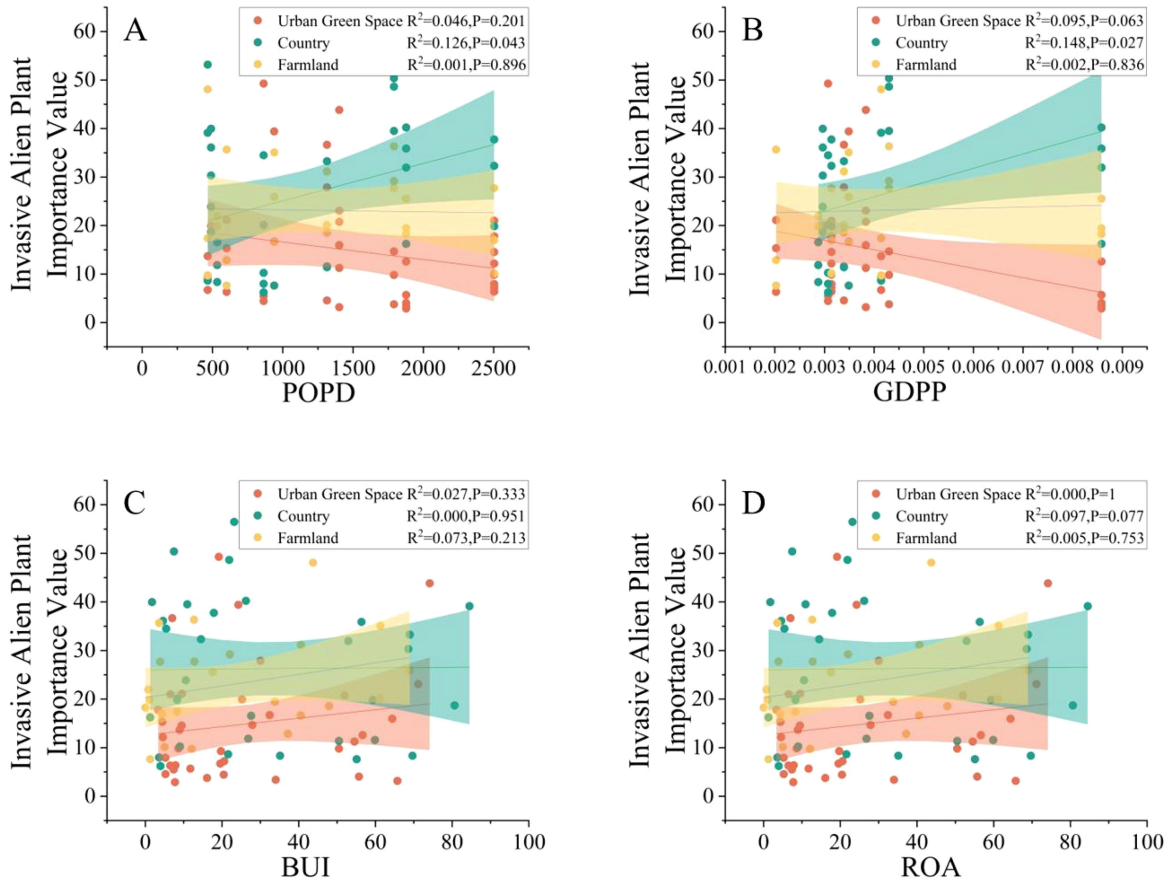

FIGURE 7
Relations between POPD **(A)**, GDPP **(B)**, BUI **(C)**,ROA **(D)** and invasive alien plant importance values in different urban areas.

The cover and importance values of alien invasive plants were significantly negatively correlated with native plant abundance in the countryside, and there was no correlation in urban green spaces or farmland areas. The results of this study were the same as those of other studies of resistance to invasive species in different habitats in tropical forest areas. The correlation between native species richness and alien invasive plant indicators varies in different habitat environments (Mungi et al., 2021) because spatial heterogeneity in cities influences the correlation between native plant species diversity and exotic invasive plants (Wang et al., 2019), high resource availability makes these areas ideal for invasive species, allowing them to establish in different communities (Karrer et al., 2020), and exotic invasive plants have different preferences for different land types in urban environments (Godefroid and Ricotta, 2018). Recent studies have shown that high biological species diversity is associated with increased resistance of grasslands to plant invasions under multiple environmental changes (Cai et al., 2024), and it is hypothesized on the basis of the results of this study that resistance to invasive alien plants may increase in relatively natural areas as native plant species diversity increases. In the countryside, where land use types are relatively diverse, there may be a variety of habitats interspersed and low levels of anthropogenic interference, the ecological environment may be more complex, the competition between species may be intense, and herbaceous plant communities with high species diversity have high biotic resistance to invasive plants because most of the ecological niches are occupied by native species, resulting in limited resources available to invasive alien plants (Yu and Li, 2020). In contrast, there are more anthropogenic influences in urban green spaces and agricultural areas, which cannot be ignored when conducting diversity-invasiveness analyses.

The cover and importance values of invasive alien plants in the countryside were significantly negatively correlated with the PD of native plants. The larger the community PD value is, the more ecological niches the community occupies and the more stable the community is. High phylogenetic diversity of native plants is associated with reduced invasion ability for alien invasive plants (Ernst et al., 2022). Habitats in the countryside are comparatively more intact than those in other areas, the phylogenetic diversity of native plants is usually greater, and plant communities are able to form complex ecological networks with strong stability and adaptability through long-term natural selection and evolution. Thus, resistance to exotic invasive plants is strong.

In summary, the resistance of native plants in different urban areas to invasive alien plants varies, especially considering genetic diversity. In the countryside, with a relatively natural environment, the diversity-invasiveness hypothesis is verified. Therefore, in urban planning and ecological conservation, the protection and enhancement of native

plant diversity should be emphasized according to field conditions to increase resistance to invasive alien plants.

4.3 The environmental factors affecting invasive alien plants vary in different urban areas

The results of the RDA showed that GDPP, BUI and ROA are the environmental factors most highly correlated with invasive alien plant abundance in Kunshan and the importance values of invasive alien plants, indicating that invasive alien plants are affected by integrated environmental factors. Additionally, the contribution of POPD is small compared with that of other environmental factors. The reasons for this may be the high urbanization of the study area, the higher the GDPP the greater the BUI and ROA, the high degree of fragmentation of the urban landscape due to the construction of built-up land, which provides suitable habitat for invasive alien plants, and the density of the roads where the spread of invasive alien plants can be carried out by vehicles. In the city the daily range of human activities is limited therefore the impact is less.

The environmental factors affecting invasive alien plants vary in different urban areas compared to the environmental factors affecting invasive alien plants in Kunshan. The invasion of alien plants in the countryside increases with the population density and GDP per capita, where there is no such trend in urban green space or farmland. The reason for this may be that in urban areas, people are more focused on their work and life, and they will not take active measures to intervene to limit the growth of invasive alien plants in urban green space and farmland, which will not have a direct impact on invasive alien plants, and only a few sanitation personnel or park managers will carry out the corresponding management. A high GDP per capita does not mean that a large amount of funds will be invested in the prevention and control of invasive alien plants in urban green spaces and farmland areas. Moreover, in urban fund allocation, economic development, infrastructure development, and social welfare are often prioritized. Unlike urban green space and farmland, in the countryside, in the countryside, a high population density means that more people many people are engaged in local activities, such as excursions, camping, and hiking. These activities increase the contact between human beings and the natural environment, and people may unintentionally bring seeds of invasive plants into the countryside or destroy the local ecological environment to create suitable conditions for invasive plants to grow. Tourism and recreational activities are more common in areas with high per capita GDP in the countryside, and the development of countryside tourism may lead to more opportunities for the introduction of exotic plants.

In this study, alien invasive plants in Kunshan were highly significantly associated with built-up land and road density, as noted in a previous study on the probability of alien invasive plant occurrence in different land use types, which was related to the percentage of impervious surfaces (Deparis et al., 2022). However, the distributions of alien invasive plants in the three different urban areas of urban green space, countryside and farmland areas in this study were not correlated with the density of built-up land or roads; additionally, some studies have shown that the probability of occurrence of invasive plants is negatively correlated with the percentage of impervious surfaces in some habitats with strong anthropogenic activities, while a positive correlation was observed for habitats with relatively limited anthropogenic activities (Li et al., 2023). Other studies have suggested that the probability of occurrence of the alien invasive plant Rudbeckia laciniata increases with increasing road density (Munemitsu et al., 2015). However, the results of this study are different. The distribution of invasive alien plants in Kunshan is related to the density of construction land and roads, but there is no correlation between the different urban areas. The reason for this may be that invasive alien plant species and their distributions in different urban areas are different, and there may be differences in the distributions of invasive alien plants when analyzed together. For example, a study of the climatic ecological niche of invasive alien plants revealed that this niche is different from that of native alien species and that the climate in the native areas of otherwise invasive alien plants is warmer, drier, and more isothermal (Chen et al., 2024); therefore, invasive alien plants exist and survive in different habitats in different urban areas at small scales. Similarly, some invasive plants prefer to inhabit places with high densities of construction land and roads, whereas some invasive plants are negatively correlated with the density of roads in construction areas; thus, in analyses of invasive alien plants, the preferences of invasive alien plants as well as other comprehensive influencing factors should be considered.

4.4 Recommendations for the prevention and control of invasive alien plants in different urban areas

The species of invasive alien plants differ in different urban areas and display a strong spatial structure. The resistance of native plant diversity to invasive alien plants varies in different urban areas, and the environmental factors affecting invasive alien plants are different in different urban areas. On the basis of the results of this study of the invasive characteristics of alien plants in different urban areas, the following recommendations are made.

In urban green areas, the daily maintenance and management of green spaces should be strengthened to maintain a good ecological environment and reduce the living space for invasive alien plants. In the countryside, the relevant departments should strengthen the ecological protection of local areas and preserve the integrity of natural vegetation and ecosystems, such as by setting up nature reserves and expanding ecological corridors, to improve resistance to invasive alien plants. In areas where activities in the countryside are carried out, public awareness of invasive plant issues should be increased, with a focus on preserving the integrity of native plants, protecting natural ecosystems and increasing knowledge regarding the prevention of alien plant invasion. The common species of invasive alien plants in farmland areas and the associated risks should be publicized to increase awareness among residents so that they can detect and remove invasive alien plants in a timely manner during the

cultivation of crops. Reasonable agricultural cultivation measures, such as crop rotation, intercropping and mulching, should be implemented to improve the stability of farmland ecosystems and reduce the chances of invasive alien plants surviving.

5 Conclusion

This study took Kunshan City, a city with rapid urbanization, as the study area, and analyzed the differences in the distribution characteristics of invasive alien plants in urban green space, countryside and farmland, and explored the mechanisms by which local plant diversity and the intensity of human activities affect invasive alien plants. The distribution of invasive alien plants in different urban areas showed species differentiation and strong spatial structure. 38 species of invasive alien plants found in Kunshan City, 9 species of invasive alien plants were distributed in all three urban areas, there were no endemic invasive alien plants in the urban green areas, 8 species of invasive alien plants were distributed in the countryside only, and 7 species of invasive alien plants were distributed only in the farmland.

The resistance of native plant diversity to invasive alien plants varied across urban areas, with alien invasive plant cover and importance values significantly decreasing with increasing native plant species diversity and phylogenetic diversity in the countryside compared to other urban areas. For the whole study area, invasive alien plants were influenced by a combination of environmental factors, and GDP per capita, proportion of built-up land and road density were the main factors influencing the distribution of invasive alien plants in Kunshan City. The environmental factors affecting the distribution of invasive alien plants were different in different urban areas. In the countryside, the importance of invasive alien plants increased significantly with the increase of population density and GDP per capita, but there was no such tendency in the urban green space and farmland.

Targeted management of invasive alien plants is recommended in urban planning and landscape management based on the characteristics of invasive plants in different urban areas. For the urban green space, it is recommended that the daily maintenance and management of green spaces be strengthened. For the countryside, it is recommended that the relevant authorities should preserve the integrity of the natural vegetation and ecosystems to enhance the resilience against invasive alien plants. For the farmland, it is recommended that reasonable agricultural cultivation measures be promoted to improve the stability of farmland ecosystems.

Data availability statement

The original contributions presented in the study are included in the article/supplementary material. Further inquiries can be directed to the corresponding author.

Author contributions

YL: Conceptualization, Data curation, Investigation, Methodology, Visualization, Writing – original draft, Writing – review & editing. YR: Investigation, Writing – review & editing. HZ: Methodology, Writing – review & editing. DQ: Methodology, Writing – review & editing. YZ: Writing – review & editing.

Funding

The author(s) declare that no financial support was received for the research and/or publication of this article.

Conflict of interest

The authors declare that the research was conducted in the absence of any commercial or financial relationships that could be construed as a potential conflict of interest.

Generative AI statement

The author(s) declare that no Generative AI was used in the creation of this manuscript.

Publisher's note

References

Afonso, L., Esler, K. J., Gaertner, M., and Geerts, S. (2020). Comparing invasive alien plant community composition between urban, peri-urban and rural areas; the City of Cape Town as a case study. Elsevier. *Urban Ecol.*, 221–236. doi: 10.1016/B978-0-12-820730-7.00013-6

Beaury, E. M., Finn, J. T., Corbin, J. D., Barr, V., and Bradley, B. A. (2020). Biotic resistance to invasion is ubiquitous across ecosystems of the United States. *Ecol. Lett.* 23, 476–482. doi: 10.1111/ele.13446

Bradley, B. A., Blumenthal, D. M., Wilcove, D. S., and Ziska, L. H. (2010). Predicting plant invasions in an era of global change. *Trends Ecol. Evol.* 25, 310–318. doi: 10.1016/j.tree.2009.12.003

Cai, C., Liu, Z. K., Song, W., Chen, X., Zhang, Z. J., Li, B., et al. (2024). Biodiversity increases resistance of grasslands against plant invasions under multiple environmental changes. *Nat. Commun.* 15, 4506. doi: 10.1038/s41467-024-48876-z

Catford, J. A., Jansson, R., and Nilsson, C. (2009). Reducing redundancy in invasion ecology by integrating hypotheses into a single theoretical framework. *Divers. Distrib.* 15, 22–40. doi: 10.1111/j.1472-4642.2008.00521.x

Chen, P. D., Shen, C. C., Tao, Z. B., Qin, W. C., Huang, W., and Siemann, E. (2024). Deterministic responses of biodiversity to climate change through exotic species invasions. *Nat. Plants.* 10, 1464–1472. doi: 10.1038/s41477-024-01797-7

Delavaux, C. S., Crowther, T. W., Zohner, C. M., Robmann, N. M., Lauber, T., van den Hoogen, J., et al. (2023). Native diversity buffers against severity of non-native tree invasions. *Nature* 622, 773–781. doi: 10.1038/s41586-023-06654-9

Deparis, M., Legay, N., Isselin-Nondedeu, F., and Bonthoux, S. (2022). Considering urban uses at a fine spatial resolution to understand the distribution of invasive plant species in cities. *Landscape Ecol.* 37, 1145–1159. doi: 10.1007/s10980-022-01415-x

Duan, T. T., He, W. L., Yang, J. Q., Lin, Z. Y., Lai, G. Z., Lu, B. C., et al. (2022). Analysis of the alien invasive plants in Zhanjiang City, Guangdong Province. *China. J. Biosaf.* 31, 245–251. doi: 10.3969/j.issn.2095-1787.2022.03.008

Dukes, J. S. (2001). Biodiversity and invasibility in grassland microcosms. *Oecologia* 126, 563–568. doi: 10.1007/s004420000549

Erickson, A. B., and Elton, C. S. (1960). The ecology of invasions by animals and plants. *J. Wildl. Manage.* 24, 231. doi: 10.2307/3796757

Ernst, A. R., Barak, R. S., Hipp, A. L., Kramer, A. T., Marx, H. E., and Larkin, D. J. (2022). The invasion paradox dissolves when using phylogenetic and temporal perspectives. *J. Ecol.* 110, 443–456. doi: 10.1111/1365-2745.13812

Faith, D. P. (1992). Conservation evaluation and phylogenetic diversity. *Biol. Conserv.* 61, 1–10. doi: 10.1016/0006-3207(92)91201-3

Feng, Y., and Kleunen, M. v. (2016). Phylogenetic and functional mechanisms of direct and indirect interactions among alien and native plants. *J. Ecol.* 104, 1136–1148. doi: 10.1111/1365-2745.12577

Fridley, J. D., Stachowicz, J. J., Naeem, S., Sax, D. F., Seabloom, E. W., Smith, M. D., et al. (2007). The invasion paradox: Reconciling pattern and process in species invasions. *Ecol* 88, 3–17. doi: 10.1890/0012-9658(2007)88[3:Tiprpa]2.0.Co;2

Godefroid, S., and Ricotta, C. (2018). Alien plant species do have a clear preference for different land uses within urban environments. *Urban Ecosyst.* 21, 1189–1198. doi: 10.1007/s11252-018-0792-4

Guo, K., Pyšek, P., Chytrý, M., Divíšek, J., Sychrová, M., Lososová, Z., et al. (2024). Stage dependence of Elton's biotic resistance hypothesis of biological invasions. *Nat. Plants.* 10, 1484–1492. doi: 10.1038/s41477-024-01790-0

Herben, T., Mandák, B., Bímová, K., and Münzbergová, Z. (2004). Invasibility and species richness of a community: a neutral model and a survey of published data. *Ecol* 85, 3223–3233. doi: 10.1890/03-0648

Holzmann, K. L., Walls, R. L., and Wiens, J. J. (2023). Accelerating local extinction associated with very recent climate change. *Ecol. Lett.* 26, 1877–1866. doi: 10.1111/ele.14303

Jia, J. J., Dai, Z. C., Li, F., and Liu, Y. J. (2016). How will global environmental changes affect the growth of alien plants? *Front. Plant Sci.* 7, 1623. doi: 10.3389/fpls.2016.01623

Karrer, S., Teodoro, A. D. A., Bustamante, M. M. C., Venterink, H. O., and Edwards, P. J. (2020). Species richness both impedes and promotes alien plant invasions in the Brazilian. *Sci. Rep.* 10, 11365. doi: 10.1038/s41598-020-68412-5

Kraft, N. J. B., Comita, L. S., Chase, J. M., Sanders, N. J., Swenson, N. G., Crist, T. O., et al. (2011). Disentangling the drivers of β diversity along latitudinal and elevational gradients. *Science* 333, 1755–1758. doi: 10.1126/science.1208584

Levine, J. M. (2000). Species diversity and biological invasions: Relating local process to community pattern. *Science* 288, 852–854. doi: 10.1126/science.288.5467.852

Levine, J. M., Adler, P. B., and Yelenik, S. G. (2004). A meta-analysis of biotic resistance to exotic plant invasions. *Ecol. Lett.* 7, 975–989. doi: 10.1111/j.1461-0248.2004.00657.x

Li, J. S., Gao, J. X., Zhang, X. L., and Zheng, X. M. (2005). Effects of urbanization on biodiversity: A review. *Chin. J. Ecol.* 24, 953–957. doi: 10.1111/ele.12522

Li, J., Zhuang, C. X., Yang, F. F., Lu, S. J., Qiu, L. S., and Zhao, J. J. (2024). Characteristics of urban invasive plants and their effects on plant diversity in the built-up area of Shen-zhen, China. *Chin. J. Ecol.* 43, 2295–2303. doi: 10.13292/j.1000-4890.202408.006

Li, L. X., He, R. X., Yang, F., Chen, J., and Cao, L. Y. (2023). Effects of urban spatial differences in Haikou on the distribution pattern of invasive alien plants. *J. Biosaf.* 32, 235–242. doi: 10.3969/j.issn.2095-1787.2023.03.006

Li, S. P., Cadotte, M. W., Meiners, S. J., Hua, Z. S., Shu, H. Y., Li, J. T., et al. (2015). The effects of phylogenetic relatedness on invasion success and impact: deconstructing Darwin's naturalisation conundrum. *Ecol. Lett.* 18, 1285–1292. doi: 10.1111/ele.12522

Liu, C. L., Diagne, C. A., Angulo, E., Banerjee, A.-K., Chen, Y., Cuthbert, R. N., et al. (2021). Economic costs of biological invasions in Asia. *NeoBiota* 67, 53–78. doi: 10.3897/neobiota.67.58147

Liu, Y., Speißer, B., Knop, E., and Kleunen, M. v. (2022). The Matthew effect: Common species become more common and rare ones become more. *Global Change Biol.* 28, 3674–3682. doi: 10.1111/gcb.16126

Ma, J. S., and Li, H. R. (2018). The checklist of the alien invasive plants in China.

Ma, K. P., and Liu, Y. M. (1994). Measurement of biotic community diversity I α diversity (Part 2). *Biodivers. Sci.* 2, 231–239. doi: 10.17520/biods.1994038

Malecore, E. M., Dawson, W., Kempel, A., Müller, G., and Kleunen, M. v. (2019). Nonlinear effects of phylogenetic distance on early-stage establishment of experimentally introduced plants in grassland communities. *J. Ecol.* 107, 781–793. doi: 10.1111/1365-2745.13059

Munemitsu, A., Takeshi, O., and Makihiko, I. (2015). The role of roads and urban area in occurrence of an ornamental invasive weed: a case of Rudbeckia laciniata L. *Urban Ecosyst.* 18, 1021–1030. doi: 10.1007/s11252-015-0466-4

Mungi, N. A., Qureshi, Q., and Jhala, Y. V. (2021). Role of species richness and human impacts in resisting invasive species in tropical forests. *J. Ecol.* 109, 3308–3321. doi: 10.1111/1365-2745.13751

Munné-Bosch, S., and Santos, J. A. S. (2024). The dramatic effects of well-intentioned but ill-designed management strategies in plant biological invasions. *Nat. Plants.* 10, 1148–1152. doi: 10.1038/s41477-024-01747-3

Murphy, S. M., Vyas, D. K., Sher, A. A., and Grenis, K. (2022). Light pollution affects invasive and native plant traits important to plant competition and herbivorous insects. *Biol. Invasions.* 24, 599–602. doi: 10.5281/zenodo.5676470

Pearson, D. E., Ortega, Y. K., Villarreal, D., Lekberg, Y., Cock, M., Eren, Ö., et al. (2018). The fluctuating resource hypothesis explains invasibility, but not exotic advantage following disturbance. *Ecol* 99, 1296–1305. doi: 10.1002/ecy.2235

Potgieter, L. J., Gaertner, M., Irlich, U. M., O'Farrell, P. J., Stafford, P. J., Stafford, L., et al. (2018). Managing urban plant invasions: a multi-criteria prioritization approach. *Environ. Manage.* 62, 1168–1185. doi: 10.1007/s00267-018-1088-4

Potgieter, L., Shrestha, N., and Cadotte, M. W. (2022). Prioritizing terrestrial invasive alien plant species for management in urban ecosystems. *J. Appl. Ecol.* 59, 872–883. doi: 10.1111/1365-2664.14103

Qiang, H., and Ma, J. S. (2022). Invasive alien plants in China: An update. *Plant Divers.* 45, 117–121. doi: 10.1016/j.pld.2022.11.004

Román-Palacios, C., and Wiens, J. J. (2020). Recent responses to climate change reveal the drivers of species extinction and survival. Proc. *Natl. Acad. Sci.* 117, 4211–4217. doi: 10.1073/pnas.1913007117

Seebens, H., Bacher, S., Blackburn, T. M., Capinha, C., Dawson, W., Dullinger, S., et al. (2020). Projecting the continental accumulation of alien species through to 2050. *Global Change Biol.* 27, 970–982. doi: 10.1111/gcb.15333

Speißer, B., Liu, Y., and van Kleunen, M. (2021). Biomass responses of widely and less-widely naturalized alien plants to artificial light at night. *J. Ecol.* 109, 1819–1827. doi: 10.1111/1365-2745.1360

Štajerová, K., Šmilauer, P., Brůna, J., and Pyšek, P. (2017). Distribution of invasive plants in urban environment is strongly spatially structured. *Landscape Ecol.* 32, 681–692. doi: 10.1007/s10980-016-0480-9

Valladares, F., Bastias, C. C., Godoy, O., Granda, E., and Escudero, A. (2015). Species coexistence in a changing world. *Front. Plant Sci.* 6. doi: 10.3389/fpls.2015.00866

Walsh, J. R., Carpenter, S. R., and Zanden, M. J. V. (2016). Invasive species triggers a massive loss of ecosystem services through a trophic cascade. *Proc. Natl. Acad. Sci.* 113, 4081–4085. doi: 10.1073/pnas.1600366113

Wang, X. K., Su, Y. B., Ren, Y. F., Zhang, H. X., Sun, X., and Ouyang, Z. Y. (2020). Urban ecosystem: human and nature compounding. *Acta Ecol. Sin.* 40, 5093–5102. doi: 10.5846/stxb201901300221

Wang, C. Y., Wu, B. D., Jiang, K., Zhou, J. W., and Du, D. L. (2019). Canada goldenrod invasion affect taxonomic and functional diversity of plant communities in heterogeneous landscapes in urban ecosystems in East China. *Urban For. Urban Green.* 38, 145–156. doi: 10.1016/j.ufug.2018.12.006

Xi, L. L., Gou, Q. Q., Wang, G. H., and Song, B. (2021). The responses of typical annual herbaceous plants to drought stress in a desert-oasis ecotone. *Acta Ecol. Sin.* 41, 5425–5434. doi: 10.5846/stxb202006211616

Yang, J. C., Wang, G. M., Jiang, C. D., Zhao, H. T., and Zhang, Z. D. (2009). Ecological characters and distribution of invasive plants under the influence of urbanization in Beijing, China. *Ecol. Environ.* 18, 1857–1862. doi: 10.16258/j.cnki.1674-5906(2009)05-1857-06

Yu, W. B., and Li, S. P. (2020). Modern coexistence theory as a framework for invasion ecology. *Biodivers. Sci.* 28, 1362–1375. doi: 10.17520/biods.2020243

Zhang, N. (2014). *Research on Plant Landscape of Urban Ecological Corridor in Beijing* (Beijing Forestry University).

Zhao, Y. F., Zhao, C. Y., Zhu, J. F., Li, F., Yang, X. Q., and Guo, C. D. (2022). Distribution pattern of alien invasive plants in typical parks in Beijing. *Acta Ecol. Sin.* 42, 3656–3665. doi: 10.5846/stxb202104140971

frontiers | Frontiers in Plant Science

TYPE Original Research
PUBLISHED 24 March 2025
DOI 10.3389/fpls.2025.1510676

OPEN ACCESS

EDITED BY
Ting Hua,
Norwegian University of Science and Technology, Norway

REVIEWED BY
Tianyu Zhan,
Beijing Normal University, China
Jiaxin Guo,
Jiangxi Academy of Agricultural Sciences (CAAS), China

*CORRESPONDENCE
Wen-hui Liu
qhliuwenhui@163.com

RECEIVED 13 October 2024
ACCEPTED 04 March 2025
PUBLISHED 24 March 2025

CITATION
Li S, Shi Z, Liu W-h, Li W, Liang G and Liu K (2025) Long-term Kentucky bluegrass cultivation enhances soil quality and microbial communities on the Qinghai-Tibet Plateau. *Front. Plant Sci.* 16:1510676. doi: 10.3389/fpls.2025.1510676

Long-term Kentucky bluegrass cultivation enhances soil quality and microbial communities on the Qinghai-Tibet Plateau

Sida Li[1,2], Zhenghai Shi[1,2], Wen-hui Liu[1,2]*, Wen Li[1,2], Guoling Liang[1,2] and Kaiqiang Liu[1,2]

[1]Key Laboratory of Superior Forage Germplasm in the Qinghai-Tibetan plateau, Qinghai Academy of Animal Science and Veterinary Medicine, Qinghai University, Xining, China, [2]Laboratory for Research and Utilization of Qinghai Tibet Plateau Germplasm Resources, Xining, Qinghai, China

Introduction: Nature-based Solutions (NbS) provide a comprehensive strategy for environmental management, focusing on the protection, sustainable use, and restoration of natural and modified ecosystems. Cultivated grasslands are a form of NbS, offering benefits such as increased biodiversity, improved soil fertility, and greater ecosystem resilience. They are widely acknowledged for their positive impact on restoring degraded grasslands. Kentucky bluegrass (Poa pratensis L.) is widely used for restoring degraded grasslands on the Qinghai-Tibet Plateau. However, long-term cultivation of Kentucky bluegrass can lead to above-ground degradation, which challenges its effectiveness in restoring ecosystem health.

Methods: This study investigates the impacts of Kentucky bluegrass cultivation on soil quality, focusing on soil nutrients, enzyme activities, and microbial communities across different recovery stages. Field experiments were conducted to analyze soil quality dynamics during early (2nd year), mid (6th year), and late (10th year) succession stages of cultivated grasslands on the Qinghai-Tibet Plateau. Our results show that in the early and mid-stages, soil total nitrogen, total phosphorus, and organic carbon storage were significantly lower compared to undegraded grasslands, with the lowest soil quality observed in the early stage ($P < 0.05$). However, by the late stage, soil quality significantly improved, with total nitrogen, total phosphorus, and organic carbon contents exceeding those of undegraded grasslands by 14.59%. These improvements were driven by enhanced microbial community dynamics and increased nitrogen and carbon cycling enzyme activities, which promoted nutrient utilization and organic matter decomposition. This process was accompanied by a rise in microbial diversity, supporting soil resilience and ecosystem function. Soil total nitrogen emerged as a key determinant of soil quality in both natural and cultivated grasslands, and appropriate nitrogen fertilization strategies were found to effectively enhance grassland productivity and ecosystem health.

Discussion: Overall, this study highlights the potential of Kentucky bluegrass in restoring degraded grasslands by improving soil fertility and microbial community structure over time, providing insights into sustainable management practices to maintain soil fertility and ecosystem services on the Qinghai-Tibet Plateau.

KEYWORDS

Qinghai-Tibet Plateau, cultivated grassland, soil microbial communities, soil quality, Kentucky bluegrass

1 Introduction

The Qinghai-Tibet Plateau serves as the source of major rivers in Asia and is recognized as one of the most biodiverse regions in China and the world. It plays a crucial role in global and regional climate, hydrology, and ecosystem dynamics (Zhang Q, et al., 2022; Liu et al., 2023; Lin et al., 2021). However, in recent years, the grasslands of the Qinghai-Tibet Plateau have experienced varying degrees of degradation, including the emergence of severely degraded grasslands such as "black soil beach" (Zhao et al., 2020; Dong et al., 2015; Zhu et al., 2010). Currently, severe and extreme degradation of grasslands is widespread across the entire plateau. The loss of vegetation cover in these degraded grasslands has resulted in severe soil erosion, the spread of noxious weeds, and conflicts between grassland and livestock (Zhang et al., 2024b). This has had a significant negative impact on the region's ecology, productivity, and socio-economic conditions (Lin L. et al., 2023; Xu Z. et al., 2023). To address the issue of severe grassland degradation on the Qinghai-Tibet Plateau, China has implemented extensive ecological conservation projects. Among these, Nature-based Solutions (NbS) have gained increasing attention for their holistic and sustainable approach to environmental challenges. NbS focus on protecting, sustainably managing, and restoring natural or modified ecosystems to address societal issues such as climate change, biodiversity loss, and land degradation. These solutions offer multiple benefits, including enhancing ecosystem resilience, improving soil and water quality, and supporting biodiversity (Hua et al., 2022). Currently, it is widely recognized that establishing cultivated grasslands using local plant species is an effective NbS measure. Cultivated grasslands involve the rapid establishment of vegetation cover through the cultivation of adaptive and fast-growing plant species (Cao et al., 2021; Mosier et al., 1991). This approach not only quickly restores vegetation cover but also significantly improves soil conditions. By enhancing soil structural stability and enriching its physical and chemical properties, cultivated grasslands effectively combat soil erosion and promote soil health (Song et al., 2023; Norderhaug et al., 2023; Kavana et al., 2024). Moreover, they provide sustained ecological functions, such as nurturing soil microbial communities, creating habitats for diverse species, and supplying food resources. As a Nature-based Solution, cultivated grasslands exemplify the use of natural processes to restore degraded ecosystems while delivering multiple benefits, including enhanced biodiversity and improved soil fertility (Tomazelli et al., 2024; Johansson et al., 2024). This approach represents a sustainable and holistic strategy for mitigating grassland degradation and fostering ecological resilience on the Qinghai-Tibet Plateau.

Kentucky bluegrass (*Poa pratensis* L.) is a rhizomatous perennial grass species that has a wide distribution in the Qinghai-Tibet Plateau region (Wei et al., 2020; Cao et al., 2019). It exhibits excellent growth adaptability and speed, quickly covering the soil surface, effectively preventing soil erosion, improving soil structure, and promoting soil carbon sequestration and moisture retention abilities (Cao et al., 2019; Wei et al., 2020). Compared to other grass species used for ecological restoration, such as *Elymus* spp. and *Festuca Linn.*, Kentucky bluegrass exhibits superior adaptability and growth speed, making it an ideal choice for rapid soil coverage and erosion control (Wang et al., 2009; Palit et al., 2021). These characteristics are particularly beneficial for stabilizing degraded grasslands in the Qinghai-Tibet Plateau region. Kentucky bluegrass is extensively used in the management of severely degraded grasslands and is considered one of the key grass species (Wang et al., 2022; Wang W. et al., 2024). However, after 4-5 years of establishment, cultivated Kentucky bluegrass grasslands are prone to secondary degradation. This process is characterized by an increase in weed species and a decline in the proportion of desirable forage grasses. Additionally, there is a significant reduction in community biomass and soil nutrient content, which further contributes to the overall degradation of the grassland ecosystem (Zhao et al., 2023; Wu et al., 2023). Therefore, secondary degradation is one of the primary issues associated with the establishment and cultivation of Kentucky bluegrass (*Poa pratensis* L.) in grasslands.

Previous studies have extensively explored and experimented with the issue of secondary degradation in cultivated grasslands. For example, Shang (Shang et al., 2018), based on a comprehensive analysis of the progress in research and restoration efforts on degraded black soil patches over the past decade, suggested that the increase in weed species, the decline in the proportion of desirable forage grasses, and the rise in aboveground biomass within cultivated grasslands may indicate the early stages of directional succession in alpine meadows. However, (Song et al., 2018) argued that the short-term high productivity of artificial grasslands often comes at the expense of soil fertility, which negatively impacts the long-term stability of grassland ecosystems. Similarly, (Dong et al., 2013) held the view that the high productivity of cultivated grasslands in the short term relies heavily on the excessive depletion of soil fertility. Based on the theory of stability maintenance, he proposed that interventions such as fertilization, weeding, and rodent control could help sustain the stability of artificial grasslands. In contrast, Li Xilai, through large-scale plot surveys and quantitative modeling, concluded that minimizing human disturbance is crucial for accelerating the recovery of cultivated grasslands from extreme degradation (Li, 2012). In summary, the precise processes underlying the degradation of cultivated grassland ecosystems remain unclear. The lack of targeted and effective conservation and management strategies is a major factor contributing to exacerbated grassland degradation and the decline in ecosystem services. Therefore, gaining a deeper understanding of the degradation processes in artificial grassland ecosystems is of critical importance for developing scientifically sound and effective conservation and management strategies to maintain the health and stability of grassland ecosystems.

Assessing soil quality facilitates timely monitoring of the current status and dynamic changes in soil. This enables sustainable management of cultivated grasslands (Karlen et al., 2003). Current research indicates that under specific climatic conditions in the Qinghai-Tibet Plateau region, the accumulation rate of organic matter is relatively slow, and soil erosion results in

severe nutrient loss. Soil nutrients are one of the primary factors limiting plant growth (Yao et al., 2021).Therefore, evaluating soil quality in cultivated grasslands is beneficial for understanding the soil conditions and trends in different stages of grassland evolution, which can facilitate better management and utilization of soil resources. Additionally, soil microorganisms play a vital role in soil and plant health, including nutrient cycling, carbon sequestration, pollutant degradation, plant disease control, and promoting plant growth (Paul et al., 2024). Exploring the soil microbial community in cultivated grasslands can assess various aspects of the soil environment and reveal soil characteristics and changes in grassland ecosystems (Pedrinho et al., 2024). Consequently, this study focuses on soil nutrient content (organic carbon, total nitrogen, and total phosphorus) and soil enzyme activities related to nutrient cycling as the main indicators for evaluating cultivated grassland soils. By analyzing the microbial community in cultivated grassland soils, the study aims to examine soil changes in different successional stages of cultivated grasslands and explore the soil evolution process, providing a basis for maintaining the health and stability of cultivated grassland ecosystems.

Current research has indicated that during the early establishment phase of cultivated grasslands, insufficient vegetation cover and underdeveloped root systems lead to inadequate protection of the soil surface and a reduction in the input of litter and root exudates. These conditions not only weaken the accumulation of soil organic matter and reduce soil fertility but also increase the risk of soil erosion due to the exposure of the soil surface (Li et al., 2025). Concurrently, management practices such as tillage significantly alter the soil's physical structure, resulting in increased soil bulk density and decreased porosity, which in turn affect soil aeration and permeability. These changes further restrict the habitat for soil microorganisms, reducing their activity and diversity, while accelerating the mineralization of soil organic matter and exacerbating nutrient loss (Liu et al., 2025; Nonxuba et al., 2025). Based on this, we propose the hypothesis that in the early stages of establishment, cultivated grasslands dominated by Kentucky bluegrass will result in a decrease in soil quality. However, as the evolution process of cultivated grasslands progresses, they will gradually approach the soil quality of undisturbed natural grasslands (i.e., climax communities). The main objectives of this study are: (1) to investigate the impact of different successional stages of cultivated grasslands dominated by Kentucky bluegrass on soil quality; (2) to explore the soil factors influencing the establishment of cultivated grasslands dominated by Kentucky bluegrass; and (3) to examine the effects of cultivated grasslands dominated by Kentucky bluegrass on soil microbial communities.

2 Materials and methods

2.1 Experimental design

A field experiment was conducted to study the changes in soil characteristics in cultivated grasslands in Qinghai Province, China. The experimental site was located near Xi Hai Town, Haibei Prefecture, Qinghai Province (elevation 3,156 m). The region has a plateau continental climate, with an average annual temperature of 0.9 °C. The average annual precipitation is 369.1 mm, and there is no absolute frost-free period. This location is representative of the Qinghai - Tibet Plateau. The high elevation and characteristic plateau continental climate, with its specific temperature and precipitation patterns, are typical of the broader region. Therefore, the selected site can effectively serve as a substitute for the Qinghai - Tibet Plateau in studying the changes in soil characteristics of cultivated grasslands.

Spatial - temporal substitution is a method that uses spatial differences to infer temporal changes. Zhao et al. used this approach to investigate the impact of different cultivation measures on soil quality over time. By comparing grasslands planted at different times but in similar locations, they deduced the temporal changes in soil quality. This method is beneficial because it can effectively eliminate the impact of inter - annual climate variations on soil quality, which are significant in the study region. In this study, a "spatial-temporal substitution" approach was employed. Cultivated grasslands established in 2014, 2018, and 2022 were selected as representative stages of the typical soil succession process (2014 represents the later stage of restoration, 2018 represents the middle stage of restoration, and 2022 represents the early stage of restoration). Additionally, un-degraded natural grassland (fenced and protected for 5 years) was selected as the control (CK) treatment. The slope direction, elevation, and precipitation conditions were similar among the different grassland plots (Figure 1).

The cultivation of different grasslands was carried out using strip sowing with a row spacing of 30 cm and a seeding rate of 22.5 kg/hm^2. Before sowing, urea at a rate of 75 kg/hm^2 and diammonium phosphate at a rate of 150 kg/hm^2 were applied, and the cultivation was rainfed. Each plot had an area of 50 m^2 and was replicated three times. After seeding, one weed removal operation is conducted in the same year, followed by enclosure.

2.2 Soil sampling

In 2023, rhizosphere soil samples were collected from cultivated grasslands at different restoration stages of Kentucky bluegrass and from undisturbed natural grasslands. For each treatment, five random replicate samples were collected, and then homogenized to provide a composite sample for each replicate site. Portions of soil were air-dried for characterization analysis, while subsamples for molecular and enzyme activity analysis were preserved with liquid nitrogen, transported in iceboxes, and stored at -80°C and 4° C, respectively.

2.3 Soil DNA extraction, PCR amplification, and Illumina sequencing

Using the MagPure Soil DNA LQ Kit (Magan) kit, following the instructions, the genomic DNA of the samples was extracted. The

concentration and purity of the DNA were determined using NanoDrop 2000 (Thermo Fisher Scientific, USA) and agarose gel electrophoresis, and the extracted DNA was stored at -20°C. The extracted genomic DNA was used as a template for PCR amplification of bacterial 16S rRNA genes and ITS genes. The V3-V4 variable region of the 16S rRNA gene was amplified using the universal primers 343F (5'-TACGGRAGGCAGCAG-3') and 798R (5'-AGGGTATCTAATCCT-3'), while the ITS1 variable region of the ITS gene was amplified using the universal primers ITS1F (5'-CTTGGTCATTTAGAGGAAGTAA-3') and ITS2 (5'-GCTGCGTTCTTCATCGATGC-3').

The PCR amplification products were analyzed using agarose gel electrophoresis. The AMPure XP beads were used for purification, and the purified products were used as templates for the second-round PCR amplification. Subsequently, another round of purification with magnetic beads was conducted, and the purified second-round products were quantified using Qubit. The concentration was adjusted for sequencing. Sequencing was performed on the Illumina NovaSeq 6000 sequencing platform, generating 250 bp paired-end reads. The sequencing was conducted by Shanghai Oe Biotech Co., Ltd.

After the raw data is sequenced, the first step involves using the Cutadapt software to trim off the primer sequences from the raw data sequences. Subsequently, DADA2 is utilized for quality filtering, denoising, merging, and chimera removal of the paired-end raw data, conducting quality control analysis to obtain representative sequences and abundance tables. Finally, the QIIME 2 software package is employed to select representative sequences of each Amplicon Sequence Variant (ASV) and annotate all representative sequences by comparing them to the Silva database.

2.4 Calculation of soil quality index

This study uses Principal Component Analysis (PCA) and correlation analysis to determine the Multidimensional Scaling (MDS) values for soil quality assessment (Zhang Z. et al., 2022). The Norm value is determined by the formula:

$$N_{ik} = \sqrt{\sum_{i}^{k}(u_{ik}^2 \times \lambda_k)}$$

where Nik is the comprehensive load on the first k principal components with the characteristic value of the ith variable ≥1. Uik is the load of the i-th variable on the k-th principal component, which reflects the importance of the i-th variable in the k principal component. λk is the kth principal component eigenvalue.

The Soil Quality Index (SQI) is calculated through an equation that determines the weights and scores of soil evaluation indicators.

$$W_i = P_i / \sum_{i=1}^{n} P_i \quad (n = 1,\ 2, 3, 4 \ldots n)$$

$$SQI = \sum_{i=1}^{n} W_i \times S_i$$

where N is the number of indicators. S_i is the membership value of the soil index. P_i represents the contribution rate of the i-th comprehensive index for each treatment. W_i is the indicator weight (Refer to Tian et al., 2018 for calculation method). The SQI ranges from 0 to 1 (Zhang F. et al., 2022).

Due to the varying impact of different soil physicochemical properties on soil quality, the membership functions for different soil indicators also differ. Membership functions can be classified as ascending and descending types. The types of membership functions for different soil physicochemical indicators are shown in Table 1.

2.5 Statistical analysis

The Mothur software package (v.1.30.1) was used to estimate community diversity using the Shannon index and calculate classification α diversity. Non-metric Multidimensional Scaling (NMDS) was employed to describe the clustering of different samples, further reflecting the changes in microbial community structure under intercropping patterns, i.e., microbial diversity. Redundancy Analysis (RDA) was conducted to study the correlations between soil microbial composition, soil nutrients, soil pH, soil bulk density and soil enzyme activities. The RDA analysis was performed using the CANOCO 4.5 software package. Spearman correlation analysis was conducted using IBM SPSS Statistics 19.0 to determine the relationships between soil microbial characteristics (abundance, α diversity, and β diversity) and soil properties (Soil nutrients, soil pH, soil bulk density) and enzyme activities. One-way Analysis of Variance (ANOVA) was used to analyze differences in soil properties (Soil nutrients, soil pH, soil bulk density), soil enzyme activities, and microbial characteristics under different intercropping patterns ($P< 0.05$). Mean differences were assessed using the LSD test ($P< 0.05$), where different letters indicate significance. Origin 9.1 was used for data visualization, including soil nutrients and enzyme activities.

3 Results

3.1 Soil physicochemical properties and soil enzyme activity

The cultivated grassland in different management stages significantly influenced the content of SOC, C stock, TN, and TP ($P<0.05$) (Figures 2a–f). In the second year of grassland cultivation (early restoration stage), the content of SOC, C stock, TN, and TP in the cultivated grassland was significantly lower compared to the CK treatment. With the increase in restoration time, the SOC, C stock, TN, and TP of the cultivated grassland showed an increasing trend (Figures 2c–f). Gradually, the differences compared to the CK treatment became non-significant ($P>0.05$) (Figures 2a–d).

For soil enzyme activity, the activity of SALPT (alkaline protease), SBAX (asic xylanase), and SUE in cultivated grasslands at different management stages significantly influenced ($P<0.05$),

10.3389/fpls.2025.1510676

TABLE 1 Soil quality iturndicators and membership function types.

Indicator	Membership function type	Membership function formula
Soil bulk density (SBD)	Descending membership function	$f(x) = \begin{cases} 1.0 & x = a \\ 0.9(b-x)/(b-a) & a < x < b \\ 0.1 & x = b \end{cases}$
pH		
Catalase (SCAT)	Ascending membership function	$f(x) = \begin{cases} 0.1 & x = a \\ 0.9(x-a)/(b-a) & a < x < b \\ 1.0 & x = b \end{cases}$
Cellulase (SCL)		
Alkaline protease (SALPT)		
Alkaline phosphatase (SAKP)		
Urease (SUE)		
Basic xylanase (SBAX)		
Sucrase (SSC)		
Bacteria Shannon		
Fungi Shannon		
Soil organic carbon (SOC)		
Total nitrogen (TN)		
Total phosphorus (TP)		
C Stock		

$f(x)$ is the membership function and x is the measured value of the evaluation index. a, b respectively indicate the minimum and maximum values of the measured values. Since the experimental site of this study is located in the Tibetan Plateau, where the soil pH values are all above 7.5, a higher soil pH is detrimental to plant growth. Therefore, the soil pH is classified as a Descending membership function.

with similar trends of changes in activity. They all showed an increase followed by a decrease with increasing years of management (Figures 2i–k). In the second year of grassland cultivation, the activity of SALPT (alkaline protease) did not differ significantly from the CK treatment (P>0.05). With the increase in management time, the activity of SALPT (alkaline protease) significantly increased in the sixth and tenth year compared to the CK treatment (P<0.05) (Figure 2i). As for SBAX, the activity did not differ significantly from the CK treatment in the second and tenth year of management, but the activity in the sixth year of cultivated grassland significantly increased compared to the CK treatment (P<0.05) (Figure 2j). Regarding SUE, the activity did

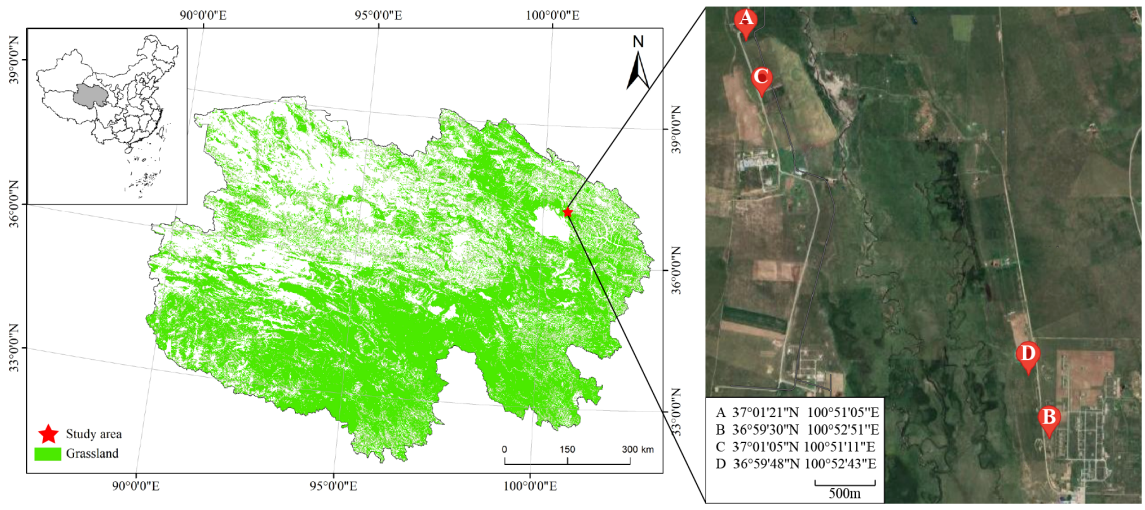

FIGURE 1
Distribution map of the experimental sites. Point A represents the later stage of restoration (2014). Point B represents the middle stage of restoration (2018). Point C represents the early stage of restoration (2022). Point D represents the un-degraded natural grassland (fenced and protected for 5 years).

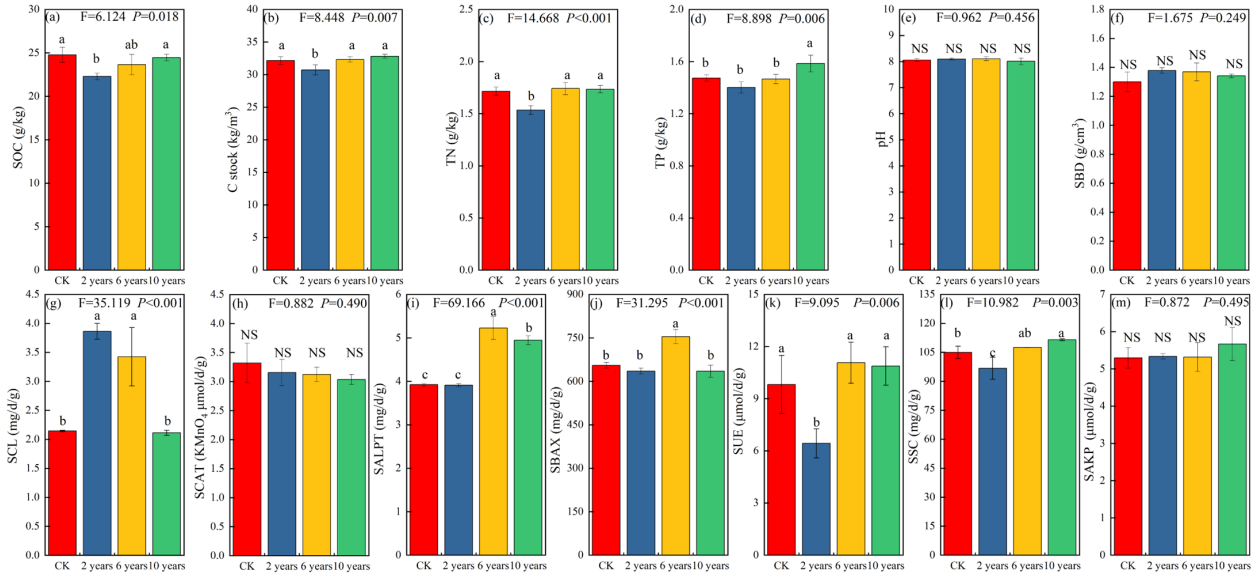

FIGURE 2
Soil physicochemical properties of different treatments. Different letters indicate significant differences (P<0.05). Panel **(a)** represents soil organic carbon content; Panel **(b)** is soil carbon stock; Panel **(c)** is soil total nitrogen content; Panel **(d)** is soil total phosphorus content; Panel **(e)** is soil pH value; Panel **(f)** is also soil pH value; Panel **(g)** is soil cellulase activity; Panel **(h)** is soil catalase activity; Panel **(i)** is soil alkaline protease activity; Panel **(j)** is soil alkaline xylanase activity; Panel **(k)** is soil urease activity; Panel **(l)** is soil sucrase activity; Figure **(m)** is soil alkaline phosphatase activity. Different letters indicate significant differences (P<0.05).

not differ significantly from the CK treatment in the sixth and tenth year of management, but in the second year of cultivated grassland, the activity of SUE significantly decreased compared to the CK treatment (P<0.05) (Figure 2k).

In addition, the activity of SCL (cellulase) and SSC (sucrase) in cultivated grasslands with different planting years significantly influenced (P<0.05). The activities of SCL (cellulase) and SCAT (catalase) decreased with the increase in management years (Figures 2g, h). In the second year of grassland cultivation, the activity of SCL (cellulase) was significantly higher than the CK treatment (P<0.05), but with the increase in management time, the activity of SCL (cellulase) did not differ significantly from the CK treatment (P>0.05) (Figures 2g, h). The activities of SSC (sucrase) and SAKP (alkaline phosphatase) showed an increasing trend with the increase in planting years, but the impact on SAKP (alkaline phosphatase) activity was not significant (P>0.05) (Figures 2l, m). The activity of SSC (sucrase) decreased the most with the increase in management time, and in the tenth year of cultivated grassland, the activities of SCL (cellulase) and SSC (sucrase) were gradually significantly higher than the CK treatment (P<0.05) (Figure 2l).

3.2 Soil microbial community

In the second year of grassland cultivation, the ACE index of bacterial and fungal communities was significantly lower than the CK treatment (P<0.05). However, with prolonged management, the ACE index gradually increased. By the tenth year, the ACE index of the bacterial community no longer showed significant differences compared to the CK treatment (P > 0.05), while the fungal community exhibited a significantly higher ACE index than the CK treatment (P< 0.05) (Figure 3a). Similar trends were observed for the Pielou and Shannon indices. In the second year, both indices were significantly lower than those of the CK treatment (P< 0.05). But with increasing management duration, their values gradually increased, and by the tenth year, no significant differences were observed compared to the CK treatment (P > 0.05) (Figures 3b, c).

Non-metric multidimensional scaling (NMDS) analysis revealed distinct clustering patterns in bacterial and fungal communities over different cultivation durations. The bacterial communities in the CK treatment, sixth-year, and tenth-year cultivated grasslands were relatively similar, while those in the second-year cultivated grasslands differed significantly from the CK treatment and later successional stages (Figure 3d). For the fungal community, the CK treatment and sixth-year cultivated grasslands displayed similarity, whereas the fungal communities in the second and tenth years exhibited significant differences compared to both the CK treatment and the sixth-year cultivated grasslands (Figure 3e).

Across different management durations, *Acidobacteriota* (23.82%), *Proteobacteria* (16.11%), *Planctomycetota* (12.06%), *Actinobacteriota* (10.06%), and *Bacteroidota* (9.91%) were the dominant bacterial phyla. The relative abundance of *Acidobacteriota* initially increased and then declined with extended management duration, while *Proteobacteria* showed a continuous decline over time. In contrast, *Actinobacteriota* and *Planctomycetota* increased with longer cultivation years. The relative abundance of *Bacteroidota* initially decreased but later increased with cultivation time (Figure 3f).

Regarding fungal communities, the dominant phyla were *Ascomycota* (56.93%), *Mortierellomycota* (14.54%), and *Basidiomycota* (9.31%). The relative abundance of *Ascomycota* initially decreased but

10.3389/fpls.2025.1510676

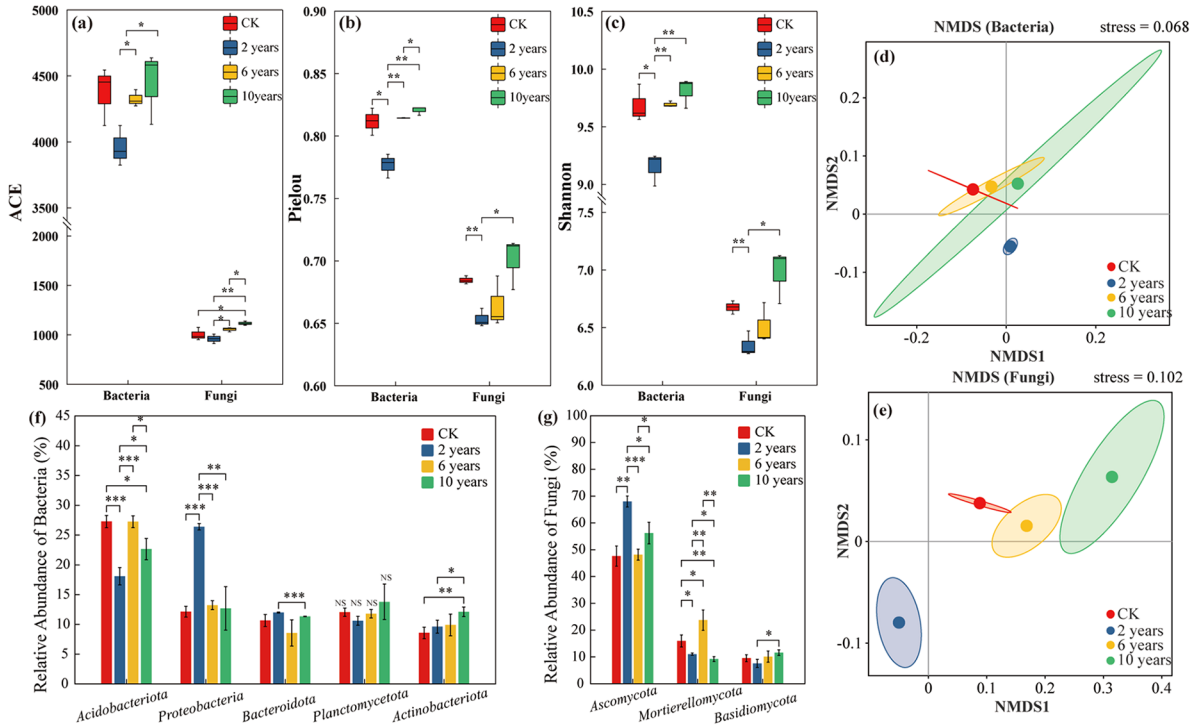

FIGURE 3
Soil microbial communities of different treatments. "*" in the figure indicates $P \leq 0.05$, "**" indicates $P \leq 0.01$, "***" indicates $P \leq 0.001$. **Panels (a–c)** represent the ACE, Pielou, and Shannon indices of microbial communities under different treatments. **Panels (d, e)** represent the β-diversity of soil bacterial and fungal communities under different treatments. **Panels (f, g)** represent the composition of soil bacterial and fungal communities under different treatments.

increased with prolonged cultivation. *Mortierellomycota* exhibited an initial increase followed by a decrease, whereas *Basidiomycota* steadily increased with extended cultivation time (Figure 3G).

LEfSe analysis further highlighted the impact of cultivation duration on microbial communities. In the early stages, cultivated grasslands significantly reduced the relative abundance of various bacterial phyla compared to the CK treatment. However, long-term cultivation resulted in minimal differences between cultivated and CK treatments. For fungal communities, the initial establishment of cultivated grasslands had a lesser impact compared to bacterial communities. Over time, multi-year cultivation increased the relative abundance of various fungal phyla compared to the CK treatment (Supplementary Figures S1, S2).

3.3 Soil quality evaluation based on minimum data set

Principal Component Analysis (PCA) was performed, and the results are shown in Table 2. For each principal component with eigenvalues ≥1, a set of soil indicators was selected based on factor loadings with absolute values >0.5. Indicators with loadings >0.5 in different components were grouped based on low correlation with other indicators (Figure 4a). Finally, total nitrogen (TN), total phosphorus (TP), soil organic carbon (SOC), and alkaline protease (SALPT) were selected as the final indicators for soil quality assessment, and PCA was conducted on these indicators (Table 2). The calculation of TN, TP, SOC, and SALPT shared common factor variances and weights (Supplementary Table S1).

According to the Soil Quality Index (SQI) calculation method, the SQI of different cultivated grasslands and control sites was calculated. The contributions of various evaluation indicators in the Multidimensional Scaling (MDS) analysis were analyzed based on the SQI of different treatments. The study reveals that the SQI of cultivated grasslands shows an increasing trend with the growth of management time, with the SQI of the grassland cultivated in the second year being the lowest. However, as the management time increases, the SQI of the cultivated grasslands gradually increases and in the tenth year (0.69 ± 0.06), significantly higher than the CK treatment (Figure 4b). From Figure 4c, it can be observed that the soil index of the entire dataset has a good linear relationship with the soil index from the Multidimensional Scaling (MDS) analysis ($R^2 = 0.957$, $P < 0.01$). This indicates that the soil quality assessment indicators based on MDS can serve as a substitute for the entire dataset in evaluating the soil quality of different cultivated grasslands in the study area.

4 Discussion

4.1 Cultivated grasslands' impact on soil nutrients and enzyme activity

From the perspective of soil total nitrogen content and nitrogen-cycling related enzyme activities, cultivated grassland

TABLE 2 Soil indicators load matrix and norm value of different treatments.

Indicator	Principal component				Norm	Grouping
	PC-1	PC-2	PC-3	PC-4		
TN	0.908	-0.089	-0.152	0.321	2.298	1
C Stock	0.904	0.216	-0.026	0.162	2.269	1
SUE	0.892	-0.138	-0.013	0.334	2.258	1
Bacteria Shannon	0.878	0.121	-0.197	0.128	2.200	1
SSC	0.784	0.361	-0.127	0.152	2.047	1
SCL	-0.746	-0.126	0.468	0.268	2.017	1
Fungi Shannon	0.729	0.433	-0.084	-0.410	2.028	1
TP	0.655	0.653	-0.114	-0.127	1.972	2
SAKP	-0.035	0.868	-0.186	-0.179	1.525	2
SCAT	-0.247	-0.789	-0.411	-0.257	1.640	2
ph	-0.115	-0.734	0.492	-0.044	1.482	2
SBD	-0.095	-0.080	0.956	0.095	1.483	3
SOC	0.581	0.183	-0.760	0.027	1.864	3
SBAX	0.121	-0.124	0.012	0.927	1.363	4
SALPT	0.531	0.270	0.219	0.710	1.744	4
Eigenvalue	6.059	2.889	2.305	2.009		
Ratio/%	40.396	19.263	15.366	13.393		
Cumulative percentage/%	40.396	59.659	75.025	88.418		

succession exhibited distinct patterns across different stages. In the early stages (2nd year), soil total nitrogen content, urease, and protease activities were significantly lower than in undegraded natural grasslands ($P< 0.05$). This decline is attributed to reduced vegetation cover and aboveground biomass, which limit nitrogen input and accelerate microbial nitrogen decomposition (Xu et al., 2025; Wu et al., 2024; Beniston et al., 2014). These effects are exacerbated by cultivation practices and soil erosion, further reducing soil nitrogen content (Ma Y. et al., 2024, von Lützow et al., 2006; Zhao Y. et al., 2024). However, as succession progresses, soil nitrogen content and enzyme activities (urease and protease) significantly recovered by the 6th and 10th years. This recovery is likely driven by increased nitrogen availability from plant residue decomposition, which enhances soil nitrogen content (De Rosa et al., 2024; Zhu et al., 2023). Additionally, improved soil microbial communities in cultivated grasslands may enhance nitrogen fixation (Xu R. et al., 2023; Ma R. et al., 2024). The increased enzyme activities indicate accelerated nitrogen cycling, benefiting plant nitrogen uptake and soil fertility (Feng et al., 2019; Xue et al., 2018).

Regarding total phosphorus, no significant changes in soil total phosphorus content were observed in the early stages compared to undegraded grasslands ($P< 0.05$). This is likely due to a balance between phosphorus input and consumption during the initial stages of Kentucky bluegrass cultivation (Sun X. et al., 2024). Despite the potential for phosphorus depletion due to cultivation practices and soil erosion, phosphorus levels were maintained through fertilization and soil weathering (Xu et al., 2024). Over time, the decomposition of plant residues continues to release mineral nutrients, increasing soil phosphorus content.

Soil organic carbon (SOC) and carbon stock showed significant reductions in the early stages of grassland succession. This change can be attributed to lower plant diversity, reduced plant input, and higher microbial decomposition rates of organic carbon (Samson et al., 2024). However, in the mid- and late stages of succession, as invasive species increased and plant diversity improved, underground carbon input also increased. This led to the accumulation of soil organic carbon, facilitated by root exudates and microbial activity (Wang A. et al., 2024; Lange et al., 2015). Additionally, changes in sucrase and basic xylanase activities indicate that, over time, the rate of organic matter decomposition in the soil accelerated, promoting soil fertility and microbial activity (Wang A. et al., 2020; Su et al., 2024).

In summary, the succession of cultivated grasslands significantly influences soil nutrients, carbon stock, and enzyme activities. Early succession is characterized by nutrient depletion and low enzyme activity, while longer recovery periods lead to increases in soil nitrogen, phosphorus, and carbon, alongside enhanced enzyme activity.

10.3389/fpls.2025.1510676

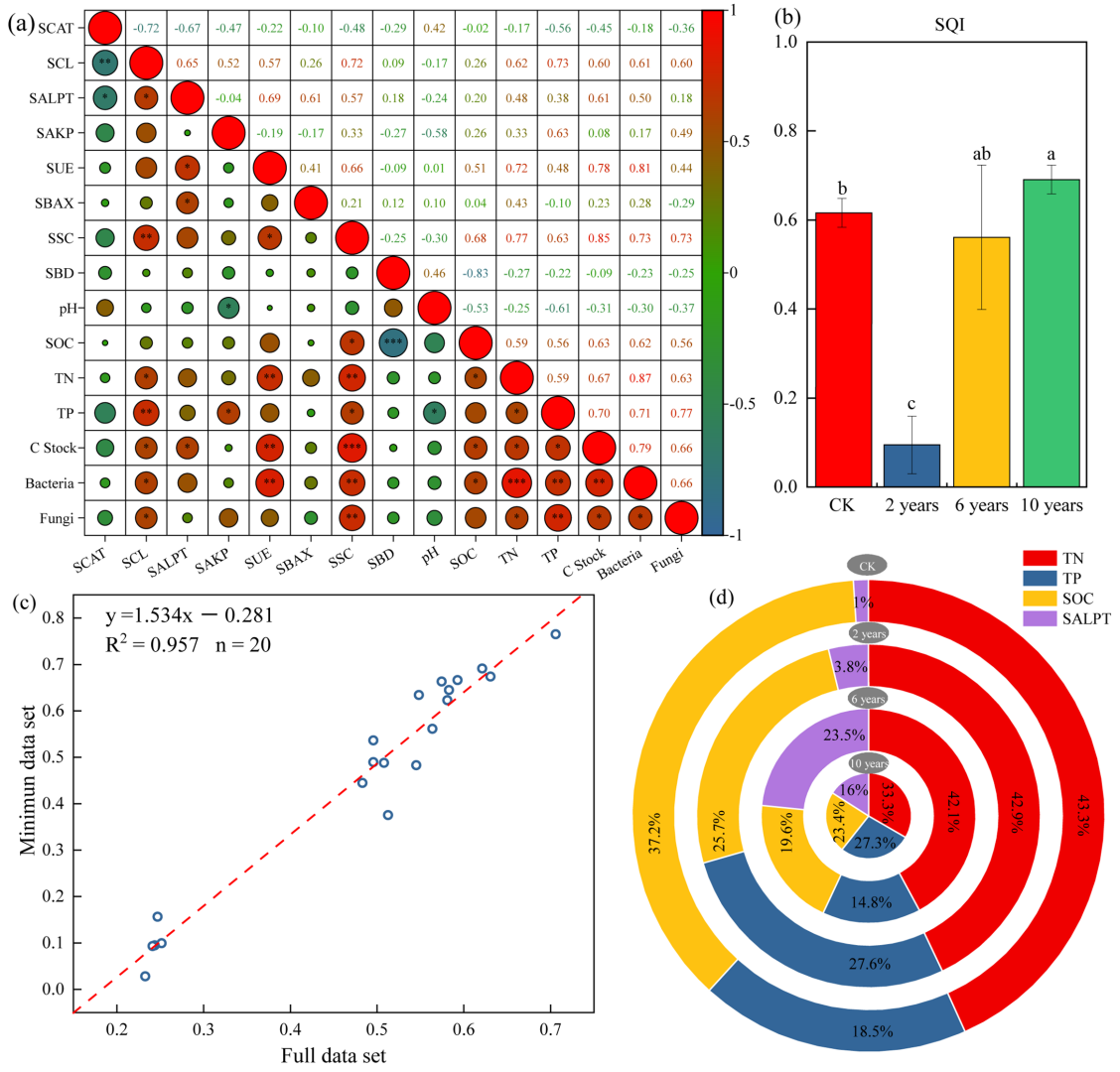

FIGURE 4
Soil quality index under different treatments. "*" in the figure indicates $P \leq 0.05$, "**" indicates $P \leq 0.01$, "***" indicates $P \leq 0.001$. **Panel (a)** represents the Pearson correlation of different soil indices. **Panel (b)** represents the soil quality index under different treatments. **Panel (c)** represents the linear relationship of the soil quality index based on MDS and the full data set. **Panel (d)** represents the percentage of different indicators in the soil quality index under different treatments.

4.2 Impact of cultivated grasslands on soil microbial community

Regarding microbial diversity, soil microbial richness, evenness, and Shannon diversity were lowest in the early stages of cultivated grassland succession. However, with increased recovery time, fungal communities showed significant improvements in richness, evenness, and Shannon diversity, reaching levels comparable to those of undegraded grasslands. In contrast, bacterial communities did not exhibit significant differences compared to natural grasslands. These findings suggest that long-term cultivation of Kentucky bluegrass can restore microbial community diversity and stability, particularly for fungal communities (Sun H. et al., 2024, Li et al., 2024).

Regarding bacterial community changes, in late-stage cultivated grasslands, the relative abundance of specific bacterial taxa shifted significantly. The abundance of *Acidobacteriota* and *Proteobacteria* decreased, while *Actinobacteriota* increased. This shift aligns with the *hypothesis* that increased soil nitrogen levels favor fast-growing bacterial groups such as Actinobacteriota, while slower-growing groups like *Acidobacteriota* and *Proteobacteria* decline (Chen et al., 2024; Pan et al., 2024; Coonan et al., 2020; Zhang et al., 2019). Our results support this trend, with soil nitrogen content increasing over time, accompanied by a decrease in *Acidobacteriota* and *Proteobacteria* and an increase in *Actinobacteriota* (Kielak et al., 2016; Li S. et al., 2024). Additionally, LEfSe analysis revealed that late-stage cultivated grasslands decreased the relative abundance of RB41, *Chthoniobacteraceae*, and *Candidatus Udaeobacter*, while increasing AKYG587. RB41 is involved in nitrogen fixation, and *Chthoniobacteraceae* plays a role in soil polysaccharide decomposition (Zou et al., 2024; Yang et al., 2024). AKYG587 is linked to organic matter decomposition and soil microbial community maintenance (Xing et al., 2020; Arellano-García et al., 2024). These

changes suggest that multi-year cultivation of Kentucky bluegrass enhances organic matter decomposition and bacterial community stability (Lin M. et al., 2023; Yusuf et al., 2021).

Regarding fungal diversity, *Mortierellomycota* initially increased but later decreased in abundance. This fungus plays a critical role in mineral phosphorus solubilization and nutrient availability (Liu et al., 2024; Baćmaga et al., 2024). The observed decline may result from a transition from sexual to asexual reproduction, which reduces phosphorus demand over time (Kruczyńska et al., 2023; Wang X. et al., 2024). Consistent with these findings, LEfSe analysis revealed that late-stage cultivated grasslands had lower relative abundances of *Mortierella, Actinomucor, Chaetomiaceae*, and *Fusicolla* compared to natural grasslands. *Mortierella* is involved in soil phosphorus cycling, while *Fusicolla* may form mycorrhizal relationships to enhance nutrient uptake (Ozimek and Hanaka, 2020; Shen et al., 2022).

In summary, the succession of cultivated grasslands promotes the diversity and stability of fungal and bacterial communities, with changes in community composition closely linked to soil nitrogen dynamics and organic matter decomposition.

4.3 Impact of cultivated grasslands on soil quality

Current soil quality evaluation methods, such as CASH (Comprehensive Assessment of Soil Health), HSHT (Haney Soil Health Test), and M-SQR (Muencheberg Soil Quality Rating), are widely used for assessing arable soil quality but have limitations when applied to grassland soils (Chang et al., 2022) (.Li et al., 2023; Zhao B. et al., 2024; Yu et al., 2018). Unlike croplands, the grasslands of the Qinghai-Tibet Plateau serve not only to meet livestock production demands but also to achieve ecological value. Therefore, this study assessed the soil quality of cultivated grasslands dominated by Kentucky bluegrass using a range of indicators that reflect ecosystem service functions, including soil bulk density, pH, carbon stock, soil organic carbon (SOC), total nitrogen (TN), total phosphorus (TP), nitrogen and carbon cycling enzymes, and microbial communities.

Results indicate that soil quality in cultivated grasslands improved with increasing recovery time, with late-stage grasslands showing significantly higher soil quality than natural grasslands. This suggests that multi-year cultivation substantially enhances soil quality compared to undegraded natural grasslands (climax communities). Analysis of the Soil Quality Index (SQI) revealed that total nitrogen content was the key factor influencing soil quality, contributing 33.3%–43.3% to the SQI (Figure 4d). During the early stages of succession, total phosphorus also contributed significantly to the SQI. These findings highlight the importance of nitrogen and phosphorus fertilization in improving soil quality in both natural and cultivated grasslands. Additionally, the proportion of SOC and TN in the SQI decreased with increasing management time, likely due to their gradual accumulation in the soil, which alleviates their limitations on Kentucky bluegrass growth.

4.4 Limitations and future research directions

This study utilized Nature-based Solutions (NbS) to investigate the effects of Kentucky bluegrass-dominated cultivated grasslands on soil quality, nutrient cycling, and microbial community dynamics. Cultivated grasslands, as an NbS, have demonstrated their ability to restore degraded ecosystems while providing multiple benefits, such as enhanced biodiversity and improved soil fertility. However, several limitations of this study highlight the need for further research to optimize the application of NbS in grassland restoration (Bardgett et al., 2021).

Firstly, this study employed a monoculture approach with Kentucky bluegrass. While this method demonstrated substantial improvements in soil quality over longer time scales, monoculture can lead to reduced plant community diversity and compromised stability. Future research should explore mixed sowing strategies that incorporate Kentucky bluegrass with other forage grasses, such as legumes, to enhance plant community diversity and stability while reducing the need for fertilizers.

Secondly, although the study initially explored the impact of Kentucky bluegrass on soil microbial community structure, revealing significant increases in fungal richness and stability, the specific mechanisms by which these microbial changes influence nutrient cycling and ecosystem functions remain unclear. Future research should delve deeper into the functional dynamics of soil microorganisms and the changes in soil metabolites to elucidate their direct and indirect impacts on soil quality.

Lastly, while the study identified soil total nitrogen and phosphorus as key indicators of soil quality, it did not validate the specific effects of fertilization on soil quality. Future research should further investigate the long-term impacts of different fertilization strategies on soil quality in grasslands to optimize management practices and enhance soil health.

In summary, although this study offers preliminary insights into the application of Kentucky bluegrass for grassland restoration, its limitations should not be overlooked. Future research should delve deeper into mixed sowing approaches, soil microbial functions, and the long-term impacts of fertilization strategies. This will help refine the management practices for using Kentucky bluegrass to restore degraded grasslands and enhance overall ecosystem health and sustainability.

5 Conclusion

This study demonstrates that Kentucky bluegrass progressively enhances soil fertility and improves microbial community structures over time. Detailed analysis of various stages of grassland recovery revealed that, in the early and mid-stages (2nd to 6th year), soil total nitrogen, total phosphorus, and organic carbon storage were lower compared to undegraded grasslands, with soil quality in the early stage ($P< 0.05$) being significantly lower. By the tenth year, Kentucky bluegrass substantially increased soil organic carbon, total nitrogen levels, and soil enzyme activities.

Compared to pristine natural grasslands, it also significantly supported healthier decomposition capabilities and the resilience of soil microbial communities. As recovery progresses, the soil quality of cultivated grasslands gradually surpasses that of undisturbed natural grasslands. Additionally, soil total nitrogen content emerges as a key determinant of soil quality for both natural and cultivated grasslands on the Qinghai-Tibet Plateau. Implementing appropriate nitrogen fertilization strategies can significantly benefit grassland development and enhance overall ecosystem health.

Data availability statement

The raw data supporting the conclusions of this article will be made available by the authors, without undue reservation.

Author contributions

SL: Conceptualization, Formal Analysis, Investigation, Methodology, Software, Writing – original draft, Writing – review & editing. ZS: Formal Analysis, Investigation, Visualization, Writing – review & editing. W-HL: Conceptualization, Data curation, Funding acquisition, Methodology, Supervision, Writing – review & editing. WL: Supervision, Validation, Writing – review & editing. GL: Data curation, Investigation, Software, Validation, Writing – review & editing. KL: Data curation, Visualization, Writing – review & editing.

Funding

The author(s) declare that financial support was received for the research and/or publication of this article. This study was supported by the Qinghai innovation platform construction project (2025) and the China Agriculture Research System (CARS-34).

Acknowledgments

We sincerely express our gratitude to the two funding for their support in conducting the experiments. At the same time, we extend our appreciation to the laboratory members for their assistance throughout the experimental process.

Conflict of interest

The authors declare that the research was conducted in the absence of any commercial or financial relationships that could be construed as a potential conflict of interest.

Generative AI statement

The author(s) declare that no Generative AI was used in the creation of this manuscript.

Publisher's note

All claims expressed in this article are solely those of the authors and do not necessarily represent those of their affiliated organizations, or those of the publisher, the editors and the reviewers. Any product that may be evaluated in this article, or claim that may be made by its manufacturer, is not guaranteed or endorsed by the publisher.

Supplementary material

The Supplementary Material for this article can be found online at: https://www.frontiersin.org/articles/10.3389/fpls.2025.1510676/full#supplementary-material

References

Arellano-García, L., Mendiola-Chávez, M., and Velázquez-Fernández, J. B. (2024). Nitrification of an anaerobic filter effluent in a flat sheet membrane aerated biofilm reactor. *Biochem. Eng. J.* 201, 109121. doi: 10.1016/j.bej.2023.109121

Baćmaga, M., Wyszkowska, J., Borowik, A., and Kucharski, J. (2024). Effect of previous crop on the structure of bacterial and fungal communities during the growth of vicia faba L. Spp. Minor. *Agriculture* 14, 370. doi: 10.3390/agriculture14030370

Bardgett, R. D., Bullock, J. M., Lavorel, S., Manning, P., Schaffner, U., Ostle, N., et al. (2021). Combatting global grassland degradation. *Nat. Rev. Earth Environ.* 2, 720–735. doi: 10.1038/s43017-021-00207-2

Beniston, J. W., DuPont, S.T., Glover, J. D., Lal, R., and Dungait, J. A. J. (2014). Soil organic carbon dynamics 75 years after land-use change in perennial grassland and annual wheat agricultural systems. *Biogeochemistry* 120, 37–49. doi: 10.1007/s10533-014-9980-3

Cao, J., Li, G., Adamowski, J. F., Holden, N. M., Deo, R. C., Hu, Z., et al. (2019). Suitable exclosure duration for the restoration of degraded alpine grasslands on the qinghai-tibetan plateau. *Land Use Policy* 86, 261–267. doi: 10.1016/j.landusepol.2019.05.008

Cao, J., Wang, H., Holden, N. M., Adamowski, J. F., Biswas, A., Zhang, X., et al. (2021). Soil properties and microbiome of annual and perennial cultivated grasslands on the qinghai–tibetan plateau. *Land Degradation Dev.* 32, 5306–5321. doi: 10.1002/ldr.4110

Chang, T., Feng, G., Paul, V., Adeli, A., Brooks, J. P., and Sparks, D. L. (2022). Soil Health Assessment Methods: Progress, Applications and Comparison. *Advances in Agronomy*. doi: 10.1016/bs.agron.2021.10.002

Chen, X., Wang, Y., Wei, H., and Zhang, J. (2024). Nitric acid rain decreases soil bacterial diversity and alters bacterial community structure in farmland soils. *Agronomy* 14, 971. doi: 10.3390/agronomy14050971

Coonan, E. C., Kirkby, C. A., Kirkegaard, J. A., Amidy, M. R., Strong, C. L., and Richardson, A. E. (2020). Microorganisms and nutrient stoichiometry as mediators of soil organic matter dynamics. *Nutrient Cycling Agroecosystems* 117, 273–298. doi: 10.1007/s10705-020-10076-8

De Rosa, D., Ballabio, C., Lugato, E., Fasiolo, M., Jones, A., and Panagos, P. (2024). Soil organic carbon stocks in european croplands and grasslands: how much have we lost in the past decade? *Global Change Biol.* 30, e16992. doi: 10.1111/gcb.16992

Dong, Q.-m., Ma, Y.-s., Xu, C.-j., Shi, J.-j., Wang, Y., Wang, Y.-l., et al. (2015). Study of classification and gradation, restoration of black-soil beach degraded grassland in the headwaters of three rivers. *Acta Agrestia Sin.* 23, 441. doi: 10.11733/j.issn.1007-0435.2015.03.001

Dong, Q.-M., Zhao, X.-Q., Wu, G.-L., Shi, J.-J., and Ren, G.-H. (2013). A review of formation mechanism and restoration measures of "black-soil-type" Degraded grassland in the qinghai-tibetan plateau. *Environ. Earth Sci.* 70, 2359–2370. doi: 10.1007/s12665-013-2338-7

Feng, C., Ma, Y., Jin, X., Wang, Z., Ma, Y., Fu, S., et al. (2019). Soil enzyme activities increase following restoration of degraded subtropical forests. *Geoderma* 351, 180–187. doi: 10.1016/j.geoderma.2019.05.006

Hua, T., Zhao, W., and Pereira, P. (2022). Opinionated views on grassland restoration programs on the qinghai-tibetan plateau. *Front. Plant Sci.* 13. doi: 10.3389/fpls.2022.861200

Johansson, A., Livsey, J., Guasconi, D., Hugelius, G., Lindborg, R., and Manzoni, S. (2024). Long-term soil organic carbon changes after cropland conversion to grazed grassland in southern Sweden. *Soil Use Manage.* 40, e13004. doi: 10.1111/sum.13004

Karlen, D. L., Andrews, S. S., Weinhold, B. J., and Doran, J. W. (2003). Soil quality: humankind's foundation for survival a research editorial by conservation professionals. *J. Soil Water Conserv.* 58, 171–179.

Kavana, P. Y., Kija, B. J., Reuben, E. P., Nkwabi, A. K., Mbwambo, B. N., Maijo, S. P., et al. (2024). Plant diversity in agro-pastoral grasslands of Tanzania. *IntechOpen*, 17–34. doi: 10.5772/intechopen.1003824

Kielak, A. M., Barreto, C. C., Kowalchuk, G. A., van Veen, J. A., and Kuramae, E. E. (2016). The ecology of acidobacteria: moving beyond genes and genomes. *Front. Microbiol.* 7. doi: 10.3389/fmicb.2016.00744

Kruczyńska, A., Kuźniar, A., Banach, A., Jurczyk, S., Podlewski, J., Słomczewski, A., et al. (2023). Changes in the mycobiome structure in response to reduced nitrogen fertilization in two cropping systems of maize. *Sci. Total Environ.* 904, 166343. doi: 10.1016/j.scitotenv.2023.166343

Lange, M., Eisenhauer, N., Sierra, C. A., Bessler, H., Engels, C., Griffiths, R. I., et al. (2015). Plant diversity increases soil microbial activity and soil carbon storage. *Nat. Commun.* 6, 6707. doi: 10.1038/ncomms7707

Li, X. (2012). *The Spatio-temporal Dynamics of Four Plant-functional Types (pfts) in Alpine Meadow as Affected By Human Disturbance, Sanjiangyuan Region, China* (Auckland: University of Auckland). Available at: http://hdl.handle.net/2292/19565 (Accessed April 20, 2024).

Li, Y., Hu, S., Lang, S., Pu, Y., Zhang, S., Li, T., et al. (2023). Soil quality and ecological benefits assessment of alpine desertified grassland following different ecological restoration measures. *Front. Plant Sci.* 14. doi: 10.3389/fpls.2023.1283457

Li, Y., Ma, J., Li, Y., Shen, X., and Xia, X. (2024). Microbial community and enzyme activity respond differently to seasonal and edaphic factors in forest and grassland ecosystems. *Appl. Soil Ecol.* 194, 105167. doi: 10.1016/j.apsoil.2023.105167

Li, S., Xiang, X., Shi, Z., Liu, W. H., Liang, G., Zhang, Y., et al. (2024). The impact of mixed planting of poaceae species in the qinghai-tibet plateau region on forage yield, soil nutrients, and soil microbial communities. *Front. Plant Sci.* 15. doi: 10.3389/fpls.2024.1370593

Li, G., Yang, T., Chen, R., Dong, H., Wu, F., Zhan, Q., et al. (2025). Experimental study on *in-situ* simulation of rainfall-induced soil erosion in forest lands converted to cash crop areas in dabie mountains. *PloS One* 20, e0317889. doi: 10.1371/journal.pone.0317889

Lin, Z.-y., Xiao, Y., and Ouyang, Z.-y. (2021). Assessment of ecological importance of the qinghai-tibet plateau based on ecosystem service flows. *J. Mountain Sci.* 18, 1725–1736. doi: 10.1007/s11629-020-6448-x

Lin, L., Xu, X., Cao, G., Zhang, F., Li, Y., Fan, B., et al. (2023). Synergies between microsites of plant communities and steady-stage alpine meadows on the qinghai–tibetan plateau. *Grassland Res.* 2, 289–298. doi: 10.1002/glr2.12057

Lin, M., Zhou, Y., Xu, R., Du, C., Wang, R., Lu, W., et al. (2023). Contrasting key bacteria and fungi related to sugar beet (beta vulgaris L.) with different resistances to beet rot under two farming modes. *Agronomy* 13, 825. doi: 10.3390/agronomy13030825

Liu, H., Liu, S., Wang, F., Liu, Y., Han, Z., Wang, Q., et al. (2023). Multilevel driving factors affecting ecosystem services and biodiversity dynamics on the qinghai-tibet plateau. *J. Cleaner Production* 396, 136448. doi: 10.1016/j.jclepro.2023.136448

Liu, D., Tian, B., Zhang, M., Jiang, L., Li, C., Qin, X., et al. (2025). Meta-analysis of the effects of different tillage methods on wheat yields under various conditions in China. *Soil Tillage Res.* 248, 106449. doi: 10.1016/j.still.2024.106420

Liu, X., Zhang, Y., Li, P., and Xiao, L. (2024). Siltation of check dams alters microbial communities and thus limits organic carbon mineralization. *Soil Tillage Res.* 236, 105949. doi: 10.1016/j.still.2023.105949

Ma, Y., Liu, Y., Rodrigo-Comino, J., López-Vicente, M., Shi, Z., and Wu, G.-L. (2024). Artificially cultivated grasslands decrease the activation of soil detachment and soil erodibility on the alpine degraded hillslopes. *Soil Tillage Res.* 243, 106176. doi: 10.1016/j.still.2024.106176

Ma, R., Tian, Z., Zhao, Y., Wu, Y., and Liang, Y. (2024). Response of soil quality degradation to cultivation and soil erosion: a case study in a mollisol region of northeast China. *Soil Tillage Res.* 242, 106159. doi: 10.1016/j.still.2024.106159

Mosier, A., Schimel, D., Valentine, D., Bronson, K., and Parton, W. (1991). Methane and nitrous oxide fluxes in native, fertilized and cultivated grasslands. *Nature* 350, 330–332. doi: 10.1038/350330a0

Nonxuba, C. S., Elephant, D. E., Nciizah, A. D., and Manyevere, A. (2025). Medium-term effects of tillage, crop rotation and crop residue management practices on selected soil physical properties in the sub-humid region of eastern cape, South Africa. *Soil Tillage Res.* 248, 106420. doi: 10.1016/j.still.2024.106420

Norderhaug, A., Clemmensen, K. E., Kardol, P., Thorhallsdottir, A. G., and Aslaksen, I. (2023). Carbon sequestration potential and the multiple functions of nordic grasslands. *Climatic Change* 176, 55. doi: 10.1007/s10584-023-03537-w

Ozimek, E., and Hanaka, A. (2020). Mortierella species as the plant growth-promoting fungi present in the agricultural soils. *Agriculture* 11, 7. doi: 10.3390/agriculture11010007

Palit, R., Gramig, G., and DeKeyser, E. S. (2021). Kentucky bluegrass invasion in the northern great plains and prospective management approaches to mitigate its spread. *Plants* 10, 817. doi: 10.3390/plants10040817

Pan, Y., Kang, P., Qu, X., Zhang, H., and Li, X. (2024). Response of the soil bacterial community to seasonal variations and land reclamation in a desert grassland. *Ecol. Indic.* 165, 112227. doi: 10.1016/j.ecolind.2024.112227

Paul, S., Parvez, SkS., Goswami, A., and Banik, A. (2024). Exopolysaccharides from agriculturally important microorganisms: conferring soil nutrient status and plant health. *Int. J. Biol. Macromolecules* 262, 129954. doi: 10.1016/j.ijbiomac.2024.129954

Pedrinho, A., Mendes, L. W., de Araujo Pereira, A. P., Araujo, A. S. F., Vaishnav, A., Karpouzas, D. G., et al. (2024). Soil microbial diversity plays an important role in resisting and restoring degraded ecosystems. *Plant Soil* 500, 325–349. doi: 10.1007/s11104-024-06489-x

Samson, V. M., Wei, Y., Guo, L., Liu, D., Heiling, M., Dercon, G., et al. (2024). Evaluation of long-term organic carbon dynamics and organic matter stability in a cultivated paddy soil using a carbon and nitrogen stable isotopes-based model. *Soil Tillage Res.* 239, 106040. doi: 10.1016/j.still.2024.106040

Shang, Z.-h., Dong, Q.-m., Shi, J.-j., Zhou, H.-k., Dong, S.-k., Shao, X.-q., et al. (2018). Research progress in recent ten years of ecological restoration for 'black soil land'degraded grassland on tibetan plateau——concurrently discuss of ecological restoration in Sangjiangyuan region. *Acta Agrestia Sin.* 26, 1. doi: 10.11733/j.issn.1007-0435.2018.01.001

Shen, M. C., Shi, Y. Z., Bo, G. D., and Liu, X. M. (2022). Fungal inhibition of agricultural soil pathogen stimulated by nitrogen-reducing fertilization. *Front. Bioengineering Biotechnol.* 10. doi: 10.3389/fbioe.2022.866419

Song, M., Guo, Y., Yu, F., Zhang, X., Cao, G., and Cornelissen, J. H. C. (2018). Shifts in priming partly explain impacts of long-term nitrogen input in different chemical forms on soil organic carbon storage. *Global Change Biol.* 24, 4160–4172. doi: 10.1111/gcb.14304

Song, G., Simpson, A. J., and Hayes, M. H. B. (2023). Compositional changes in the humin fraction resulting from the long-term cultivation of an irish grassland soil: evidence from FTIR and multi-NMR spectroscopies. *Sci. Total Environ.* 880, 163280. doi: 10.1016/j.scitotenv.2023.163280

Su, H., Zhang, Y., Wu, G., Chen, Z., Jiang, N., Qiu, W., et al. (2024). Effects of different maize residue managements on soil organic nitrogen cycling in different soil layers in northeast China. *Gcb Bioenergy* 16, e13123. doi: 10.1111/gcbb.13123

Sun, X., Amelung, W., Klumpp, E., Walk, J., Mörchen, R., Böhm, C., et al. (2024). Fog controls biological cycling of soil phosphorus in the coastal cordillera of the Atacama Desert. *Global Change Biol.* 30, e17068. doi: 10.1111/gcb.17068

Sun, H., Liu, J., Wu, J., Hu, H., Chen, Q., Fang, H., et al. (2024). Effects of alpine grassland degradation on soil microbial community structure and metabolic activity in the qinghai-tibet plateau. *Appl. Soil Ecol.* 200, 105458. doi: 10.1016/j.apsoil.2024.105458

Tian, W., Zhang, G., Zhang, X., and Dong, Y. (2018). PCA weight and Johnson transformation based alarm threshold optimization in chemical processes. *Chin. J. Chem. Eng.* 26, 1653–1661. doi: 10.1016/j.cjche.2017.10.027

Tomazelli, D., dos Santos Peron, R. A., Mendes, S. D. C., Pinto, C. E., Baldissera, T. C., Baretta, D., et al. (2024). Plant diversity and root traits shape rhizosphere microbial communities in natural grasslands and cultivated pastures. *Rhizosphere* 29, 100864. doi: 10.1016/j.rhisph.2024.100864

von Lützow, M., Kögel-Knabner, I., Ekschmitt, K., Matzner, E., Guggenberger, G., Marschner, B., et al. (2006). Stabilization of organic matter in temperate soils: mechanisms and their relevance under different soil conditions–a review. *Eur. J. Soil Sci.* 57, 426–445. doi: 10.1111/j.1365-2389.2006.00809.x

Wang, X.-y., Hu, T.-m., Wang, Q.-z., Tian, L.-m., Zhang, X.-l., and Tian, K. (2009). Growth of kentucky bluegrass as influenced by nitrogen and trinexapacethyl. *Agric. Sci. China* 8, 1498–1502. doi: 10.1016/S1671-2927(08)60364-8

Wang, C., Tang, Y., Li, X., Zhang, W., Zhao, C., and Li, C. (2020). Negative impacts of plant diversity loss on carbon sequestration exacerbate over time in grasslands. *Environ. Res. Lett.* 15, 104055. doi: 10.1088/1748-9326/abaf88

Wang, L., Xie, X., Li, Q., Yu, Z., Hu, G., Wang, X., et al. (2022). Accumulation of potentially toxic trace elements (ptes) by native plant species growing in a typical gold mining area located in the northeast of qinghai-tibet plateau. *Environ. Sci. pollut. Res.* 29, 6990–7000. doi: 10.1007/s11356-021-16076-7

Wang, W., Yang, Y., Li, J., Bu, P., Lu, A., Wang, H., et al. (2024). Consecutive fertilization-promoted soil nutrient availability and altered rhizosphere bacterial and bulk fungal community composition. *Forests* 15, 514. doi: 10.3390/f15030514

Wang, A., Zhang, Y., Wang, G., and Zhang, Z. (2024). Soil physicochemical properties and microorganisms jointly regulate the variations of soil carbon and nitrogen cycles along vegetation restoration on the loess plateau, China. *Plant Soil* 494, 413–436. doi: 10.1007/s11104-023-06290-2

Wang, X., Zhang, C., Zhao, N., Sun, X., Hou, S., and Wang, P. (2024). Physiological nitrogen uptake and utilisation responses in two native plants from the qinghai-tibet plateau under different water and fertiliser conditions. *Agronomy* 14, 440. doi: 10.3390/agronomy14030440

Wei, L., Zhang, C., Dong, Q., Yu, Y., and Yang, X. (2020). Characterization of the complete chloroplast genome of poa pratensis L. Cv. Qinghai (gramineae). *Mitochondrial DNA Part B* 5, 532–533. doi: 10.1080/23802359.2019.1710276

Wu, J.-l., Shi, J.-j., Wang, X.-l., Zhao, Z.-z., Wang, Y.-l., Wang, H.-b., et al. (2023). Analysis of soil management effect of different measures on "bare land of mountain" in the three rivers source region. *Acta Agrestia Sin.* 31, 220. doi: 10.11733/j.issn.1007-0435.2023.01.026

Wu, Y., Wang, P., Hu, X., Li, M., Ding, Y., Peng, T., et al. (2024). Plant diversity, productivity, and soil nutrient responses to different grassland degradation levels in Hulunbuir, China. *Land* 13, 2001. doi: 10.3390/land13122001

Xing, W., Wang, Y., Hao, T., He, Z., Jia, F., and Yao, H. (2020). pH control and microbial community analysis with HCl or CO_2 addition in H2-based autotrophic denitrification. *Water Res.* 168, 115200. doi: 10.1016/j.watres.2019.115200

Xu, S., Gu, C., Rodrigues, J. L. M., Li, C., Bohannan, B., Nüsslein, K., et al. (2024). Soil phosphorus cycling across a 100-year deforestation chronosequence in the amazon rainforest. *Global Change Biol.* 30, e17077. doi: 10.1111/gcb.17077

Xu, X., Jin, Y., Xu, J., Zhang, Y., and Yang, J. (2025). Effects of herbaceous plant encroachment on the soil carbon pool in the shrub tundra of the Changbai mountains. *Forests* 16, 197. doi: 10.3390/f16020197

Xu, Z., Li, X., and Zhang, L. (2023). A bibliometric analysis of research trends and hotspots in alpine grassland degradation on the qinghai-tibet plateau. *Peerj* 11, e16210. doi: 10.7717/peerj.16210

Xu, R., Shi, W., Kamran, M., Chang, S., Jia, Q., and Hou, F. (2023). Grass-legume mixture and nitrogen application improve yield, quality, and water and nitrogen utilization efficiency of grazed pastures in the loess plateau. *Front. Plant Sci.* 14. doi: 10.3389/fpls.2023.1088849

Xue, W., Peng, Z., Huang, D., Zeng, G., Wan, J., Xu, R., et al. (2018). Nanoremediation of cadmium contaminated river sediments: microbial response and organic carbon changes. *J. Hazardous Materials* 359, 290–299. doi: 10.1016/j.jhazmat.2018.07.062

Yang, Y., Liu, L., Liu, X., Ma, Q., and Liu, J. (2024). Impact of maize growth stage on soil bacterial communities and functions in dryland under P fertilization: a comprehensive analysis. *J. Soil Sci. Plant Nutr.* 16, 1–11. doi: 10.1007/s42729-024-01619-x

Yao, L., Guo, N., He, Y., Xiao, Y., Li, Y., Gao, J., et al. (2021). Variations of soil organic matters and plant cuticular waxes along an altitude gradient in qinghai-tibet plateau. *Plant Soil* 458, 41–58. doi: 10.1007/s11104-019-04304-6

Yu, P., Han, D., Liu, S., Wen, X., Huang, Y., and Jia, H. (2018). Soil quality assessment under different land uses in an alpine grassland. *Catena* 171, 280–287. doi: 10.1016/j.catena.2018.07.021

Yusuf, M., Fernandes, A. A. R., Kurniawan, S., and Arisoesilaningsih, E. (2021). Spatial variation of soil bacteria communities and its alpha diversity as a potential bioindicator of land degradation. *J. Degraded Min. Lands Manage.* 8, 2847. doi: 10.15243/jdmlm.2021.084.2847

Zhang, Z., Han, J., Yin, H., Xue, J., Jia, L., Zhen, X., et al. (2022). Assessing the effects of different long-term ecological engineering enclosures on soil quality in an alpine desert grassland area. *Ecol. Indic.* 143, 109426. doi: 10.1016/j.ecolind.2022.109426

Zhang, F. W., Li, H. Q., Yi, L. B., Luo, F. L., Zhang, G. R., Wang, C. Y., et al. (2022). Spatial response of topsoil organic carbon, total nitrogen, and total phosphor content of alpine meadows to grassland degradation in the Sanjiangyuan national park. *Acta Ecol. Sin.* 14, 1–8. doi: 10.5846/stxb202106111566

Zhang, M., Sun, J., Wang, Y., Li, Y., and Duo, J. (2024b). State-of-the-art and challenges in global grassland degradation studies. *Geogr. Sustainability* 6, 100229. doi: 10.1016/j.geosus.2024.08.008

Zhang, B., Wu, X., Tai, X., Sun, L., Wu, M., Zhang, W., et al. (2019). Variation in actinobacterial community composition and potential function in different soil ecosystems belonging to the arid Heihe river basin of northwest China. *Front. Microbiol.* 10. doi: 10.3389/fmicb.2019.02209

Zhang, Q., Yuan, R., Singh, V. P., Xu, C.-Y., Fan, K., Shen, Z., et al. (2022). Dynamic vulnerability of ecological systems to climate changes across the qinghai-tibet plateau, China. *Ecol. Indic.* 134, 108483. doi: 10.1016/j.ecolind.2021.108483

Zhao, B., Gao, R., Zhang, X., Xia, L., Zhang, L., Xia, D., et al. (2024). Comparison of soil quality assessment methods for different vegetation eco-restoration techniques at engineering disturbed areas. *Peerj* 12, e18033. doi: 10.7717/peerj.18033

Zhao, X., Xu, S., Zhao, L., Zhang, T., Hu, L., Li, Q., et al. (2023). Innovation and practice on biodiversity conservation in Sanjiangyuan national park. *Bull. Chin. Acad. Sci. (chinese Version)* 38, 1833–1844. doi: 10.16418/j.issn.1000-3045.20230920004

Zhao, W., Yin, Y., Li, S., Liu, Y., Liu, J., and Wang, Y. (2020). Effects of vegetation reconstruction on vegetation and microbial community characteristics of black soil beach grassland. *Ecol. Environ.* 29, 71. doi: 10.16258/j.cnki.1674-5906.2020.01.008

Zhao, Y., Zhang, M., Liu, Z., and Yang, F. (2024). Migration and transformation of soil phosphorus by organic acids: a global meta-analysis. *J. Soils Sediments* 24, 589–602. doi: 10.1007/s11368-023-03665-x

Zhu, L., Dong, S. K., Wen, L., Li, Y. L., Shi, J. J., Wang, Y. L., et al. (2010). Effect of cultivated pasture on recovering soil nutrient of "black-beach" in the alpine region of headwater areas of qinghai-tibetan plateau, China. *Proc. Environ. Sci.* 2, 1355–1360. doi: 10.1016/j.proenv.2010.10.146

Zhu, N., Yan, Y., Bai, K., Zhang, J., Wang, C., Wang, X., et al. (2023). Conversion of croplands to shrublands does not improve soil organic carbon and nitrogen but reduces soil phosphorus in a temperate grassland of northern China. *Geoderma* 432, 116407. doi: 10.1016/j.geoderma.2023.116407

Zou, Y., Chen, X., Zhang, S., Zhang, B., Bai, Y., Zhang, T., et al. (2024). Co-applied biochar and PGPB promote maize growth and reduce CO_2 emission by modifying microbial communities in coal mining degraded soils. *J. Environ. Manage.* 354, 120280. doi: 10.1016/j.jenvman.2024.120280

frontiers | Frontiers in Plant Science

TYPE Original Research
PUBLISHED 15 May 2025
DOI 10.3389/fpls.2025.1567414

OPEN ACCESS

EDITED BY
Ting Hua,
Norwegian University of Science and Technology, Norway

REVIEWED BY
Yanfu Bai,
Sichuan Agricultural University, China
Weiwei Wang,
Guizhou University, China

*CORRESPONDENCE
Lihua Tian
lhtian@yeah.net

RECEIVED 27 January 2025
ACCEPTED 22 April 2025
PUBLISHED 15 May 2025

CITATION
Xue G, Tian L and Zhao J (2025) Effects of simulated warming and litter removal on structure and function of semi-humid alpine grassland in the Qinghai-Tibet Plateau. *Front. Plant Sci.* 16:1567414. doi: 10.3389/fpls.2025.1567414

Effects of simulated warming and litter removal on structure and function of semi-humid alpine grassland in the Qinghai-Tibet Plateau

Guomin Xue[1], Lihua Tian[1]* and Jingxue Zhao[2]

[1]Sichuan Zoige Alpine Wetland Ecosystem National Observation and Research Station, and College of Grassland Resources, Southwest Minzu University, Chengdu, China, [2]State Key Laboratory of Herbage Improvement and Grassland Agro-Ecosystems, and College of Ecology, Lanzhou University, Lanzhou, China

Climate warming and human activities are modifying plant litter inputs in alpine grasslands, which is predicted to affect ecosystem structure and function. However, the effects of plant litter removal and warming as well as the combined impacts on the ecological functions of alpine grasslands are not well understood. A field experiment was conducted to investigate the effects of experimental warming, litter removal, and their interaction on ecosystem multifunctionality (EMF) of alpine grasslands. Our results demonstrated a significant decrease in plant diversity ($p < 0.05$) and vegetation cover ($p < 0.01$) under experimental warming treatment, whereas the richness index (R) and belowground biomass (BGB) significantly increased under litter removal treatment ($p < 0.05$). The interaction effect of experimental warming and litter removal results in a neutralizing effect on the ecological functions in alpine grasslands. Meanwhile, the EMF tended to increase under all treatments of experimental warming, litter removal, and experimental warming-litter removal. However, there are differences in the response of aboveground and belowground multifunctionality to experimental warming and litter removal. The aboveground ecosystem multifunctionality (AEMF) showed a decreasing trend, while belowground ecosystem multifunctionality (BEMF) increased significantly ($p < 0.01$) under the experimental warming treatment. In contrast, AEMF and BEMF showed an increasing trend in litter removal treatment. In addition, the study found that litter removal could alleviate the negative effect of experimental warming on multiple ecological functions. These research findings can serve as a reference for maintaining ecosystem functions in alpine grasslands under climate change conditions and provide effective measures to enhance the capacity of grassland ecosystems to respond to climate change. The application of appropriate litter management measures and other nature-based solutions (NbS) to improve ecosystem functions, aiming to adopt sustainable approaches to address environmental challenges, holds significant importance for ecological conservation.

KEYWORDS

alpine grasslands, experimental warming, ecosystem multifunctionality, litter removal, plant diversity

Highlights

- Litter removal could alleviate the negative effect of experimental warming on aboveground ecosystem multifunctionality.
- There are differences in the response of aboveground and belowground multifunctionality to experimental warming and litter removal.
- Changes in ecosystem functioning due to experimental warming and litter removal are primarily driven by plant diversity, productivity, and soil nutrients.

1 Introduction

The interference of climate change affects ecosystem functions, specifically reflected in the relationship between climate-determined ecosystem functions and their driving factors (Jing et al., 2015). Similarly, global temperature changes, drought severity, and historical climate are important driving factors for ecosystem functioning (Ye et al., 2019). In the background of temperature changes, community structure and composition serve as the foundation of ecosystem functions, specifically reflected in changes in vegetation species and functional diversity, which may affect the potential ecosystem feedback to climate change (Ganjurjav et al., 2018; Shangguan et al., 2024). The relevant research indicated that warming affects plant growth and development by altering soil water and temperature, which in turn changes interspecies relationships within communities (Niu and Wan, 2008), consequently affecting the structure and composition of plant communities (Young et al., 2024). Among others, warming can affect soil moisture conditions and further contribute to the reduction of ecosystem functions through a decrease in plant diversity and vegetation productivity (Ma et al., 2023). Studies also indicated that the changes in temperature affect ecosystem functioning by altering the composition of grassland plant communities (Zhu et al., 2024). More specifically, warming affects grassland primary productivity by influencing plant community composition (Zhu et al., 2016), and this further affects the ecosystem functioning.

The global grasslands are not only experiencing severe climate change, but also withstanding high-intensity grazing activities (Fekete et al., 2016). Grazing is the main utilization method for grassland ecosystems, and long-term overgrazing will significantly compromise the functioning and structure of grassland ecosystems by reducing biodiversity, litter inputs, and plant productivity (Liu et al., 2023a). Meanwhile, the accumulation of litter was always considered a limiting factor for plant symbiotic structures and an important link between productivity, community, and ecosystem processes. A previous study suggested that overgrazing impacts on grassland ecosystem functions are mainly influenced by the reduction of litter inputs (Weltzin et al., 2005). Specifically, the indirect impact of grazing on plant communities is achieved by the litter removal, which leads to changes in species composition (Wang et al., 2011). Human disturbances such as burning and grazing combined with climate change factors like drought can significantly reduce plant litter production, thereby modifying plant diversity and subsequently affecting productivity and ecosystem functions (Zhang et al., 2023a; Liu et al., 2023b). Changes in plant litter can also impact ecosystem function by regulating soil temperature, moisture, and nutrient availability (Liu et al., 2023c). Specifically, litter removal can affect ecosystem functions through reductions in soil temperature and alterations in soil carbon and nitrogen content (Yan et al., 2018; Osborne et al., 2021). Sustainable management and nature restoration measures such as moderate grazing and litter removal can be incorporated into Nature-based Solutions (NbS). Studies have suggested that such restoration measures can enhance ecosystems by reducing external disturbances while leveraging ecosystem resilience and natural succession (Hua et al., 2022). However, the impact of reduced plant litter on ecosystem function is easily confused with the impacts of other disturbances (Chen et al., 2024). Therefore, it is crucial to understand how the loss of plant litter affects the response of grasslands to warming.

The Qinghai-Tibetan Plateau (QTP) is a key ecological region in China, with alpine grasslands representing its most important ecosystem. In recent years, the alpine grasslands on the QTP have been experiencing more rapid climate warming and higher-intensity livestock grazing than the global average rates (Yang et al., 2014), leading to a substantial impact on ecosystem functions. The alpine grassland ecosystem on the QTP is becoming increasingly vulnerable (Wang et al., 2024). Studies have shown that experimental warming significantly impacts the biological processes, structures, and functions in alpine grasslands (Liu et al., 2018; Zhao et al., 2019, 2024). Meanwhile, ecological functions are negatively responded to the accumulation of plant litter (Zhang et al., 2022). The accumulation of litter in grassland ecosystems influences community productivity, diversity, and species composition by affecting soil moisture and temperature (Hou et al., 2019), further impacting the ecosystem functions of alpine grasslands. Early research primarily focused on single ecosystem functions, such as productivity, litter decomposition, soil nutrients, and biodiversity. However, real-world ecosystems can provide multiple ecosystem functions simultaneously, with complex interactions such as promotion or antagonism occurring between these ecosystem functions (Byrnes et al., 2014). Therefore, ecologists have proposed the concept of ecosystem multifunctionality (EMF) in recent years, and research on the relationship between biodiversity and EMF has gradually increased (Van Der Plas, 2019; Duffy et al., 2017). Nevertheless, most research on multiple ecosystem functions has focused on overall EMF. The effects of warming, litter removal treatments, and their interactions on the functioning of the aboveground and belowground ecosystems remain largely unknown.

In this study, we hypothesize that experimental warming will decrease ecosystem functions, while litter removal will mitigate these effects by improving plant diversity, productivity, and soil conditions. Field experiments were conducted to investigate the effects of experimental warming and litter removal on the ecosystem structure and function of alpine grassland using four different treatments: control, experimental warming, litter removal, and experimental warming-litter removal. The main purpose of this

study is to determine the changes in the aboveground and belowground ecological functions of alpine grasslands caused by experimental warming and litter removal, as well as their interaction, and to explore the key factors affecting the dynamic changes in ecological functions. This study is of great significance for understanding the impacts of global climate change and human activities on the ecological function of alpine grasslands, while providing measures and a theoretical basis for adopting natural restoration measures to improve ecosystems.

2 Materials and methods

2.1 Site description

The study was conducted at the Sichuan Zoige Alpine Wetland Ecosystem National Observation and Research Station, located in Hongyuan County, Sichuan Province, on the eastern edge of the QTP (Figure 1). The average altitude of the region is 3,507 m, and the average annual temperature is 1.5°C. January is the coldest month, with an average temperature of -9.5°C, while July is the hottest month, averaging 11°C. The annual rainfall reaches 749 mm, and 80% of the rain falls between May and September. The dominant vegetation species including *Anemone rivularis, Elymus nutans*, *Agrostis gigantea*, *Carex setschwanensis*, *Carex parvula*, *Oxytropis kansuensis*, and *Koeleria cristata*. The main soil type is alpine meadow soil, with a high organic matter content and a weakly acidic pH.

2.2 Experimental design

In November 2018, we conducted a rigorous field survey to select a typical homogeneous area representing the main characteristics of alpine meadows. Subsequently, we established a randomized complete block design experiment with experimental warming and litter removal treatments, and annual monitoring was conducted from 2019 to 2023. In this experiment, open-top chambers (OTCs) were used to simulate climate warming. The OTCs are constructed from polycarbonate panels (transmittance >95%), which enhance the penetration of solar radiation through the transparent panels while blocking wind to minimize heat loss, thereby achieving a warming effect, and the average surface temperature within the warming range of the OTCs increased by 1.31 (± 0.3) °C compared to the control. The experiment has 4 treatments (CK, W, L, WL, representing control, experimental warming, litter removal, and experimental warming-litter removal, respectively) and 5 replicates. The experimental area was divided into 20 quadrats (4 treatments × 5 replicates), each with an area of 4 m^2 (2 m × 2 m). The litter removal treatment was carried out annually during the withering period, with both upright and fallen plant litter removed completely in each litter removal plot and the experimental warming-litter removal plot.

2.3 Vegetation and soil sampling

A field vegetation community survey and soil sampling were conducted during the peak period of the growing season from 2021

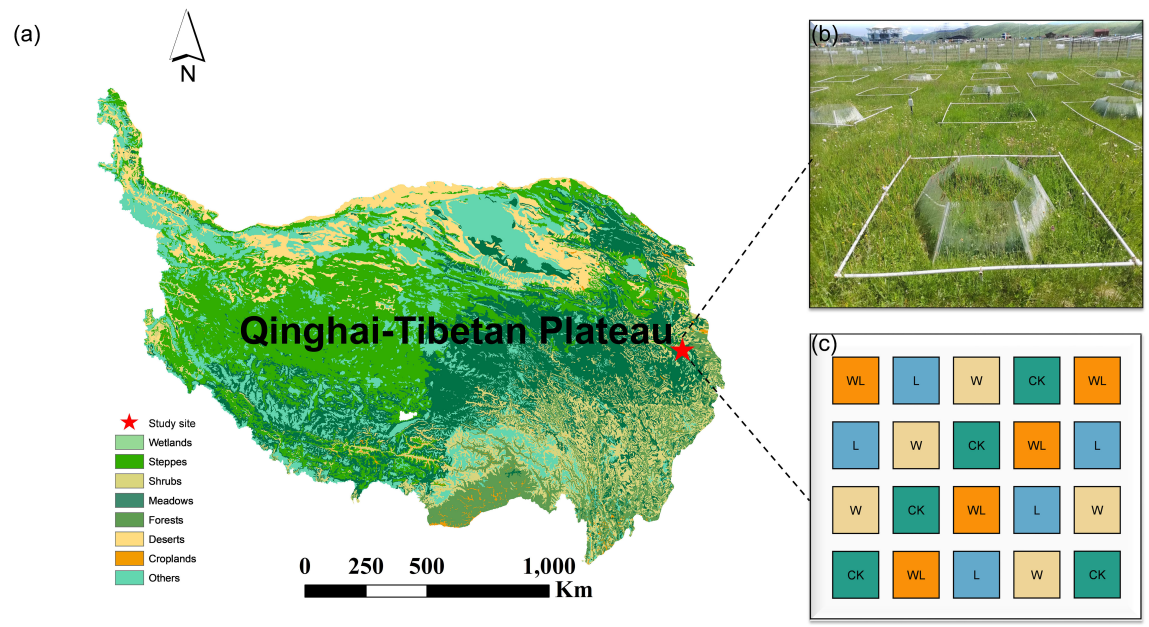

FIGURE 1
(a) Location of study area in Hongyuan county on the eastern Qinghai-Tibetan Plateau. **(b)** The landscape of the present litter removal, experimental warming and experimental warming-litter removal treatments experiment. **(c)** The experimental design of the litter removal, experimental warming and experimental warming-litter removal treatments.

to 2023. Individual plants were identified at the species level in each of the quadrats. The coverage and natural height of each species were measured for each species within the sample quadrat. After the vegetation community survey, aboveground plant tissue was harvested from the sample quadrat to obtain the aboveground biomass (AGB). The soil samples were collected using a soil drill and sieved through a 2 mm mesh, and the root systems were subsequently washed with flowing water for belowground biomass (BGB) calculation. The AGB and BGB samples were weighed after oven-drying for 48 h at 65°C.

Bulk density was taken by a bulk density drill, and the soil moisture content (SM) was oven-dried to a constant weight treatment at 105°C for 72 hours. Soil samples of 0–10 cm depths were collected from the four corners of the quadrats for measurement of soil inorganic nitrogen (NH_4^+–N; NO_3^-–N), soil pH (pH), soil total nitrogen (STN), soil organic matter (SOM). The soil pH was measured with a pH meter. The SOC and STN contents were measured using the elementary analyzer (Vario EL III, Elementar, Germany). Soil NH_4^+–N and NO_3^-–N contents were determined by auto-analyzer (Auto Analyzer 3, Bran Luebbe, Germany).

2.4 Statistical analysis

Plants were divided into three functional groups, including grasses, sedges, and forbs, to evaluate the impact of treatment on these functional groups.

The importance value (IV), species richness index *(R)*, and plant diversity index *(H)* were used as indicators of plant biodiversity and were calculated as follows:

IV:

$$\mathbf{IV} = \frac{\boldsymbol{RH} + \boldsymbol{RC}}{\mathbf{2}}$$

where *RC and RH* represent the mean values of relative cover and relative height.

Species richness index (*R*):

$$\boldsymbol{R} = \boldsymbol{S}$$

Plant diversity index (*H*):

$$\boldsymbol{H} = -\sum_{i=1}^{S}(\boldsymbol{pi}\ln \boldsymbol{pi})$$

where *S* represents the total number of species, *Pi* is the relative IV of the *i*th species.

To evaluate the differences in ecosystem function between litter removal and experimental warming treatments more accurately, we employed a Random Forest method to identify the ecological factors that contribute significantly to EMF. The results indicated that height, Cover, *R*, *H*, STN, SOM, NH_4^+–N, and pH are the primary predictors of ecosystem functions (Supplementary Figure S5). Thus, the aboveground ecosystem multifunctionality (AEMF) index was calculated by height, Cover, *R*, and *H*, while the belowground ecosystem multifunctionality (BEMF) index was calculated by STN, SOM, NH_4^+–N, and pH. Finally, these primary predictor factors were utilized to calculate the EMF index. The EMF index can be calculated in the following way (Maestre et al., 2012):

$$\boldsymbol{EMF} = \frac{\mathbf{1}}{\mathbf{N}}\sum_{i=1}^{N}\boldsymbol{f}(\boldsymbol{x_i})$$

where N represents the number of functions and f(x_i) is the standardization of the measured value obtained by:

$$\boldsymbol{f(xi)} = (\boldsymbol{x_i} - \boldsymbol{x_{mean}})/\boldsymbol{std}$$

where x_i, x_{mean} and *std* represents the measured value, mean value and standard deviation of all observations, respectively.

Structural equation modeling (SEM) was used to examine the direct and indirect effects of experimental warming treatment, litter removal treatment, plant productivity, plant diversity, and soil nutrients on EMF. Duncan method was used to analyze the significant differences in height, cover, IV, plant community characteristics, and soil physicochemical factors among different functional groups under various treatment conditions. Two factors analysis of variance was used to analyze the effects of experimental warming, litter removal, and their interaction on plant community characteristics and soil physicochemical factors. Pearson correlation is used to evaluate the relationship between individuals and multiple ecological functions. The SEM models were conducted using the AMOS 26 software, while other statistical analyses were executed using the SPSS 24.0 software. Graphics were accomplished using the Origin 2021 software.

3 Results

3.1 Plant community composition and structure under experimental warming, litter removal and experimental warming-litter removal

The experimental warming treatment, experimental warming-litter removal treatment, and the control were dominated by *Elymus dahuricus*, with relative important values (IV) of 0.23, 0.18, and 0.13, respectively. However, litter removal treatment is primarily dominated by *Agrostis matsumurae*, with the IV of 0.12. In terms of functional groups, the grasses exhibited the highest dominance in control and experimental warming treatment, while the forbs exhibited the highest dominance in litter removal and experimental warming-litter removal treatment (Figure 2a). Overall, experimental warming, litter removal, and experimental warming-litter removal treatments all caused changes in each functional group. Specifically, compared with the control, experimental warming treatment resulted in a significant decrease in the height and cover of the sedges ($p < 0.05$) and a significant increase in the IV and cover of grasses ($p < 0.05$; Supplementary Figure S4a). The litter removal treatment led to a significant decrease in the height of the sedges ($p < 0.05$), while at the same time causing a significant increase in the cover of the forbs ($p < 0.001$; Supplementary Figure S4b). Experimental warming-litter removal treatment resulted in a significant decrease in the cover of sedges ($p < 0.05$), while simultaneously leading to a significant increase in the cover and IV of grasses ($p < 0.05$; Supplementary Figure S4c).

10.3389/fpls.2025.1567414

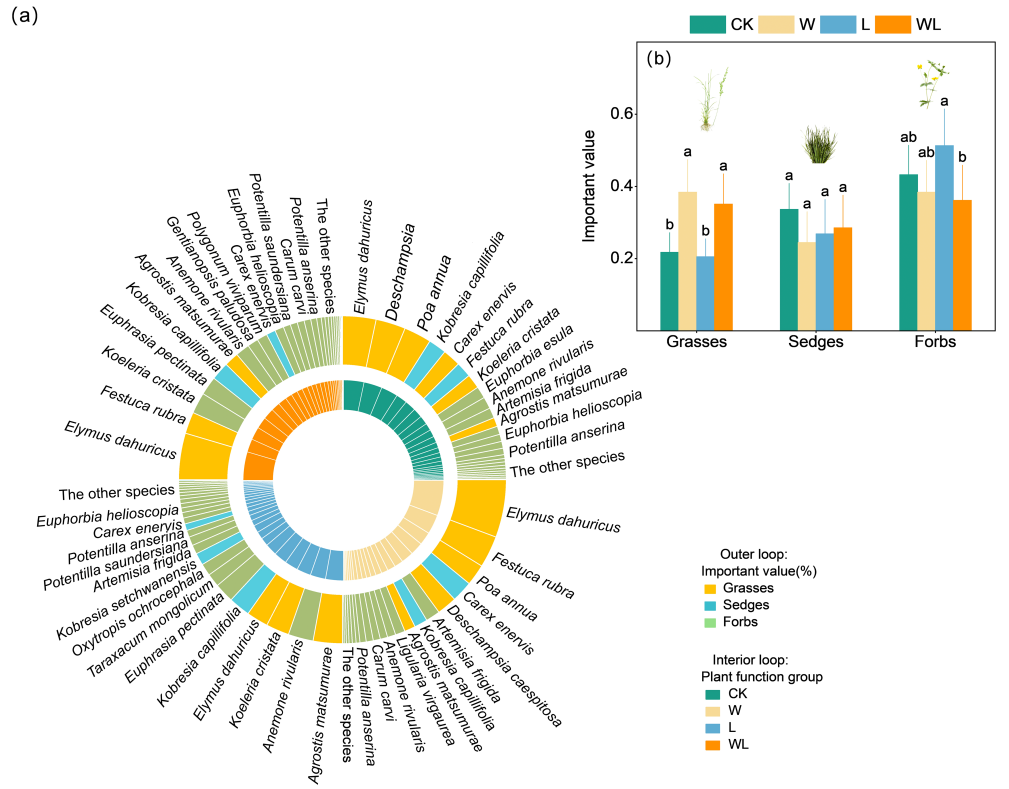

FIGURE 2
(a) The species and functional groups found in the present study. The colors of the internal loop represent the control (CK), experimental warming (W), litter removal (L) and experimental warming-litter removal (WL) treatments. In panel **(b)**, the colors of the external loop show the plant functional groups including sedges, grasses, and forbs. The areas of the loop segments are proportional to the relative importance value of each species. Different letters indicate significant differences among treatments.

The response of vegetation cover, height, AGB, BGB, *R*, and *H* to experimental warming treatment and litter removal treatment are inconsistent. Specifically, our results demonstrated a significant decrease in *R*, *H* ($p < 0.05$), and vegetation cover ($p<0.01$) under experimental warming treatment, with the average results showing that experimental warming treatment decreased the Cover, *R*, and *H* by an average of 7%, 17% and 10% (Figures 3, 4). And the Height, AGB, BGB showed upward trend under experimental warming treatment (Supplementary Figure S1). The *R* and BGB significantly increased under litter removal treatment ($p < 0.05$; Figure 4). Litter removal treatment increased the *R* and BGB by an average of 25% and 49%, respectively (Figure 3). And the Height decreased, while Cover, *H*, and AGB showed an upward trend under litter removal treatment. The Height, Cover, *R*, *H*, AGB, and BGB all increased, but did not reach a significant level under experimental warming-litter removal treatment (Supplementary Figure S1).

3.2 Soil physical and chemical properties following experimental warming, litter removal and experimental warming-litter removal

The response of SOM, STN, NH_4^+–N, NO_3^-–N, pH, and SM to experimental warming treatment and litter removal treatment is not consistent. Compared to the control, pH all significantly increased under experimental warming, litter removal, and experimental warming-litter removal treatments ($p < 0.001$; Figure 4). Results showed that the pH increased by 4% under experimental warming treatment and litter removal treatment. Experimental warming-litter removal treatment increased the pH by 5% (Figure 3). In addition, the SOM, STN, and NH_4^+–N showed an upward trend under experimental warming treatment, meanwhile, the NO_3^-N and SM showed a downward trend. Under litter removal treatment, all the SOM, STN, NH_4^+–N, and NO_3^-N showed a downward trend, but the SM showed an upward trend. Under experimental warming-litter removal treatment, all the SOM, STN, NH_4^+–N, NO_3^-–N, and SM showed a downward trend (Supplementary Figure S2).

3.3 Changes in ecosystem functioning following experimental warming, litter removal and warming-litter removal

The EMF indexes of control, experimental warming treatment, litter removal treatment, and experimental warming-litter removal treatment were -0.26, -0.08, 0.27, and 0.06, respectively. Our results indicated that experimental warming, litter removal, and experimental warming-litter removal treatments had no significant effects on the EMF index. However, the aboveground ecosystem multifunctionality

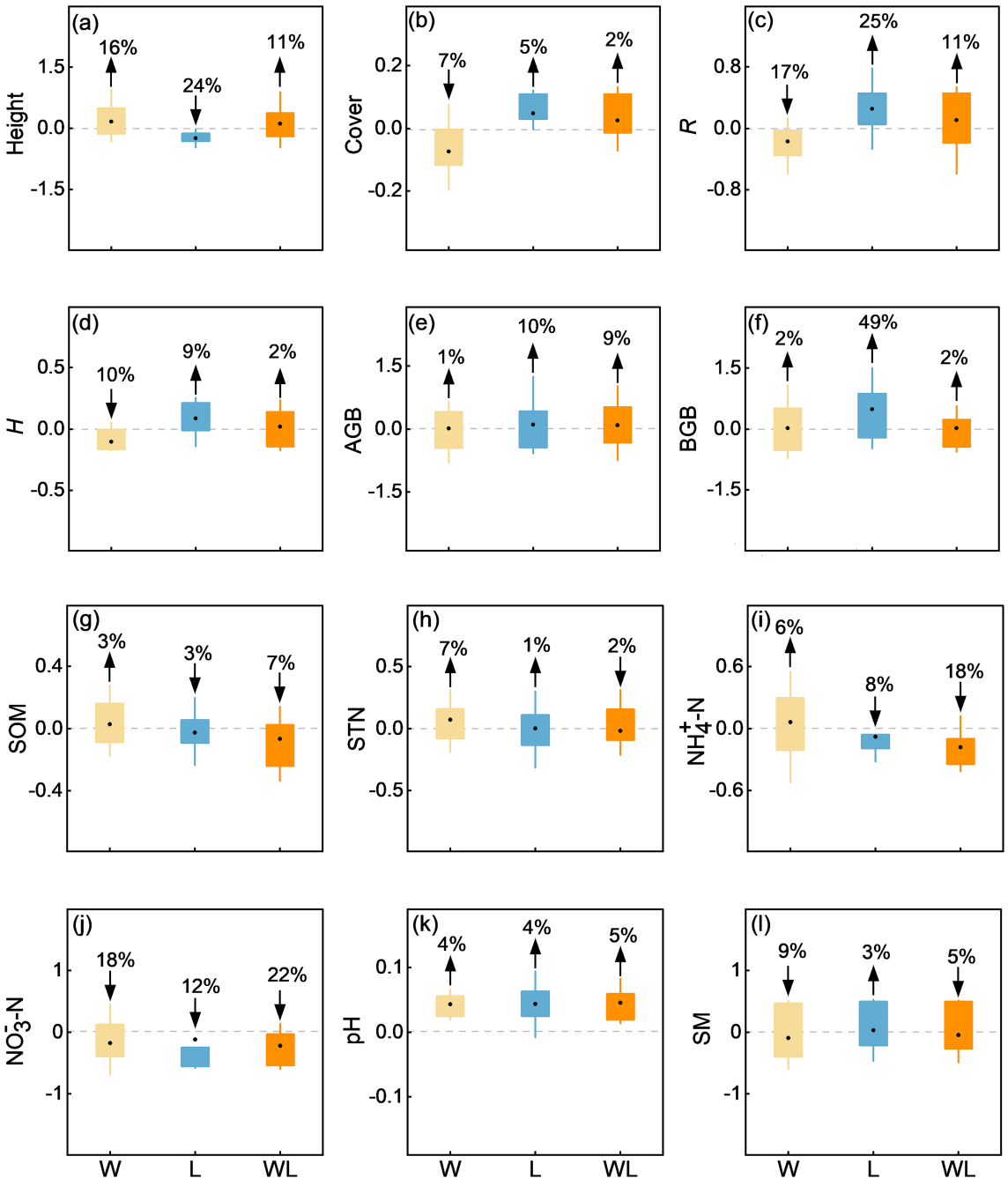

FIGURE 3
Differences in **(a)** community height (Height), **(b)** coverage (Cover), **(c)** species richness (*R*), **(d)** plant diversity (*H*), **(e)** aboveground biomass (AGB), **(f)** belowground biomass (BGB), **(g)** soil organic matter (SOM), **(h)** soil total nitrogen (STN), **(i)** soil ammonia nitrogen (NH_4^+–N), **(j)** soil nitrate nitrogen (NO_3^-N), **(k)** soil pH (pH), and **(l)** soil moisture content (SM) between experimental warming (W), litter removal (L), and experimental warming-litter removal (WL) treatments, compared to the control (CK).

(AEMF) index and belowground ecosystem multifunctionality (BEMF) showed differential responses to experimental warming and litter removal treatments. The AEMF index showed a decreasing trend under experimental warming but showed an upward trend under both litter removal and experimental warming-litter removal treatments (Figure 5b). The BEMF index significantly increased under experimental warming ($p < 0.01$) but showed an upward trend under litter removal and experimental warming-litter removal treatments (Figure 5c). Under the experimental warming treatment, AEMF and BEMF exhibited opposite trends, which resulted in a balancing effect on EMF. Specifically, AEMF showed a decreasing trend, while BEMF increased significantly ($p < 0.01$), leading to an overall increase in EMF after balancing. In contrast, both AEMF and BEMF showed an increasing trend in litter removal and experimental warming-litter removal treatments, resulting in a corresponding increase in EMF.

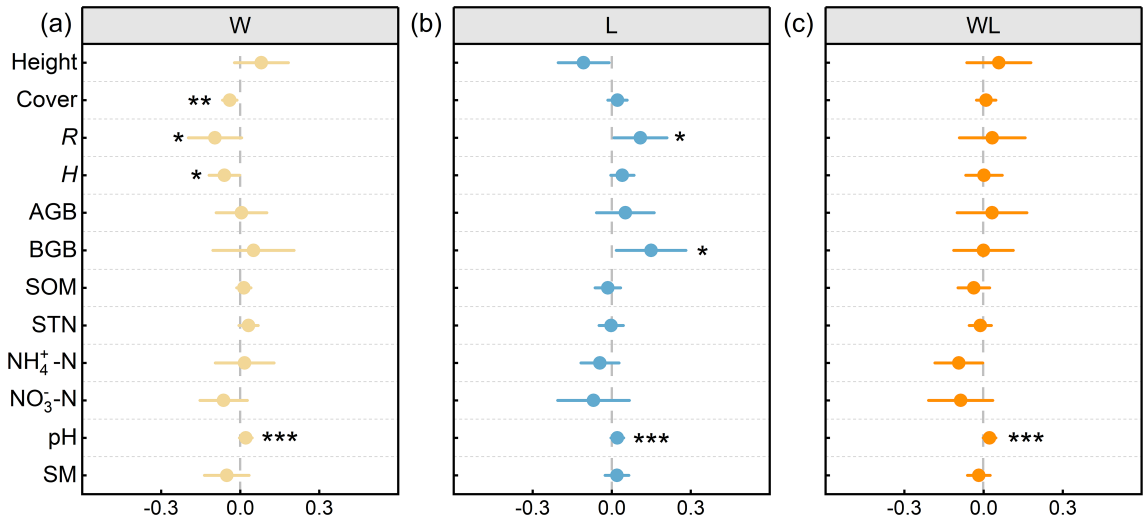

FIGURE 4
The effects of experimental warming (W), litter removal (L), and experimental warming-litter removal (WL) on plant communities and soil indicators. Asterisks indicate significant differences between each treatment (W, L, WL) and the control (CK). *, $p < 0.05$; **, $p < 0.01$; ***, $p < 0.001$.

3.4 Relationships of individual ecological functions with EMF, AEMF and BEMF

We analyzed the relationships among plant and soil functions, and the results showed that plant height was significantly correlated with STN and NO_3^-–N. The AGB was significantly correlated with SOM and NO_3^-–N. In addition, *H* was significantly correlated with STN and SM (Figure 6). We further analyzed the correlation between EMF, AEMF, and BEMF indexes with plant and soil functions. The results showed that EMF, AEMF, and BEMF indexes were significantly correlated with STN. The EMF index was significantly correlated with height, cover, *R*, *H*, SOM, STN, NH_4^+–N, pH, and SM, AEMF index was significantly correlated with height, cover, *R*, *H*, STN, NO_3^-N, and SM, BEMF index was significantly correlated with SOM, STN, NH_4^+–N, and pH (Figure 6). Path analysis of the structural equation model showed that experimental warming and litter removal treatments influence the EMF and AEMF indexes mainly directly by affecting BGB. In the total impact on EMF and BEMF index, the contribution of soil nutrients is much higher than other indicators, while in the AEMF index, the contributions of AGB and BGB are higher than the other functions (Figures 7, 8).

4 Discussion

4.1 The impact of experimental warming on ecosystem structure and function

Temperature is a pivotal factor influencing plant growth and development. In cold and high-altitude regions, climate warming is more likely to impact the structure and traits of plant communities (Quan et al., 2024). The main reason for this result is that at high altitudes, certain highly temperature-sensitive plant species are more vulnerable to climate change, leading to species decline or extinction, which further leads to changes in community composition and structure (Ma et al., 2017). Our findings indicate that under experimental warming treatment, both the cover and importance value (IV) of grasses significantly increased ($p < 0.05$), while the cover and height of sedges significantly decreased ($p < 0.05$; Supplementary Figures S3, S4). The reason for this result is the difference in resistance between sedges and grasses. Warming could increase the abundance of grasses at the expense of the biomass of sedge and other non-grasses (Liu et al., 2018). On the one hand, the response of sedges to climate warming is primarily due to moisture limitation, the decrease in moisture levels caused by climate warming has been shown to have a detrimental effect on the growth of sedges (Yuan et al., 2021); on the other hand, the low-temperature limitation of alpine meadows is broken by warming, and the increase in vegetation height and AGB enhances the ability to compete for light, with sedges and some low forbs being excluded from competition by grasses (Hu et al., 2021). For a specific functional group type, warming may have opposite effects on the relative abundance between species (Ganjurjav et al., 2016). This finding indicates that functional groups may not adequately represent changes at the species level, thus emphasizing the necessity for further research in this area. Additionally, changes in vegetation functional groups can also explain the response of cover to warming (Niu et al., 2025), which means that warming decreases plant diversity and further affects cover.

Research on alpine meadows has revealed that, under 20 years of experimental warming treatment, the effect of temperature on soil pH increase showed significant differences (Alatalo et al., 2017). Our results indicate that experimental warming significantly increased soil pH ($p < 0.001$; Figure 4a). Changes in microbial activity as a result of warming, where microbial decomposition of organic matter releases alkaline compounds, can be used to explain the increase in pH (Han et al., 2022). Meanwhile, under warming, the soil moisture content decreases (Supplementary Figure S2). Warming-induced declines in soil

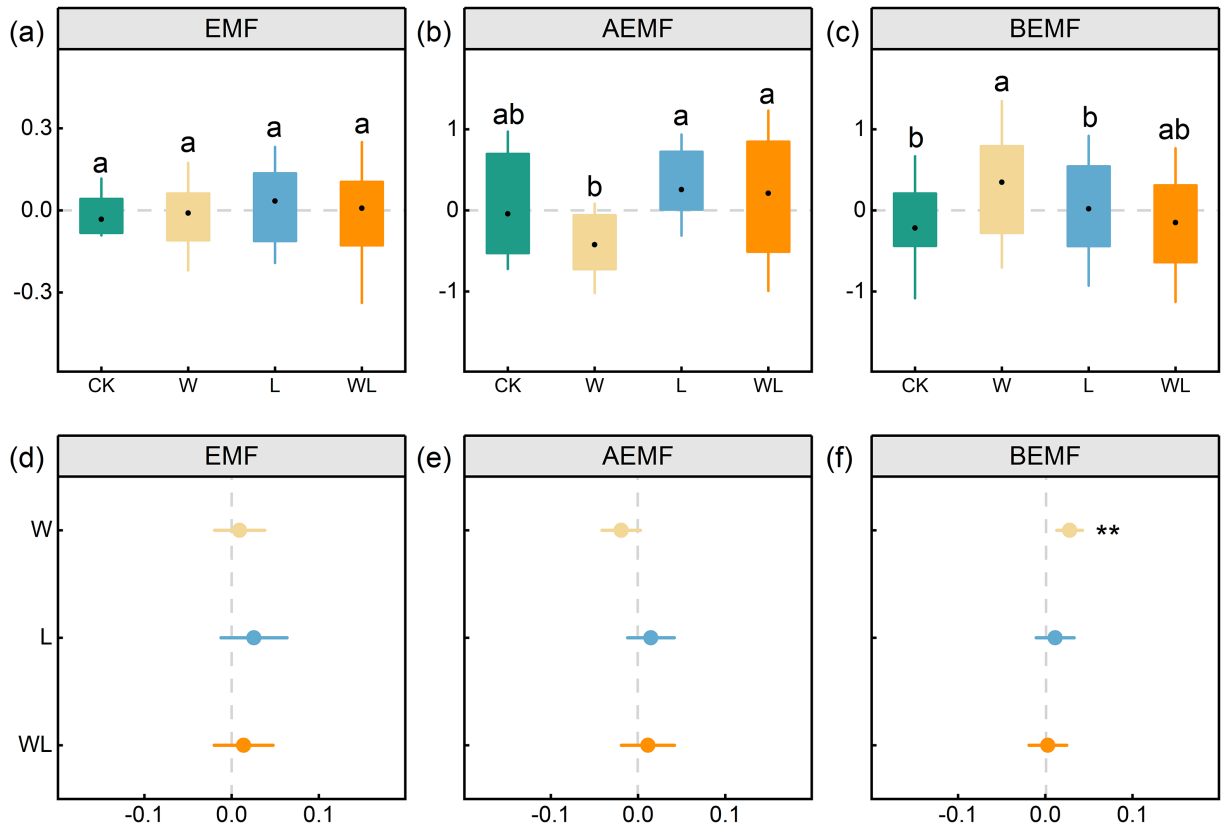

FIGURE 5
Changes of EMF (ecosystem multifunctionality), AEMF (aboveground ecosystem multifunctionality), BEMF (belowground ecosystem multifunctionality) in four different treatments plots **(a-c)**. Different letters indicate significant differences among treatments. The effects of experimental warming (W), litter removal (L), and experimental warming-litter removal (WL) on **(d)** EMF, **(e)** AEMF, **(f)** BEMF. Asterisks indicate significant differences between each treatment (W, L, WL) and the control (CK) *, $p < 0.05$; **, $p < 0.01$; ***, $p < 0.001$.

moisture are usually accompanied by changes in nitrification intensity, which affects the conversion of NH_4^+ and NO_3^-, while increased nitrogen leaching and gaseous nitrogen losses accelerate the depletion of soil nitrogen pools (Fang et al., 2023). The observed decreases in NO_3^-–N and SM in this study indicate a response to warming. However, the absence of significant changes may be attributed to the relatively short duration of the experimental warming treatment. Therefore, future long-term monitoring is essential for a deeper understanding of nutrient cycling responses to climate warming.

4.2 The impact of litter removal on ecosystem structure and function

The results of this study indicate that under litter removal, the height and IV of grasses have exhibited a declining trend, while the cover of forbs has significantly increased ($p < 0.001$), and IV of forbs has shown an upward trend (Supplementary Figure S4). The following factors are considered to be the underlying causes of the observed changes in functional groups. Firstly, with litter removal, sedges and low-growing forbs received sufficient light, which significantly enhanced their dominance in the grass layer (Wu et al., 2004). Meanwhile, litter removal can affect the nutritional utilization strategies of plants, indirectly affecting their competitiveness and biomass of plants. It is evident that litter removal dramatically reduces the dominant position of dominant species in grasslands (Li et al., 2020). In contrast, the dominance of secondary and associated species increases, affecting grassland productivity and species diversity and further affecting the EMF.

In the analysis of soil properties, the decomposition process of litter releases organic acids. In this experiment, litter removal resulted in a decrease in organic acid content, leading to a significant increase in pH ($p < 0.05$; Figure 4a). In addition, litter can be leached and decomposed to provide soluble nutrients to the soil directly and nitrogen content is the main influencing factor in the process of litter decomposition (Błońska et al., 2021); in this study, there was no significant change in soil total nitrogen content and soil organic matter under litter removal, which is consistent with the previous research results (Lajtha et al., 2014). This can be attributed to the relatively slow mineralization and nutrient accumulation process of soil organic matter, so the short-term effect of litter removal on soil total nitrogen content may not yet be apparent. Regarding the analysis of soil available nitrogen, previous studies have found that litter removal will reduce the soil nitrogen pool and increase NO_3^- leaching, indicating that litter removal decreases the storage and availability of nitrogen in the soil (Zhang et al., 2023b); our

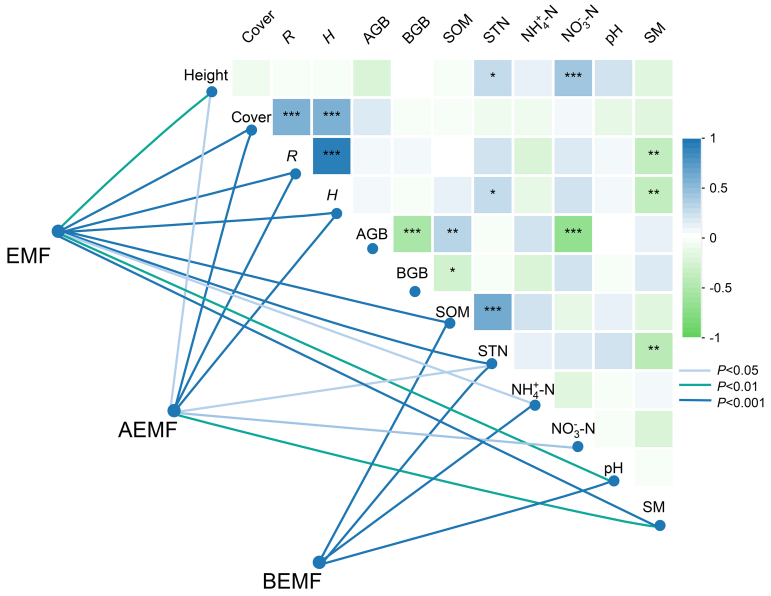

FIGURE 6
Correlation coefficients between the vegetation characteristics, soil properties, and the ecosystem multifunctionality (EMF) index. Cover, vegetation cover (%), Height, plant height (cm), *R*, species richness, *H*, plant diversity, AGB, aboveground biomass (g m^{-2}), BGB, belowground biomass (g m^{-2}), SOM, soil organic matter(SOM) (g kg^{-1}), STN, soil total nitrogen (g kg^{-1}), NH_4^+–N, soil ammonia nitrogen (mg kg^{-1}), NO_3^-N, soil nitrate nitrogen (mg kg^{-1}), pH, soil pH; SM, Soil moisture content (%). Asterisk was considered to be significant. *, $p < 0.05$; **, $p < 0.01$; ***, $p < 0.001$.

research findings also demonstrate that litter removal results in a decrease in NH_4^+–N and NO_3^-–N, although these changes did not achieve statistical significance, this may be because the duration of litter removal was relatively short and has not yet had a significant impact on soil NH_4^+–N and NO_3^-–N.

4.3 Controls of the multiple ecosystem functions under experimental warming and litter removal

In fact, ecosystem function can be influenced by many factors, such as climate conditions, biodiversity levels, and even experimental design. Most previous studies have shown a general positive correlation between plant diversity and ecosystem functions, indicating that plant diversity has a limiting effect on ecosystem functions, as communities with high species diversity can maintain more functions at high levels (Xu et al., 2021). Research has demonstrated that litter indirectly drives changes in EMF by mediating plant cover and species richness in alpine meadows (Ma et al., 2021). Moreover, plant litter affects changes in soil physico-chemical properties in alpine meadows, thereby impacting ecosystem function (Tian et al., 2021). The findings of our study demonstrated that the response of AEMF to litter removal was predominantly contingent on alterations in plant diversity and that diversity exhibited a significant correlation with ecosystem function (Figure 6). The positive responses of ecosystem functions to litter removal can be explained by the litter removal-induced increases in primary productivity and species diversity and decreases in soil nutrient. The improvement in productivity and diversity offsets the adverse effects of other ecosystem functions, ultimately leading to an upward trend in ecosystem functions because of litter removal.

Studies have shown that experimental warming can influence EMF by affecting the plant diversity and productivity of alpine grasslands (Zhao et al., 2024). A plethora of research has demonstrated a correlation between plant diversity and vegetation productivity in alpine grasslands and ecosystem function (Jing et al., 2015). Plant diversity is identified as the key factor mediating the effects of human activities on EMF (Zhang et al., 2021), and may decrease with increasing temperature (Ma et al., 2022), further impacting the ecosystem functions. Specifically, due to some species being more sensitive to warming than others, warming can reduce the species richness (Gruner et al., 2017) and alter species composition (Perkins et al., 2010), affecting both individual ecosystem functions and overall multifunctionality (Perkins et al., 2010, 2015). Our study has demonstrated that experimental warming would primarily affect the AEMF through alterations to plant diversity and vegetation productivity (Figure 7). In addition, the correlation between productivity and diversity may also change under climate change. Warming has altered the positive correlation between AGB and species diversity in alpine grasslands under natural conditions, thereby weakening the dependence of AGB on species diversity (Ma et al., 2022). Warming reduces the correlation between species diversity and vegetation productivity, suggesting that environmental factors significantly impact the relationship between the two. In conclusion, experimental warming decreased diversity and cover (Figure 4a), which further affected AEMF by affecting productivity (Figure 7). Research demonstrates that soil pH significantly correlates with EMF in alpine meadows and that it indirectly influences EMF through structural, compositional, and functional modulation of soil communities (Shi et al., 2024; Hu et al.,

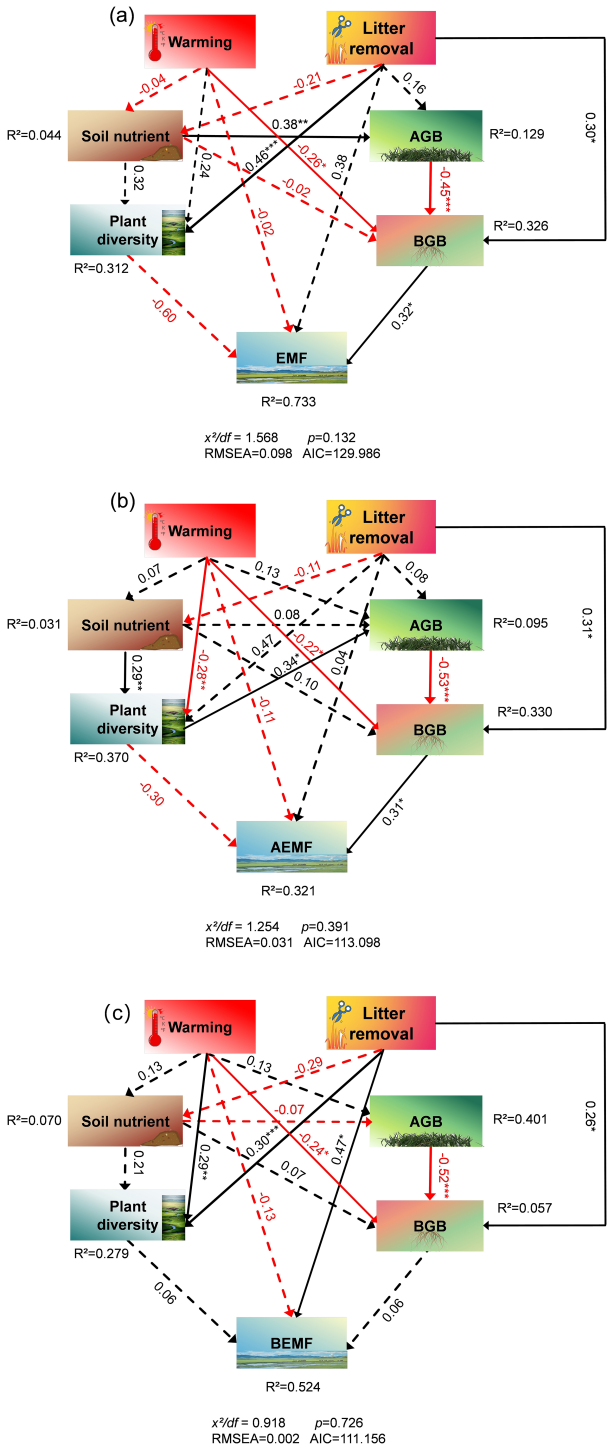

FIGURE 7
Effects of the experimental warming and litter removal on **(a)** ecosystem multifunctionality (EMF), **(b)** aboveground ecosystem multifunctionality (AEMF), **(c)** belowground ecosystem multifunctionality (BEMF) analyzed using structural equation model with path analysis based on observed data. Effects were calculated according to the standardized path coefficients. Black solid arrows represent positive effects. Red solid arrows represent negative effects. Significance is proportional to the thickness of the solid line. Dashed arrows indicate non-significant effects. Numbers next to arrows indicate standardized path coefficients. R^2 represent the proportion of variance explained for each dependent variable in the model.

2024). In addition, nitrogen availability has been shown to mediate EMF through coordinated regulation of species richness and functional diversity (Pichon et al., 2024). Specifically in alpine meadows, experimental analyses reveal that nitrogen-induced variations in multifunctionality are fundamentally governed by plant diversity-mediated ecological mechanisms (Liu et al., 2021). The decrease in moisture caused by warming led to the migration of nitrogen pools (Fang et al., 2023), while the increase in pH, SOM, and NH_4^+–N

10.3389/fpls.2025.1567414

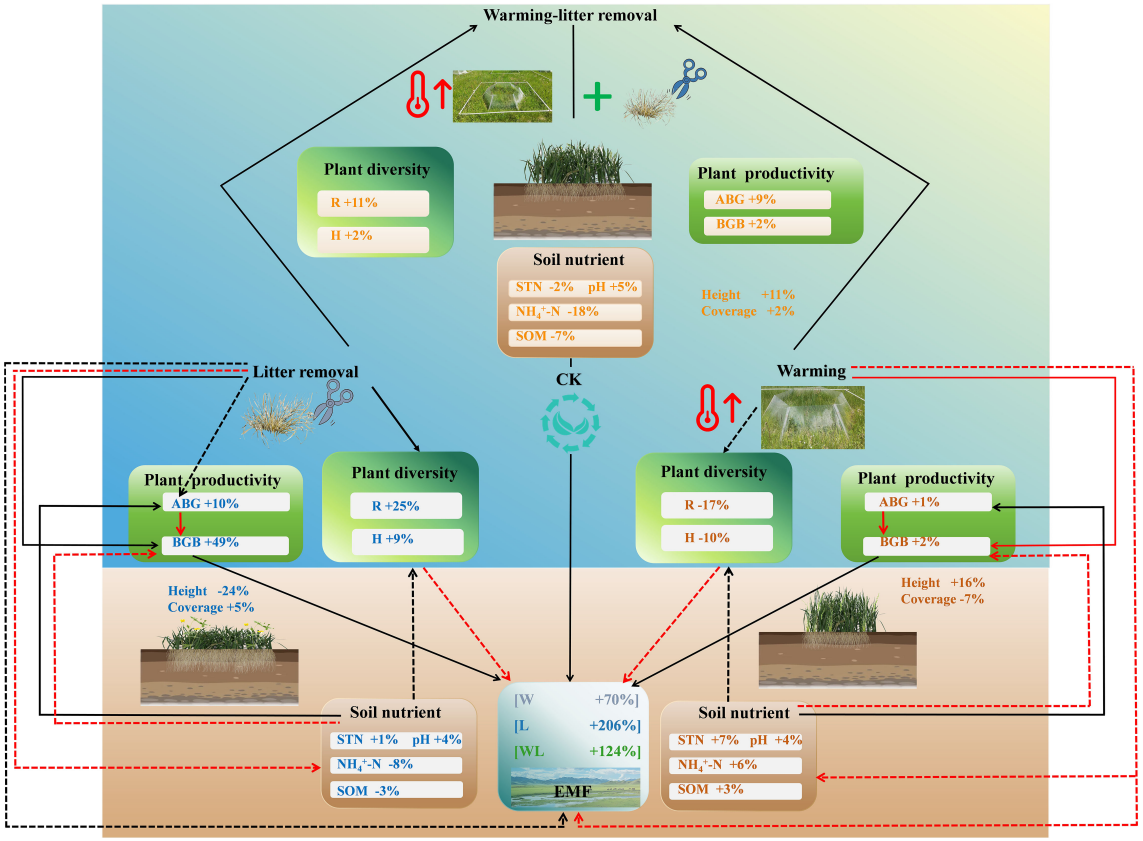

FIGURE 8
A conceptual framework diagram for understanding the potential effects of experimental warming and litter removal on the ecological functioning in semi-humid alpine grasslands. Black solid arrows represent positive effects. Red solid arrows represent negative effects. Dashed arrows indicate non-significant effects.

affected BEMF. The positive effects of soil nutrients offset the negative impacts on other ecosystem functions, ultimately achieving a balance in ecosystem functions. In the interaction between experimental warming and litter removal, litter removal diminished the limiting effects of warming, enhanced the *R* and *H*, and consequently influenced AEMF by affecting AGB and BGB. Ultimately, this led to litter removal, mitigating the decline in aboveground ecosystem multifunctioning caused by warming. In addition, it has been shown that litter is closely related to the formation of SOC (Angst et al., 2021), our results confirm that litter removal leads to a downward trend in SOC (Figure 3). However, the significant increase in pH offset the decreasing trend of other soil nutrients, and BEMF still showed an increasing trend under litter removal treatment. Therefore, the interaction between experimental warming and litter removal promoted upward trends in AEMF and BEMF by mediating plant diversity, productivity, and soil nutrients, thereby further enhancing EMF.

4.4 Limitations and future research

The present research has certain limitations that should be acknowledged. Our study plots were established within fenced areas, and grazing exclusion may affect changes in ecosystem functions. Therefore, grazing exclusion and the two experimental treatments (experimental warming and litter removal) may exert interactive effects that could confound the interpretation of experimental outcomes. In addition, litter removal can serve as an experimental treatment to simulate grazing, and the results of this experiment explain the effects of grazing on EMF to a certain extent. However, the actual effects depend on factors such as environmental conditions, soil type, and plant species. Our future studies should focus on the individual and interactive effects of experimental warming, different grazing intensities, and grazing exclusion on alpine grassland ecosystems.

Another important point to note is that the duration of the experimental warming and litter removal experiments in this study was relatively short, which may limit our ability to assess fully the effects of these two factors on ecosystem functioning. Therefore, future research should focus on simulating the long-term effects of experimental warming and litter removal on individual and multiple ecosystem functions. This will help elucidate the specific mechanisms underlying ecosystem responses to climate change and provide more NbS, such as litter management measures to enhance ecosystem functionality.

5 Conclusions

Our findings provided novel experimental evidence that litter removal could mitigate the negative effects of warming on ecosystem functions in semi-humid alpine grasslands. This response is mainly driven by the direct and indirect effects of warming and litter removal on plant diversity, productivity, and soil nutrients. However, warming affected the aboveground and belowground ecosystem functions of alpine grasslands differently, with the AEMF index decreasing while the BEMF index increased under experimental warming. Consequently, the balancing effect of litter removal on ecological functions varies, which is primarily reflected in the AEMF index in alpine grasslands.

Our findings highlight the importance of plant litter removal in maintaining ecological functions by altering plant diversity and productivity in semi-humid alpine grasslands under climate change. We further emphasize the need to implement appropriate grassland management measures to regulate plant litter accumulation and apply suitable litter management practices along with other NbS to enhance ecosystem functionality. These practices include controlling grazing intensity to maintain the balance of plant communities and prevent excessive litter build-up, as well as applying scientific fertilization and improving soil quality to accelerate litter decomposition. By adopting these measures, we can enhance ecosystem biodiversity and the multifunctionality of alpine grasslands in semi-humid areas of the QTP, thereby further strengthening the capacity of grassland ecosystems to cope with climate change.

Data availability statement

The raw data supporting the conclusions of this article will be made available by the authors, without undue reservation.

Author contributions

GX: Conceptualization, Data curation, Formal Analysis, Investigation, Writing – original draft, Writing – review & editing. LT: Conceptualization, Data curation, Formal Analysis, Investigation, Visualization, Writing – original draft, Writing – review & editing, Funding acquisition, Methodology, Project administration, Resources, Supervision. JZ: Conceptualization, Data curation, Formal Analysis, Funding acquisition, Investigation, Methodology, Project administration, Resources, Writing – original draft, Writing – review & editing.

Funding

The author(s) declare that financial support was received for the research and/or publication of this article. This research was funded by the National Natural Science Foundation of China (32230068; 42071058), Southwest Minzu University Double World-Class Project (CX2023016), and the Fundamental Research Funds for the Central Universities, Southwest Minzu University (ZYN2024051).

Acknowledgments

We thank Hu S.Y., Xiao Y., Ma Y.H., Ji-Shi A.W., Yang W., Zhao W.X., Wu J., Zhao Q., and Bai S.H. for their great work on field observations.

Conflict of interest

The authors declare that the research was conducted in the absence of any commercial or financial relationships that could be construed as a potential conflict of interest.

Generative AI statement

The author(s) declare that no Generative AI was used in the creation of this manuscript.

Publisher's note

Supplementary material

The Supplementary Material for this article can be found online at: https://www.frontiersin.org/articles/10.3389/fpls.2025.1567414/full#supplementary-material

SUPPLEMENTARY FIGURE 1
Differences in **(a)** plant height (Height), **(b)** vegetation coverage (Cover), **(c)** species richness (*R*), **(d)** plant diversity (*H*), **(e)** aboveground biomass (AGB), and **(f)** belowground biomass (BGB) among the control (CK), experimental warming (W), litter removal (L), and experimental warming-litter removal (WL) treatments. Different letters indicate significant differences among four treatments.

SUPPLEMENTARY FIGURE 2
Differences in **(a)** soil organic matter (SOM), **(b)** soil total nitrogen (STN), **(c)** soil ammonia nitrogen (NH_4^+–N), **(d)** soil nitrate nitrogen (NO_3^-N), **(e)** soil pH and **(f)** soil moisture content (SM) among the control (CK), experimental warming (W), litter removal (L) and experimental warming-litter removal (WL) treatments. Different letters indicate significant differences among four treatments.

SUPPLEMENTARY FIGURE 3
Differences in plant height (Height), vegetation coverage (Cover), Important value of three different vegetation functional groups including sedges, grasses and forbs among the control (CK), experimental warming (W), litter removal (L) and experimental warming-litter removal (WL) treatments. Different letters indicate significant differences among four treatments.

SUPPLEMENTARY FIGURE 4
The effects of experimental warming (W), litter removal (L), and experimental warming-litter removal (WL) on plant height (Height), vegetation coverage (Cover), and important value (IV) of three vegetation functional groups, including sedges, grasses, and forbs. Asterisks indicate significant differences between each treatment (W, L, WL) and the control (CK). *, $p < 0.05$; **, $p < 0.01$; ***, $p < 0.001$.

SUPPLEMENTARY FIGURE 5
A total of 8 factors with significant influence on EMF were screened out by a random forest model, including: plant diversity (*H*), soil total nitrogen (STN), soil organic matter (SOM), species richness (*R*), vegetation coverage (Cover), soil ammonia nitrogen (NH_4^+–N), plant height (Height), and soil pH (pH).

References

Alatalo, J. M., Jägerbrand, A. K., Juhanson, J., Michelsen, A., and Ľuptáčik, P. (2017). Impacts of twenty years of experimental warming on soil carbon, nitrogen, moisture and soil mites across alpine/subarctic tundra communities. *Sci. Rep.* 7, 44489. doi: 10.1038/srep44489

Angst, G., Pokorný, J., Mueller, C. W., Prater, I., Preusser, S., Kandeler, E., et al. (2021). Soil texture affects the coupling of litter decomposition and soil organic matter formation. *Soil Biol. Biochem.* 159, 108302. doi: 10.1016/j.soilbio.2021.108302

Błońska, E., Piaszczyk, W., Staszel, K., and Lasota, J. (2021). Enzymatic activity of soils and soil organic matter stabilization as an effect of components released from the decomposition of litter. *Appl. Soil. Ecol.* 157, 103723. doi: 10.1016/j.apsoil.2020.103723

Byrnes, J. E. K., Gamfeldt, L., Isbell, F., Lefcheck, J. S., Griffin, J. N., Hector, A., et al. (2014). Investigating the relationship between biodiversity and ecosystem multifunctionality: challenges and solutions. *Methods Ecol. Evol.* 5, 111–124. doi: 10.1111/2041-210X.12143

Chen, W. J., Jiang, L., Jia, R. Y., Tang, B., Jiang, H. Z., Wang, Y., et al. (2024). Plant litter loss exacerbates drought influences on grasslands. *New Phytol.* 241, 142–153. doi: 10.1111/nph.19374

Duffy, J. E., Godwin, C. M., and Cardinale, B. J. (2017). Biodiversity effects in the wild are common and as strong as key drivers of productivity. *Nature* 549, 261–264. doi: 10.1038/nature23886

Fang, C., Verbrigghe, N., Sigurdsson, B. D., Ostonen, I., Leblans, N. I. W., Marañón-Jiménez, S., et al. (2023). Decadal soil warming decreased vascular plant above and belowground production in a subarctic grassland by inducing nitrogen limitation. *New Phytol.* 240, 565–576. doi: 10.1111/nph.19177

Fekete, I., Varga, C., Biró, B., Tóth, J. A., Várbíró, G., Lajtha, K., et al. (2016). The effects of litter production and litter depth on soil microclimate in a central european deciduous forest. *Plant Soil* 398, 291–300. doi: 10.1007/s11104-015-2664-5

Ganjurjav, H., Gao, Q., Gornish, E. S., Schwartz, M. W., Liang, Y., Cao, X., et al. (2016). Differential response of alpine steppe and alpine meadow to climate warming in the central Qinghai-Tibetan Plateau. *Agric. For. Meteorol.* 223, 233–240. doi: 10.1016/j.agrformet.2016.03.017

Ganjurjav, H., Gornish, E. S., Hu, G. Z., Wan, Y. F., Li, Y., Danjiu, L., et al. (2018). Temperature leads to annual changes of plant community composition in alpine grasslands on the Qinghai-Tibetan Plateau. *Environ. Monit. Assess.* 190, 585. doi: 10.1007/s10661-018-6964-0

Gruner, D. S., Bracken, M. E. S., Berger, S. A., Eriksson, B. K., Gamfeldt, L., Matthiessen, B., et al. (2017). Effects of experimental warming on biodiversity depend on ecosystem type and local species composition. *Oikos* 126, 8–17. doi: 10.1007/s11104-015-2664-5

Han, Y. F., Qu, C. C., Hu, X. P., Wang, P., Wan, D., Cai, P., et al. (2022). Warming and humidification mediated changes of DOM composition in an Alfisol. *Sci. Total Envir.* 805, 150198. doi: 10.1016/j.scitotenv.2021.150198

Hou, D. J., He, W. M., Liu, C. C., Qiao, X. G., and Guo, K. (2019). Litter accumulation alters the abiotic environment and drives community successional changes in two fenced grasslands in Inner Mongolia. *Ecol. Evol.* 9, 9214–9224. doi: 10.1002/ece3.5469

Hu, Z. K., Delgado-Baquerizo, M., Fanin, N., Chen, X. Y., Zhou, Y., Du, G. Z., et al. (2024). Nutrient-induced acidification modulates soil biodiversity-function relationships. *Nat. Commun.* 15, 2858. doi: 10.1038/s41467-024-47323-3

Hu, X. L., Zhou, W. L., Li, X. N., Niklas, K. J., and Sun, S. C. (2021). Changes in community composition induced by experi- mental warming in an alpine meadow: beyond plant functional type. *Front. Ecol. Evol.* 9. doi: 10.3389/fevo.2021.569422

Hua, T., Zhao, W. W., and Pereira, P. (2022). Opinionated views on grassland restoration programs on the qinghai-Tibetan plateau. *Front. Plant Sci.* 13, 861200. doi: 10.3389/fpls.2022.861200

Jing, X., Sanders, N. J., Shi, Y., Chu, H. Y., Classen, A. T., Zhao, K., et al. (2015). The links between ecosystem multifunctionality and above - and belowground biodiversity are mediated by climate. *Nat. Commun.* 6, 8159. doi: 10.1038/ncomms9159

Lajtha, K., Bowden, R. D., and Nadelhoffer, K. (2014). Litter and root manipulations provide insights into soil organic matter dynamics and stability. *Soil Sci. Soc Am. J.* 78, S261–S269. doi: 10.2136/sssaj2013.08.0370nafsc

Li, W. B., Huang, G. Z., and Zhang, H. X. (2020). Enclosure increases nutrient resorption from senescing leaves in a subalpine pasture. *Plant Soil* 457, 269–278. doi: 10.1007/s11104-020-04733-8

Liu, H. Y., Mi, Z. R., Lin, L., Wang, Y. H., Zhang, Z. H., Zhang, F. W., et al. (2018). Shifting plant species composition in response to climate change stabilizes grassland primary production. *P. Natl. Acad. Sci. USA.* 115, 4051–4056. doi: 10.1073/pnas.1700299114

Liu, S. G., Plaza, C., Ochoa-Hueso, R., Trivedi, C., Wang, J. T., Trivediet, P., et al. (2023c). Litter and soil biodiversity jointly drive ecosystem functions. *Global Change Biol.* 29, 6276–6285. doi: 10.1111/gcb.16913

Liu, X. C., Shi, X. M., and Zhang, S. T. (2021). Soil abiotic properties and plant functional diversity co-regulate the impacts of nitrogen addition on ecosystem multifunctionality in an alpine meadow. *Sci. Total Environ.* 780, 146476. doi: 10.1016/j.scitotenv.2021.146476

Liu, J., Wang, J., Morreale, S. J., Schneider, R. L., Li, Z. G., and Wu, G. L. (2023b). Contributions of plant litter to soil microbial activity improvement and soil nutrient enhancement along with herb and shrub colonization expansions in an arid sandy land. *Catena* 227, 107098. doi: 10.1016/j.catena.2023.107098

Liu, M. X., Yin, F. L., Xiao, Y. D., and Yang, C. L. (2023a). Grazing alters the relationship between alpine meadow biodiversity and ecosystem multifunctionality. *Sci. Total Environ.* 898, 165445. doi: 10.1016/j.scitotenv.2023.165445

Ma, Z. Y., Liu, H. Y., Mi, Z. R., Zhang, Z. H., Wang, Y. H., Xu, W., et al. (2017). Climate warming reduces the temporal stability of plant community biomass production. *Nat. Commun.* 8, 15378. doi: 10.1038/ncomms15378

Ma, Z. W., Wu, J., Li, L., Zhou, Q. P., and Hou, F. J. (2021). Litter-induced reduction in ecosystem multifunctionality is mediated by plant diversity and cover in an alpine meadow. *Front. Plant Sci.* 12. doi: 10.3389/fpls.2021.773804

Ma, L., Zhang, Z. H., Shi, G. X., Su, H. Y., Qin, R. M., Chang, T., et al. (2022). Warming changed the relationship between species diversity and primary productivity of alpine meadow on the Tibetan Plateau. *Ecol. Indic.* 145, 109691. doi: 10.1016/j.ecolind.2022.109691

Ma, P. F., Zhao, J. X., Zhang, H. Z., Zhang, L., and Luo, T. X. (2023). Increased precipitation leads to earlier green-up and later senescence in Tibetan alpine grassland regardless of warming. *Sci. Total Environ.* 871, 162000. doi: 10.1016/j.scitotenv.2023.162000

Maestre, F. T., Quero, J. L., Gotelli, N. J., Escudero, A., Ochoa, V., Delgado-Baquerizo, M., et al. (2012). Plant species richness and ecosystem multifunctionality in global drylands. *Science* 335, 214–218. doi: 10.1126/science.1215442

Niu, Q. C., Jin, G. F., Yin, S. X., Gan, L., Yang, Z. Y., Dorji, T., et al. (2025). Transcriptional changes underlying the degradation of plant community in alpine meadow under seasonal warming impact. *Plant Cell Environ.* 48, 526–536. doi: 10.1111/pce.15160

Niu, S. L., and Wan, S. Q. (2008). Warming changes plant competitive hierarchy in a temperate steppe in Northern China. *J. Plant Ecol.* 1, 103–110. doi: 10.1093/jpe/rtn003

Osborne, B. B., Soper, F. M., Nasto, M. K., Bru, D., Hwang, S., Machmuller, M. B., et al. (2021). Litter inputs drive patterns of soil nitrogen heterogeneity in a diverse tropical forest: Results from a litter manipulation experiment. *Soil Biol. Biochem.* 158, 108247. doi: 10.1016/j.soilbio.2021.108247

Perkins, D. M., Bailey, R. A., Dossena, M., Gamfeldt, L., Reiss, J., Trimmer, M., et al. (2015). Higher biodiversity is required to sustain multiple ecosystem processes across temperature regimes. *Glob. Change Biol.* 21, 396–406. doi: 10.1111/gcb.12688

Perkins, D. M., McKie, B. G., Malmqvist, B., Gilmour, S. G., Reiss, J., and Woodward, G. (2010). Environmental warming and biodiversity - ecosystem functioning in freshwater microcosms: partitioning the effects of species identity, richness and metabolism. *Adv. Ecol. Res.* 43, 177–209. doi: 10.1016/B978-0-12-385005-8.00005-8

Pichon, N. A., Cappelli, S. L., Soliveres, S., Mannall, T., Nwe, T. Z., Hölzel, N., et al. (2024). Nitrogen availability and plant functional composition modify biodiversity-multifunctionality relationships. *Ecol. Lett.* 27, 14361. doi: 10.1111/ele.14361

Quan, Q., He, N. P., Zhang, R. Y., Wang, J. S., Luo, Y. Q., Ma, F. F., et al. (2024). Plant height as an indicator for alpine carbon sequestration and ecosystem response to warming. *Nat. Plants* 10, 890–900. doi: 10.1038/s41477-024-01705-z

Shangguan, Z. J., Jing, X., Wang, H., Liu, H. Y., Gu, H. J., and He, J.-S. (2024). Plant biodiversity responds more strongly to climate warming and anthropogenic activities than microbial biodiversity in the Qinghai–Tibetan alpine grasslands. *J. Ecol.* 112, 110–125. doi: 10.1111/1365-2745.14222

Shi, L. N., Lin, Z. R., Yao, Z. Y., Peng, C. J., Hu, M. A., Yin, N., et al. (2024). Increased precipitation rather than warming increases ecosystem multifunctionality in an alpine meadow. *Plant Soil* 498, 357–370. doi: 10.1007/s11104-023-06441-5

Tian, L. H., Bai, Y. F., Wang, W. W., Qu, G. P., Deng, Z. H., Li, R. C., et al. (2021). Warm- and cold- season grazing affect plant diversity and soil carbon and nitrogen sequestration differently in Tibetan alpine swamp meadows. *Plant Soil* 458, 151–164. doi: 10.1007/s11104-020-04573-6

Van Der Plas, F. (2019). Biodiversity and ecosystem functioning in naturally assembled communities. *Biol. Rev.* 94, 1220–1245. doi: 10.1111/brv.12499

Wang, Y. J., Liu, Y. X., Chen, P., Song, J. X., and Fu, B. J. (2024). Interannual precipitation variability dominates the growth of alpine grassland above-ground biomass at high elevations on the Tibetan Plateau. *Sci. Total Environ.* 931, 172745. doi: 10.1016/j.scitotenv.2024.172745

Wang, J., Zhao, M. L., Willms, W. D., Han, G. D., Wang, Z. W., and Bai, Y. F. (2011). Can plant litter affect net primary production of a typical steppe in Inner Mongolia? *J. Veg. Sci.* 22, 367–376. doi: 10.1111/j.1654-1103.2011.01257.x

Weltzin, J. F., Keller, J. K., Bridgham, S. D., Pastor, J., Allen, P. B., and Chen, J. (2005). Litter controls plant community composition in a northern fen. *Oikos* 110, 537–546. doi: 10.1111/j.0030-1299.2005.13718.x

Wu, N., Liu, J., and Yan, Z. L. (2004). Grazing intensity on the plant diversity of alpine meadow in the eastern Tibetan plateau. *Rangifer* 15, 9–15. doi: 10.7557/2.24.4.1664

Xu, Q. N., Yang, X., Yan, Y., Wang, S. P., Loreau, M., and Jiang, L. (2021). Consistently positive effect of species diversity on ecosystem, but not population, temporal stability. *Ecol. Lett.* 24, 2256–2266. doi: 10.1111/ele.13777

Yan, Y. C., Yan, R. R., Chen, J. Q., Xin, X. P., Eldridge, D. J., Shao, C. L., et al. (2018). Grazing modulates soil temperature and moisture in a Eurasian steppe. *Agric. For. Meteorol.* 262, 157–165. doi: 10.1016/j.agrformet.2018.07.011

Yang, K., Wu, H., Qin, J., Lin, C. G., Tang, W. J., and Chen, Y. Y. (2014). Recent climate changes over the Tibetan Plateau and their impacts on energy and water cycle: A review. *Global Planet. Change* 112, 79–91. doi: 10.1016/j.gloplacha.2013.12.001

Ye, J. S., Delgado-Baquerizo, M., Soliveres, S., and Maestre, F. T. (2019). Multifinctionality debt in global drylands linked to past biome and climate. *Global Change Biol.* 25, 2152–2161. doi: 10.1111/gcb.14631

Young, M. L., Dobson, K. C., Hammond, M. D., and Zarnetske, P. L. (2024). Plant community responses to the individual and interactive effects of warming and herbivory across multiple years. *Ecology* 105, e4441. doi: 10.1002/ecy.4441

Yuan, X., Chen, Y., Qin, W., Xu, T. L., Mao, Y. H., Wang, Q., et al. (2021). Plant and microbial regulations of soil carbon dynamics under warming in two alpine swamp meadow ecosystems on the Tibetan Plateau. *Sci. Total Environ.* 790, 148072. doi: 10.1016/j.scitotenv.2021.148072

Zhang, W. P., Fornara, D., Yang, H., Yu, R. P., Callaway, R. M., Li, L., et al. (2023a). Plant litter strengthens positive biodiversity–ecosystem functioning relationships over time. *Trends Ecol. Evol.* 38, 473–484. doi: 10.1016/j.tree.2022.12.008

Zhang, X. Y., Ni, X. Y., Heděnec, P., Yue, K., Wei, X. Y., Yang, J., et al. (2022). Litter facilitates plant development but restricts seedling establishment during vegetation regeneration. *Funct. Ecol.* 36, 3134–3147. doi: 10.1111/1365-2435.14200

Zhang, X. B., Pei, G. T., Sun, J. F., Huang, Y. X., Huang, Q. Q., Xie, H. X., et al. (2023b). Responses of soil nitrogen cycling to changes in aboveground plant litter inputs: A meta-analysis. *Geoderma* 439, 116678. doi: 10.1016/j.geoderma.2023.116678

Zhang, R. Y., Wang, Z. W., Niu, S. L., Tian, D. S., Wu., Q., Gao, X. F., et al. (2021). Diversity of plant and soil microbes mediates the response of ecosystem multifunctionality to grazing disturbance. *Sci. Total Environ.* 776, 145730. doi: 10.1016/j.scitotenv.2021.145730

Zhao, J. X., Luo, T. X., Wei, H. X., Deng, Z. H., Li, X., Li, R. C., et al. (2019). Increased precipitation offsets the negative effect of warming on plant biomass and ecosystem respiration in a Tibetan alpine steppe. *Agr. For. Meteorol.* 279, 107761. doi: 10.1016/j.agrformet.2019.107761

Zhao, J. X., Yang, W., Tian, L. H., Qu, G. P., and Wu, G.-L. (2024). Warming differentially affects above-and belowground ecosystem functioning of the semi-arid alpine grasslands. *Sci. Total Environ.* 914, 170061. doi: 10.1016/j.scitotenv.2024.170061

Zhu, K., Chiariello, N. R., Tobecontrast, T., Fukami, T., and Field, C. B. (2016). Nonlinear, interacting responses to climate limit grassland production under global change. *P. Natl. Acad. Sci. USA.* 113, 10589–10594. doi: 10.1073/pnas.1606734113

Zhu, K., Song, Y. L., Lesage, J. C., Luong, J. C., Bartolome, J. W., Chiariello, N. R., et al. (2024). Rapid shifts in grassland communities driven by climate change. *Nat. Ecol. Evol.* 8, 2252–2264. doi: 10.1038/s41559-024-02552-z

frontiers | Frontiers in Plant Science

TYPE Original Research
PUBLISHED 20 May 2025
DOI 10.3389/fpls.2025.1570005

OPEN ACCESS

EDITED BY
Ting Hua,
Norwegian University of Science and Technology, Norway

REVIEWED BY
Zhijie Zhang,
Chinese Academy for Environmental Planning, China
Han Wang,
Peking University, China

*CORRESPONDENCE
Ruonan Li
rnli@rcees.ac.cn

RECEIVED 02 February 2025
ACCEPTED 21 April 2025
PUBLISHED 20 May 2025

CITATION
Hai Y, Han T, Wang Y, Li R, Yang Y, Wen Z and Zheng H (2025) Quantifying the impact of precipitation fluctuations on forest growth in Northeast China. *Front. Plant Sci.* 16:1570005. doi: 10.3389/fpls.2025.1570005

Quantifying the impact of precipitation fluctuations on forest growth in Northeast China

Yue Hai[1,2], Tian Han[1,3], Yu Wang[1,2,4], Ruonan Li[1,2]*, Yanzheng Yang[1,2], Zhi Wen[1,2] and Hua Zheng[1,2]

[1]State Key Laboratory for Ecological Security of Regions and Cities, Research Center for Eco-Environmental Sciences, Chinese Academy of Sciences, Beijing, China, [2]University of Chinese Academy of Sciences, Beijing, China, [3]College of Geoscience and Surveying Engineering, China University of Mining and Technology-Beijing, Beijing, China, [4]Solux College of Architecture and Design, University of South China, Hengyang, Hunan, China

Introduction: In the context of climate change, the escalating frequency of global precipitation fluctuations amplifies uncertainties in assessing the impact on forest ecosystem productivity. Hence, elucidating the dynamic relationship between precipitation characteristics and forest growth can provide effective management strategies for addressing climate change.

Methods: This study utilizes precipitation data from 1982 to 2022 to construct the frequency and amplitude of precipitation fluctuations and analyzes the response of forest growth in northern China to these precipitation variations.

Results: The growth of 13.7% of the region's forest is declining, with 8.1% of the area showing significant degradation. The core degradation zones for forest growth are located in semi-arid regions with precipitation frequencies ≥ 12 and amplitudes ≤ 60 mm and subhumid regions with precipitation frequencies ≥ 14 and amplitudes ≤ 65 mm. In the core semi-arid zone, deciduous broadleaf shrublands have greatest degraded area (2.8×104 ha), but deciduous needleleaf forests have the highest proportion of degradation (57.1%), while in the subhumid core degradation zone, deciduous broadleaf forests have the highest area (1.7×105 ha) and proportion of degradation (9.3%).

Discussion: This study not only provides a novel perspective for evaluating forest ecosystem responses to precipitation characteristics, but also offers crucial theoretical support for advancing the implementation of Nature-based Solutions in practical applications.

KEYWORDS

Northeast China, semi-arid region, subhumid region, precipitation variability, forest growth

1 Introduction

Forest growth converts solar energy into organic matter through photosynthesis, and the stronger the biomass accumulation capacity of healthy forest ecosystems (Liang and Wang, 2020). Precipitation is a decisive factor for tree growth and the ecological services of forest ecosystems. In semi-arid to subhumid regions, an annual rainfall of 400 mm represents a critical threshold for maintaining the health (Gessner et al., 2013; Chen et al., 2019; Liu, 2019), an increase in precipitation generally leads to a rise in forest growth (Hu et al., 2010; Reichstein et al., 2013; Li et al., 2024). However, changes in precipitation characteristics and the global hydrological cycle owing to climate change (Durack et al., 2012; IPCC, 2021; Ndehedehe et al., 2023) affect the dynamic response of forests to the original precipitation regimes. These changes impact not only forest growth but also the ecosystem services provided by forests, such as soil and water conservation, windbreaks, sand fixation, and climate regulation, especially in ecologically vulnerable areas. Therefore, clarifying the dynamic relationship between precipitation characteristics and forest growth is crucial for understanding the response of natural ecosystems to global climate change (Giorgi et al., 2019; Zhang et al., 2025).

Current research has analyzed the impact of precipitation on forest ecosystem from the perspectives of intensity and spatiotemporal scales (Guan et al., 2018; Wise and Dannenberg, 2022; Feng et al., 2024; Hu et al., 2025). The impact of rainfall intensity on forest significantly differs based on variations among stands. For example, as precipitation intensity increases, the productivity of temperate deciduous broadleaf forests may decrease, whereas that of deciduous needleleaf forests may increase (Fang et al., 2005). The temporal scale of precipitation primarily focuses on inter-annual and intra-annual variations (Viles and Goudie, 2003; Fatichi et al., 2012; Lyu et al., 2025). A greater inter-annual precipitation variability corresponds to lower vegetation growth (Liu et al., 2020a), and exceeding the variability threshold can lead to ecosystem mortality (Ye et al., 2013; Gherardi and Sala, 2015). Because of the phenological cycle of vegetation, seasonal precipitation characteristics are more significantly correlated with vegetation growth than annual totals (Robinson et al., 2013; Yuan et al., 2022; Chen and Zhang, 2023), and earlier rainfall during the growing season has a more pronounced effect on enhancing vegetation growth (Robinson et al., 2013; Lian et al., 2024; Zhu et al., 2025). Additionally, the increasingly extreme intra-annual distribution of precipitation significantly affects the response of forest ecosystems to inter-annual precipitation (Zhang et al., 2013; Zeppel et al., 2014). The spatial distribution of precipitation is mainly influenced by monsoons, but climate change has exacerbated its variability (Loo et al., 2015), making arid regions even drier and leading to the decline and even widespread mortality of forests in semi-arid regions (Liu et al., 2013).

Evidently, forest ecosystems exhibit complex dynamic responses to precipitation. However, current analyses of precipitation characteristics often focus on annual precipitation amounts or precipitation distribution within the year, with insufficient attention to the spectral properties and stochastic dynamics of precipitation variability. Hence, the impact of precipitation on forest has not been fully elucidated. Precipitation variability includes frequency and amplitude, referring to the number of precipitation events and the degree of variation in the amount of precipitation (Zhang et al., 2021), respectively. Precipitation frequency determines the interval at which forests receive precipitation; excessively frequent or infrequent precipitation events can trigger floods or droughts, suppress forest autotrophic respiration and photosynthesis, and affect forest growth (Craine et al., 2012; Marra et al., 2019). Precipitation amplitude directly affects the soil moisture supply; an appropriate amount of precipitation is beneficial for forest growth, whereas amounts exceeding or falling below certain thresholds can be detrimental (Zhang et al., 2018; Liu et al., 2024). Against the backdrop of climate change, precipitation events are expected to become more complex and vary in the future (IPCC, 2021), thereby increasing the risk to forest growth. Therefore, quantifying the impact of precipitation fluctuations on forest can enhance our understanding of the response and adaptive capacity of forest ecosystems to climate change and aid in the development of forest ecosystem management strategies.

This study introduces a novel approach for quantifying both precipitation frequency and amplitude as key indicators of precipitation fluctuation, and explores their impact on forest ecosystems dynamics. Specifically, the research aimed to analyze the dynamic characteristics of precipitation fluctuations and forest growth of forest ecosystems in Northeast China from 1982 to 2022. The objectives of the study were to: (1) establish indicators for assessing precipitation fluctuation and identify regions with precipitation variability and their characteristics, (2) elucidate the response relationship between precipitation fluctuation characteristics and forest dynamics and determine the thresholds at which precipitation fluctuation leads to significant differences in forest change trends, and (3) examine the growth trend conditions of different forest types within precipitation fluctuation threshold zones. The novelty of this study lies in the development of an integrated index for quantifying precipitation variability in terms of fluctuation frequency and amplitude. This study provides a scientific basis for addressing forest degradation under climate change, facilitating the implementation and application of Nature-based Solutions (NbS) in forest ecosystem management.

2 Study area and methods

2.1 Study area

The northeast forest region accounts for 28.9% of the total forest area in China and is the largest natural forest area in the country (Nkonya et al., 2016). This region encompasses four main types of forests: deciduous broadleaf shrubland, deciduous needleleaf forest, evergreen needleleaf forest, and deciduous broadleaf forest. The forest ecosystems of northeast China, located in the semi-arid to humid transition zone, play a critical role in maintaining ecological security, and serve as a significant ecological barrier (Yu et al., 2011). Over the past few decades, the Northeast

region has witnessed a substantial expansion in forest cover, driven by the implementation of large-scale ecological restoration programs, such as the Three-North Shelterbelt Forest Program and the Grain for Green Project (Nkonya et al., 2016; Song et al., 2022a). This expansion has been further facilitated by a shift in forest management policies, transitioning from timber production-oriented practices to ecological restoration and conservation (Yu et al., 2011). However, influenced by climate change, 400 mm isohyet (the forest-grassland boundary) has expanded eastward by 1850 km over the past few decades (Ma et al., 2016), profoundly affecting the ecosystem. To quantify the impact of precipitation fluctuations on the forest ecosystems of northeast China, we selected the area of spatial fluctuation around the 400mm isohyet as the study area, focusing on the forests within this region to analyze the dynamic relationship between precipitation characteristics and forest ecosystem. Based on multi-year precipitation data, we have divided the study area into semi-arid and subhumid zones (Figure 1).

2.2 Data sources

This study used unchanged stable forest ecosystems from 1980 to 2020 as the research subjects. The accuracy of land use data exceeds 95%, providing a comprehensive and objective understanding of the quantity and distribution of land use changes in China, as well as the patterns and characteristics of interactions among various land use types (Jiyuan et al., 2002). The NDVI data used in this study underwent a Bayesian calibration and correction procedure, ensuring the reliability of data quality (Pinzon and Tucker, 2014). Numerous studies have demonstrated a strong correlation between the normalized difference vegetation index (NDVI) and vegetation growth dynamics (Fensholt et al., 2012); hence, this study employed NDVI data to represent forest growth. To negate false NDVI signals due to winter snow cover, this study used values from the growing season (June to October) for analysis, with the sum of the NDVI values during the growing season indicating forest growth dynamics (Fang et al., 2005). Precipitation data were generated using the globally available 0.5° climate data released by CRU and the high-resolution global climate data provided by WorldClim, employing the delta spatial downscaling method. Validation was conducted using 496 independent meteorological observation points, which indicated a reduction in the mean absolute error of 25.7% (Peng et al., 2019). Annual precipitation data from 1982 to 2022 were used to extract 400 mm isohyet and calculate frequency and amplitude of precipitation fluctuations. Land use and NDVI data were sampled to a resolution of 1 km using precipitation grid data as the capture object. The specific descriptions of the data are presented in Table 1.

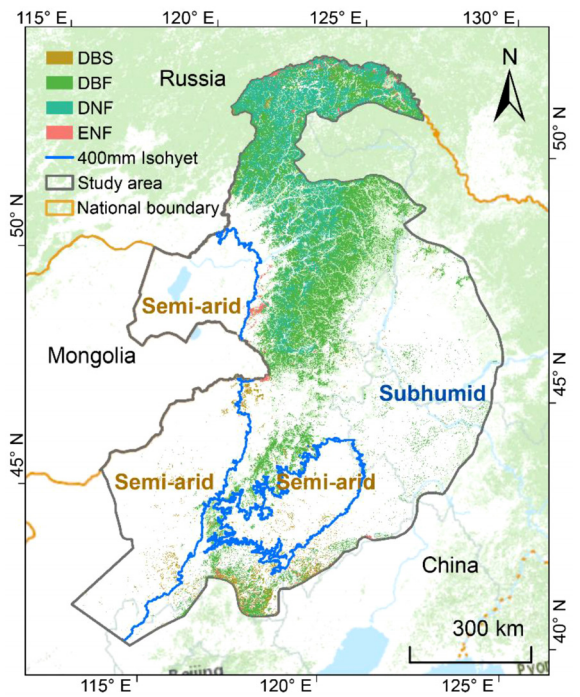

FIGURE 1
Spatial distribution of the main forest types and extent of the 400 mm isohyet averaged in the study area. DBS, Deciduous broadleaf shrubland, DBF, Deciduous broadleaf forest, DNF, Deciduous needleleaf forest, ENF, Evergreen needleleaf forest.

2.3 Calculation and spatial distribution of precipitation fluctuation characteristics

Based on ecohydrological principles, the 400 mm isohyet serves as a critical ecological threshold for forest distribution (Rishmawi et al., 2016; Chen et al., 2019). To quantify precipitation fluctuations, we define the frequency of precipitation fluctuation as the number of times the 400 mm isohyet crosses a grid, reflecting the recurrence of drought events. Frequent precipitation fluctuations may intermittently limit soil water availability and impair root absorption of water, thereby exerting stress on forests (Gu et al., 2016; Ke, 2022). The amplitude of precipitation fluctuation indicates the deviation of annual precipitation relative to the 400 mm threshold, reflecting the intensity of drought. Greater amplitudes directly alter water availability and influence physiological processes such as photosynthesis and growth (Liu et al., 2020a; Yu et al., 2022). By analyzing these two indicators, this study reveals how the frequency and amplitude of precipitation fluctuations jointly regulate forest growth, providing a basis for predicting the responses of forest ecosystems to climate change.

Precipitation Fluctuation Frequency: Over a given time period, this represents the number of times the same isohyet line spatially overlaps in two consecutive years and is used to characterize the spatial variation of precipitation fluctuation (Quesada-Hernández et al., 2019). The calculation of precipitation fluctuation frequency was conducted as follows: First, based on annual precipitation raster data, the region was classified into two categories using 400 mm as a threshold: areas with annual precipitation ≥ 400 mm were assigned a value of 1, while other areas were assigned a value of 0. Next, a logical exclusive OR (XOR) operation was performed on the assigned data for adjacent years (Figure 2), while if they differed, the result was 1, thus reflecting

10.3389/fpls.2025.1570005

TABLE 1 Requisite data used in this study.

Data type	Acronym	Time	Spatial resolution	Temporal resolution	Data source
Precipitation	Pre	1982–2022	1 km	Mon	National Earth System Science Data Center, National Science & Technology Infrastructure of China (http://www.geodata.cn)
Land Use and Land Cover Change	LUCC	1980–2020	1 km	Year	Resource and Environmental Science Data Platform (https://www.resdc.cn/)
Normalized Difference Vegetation Index	NDVI	1982–2022	1/12°	15 d	National Oceanic and Atmospheric Administration, NOAA (https://ecocast.arc.nasa.gov/data/pub/gimms/)

changes in the spatial distribution of precipitation. Subsequently, the results of the XOR operation were summed across grids to obtain the precipitation fluctuation frequency for adjacent years. Finally, the precipitation fluctuation frequencies for all adjacent years within the study period were aggregated to derive the overall precipitation fluctuation frequency, which characterizes the spatial variability of precipitation during the entire study period. We define the study area as the region where the frequency of precipitation fluctuations is greater than 0, referred to as the precipitation fluctuation zone.

Precipitation Fluctuation Amplitude: Over a given period, the deviation relative to the 400 mm precipitation line was quantified. The formula used is as follows (Equation 1):

$$D_{400} = \frac{\sum_{i=1982}^{n}(x_i - 400)}{N} \quad (1)$$

where x_i represents the grid precipitation amount for year i, n represents the final year of observation, N represents the number of years observed and D_{400} is the amplitude of the precipitation fluctuation. Areas with $D_{400} > 0$ were classified as subhumid fluctuation zones, and areas with $D_{400} < 0$ were classified as semi-arid fluctuation zones.

Figure 3 illustrates the spatial distribution of the frequency and amplitude of precipitation fluctuation within the study area from 1982 to 2022. The highest precipitation fluctuation frequency was 27, with 41.7% of the study area experiencing more than 14 fluctuations. The amplitude of precipitation fluctuation ranged from −186 to 238 mm; within this, the semi-arid fluctuation zone had a precipitation fluctuation amplitude ranging from −186 to 0 mm, while the subhumid fluctuation zone had an amplitude ranging from 0 to 238 mm.

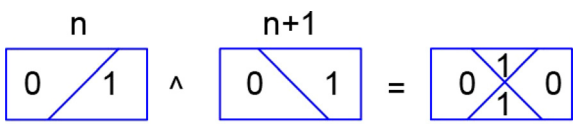

FIGURE 2
Calculation of precipitation fluctuation frequency in adjacent years.

2.4 Identification of forest degradation

In this study, the least squares method was used to analyze the trends in forest dynamics changes, a technique widely used in assessing vegetation dynamics (Lin et al., 2016; Mehmood et al., 2024). In assessing forest dynamics changes, this study employs residual analysis to filter out NDVI outliers, thereby effectively enhancing the accuracy and stability of the model estimates. The sign of the slope was employed to characterize the increase or decrease in forest, whereas the absolute value of the slope was used to represent the amplitude of the forest change. In addition, an F-test was used to assess the significance of the slope, and the classification levels were delineated (Table 2). The trends in forest changes were calculated as follows (Equation 2):

$$S_{NDVI} = \frac{n \times \sum_{i=1}^{n}(i \times NDVI_i) - \sum_{i=1}^{n} i \times \sum_{i=1}^{n} NDVI_i}{n \times \sum_{i=1}^{n} i^2 - (\sum_{i=1}^{n} i)^2} \quad (2)$$

where S_{NDVI} represents the slope of the linear regression equation for NDVI, n denotes the study period (y), and $NDVI_i$ represents the observed NDVI value for year i.

2.5 Change point detection

The Pettitt test is a rank-based non-parametric statistical test designed to detect change points within a data series (Pettitt, 1979; Hai et al., 2020). It has been used extensively to detect changes in hydrological and climatological records (Verstraeten et al., 2006; Zhang et al., 2009), and the method is as follows (Equations 3–6):

$$U_{t,\ n} = U_{t\ -1} + \sum_{j=1}^{n} sgn(x_i - x_j) \quad (3)$$

$$sgn(x_i - x_j) = \begin{cases} 1 & x_i - x_j > 0 \\ 0 & x_i - x_j = 0 \\ -1 & x_i - x_j < 0 \end{cases} \quad (4)$$

$$K = max\left|U_{t,\ n}\right|, t = 1, 2, \ldots, n \quad (5)$$

$$P \cong 2exp\left(-\frac{6K^2}{n^3 + n^2}\right) \quad (6)$$

10.3389/fpls.2025.1570005

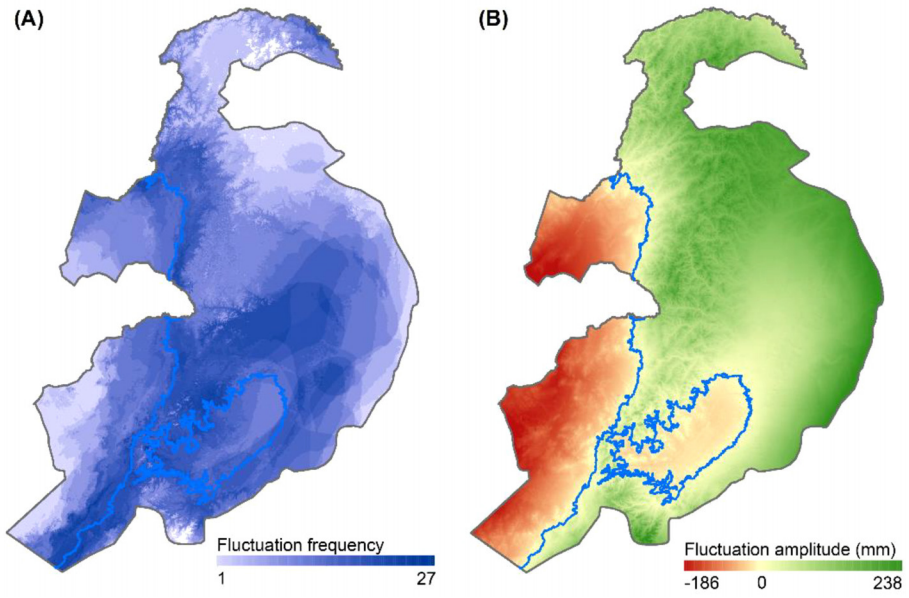

FIGURE 3
Spatial distribution of precipitation fluctuation **(A)** frequency and **(B)** amplitude.

where $U_{t,\,n}$ represents the defined statistic; n is the number of interval groups; x_i and x_j are the forest dynamics trends of the i-th and j-th groups, respectively; K is the year of the change point; if $P \leq 0.05$, then the change point year is statistically significant. This study employs the Pettitt test to identify turning points in significantly degraded forest dynamics trends at precipitation fluctuation frequency and the amplitude. Additionally, a one-way analysis of variance (ANOVA) is conducted to ascertain the differences in forest dynamics trends before and after these turning points ($P < 0.05$), as referenced by Lix et al. (1996), where a lower mean of forest dynamics trends indicates more severe forest degradation. The article defines regions exhibiting greater forest degradation in relation to precipitation fluctuation frequency and amplitude as core areas, and evaluates the degradation trends of different forest types within these core areas.

3 Results

3.1 Forest degradation

In the precipitation fluctuation zone, the total area decreased by 2.5×10^6 ha, accounting for 13.7% of the total forest area in these regions. Specifically, the forest degradation in the subhumid and semi-arid fluctuation zones was 2.3×10^6 ha and 1.6×10^5 ha, representing 13.2% and 30.4% of their respective forest areas. Further analysis revealed that 4.2% (7.5×10^5 ha) of the forest area within the precipitation fluctuation zone experienced significant decline, primarily concentrated in the central part of the subhumid fluctuation zone and the transitional areas between the semi-arid and subhumid fluctuation zones. In detail, the significantly declined forest area accounted for 4.0% (7.0×10^5 ha) and 10.9% (5.7×10^4 ha) of the forest area in the subhumid and semi-arid fluctuation zones, respectively (Figures 4A, B). An analysis of the different forest types revealed that the semi-arid fluctuation zone has the largest proportion of significant decline in deciduous broadleaf shrublands (12.6%, 3.7×10^4 ha), followed by deciduous broadleaf forests (10.3%, 1.4×10^4 ha), evergreen needleleaf forests (9.9%, 2.6×10^3 ha), and deciduous needleleaf forests (5.3%, 3.8×10^3 ha). In the subhumid fluctuation zone, deciduous broadleaf forests show the highest proportion of significant decline at 4.3% (4.6×10^5 ha), followed by deciduous needleleaf forests (3.7%, 2.1×10^5 ha), evergreen needleleaf forests (3.1%, 1.3×10^4 ha), and deciduous broadleaf shrublands (2.3%, 1.5×10^4 ha) (Figure 4C).

TABLE 2 Trend grade of forest dynamics.

Steady increase (SI)	Insignificant degradation (ID)	Significant degradation (SD)
$S_{NDVI}>0$	$S_{NDVI}<0$	$S_{NDVI}<0$
Other	$P>0.05$	$P \leq 0.05$

3.2 Qualitative impact of precipitation change frequency and amplitude on forest dynamics

Overall, forest dynamics exhibited a stability trend followed by a decline as the precipitation fluctuation frequency increased. Meanwhile, an initial rise followed by stabilization as the precipitation fluctuation amplitude increased (Figure 5). This indicates that areas with high-frequency and low-amplitude precipitation fluctuations have lower forest growth and more

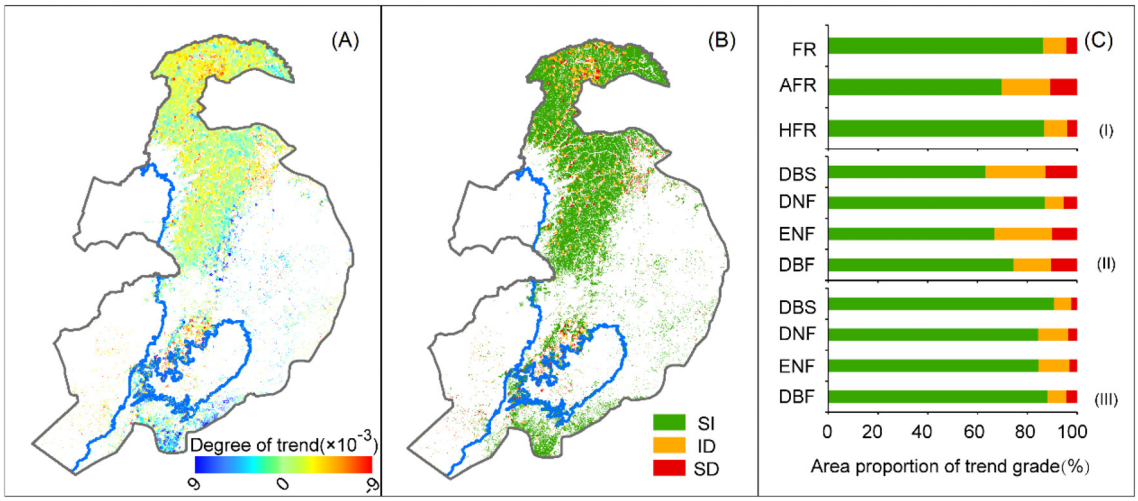

FIGURE 4
Spatial distribution of **(A)** forest dynamics trends and **(B)** trend significance and **(C)** trend-level statistics in terms of area and forest type in the (I) study area, (II) semi-arid fluctuation area, and (III) subhumid fluctuation area. FR, AFR, and HFR represent the entire study area, semi-arid, and subhumid fluctuation areas, respectively. SI indicates steady increase, ID indicates an insignificant decline, and SD indicates a significant decline. DBS, Deciduous broadleaf shrubland; DBF, Deciduous broadleaf forest; DNF, Deciduous needleleaf forest; ENF, Evergreen needleleaf forest.

dramatic change, whereas areas with low-frequency and high-amplitude precipitation fluctuations have higher forest growth and are relatively stable. For precipitation fluctuation frequency, the inflection points for forest growth did not significantly differ across different climatic zones, being 12 and 14 times in semi-arid and subhumid areas, respectively. Furthermore, the relationship between forest dynamics and precipitation fluctuation amplitude had an inflection point in semi-arid zones that was lower than that in subhumid zones (60 and 65 mm, respectively) (Figure 5).

3.3 Differences in forest dynamics in the core areas

This study further identified the relationships between precipitation characteristics and forest types in the core areas characterized by high-frequency but low-amplitude precipitation fluctuations (Figure 6). In the semi-arid fluctuation zone, the most significant decline in forest dynamics was observed in deciduous needleleaf forests (57.1%), followed by deciduous broadleaf shrublands (12.0%), deciduous broadleaf forests (11.0%), and evergreen needleleaf forests (2.9%). In terms of area, deciduous broadleaf shrublands showed the largest significant decline, accounting for 72.6% of the total significantly degraded area, followed by deciduous broadleaf forests (25.6%), deciduous needleleaf forests (1.0%), and evergreen needleleaf forests (0.8%). In the sub-humid fluctuation zone, deciduous broadleaf forests exhibited the largest proportion of significant decline (9.1%), followed by evergreen needleleaf forests (4.9%), deciduous needleleaf forests (3.6%), and deciduous broadleaf shrublands (2.8%). In terms of area, deciduous broadleaf forests accounted for the largest significant decline, comprising 88.7% of the degraded area, followed by deciduous broadleaf shrublands (5.2%), evergreen needleleaf forests (3.2%), and deciduous needleleaf forests (2.9%).

4 Discussion

4.1 Identified forest degradation

This study analyzed forest dynamics trends in the precipitation fluctuation zone of Northeastern China, revealing that 13.7% of the forest area experienced a decline, with 4.2% showing significant downward trends, and notable differences were observed between semi-arid and subhumid regions (Figure 4). Forest degradation in Northeast China has been corroborated by multiple studies. For instance, long-term (1982–2012) and segmented (1982–1997 and 1997–2012) analyses based on GIMMS NDVI data indicates that 38.91–46.21% of vegetation in China has exhibited a declining trend, with significant decreases in the Northeast region (Liu et al., 2015). Furthermore, dendrochronology analyses indicate that since 1994, forest growth trends in China's semi-arid to subhumid forests have generally decreased (Liu et al., 2013), with the correlation between forest growth and precipitation being significantly stronger than that with temperature (Poulter et al., 2013). This phenomenon may be closely related to the reductions in precipitation and the intensification of droughts caused by climate change. Studies have shown that both the frequency and intensity of precipitation decrease and drought events in Northeastern China are on the rise (Sheffield et al., 2009; Huang et al., 2016), and more frequent and severe droughts significantly increase the likelihood of reduced forest growth (Allen et al., 2010). Notably, forests in ecologically vulnerable areas exhibit high sensitivity to climate change (Liu and Yin, 2013; Shi et al., 2021). However, there are

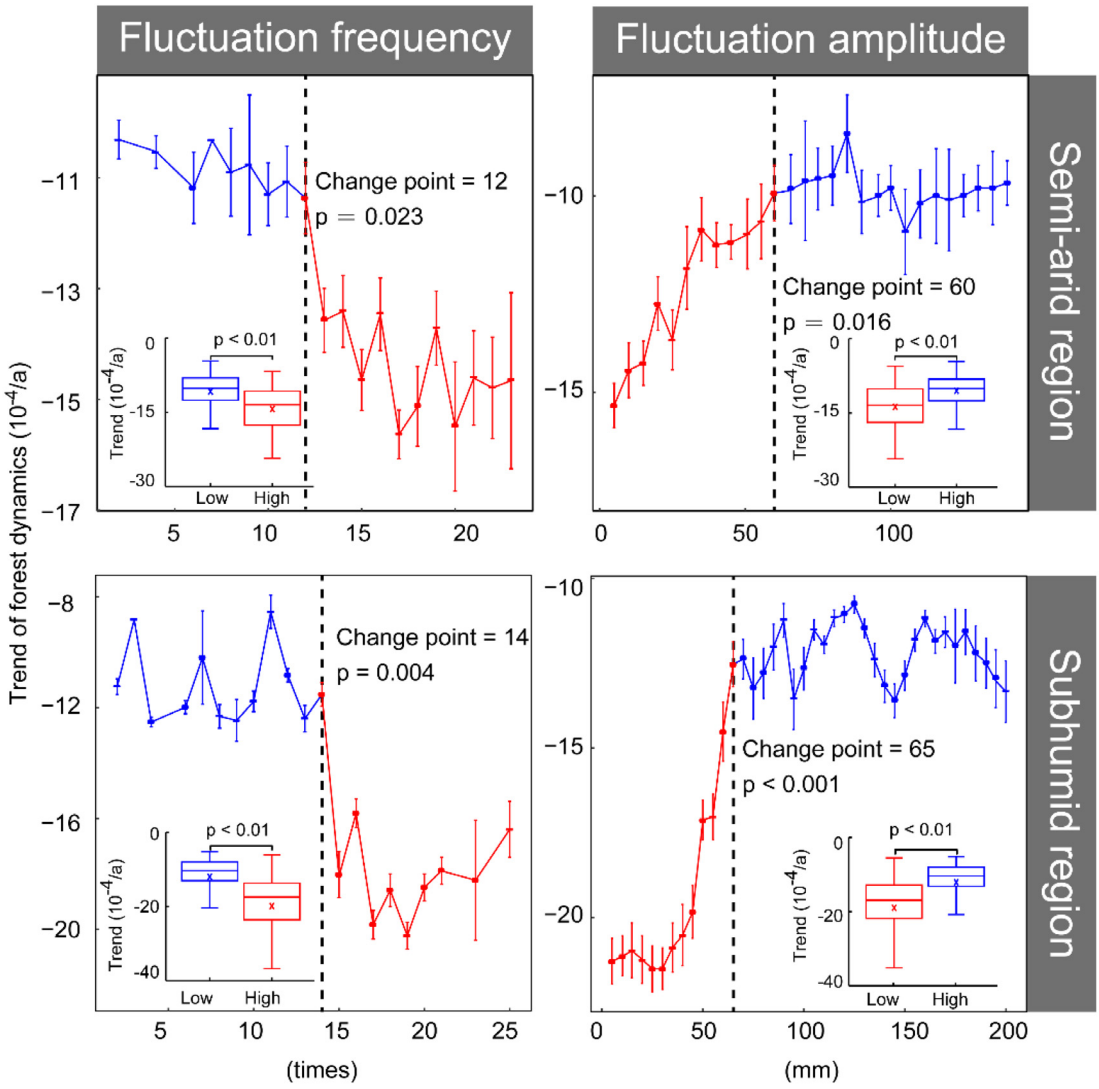

FIGURE 5
Forest dynamics trend of significantly degraded forests based on the frequency and amplitude of precipitation fluctuation. The dashed line indicates the threshold for abrupt changes, the red dotted line represents the significant relationship between forest trends and changes in precipitation frequency and amplitude, while the blue dotted line represents the absence of a significant relationship between forest trends and changes in precipitation frequency and amplitude. The subgraph shows the differences in the trend of forest growth before and after the threshold for abrupt changes.

differences in the adaptive capacities of different vegetation zones to climate change (Maherali et al., 2004; Jiang et al., 2023), which may be an important reason for the differences observed in forest dynamics trends between semi-arid and subhumid regions.

In terms of forest community structure, evergreen needleleaf forest exhibit the highest rates of degradation in semi-arid regions, which may be related to their higher water requirements (Wang et al., 2018). Under drought conditions, their resilience is relatively weak (Lv et al., 2022), making them more susceptible to water stress. Deciduous needleleaf forests exhibit comparable degradation rates in semi-arid and subhumid regions, demonstrating robust adaptive capacity. This resilience may be attributed to the fact that, under drought conditions, deciduousness reduces water transpiration (Zeng et al., 2025), thereby enhancing their drought resistance. Deciduous broadleaf forests exhibit significant degradation in arid environments, primarily due to their high sensitivity to drought stress (Kang et al., 2025). Reduced moisture availability leads to premature leaf abscission (Singh and Kushwaha, 2016), thereby restricting the normal growth and development of trees and exacerbating the process of forest degradation. Deciduous broadleaf shrublands in semi-arid regions are more prone to degradation than those in subhumid areas. This heightened degradation is attributed to the shrubs' lack of effective self-regulation mechanisms under more adverse conditions (Kooch et al., 2022).

4.2 Role of precipitation characteristics on forest growth and change point

This study identifies significant change points in forest dynamics that correspond to the frequency and amplitude of

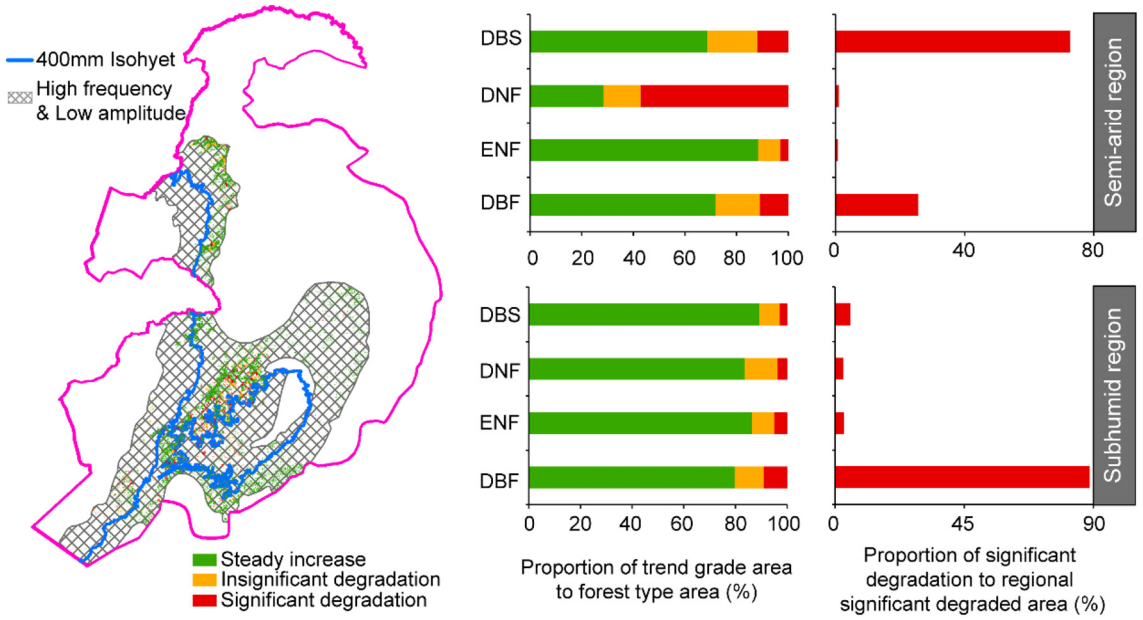

FIGURE 6
Spatial distribution of forest dynamics trend in areas with high-frequency and low-amplitude precipitation fluctuation. The histogram shows the trend-level statistics of different forest types in the two fluctuation zones. DBS, Deciduous broadleaf shrubland; DBF, Deciduous broadleaf forest; DNF, Deciduous needleleaf forest; ENF, Evergreen needleleaf forest.

precipitation fluctuations. Specifically, regions characterized by high-frequency and low-amplitude precipitation fluctuations experience more severe forest degradation than others, due to the resulting instability of available water resources for vegetation. In subhumid regions, the high frequency of precipitation fluctuations indicates that the precipitation amount falls below the critical threshold of 400 mm in multiple years. These frequent drought conditions weaken the moisture supply in forest soils (Liu et al., 2020a), making it difficult for trees to acquire sufficient water to maintain normal physiological activities, thereby exacerbating forest degradation. In semi-arid regions, areas characterized by large precipitation fluctuation amplitudes are primarily dominated by herbaceous plants, shrubs, or sparse forests rather than forest ecosystems. These types of vegetation exhibit strong adaptability and resilience to precipitation fluctuations (Zhao et al., 2015; Hu et al., 2021), which results in a relatively minor impact of such fluctuations on the overall ecosystem.

In addition to the amount of precipitation (e.g., surplus or deficit), the temporal characteristics of precipitation (e.g. extreme events, consecutive droughts, and precipitation variability) also play a significant role in ecosystem dynamics (Liu et al., 2020a). The impacts of precipitation characteristics on forest dynamics exhibit regional differences and vary among forest types (Knapp et al., 2002; Heisler-White et al., 2008; Guan et al., 2018). The direction of the impact of extreme precipitation events on forest growth also varies by geographical region. For example, in arid regions, extremely wet conditions can stimulate forest growth to compensate for the decline caused by extreme drought (Jiang et al., 2019). In humid regions, extreme precipitation can negatively affect forest growth and even lead to tree mortality (Zhao et al., 2005). Moreover, the degree of impact of precipitation surplus or deficit on forest dynamics varies regionally. For example, in arid regions, forest growth generally increases in wet years, while the decrease in dry years is relatively small; in humid regions, the increase in wet years is smaller, while the decrease in dry years is relatively larger (Al-Yaari et al., 2020). In this study, the core areas of declining forest growth were primarily located in areas with high-frequency and low-amplitude precipitation fluctuation distributed across both the semi-arid and subhumid zones (Figure 5). The diversity in the impact of precipitation characteristics on forest types is reflected in the dynamic relationship between drought persistence and forest growth. For instance, consecutive droughts have exacerbated the decline in needleleaf forests, whereas the impact of initial droughts is more pronounced in broadleaf forests (Anderegg et al., 2020; Liu et al., 2020b). Deciduous broadleaf shrublands had a lower proportion of significant decline in the core areas compared with that in deciduous broadleaf, evergreen needleleaf, and deciduous needleleaf forests (Figure 6). The above analysis indicated that quantifying precipitation characteristics from different perspectives can better identify the dynamic response of forests to precipitation.

4.3 Implications for forest management

By exploring the impact of precipitation fluctuation characteristics on forest growth, this study quantified the variability in the growth response of different forest types to precipitation fluctuations. These findings provide critical insights

for shaping effective forest conservation and restoration policies, particularly in the context of climate variability and change.

Region-specific management strategies should be developed to address unique environmental conditions. For instance, in forest-steppe ecotones, ecological afforestation projects should prioritize drought-resistant species and optimize shrub density to enhance water-use efficiency (Chen et al., 2015), thereby addressing current and future climate changes (Deng et al., 2019; Xiao et al., 2021). Forest composition should be diversified by selecting resilient forest types. Deciduous broadleaf forests, which cover the largest areas and higher degradation rate, often shed leaves to cope with drought, reducing water loss but resulting in relatively poor drought resistance (Lv et al., 2022). Therefore, selecting drought-resistant deciduous broadleaf species is essential to respond to precipitation changes. Because of their lower evapotranspiration rates, evergreen needleleaf forests show strong resistance in areas of fluctuating precipitation (Song et al., 2022b), suggesting that increasing their proportion can mitigate growth decline and enhance the stability of future forest ecosystems. Afforestation practices must consider the water adaptability of trees, and projects should incorporate water-adaptive measures into planning and implementation. Widespread forest growth decline (Figure 4) has been observed, with related studies showing that the afforestation survival rate in China's Three-North Shelterbelt Program is only 60% (Xiao et al., 2021). The failure to account for water adaptability in afforestation is a significant factor contributing to large-scale plantation losses (Deng et al., 2019).

In the future, global warming will intensify hydrological cycle (IPCC, 2021; Ndehedehe et al., 2023), and extreme weather will alter precipitation characteristics (Jiang et al., 2019), inevitably having a profound impact on global forest and forest ecosystem services and functions (Aleixo et al., 2019). In the face of complex environmental challenges, continuous monitoring of forest dynamics and precipitation patterns is essential to inform adaptive management strategies. Policymakers should invest in research to better understand the interactions between climate change, precipitation fluctuations, and forest growth. In particular, forests in northern China are mostly even-aged monoculture plantations, which have poorer ecosystem stability and resilience compared to natural forests (Huang et al., 2016), and will face significant risks in adapting to future climate change (Figure 6). In the management of ecological projects and policy-making processes in northern China, increasing forest tree species diversity can be a valuable strategy to enhance the resilience of forests against frequent and intense precipitation changes, and this positive effect is most pronounced in arid zone forests (Peng et al., 2020; Liu et al., 2022).

4.4 Limitations and future research directions

Despite the widespread use of NDVI as an indicator for monitoring forest growth dynamics, its effectiveness varies significantly across different ecological systems. In humid regions with high vegetation cover, NDVI tends to saturate, rendering it incapable of detecting subtle changes in plant growth. Conversely, in arid areas with low vegetation cover, soil background signals can obscure vegetation signals, leading to insufficient sensitivity of NDVI for accurately detecting vegetation changes. In the semi-arid and semi-humid transitional zones addressed in this study, where vegetation density is moderate, NDVI proves effective in capturing variations in plant growth. Clearly, selecting appropriate remote sensing indices based on the specific climatic and vegetation characteristics is crucial for accurately representing forest growth conditions. It is recommended to use the Enhanced Vegetation Index (EVI) in areas with high vegetation cover and the Modified Soil-Adjusted Vegetation Index (MSAVI) in arid regions to overcome the inherent limitations of NDVI in extreme biomes.

This study focuses on forest areas that remained unchanged between 1980 and 2020. While this approach effectively controls for the natural processes of forest succession influencing growth, it may underestimate the true impact of precipitation fluctuations on forest growth. By concentrating solely on stable forest regions, the research overlooks the reductions in forest area caused by degradation, logging, or land cover change during this period, potentially limiting the findings' capacity to fully capture the dynamic changes within forest ecosystems. Future studies should integrate considerations of both increases and decreases in forest area to formulate more comprehensive forest management and conservation strategies.

5 Conclusion

The results of this study clearly indicated that the frequency and amplitude of precipitation fluctuations were significant determinants of the state of forest ecosystems, with high-frequency and low-amplitude precipitation fluctuations being particularly impactful, as 8.14% of forests exhibited notable degradation. This had to be taken into consideration in the context of increasingly complex and variable precipitation characteristics in the past. With the use of NDVI, precipitation, and land use data, our findings indicated that in the semi-arid core degradation zone, deciduous broadleaf shrublands covered the largest degraded area, whereas deciduous needleleaf forests had the highest proportion of degradation; In the subhumid core degradation zone, deciduous broadleaf forests had the highest area and proportion of degradation, amounting to 1733 km^2 and 9.13%, respectively. This study evaluated the response of forest ecosystems to precipitation characteristics in terms of fluctuation frequency and amplitude, providing a basis for the restoration and management of forest ecosystems in arid regions, and for addressing climate change.

Data availability statement

The original contributions presented in the study are included in the article/supplementary material. Further inquiries can be directed to the corresponding author.

Author contributions

YH: Conceptualization, Data curation, Investigation, Methodology, Writing – original draft. TH: Data curation,

Writing – review & editing. YW: Data curation, Writing – review & editing. RL: Data curation, Investigation, Methodology, Writing – original draft. YY: Data curation, Formal Analysis, Writing – review & editing. ZW: Data curation, Investigation, Writing – review & editing. HZ: Conceptualization, Writing – review & editing.

Funding

The author(s) declare that financial support was received for the research and/or publication of this article. This research was funded and supported by National Natural Science Foundation of China, Grant/Award Number: 42361144872; National Key R&D Program of China, Grant/Award Number: 2022YFF1301802; National Natural Science Foundation of China, Grant/Award Number: 52179083 and 42171099.

Acknowledgments

We are grateful to the reviewers for their valuable suggestions in improving the manuscript.

Conflict of interest

The authors declare that the research was conducted in the absence of any commercial or financial relationships that could be construed as a potential conflict of interest.

Generative AI statement

The author(s) declare that no Generative AI was used in the creation of this manuscript.

Publisher's note

References

Aleixo, I., Norris, D., Hemerik, L., Barbosa, A., Prata, E., Costa, F., et al. (2019). Amazonian rainforest tree mortality driven by climate and functional traits. *Nat. Clim. Change* 9, 384–388. doi: 10.1038/s41558-019-0458-0

Allen, C. D., Macalady, A. K., Chenchouni, H., Bachelet, D., McDowell, N., Vennetier, M., et al. (2010). A global overview of drought and heat-induced tree mortality reveals emerging climate change risks for forests. *For. Ecol. Manage.* 259, 660–684. doi: 10.1016/j.foreco.2009.09.001

Al-Yaari, A., Wigneron, J., Ciais, P., Reichstein, M., Ballantyne, A., Ogée, J., et al. (2020). Asymmetric responses of ecosystem productivity to rainfall anomalies vary inversely with mean annual rainfall over the conterminous United States. *Global Change Biol.* 26, 6959–6973. doi: 10.1111/gcb.15345

Anderegg, W. R. L., Trugman, A. T., Badgley, G., Konings, A. G., and Shaw, J. (2020). Divergent forest sensitivity to repeated extreme droughts. *Nat. Clim. Change* 10, 1091–1095. doi: 10.1038/s41558-020-00919-1

Chen, C., Park, T., Wang, X., Piao, S., Xu, B., Chaturvedi, R. K., et al. (2019). China and India lead in greening of the world through land-use management. *Nat. Sustain.* 2, 122–129. doi: 10.1038/s41893-019-0220-7

Chen, Y., Wang, K., Lin, Y., Shi, W., Song, Y., and He, X. (2015). Balancing green and grain trade. *Nat. Geosci* 8, 739–741. doi: 10.1038/ngeo2544

Chen, X., and Zhang, Y. (2023). The impact of vegetation phenology changes on the relationship between climate and net primary productivity in Yunnan, China, under global warming. *Front. Plant Sci.* 14. doi: 10.3389/fpls.2023.1248482

Craine, J. M., Nippert, J. B., Elmore, A. J., Skibbe, A. M., Hutchinson, S. L., and Brunsell, N. A. (2012). Timing of climate variability and grassland productivity. *Proc. Natl. Acad. Sci.* 109, 3401–3405. doi: 10.1073/pnas.1118438109

Deng, C., Zhang, B., Cheng, L., Hu, L., and Chen, F. (2019). Vegetation dynamics and their effects on surface water-energy balance over the Three-North Region of China. *Agric. For. Meteorology* 275, 79–90. doi: 10.1016/j.agrformet.2019.05.012

Durack, P. J., Wijffels, S. E., and Matear, R. J. (2012). Ocean salinities reveal strong global water cycle intensification during 1950 to 2000. *Science* 336, 455–458. doi: 10.1126/science.1212222

Fang, J., Piao, S., Zhou, L., He, J., Wei, F., Myneni, R. B., et al. (2005). Precipitation patterns alter growth of temperate vegetation. *Geophys. Res. Lett.* 32, L21411. doi: 10.1029/2005GL024231

Fatichi, S., Ivanov, V., Yu,, and Caporali, E. (2012). Investigating interannual variability of precipitation at the global scale: is there a connection with seasonality? *J. Climate* 25, 5512–5523. doi: 10.1175/JCLI-D-11-00356.1

Feng, Q., Yang, H., Liu, Y., Liu, Z., Xia, S., Wu, Z., et al. (2024). Interdisciplinary perspectives on forest ecosystems and climate interplay: a review. *Environ. Rev.* 33, 1–21. doi: 10.1139/er-2024-0010

Fensholt, R., Langanke, T., Rasmussen, K., Reenberg, A., Prince, S. D., Tucker, C., et al. (2012). Greenness in semi-arid areas across the globe 1981–2007 — an Earth Observing Satellite based analysis of trends and drivers. *Remote Sens. Environ.* 121, 144–158. doi: 10.1016/j.rse.2012.01.017

Gessner, U., Naeimi, V., Klein, I., Kuenzer, C., Klein, D., and Dech, S. (2013). The relationship between precipitation anomalies and satellite-derived vegetation activity in Central Asia. *Global Planetary Change* 110, 74–87. doi: 10.1016/j.gloplacha.2012.09.007

Gherardi, L. A., and Sala, O. E. (2015). Enhanced interannual precipitation variability increases plant functional diversity that in turn ameliorates negative impact on productivity. *Ecol. Lett.* 18, 1293–1300. doi: 10.1111/ele.12523

Giorgi, F., Raffaele, F., and Coppola, E. (2019). The response of precipitation characteristics to global warming from climate projections. *Earth System Dynamics* 10, 73–89. doi: 10.5194/esd-10-73-2019

Gu, L., Pallardy, S. G., Hosman, K. P., and Sun, Y. (2016). Impacts of precipitation variability on plant species and community water stress in a temperate deciduous forest in the central US. *Agric. For. Meteorology* 217, 120–136. doi: 10.1016/j.agrformet.2015.11.014

Guan, K., Good, S. P., Caylor, K. K., Medvigy, D., Pan, M., Wood, E. F., et al. (2018). Simulated sensitivity of African terrestrial ecosystem photosynthesis to rainfall frequency, intensity, and rainy season length. *Environ. Res. Lett.* 13, 025013. doi: 10.1088/1748-9326/aa9f30

Hai, Y., Yang, g., Li, R., and Zheng, H. (2020). Recognition of vegetation spatial variation based on time-series mutation detection: A case study of the mountainous area of Northern Haihe River Basin. *Acta Ecologica Sin.* 40, 9138–9147.

Heisler-White, J. L., Knapp, A. K., and Kelly, E. F. (2008). Increasing precipitation event size increases aboveground net primary productivity in a semi-arid grassland. *Oecologia* 158, 129–140. doi: 10.1007/s00442-008-1116-9

Hu, Y., Li, H., Wu, D., Chen, W., Zhao, X., Hou, M., et al. (2021). LAI-indicated vegetation dynamic in ecologically fragile region: A case study in the Three-North Shelter Forest program region of China. *Ecol. Indic.* 120, 106932. doi: 10.1016/j.ecolind.2020.106932

Hu, H., Liu, X., He, Y., Feng, J., Xu, Y., and Jing, J. (2025). Legacy effects of precipitation change: Theories, dynamics, and applications. *J. Environ. Manage.* 373, 123729. doi: 10.1016/j.jenvman.2024.123729

Hu, Z., Yu, G., Fan, J., Zhong, H., Wang, S., and Li, S. (2010). Precipitation-use efficiency along a 4500-km grassland transect: Rain-use efficiency in Chinese grasslands. *Global Ecol. Biogeography* 19, 842–851. doi: 10.1111/j.1466-8238.2010.00564.x

Huang, J., Ji, M., Xie, Y., Wang, S., He, Y., and Ran, J. (2016). Global semi-arid climate change over last 60 years. *Clim Dyn* 46, 1131–1150. doi: 10.1007/s00382-015-2636-8

IPCC (2021). *Climate Change 2021: The Physical Science Basis* (United Kingdom and New York: Cambridge University Press).

Jiang, L., Liu, W., Liu, B., Yuan, Y., and Bao, A. (2023). Monitoring vegetation sensitivity to drought events in China. *Sci. Total Environ.* 893, 164917. doi: 10.1016/j.scitotenv.2023.164917

Jiang, P., Liu, H., Piao, S., Ciais, P., Wu, X., Yin, Y., et al. (2019). Enhanced growth after extreme wetness compensates for post-drought carbon loss in dry forests. *Nat. Commun.* 10, 195. doi: 10.1038/s41467-018-08229-z

Jiyuan, L., Mingliang, L., Xiangzheng, D., Dafang, Z., Zengxiang, Z., and Di, L. (2002). The land use and land cover change database and its relative studies in China. *J. Geogr. Sci.* 12, 275–282. doi: 10.1007/BF02837545

Kang, J., Shen, H., Liu, Y., Ma, P., Wu, B., Xu, L., et al. (2025). Drought dimensions impact birch resistance and resilience and their determining factors across semiarid forests of northern China. *Agric. For. Meteorology* 360, 110314. doi: 10.1016/j.agrformet.2024.110314

Ke, P.-J. (2022). Water shifts the balance of coexistence. *Nat. Ecol. Evol.* 6, 496–497. doi: 10.1038/s41559-022-01725-y

Knapp, A. K., Fay, P. A., Blair, J. M., Collins, S. L., Smith, M. D., Carlisle, J. D., et al. (2002). Rainfall variability, carbon cycling, and plant species diversity in a Mesic grassland. *Science* 298, 2202–2205. doi: 10.1126/science.1076347

Kooch, Y., Amani, M., and Abedi, M. (2022). The effect of shrublands degradation intensity on soil organic matter-associated properties in a semi-arid ecosystem. *Sci. Total Environ.* 853, 158664. doi: 10.1016/j.scitotenv.2022.158664

Li, T., He, B., Chen, D., Chen, H. W., Guo, L., Yuan, W., et al. (2024). Increasing sensitivity of tree radial growth to precipitation. *Geophysical Res. Lett.* 51, e2024GL110003. doi: 10.1029/2024GL110003

Lian, X., Peñuelas, J., Ryu, Y., Piao, S., Keenan, T. F., Fang, J., et al. (2024). Diminishing carryover benefits of earlier spring vegetation growth. *Nat. Ecol. Evol.* 8, 218–228. doi: 10.1038/s41559-023-02272-w

S. Liang and J. Wang (Eds.) (2020). "Chapter 15 - Estimate of vegetation production of terrestrial ecosystem," in *Advanced Remote Sensing, 2nd ed.* (Cambridge: Academic Press), 581–620. doi: 10.1016/B978-0-12-815826-5.00015-5

Lin, X., Tang, J., Li, Z., and Li, H. (2016). Vegetation greenness modelling in response to interannual precipitation and temperature changes between 2001 and 2012 in Liao River Basin in Jilin Province, China. *Springerplus* 5, 1173. doi: 10.1186/s40064-016-2737-9

Liu, H. (2019). It is difficult for China's greening through large-scale afforestation to cross the Hu Line. *Sci. China-Earth Sci.* 62, 1662–1664. doi: 10.1007/s11430-019-9381-3

Liu, J., Ma, X., Duan, Z., Jiang, J., Reichstein, M., and Jung, M. (2020a). Impact of temporal precipitation variability on ecosystem productivity. *WIREs Water* 7, e1481. doi: 10.1002/wat2.1481

Liu, H., Park Williams, A., Allen, C. D., Guo, D., Wu, X., Anenkhonov, O. A., et al. (2013). Rapid warming accelerates tree growth decline in semi-arid forests of Inner Asia. *Glob Change Biol.* 19, 2500–2510. doi: 10.1111/gcb.12217

Liu, D., Wang, T., Peñuelas, J., and Piao, S. (2022). Drought resistance enhanced by tree species diversity in global forests. *Nat. Geosci.* 15, 800–804. doi: 10.1038/s41561-022-01026-w

Liu, M., Wang, H., Zhai, H., Zhang, X., Shakir, M., Ma, J., et al. (2024). Identifying thresholds of time-lag and accumulative effects of extreme precipitation on major vegetation types at global scale. *Agric. For. Meteorology* 358, 110239. doi: 10.1016/j.agrformet.2024.110239

Liu, J., Wen, Z., and Gang, C. (2020b). Normalized difference vegetation index of different vegetation cover types and its responses to climate change in the Loess Plateau. *Acta Ecologica Sin.* 40, 678–691. doi: 10.5846/stxb201901090082

Liu, H., and Yin, Y. (2013). Response of forest distribution to past climate change: An insight into future predictions. *Chin. Sci. Bull.* 58, 4426–4436. doi: 10.1007/s11434-013-6032-7

Liu, X., Zhu, X., Pan, Y., Li, Y., and Zhao, A. (2015). Spatiotemporal changes in vegetation coverage in China during 1982—2012. *Acta Ecologica Sin.* 35, 5331–5342.

Lix, L. M., Keselman, J. C., and Keselman, H. J. (1996). Consequences of assumption violations revisited: A quantitative review of alternatives to the one-way analysis of variance F test. *Rev. Educ. Res.* 66, 579–619. doi: 10.3102/00346543066004579

Loo, Y. Y., Billa, L., and Singh, A. (2015). Effect of climate change on seasonal monsoon in Asia and its impact on the variability of monsoon rainfall in Southeast Asia. *Geosci. Front.* 6, 817–823. doi: 10.1016/j.gsf.2014.02.009

Lv, Y., He, H., Ren, X., Zhang, L., Qin, K., Wu, X., et al. (2022). High resistance of deciduous forests and high recovery rate of evergreen forests under moderate droughts in China. *Ecol. Indic.* 144, 109469. doi: 10.1016/j.ecolind.2022.109469

Lyu, X., Du, J., Qiu, Y., Jia, Y., Hao, C., and Dong, H. (2025). Spatiotemporal characteristics of future precipitation variability in the Tianshan Mountain region of China. *J. Hydrology: Regional Stud.* 57, 102124. doi: 10.1016/j.ejrh.2024.102124

Ma, C., Ma, W., Wang, C., Liu, W., Zhang, Y., and Ma, M. (2016). Migration and its inducements of 400 mm precipitation contour in the mainland China from 1951 to 2012 year. *J. Henan Polytechnic University(Natural Science)* 35, 520–525.

Maherali, H., Pockman, W. T., and Jackson, R. B. (2004). Adaptive variation in the vulnerability of woody plants to xylem cavitation. *Ecology* 85, 2184–2199. doi: 10.1890/02-0538

Marra, F., Nikolopoulos, E. I., Anagnostou, E. N., Bárdossy, A., and Morin, E. (2019). Precipitation frequency analysis from remotely sensed datasets: A focused review. *J. Hydrology* 574, 699–705. doi: 10.1016/j.jhydrol.2019.04.081

Mehmood, K., Anees, S. A., Muhammad, S., Hussain, K., Shahzad, F., Liu, Q., et al. (2024). Analyzing vegetation health dynamics across seasons and regions through NDVI and climatic variables. *Sci. Rep.* 14, 11775. doi: 10.1038/s41598-024-62464-7

Ndehedehe, C. E., Ferreira, V. G., Adeyeri, O. E., Correa, F. M., Usman, M., Oussou, F. E., et al. (2023). Global assessment of drought characteristics in the Anthropocene. *Resources Environ. Sustainability* 12, 100105. doi: 10.1016/j.resenv.2022.100105

E. Nkonya, A. Mirzabaev and J. Von Braun (Eds.) (2016). *Economics of Land Degradation and Improvement – A Global Assessment for Sustainable Development* (Cham: Springer International Publishing). doi: 10.1007/978-3-319-19168-3

Peng, S., Ding, Y., Liu, W., and Li, Z. (2019). 1 km monthly temperature and precipitation dataset for China from 1901 to 2017. *Earth System Sci. Data* 11, 1931–1946. doi: 10.5194/essd-11-1931-2019

Peng, J., Hu, Y., Dong, J., Mao, Q., Liu, Y., Du, Y., et al. (2020). Linking spatial differentiation with sustainability management: Academic contributions and research directions of physical geography in China. *Prog. Phys. Geography: Earth Environ.* 44, 14–30. doi: 10.1177/0309133319878107

Pettitt, A. N. (1979). A non-parametric approach to the change-point problem. *J. R. Stat. Society: Ser. C (Applied Statistics)* 28, 126–135. doi: 10.2307/2346729

Pinzon, J. E., and Tucker, C. J. (2014). A non-stationary 1981–2012 AVHRR NDVI3g time series. *Remote Sens.* 6, 6929–6960. doi: 10.3390/rs6086929

Poulter, B., Pederson, N., Liu, H., Zhu, Z., D'Arrigo, R., Ciais, P., et al. (2013). Recent trends in Inner Asian forest dynamics to temperature and precipitation indicate high sensitivity to climate change. *Agric. For. Meteorology* 178–179, 31–45. doi: 10.1016/j.agrformet.2012.12.006

Quesada-Hernández, L. E., Calvo-Solano, O. D., Hidalgo, H. G., Pérez-Briceño, P. M., and Alfaro, E. J. (2019). Dynamical delimitation of the Central American Dry Corridor (CADC) using drought indices and aridity values. *Prog. Phys. Geography: Earth Environ.* 43, 627–642. doi: 10.1177/0309133319860224

Reichstein, M., Bahn, M., Ciais, P., Frank, D., Mahecha, M. D., Seneviratne, S. I., et al. (2013). Climate extremes and the carbon cycle. *Nature* 500, 287–295. doi: 10.1038/nature12350

Rishmawi, K., Prince, S. D., and Xue, Y. (2016). Vegetation responses to climate variability in the northern arid to sub-humid zones of sub-Saharan Africa. *Remote Sens.* 8, 910. doi: 10.3390/rs8110910

Robinson, T. M. P., La Pierre, K. J., Vadeboncoeur, M. A., Byrne, K. M., Thomey, M. L., and Colby, S. E. (2013). Seasonal, not annual precipitation drives community productivity across ecosystems. *Oikos* 122, 727–738. doi: 10.1111/j.1600-0706.2012.20655.x

Sheffield, J., Andreadis, K. M., Wood, E. F., and Lettenmaier, D. P. (2009). Global and continental drought in the second half of the twentieth century: severity–area–duration analysis and temporal variability of large-scale events. *J. Climate* 22, 1962–1981. doi: 10.1175/2008JCLI2722.1

Shi, L., Liu, H., Xu, C., Liang, B., Cao, J., Cressey, E. L., et al. (2021). Decoupled heatwave-tree growth in large forest patches of *Larix sibirica* in northern Mongolian Plateau. *Agric. For. Meteorology* 311, 108667. doi: 10.1016/j.agrformet.2021.108667

Singh, K. P., and Kushwaha, C. P. (2016). Deciduousness in tropical trees and its potential as indicator of climate change: A review. *Ecol. Indic.* 69, 699–706. doi: 10.1016/j.ecolind.2016.04.011

Song, W., Feng, Y., and Wang, Z. (2022a). Ecological restoration programs dominate vegetation greening in China. *Sci. Total Environ.* 848, 157729. doi: 10.1016/j.scitotenv.2022.157729

Song, Y., Sterck, F., Sass-Klaassen, U., Li, C., and Poorter, L. (2022b). Growth resilience of conifer species decreases with early, long-lasting and intense droughts but cannot be explained by hydraulic traits. *J. Ecol.* 110, 2088–2104. doi: 10.1111/1365-2745.13931

Verstraeten, G., Poesen, J., Demarée, G., and Salles, C. (2006). Long-term (105 years) variability in rain erosivity as derived from 10-min rainfall depth data for Ukkel (Brussels, Belgium): Implications for assessing soil erosion rates. *J. Geophysical Research: Atmospheres* 111. doi: 10.1029/2006JD007169

Viles, H. A., and Goudie, A. S. (2003). Interannual, decadal and multidecadal scale climatic variability and geomorphology. *Earth-Science Rev.* 61, 105–131. doi: 10.1016/S0012-8252(02)00113-7

Wang, M., Chen, Y., Wu, X., and Bai, Y. (2018). Forest-type-dependent water use efficiency trends across the northern hemisphere. *Geophysical Res. Lett.* 45, 8283–8293. doi: 10.1029/2018GL079093

Wise, E. K., and Dannenberg, M. P. (2022). Simulating the impacts of changes in precipitation timing and intensity on tree growth. *Geophysical Res. Lett.* 49, e2022GL100863. doi: 10.1029/2022GL100863

Xiao, Y., Xie, G., Lu, C., Zhang, C., Xu, J., Liu, J., et al. (2021). Suggestions for revegetation over the next 30 years based on precipitation in the three north region of China. *Sustainability* 13, 12649. doi: 10.3390/su132212649

Ye, J.-S., Reynolds, J. F., Sun, G.-J., and Li, F.-M. (2013). Impacts of increased variability in precipitation and air temperature on net primary productivity of the Tibetan Plateau: a modeling analysis. *Climatic Change* 119, 321–332. doi: 10.1007/s10584-013-0719-2

Yu, J., Zhang, Y., Wang, Y., Luo, X., Liang, X., Huang, X., et al. (2022). Ecosystem photosynthesis depends on increased water availability to enhance carbon assimilation in semiarid desert steppe in northern China. *Global Ecol. Conserv.* 38, e02202. doi: 10.1016/j.gecco.2022.e02202

Yu, D., Zhou, L., Zhou, W., Ding, H., Wang, Q., Wang, Y., et al. (2011). Forest management in northeast China: history, problems, and challenges. *Environ. Manage.* 48, 1122–1135. doi: 10.1007/s00267-011-9633-4

Yuan, Y., Bao, A., Jiapaer, G., Jiang, L., and De Maeyer, P. (2022). Phenology-based seasonal terrestrial vegetation growth response to climate variability with consideration of cumulative effect and biological carryover. *Sci. Total Environ.* 817, 152805. doi: 10.1016/j.scitotenv.2021.152805

Zeng, Y., Liu, Y., Hong, P., He, P., and Ma, J. (2025). Main environmental driver and seasonality of water use efficiency in tropical forests. *J. Hydrology* 654, 132944. doi: 10.1016/j.jhydrol.2025.132944

Zeppel, M. J. B., Wilks, J. V., and Lewis, J. D. (2014). Impacts of extreme precipitation and seasonal changes in precipitation on plants. *Biogeosciences* 11, 3083–3093. doi: 10.5194/bg-11-3083-2014

Zhang, W., Brandt, M., Tong, X., Tian, Q., and Fensholt, R. (2018). Impacts of the seasonal distribution of rainfall on vegetation productivity across the Sahel. *Biogeosciences* 15, 319–330. doi: 10.5194/bg-15-319-2018

Zhang, W., Furtado, K., Wu, P., Zhou, T., Chadwick, R., Marzin, C., et al. (2021). Increasing precipitation variability on daily-to-multiyear time scales in a warmer world. *Sci. Adv.* 7, eabf8021. doi: 10.1126/sciadv.abf8021

Zhang, Y., Susan Moran, M., Nearing, M. A., Ponce Campos, G. E., Huete, A. R., Buda, A. R., et al. (2013). Extreme precipitation patterns and reductions of terrestrial ecosystem production across biomes. *JGR Biogeosciences* 118, 148–157. doi: 10.1029/2012JG002136

Zhang, X., Wang, X., Zohner, C. M., Peñuelas, J., Li, Y., Wu, X., et al. (2025). Declining precipitation frequency may drive earlier leaf senescence by intensifying drought stress and enhancing drought acclimation. *Nat. Commun.* 16, 910. doi: 10.1038/s41467-025-56159-4

Zhang, W., Yan, Y., Zheng, J., Li, L., Dong, X., and Cai, H. (2009). Temporal and spatial variability of annual extreme water level in the Pearl River Delta region, China. *Global Planetary Change* 69, 35–47. doi: 10.1016/j.gloplacha.2009.07.003

Zhao, Z., Liu, J., Peng, J., Li, S., and Wang, Y. (2015). Nonlinear features and complexity patterns of vegetation dynamics in the transition zone of North China. *Ecol. Indic.* 49, 237–246. doi: 10.1016/j.ecolind.2014.08.038

Zhao, Y., Wang, C., Wang, S., and Tibig, L. V. (2005). Impacts of present and future climate variability on agriculture and forestry in the humid and sub-humid tropics. *Climatic Change* 70, 73–116. doi: 10.1007/s10584-005-5938-8

Zhu, J., Wang, H., Wang, H., Pan, Y., Bai, Y., Li, W., et al. (2025). Precipitation and nitrogen enrichment impact carbon exchange and stability: From antagonism to synergy with increasing shrub encroachment. *Funct. Ecol.* 39, 1001–1015. doi: 10.1111/1365-2435.14725

frontiers | Frontiers in Plant Science

TYPE Methods
PUBLISHED 03 June 2025
DOI 10.3389/fpls.2025.1507804

OPEN ACCESS

EDITED BY
Amrit Mishra,
James Cook University, Australia

REVIEWED BY
Sebastian Leuzinger,
Auckland University of Technology, New Zealand
Ioannis-Dimosthenis S. Adamakis,
National and Kapodistrian University of Athens, Greece

*CORRESPONDENCE
Silvia Bianchelli
silvia.bianchelli@univpm.it

†These authors have contributed equally to this work

RECEIVED 08 October 2024
ACCEPTED 12 May 2025
PUBLISHED 03 June 2025

CITATION
Marletta G, Sacco D, Danovaro R and Bianchelli S (2025) Effectiveness of growth promoters for the seagrass (*Cymodocea nodosa*) restoration. *Front. Plant Sci.* 16:1507804. doi: 10.3389/fpls.2025.1507804

Effectiveness of growth promoters for the seagrass (*Cymodocea nodosa*) restoration

Giuliana Marletta[1,2†], Domenico Sacco[1†], Roberto Danovaro[1,2] and Silvia Bianchelli[1,2*]

[1]Dipartimento di Scienze della Vita e dell'Ambiente, Università Politecnica delle Marche, Ancona, Italy, [2]National Biodiversity Future Centre, Palermo, Italy

Seagrass meadows are regressing due to the cumulative impacts that affect coastal ecosystems worldwide. Seagrass restoration has been repeatedly proposed to reverse this trend, although with contrasting results due to the difficulty in maintaining the transplanted rhizomes. Enhancing the vegetative propagation of the rhizome plantings (e.g., employing growth-promoters) could represent a reliable tool to increase the success of seagrass restoration. Here we tested the effects of physio-activators, as plant growth-promoting bacteria (PGPB), and synthetic hormones, as plant growth regulators (PGRs), on a seagrass species to assess their potential utilization to enhance restoration efficiency. We conducted two separate experiments in aquaria on *Cymodocea nodosa* fragments: in the first one, the fragments were exposed to PGRs for six weeks, while in the second experiment, the fragments were exposed to PGPB for four weeks. For each experiment (PGRs and PGPB), the formation of new roots and new leaves, the survivorship, and the trend of maximum leaf length were compared between the treated and control (not exposed to PGRs or PGPB) fragments. It was observed that only the PGPB had a significant effect on the fragments' survivorship (90% in treated fragments vs. 25% in control ones) and contributed significantly to the formation of new leaves and roots of *C. nodosa* fragments. On the contrary, in the experiments with PGRs, no significant effects were observed between treated and control fragments, and both showed a survivorship of 100% at the end of the experiment. Our study showed that the application of growth-promoters (particularly PGPB) on fragments could increase their survival and the formation of new roots and leaves. Therefore, the use of PGPB on *C. nodosa* fragments can allow their re-employment in restoration interventions, without damaging the individuals of natural populations.

KEYWORDS

habitat-forming species, seagrass, Mediterranean Sea, complementary actions, active restoration

1 Introduction

Seagrasses are marine angiosperms playing a crucial role in temperate and tropical coastal habitats, as they provide important ecosystem services (Costanza et al., 1997; Boudouresque et al., 2021). They include 67 species worldwide, 7 of which are present in the Mediterranean Sea: *Posidonia oceanica* is the only endemic species of the Mediterranean Sea, whereas *Cymodocea nodosa*, *Zostera marina* and *Z. noltei* show a broader distribution at temperate latitudes (Boudouresque et al., 2009; Ruiz et al., 2009), *Ruppia maritima* is almost entirely restricted to brackish lagoons and salt marshes (Shili et al., 2007), and *Halophila stipulacea* and *H. decipiens* are non-indigenous species (Winters et al., 2020; Gerakaris et al., 2020).

Over the last decades, seagrasses have severely declined due to anthropogenic activities, and only a few meadows recovered (Waycott et al., 2009; Orth et al., 2006; de los Santos et al., 2019; Sinclair et al., 2021). As a result of direct and indirect anthropogenic pressures, seagrass meadows are shrinking their global distribution at a rate ranging from 1% per year (till 1940) to 7% per year (after 1990, Waycott et al., 2009). In the Mediterranean Sea, the main causes of this decline are coastal development, increased maritime traffic, eutrophication, and chemical contamination (Pergent et al., 2014). Between 1973 and 1989, it was observed that the seagrass meadows of the northern Adriatic Sea were subjected to a decrease in extension due to the explosion of coastal urbanization, the intensification of tourism flow, and a significant increase in eutrophication caused by the Po River flow (Danovaro et al., 2020). Even a long-term analysis conducted from 1869 to 2016 in the European Seas showed that between the 1970s and 1980s, there was a sharp decline in seagrass meadows due to disease, deteriorated water quality, and coastal development (de los Santos et al., 2019).

Climate change and extreme events such as heat waves can exacerbate the rapid loss of shoot density and increase the energy needed to reproduce and produce defense compounds (Pergent et al., 2008). In the Greek Seas, the increase in the thermal regime over two decades (1997-2018) was followed by a decline in *P. ocenica* production (Litsi-Mizan et al., 2023). Stipcich et al. (2022) tested the effects of current and future Marine Heatwaves (MHWs) through a manipulative experiment in Sardinia (Italy) and observed significant changes in the morphological and biochemical variables of *P. oceanica* shoots. They found that current and future MHWs could have similar effects, with a difference depending on the intensity of the waves: the number of leaves, the maximum leaf length, and lipid content decreased, while the leaf necrosis and carbohydrate content increased (Stipcich et al., 2022). Beca-Carretero et al. (2024) applied a novel ecological and spatial model, considering two climate scenarios (RCP 2.6 and RCP 8.5) projected from 2020 to 2100 in four different regions within the Mediterranean (West, Central West, Central East, East Mediterranean). They foresee that with rising temperature and salinity, the habitat of *P. ocenica* will be lost and colonized by more resilient species such as *C. nodosa* and the invasive species *H. stipulacea*. Under the worst scenario (RCP 8.5), the most negative effects have been foreseen in warmer regions (Central and East Mediterranean), while the western region will represent a refuge area for *P. oceanica* (Beca-Carretero et al., 2024).

In recent decades, thanks to the enforcement of conservation measures (e.g., Habitat Directive, Water and Marine Strategy Framework Directives, Marine Protected Areas institution), some meadows displayed encouraging signs of stabilization or recovery (de los Santos et al., 2019). Moreover, in the last two decades, several restoration interventions have been implemented (Orth et al., 2006; Marbà et al., 2014). Although active restoration is considered an increasingly reliable approach to enhancing the recovery of seagrass ecosystems, to date, restoration results have not always been fully successful, due to many factors, such as the seagrass's low growth rate and complex reproduction cycle (Bekkby et al., 2020), site selection (Paling et al., 2009; Bayraktarov et al., 2016), and used methodology (Da Ros et al., 2020).

Previous studies demonstrated that one of the major causes of restoration failure is the difficulty in maintaining *in situ* the transplanted rhizomes (Lepoint et al., 2002). During vegetative propagation, the formation of adventitious roots enables the plant to remain firmly attached to the substrate and to absorb the nutrients (Duguma, 1988; Swamy et al., 2002). Therefore, techniques enabling the development of a robust root system could facilitate the vegetative expansion of the transplanted rhizomes (Balestri and Lardicci, 2006). To accelerate vegetation expansion and improve transplant success (Loquès et al., 1990; Balestri et al., 1998; Balestri and Cinelli, 2001), other studies proposed the transplant of entire plants with the surrounding sediments contained in organic and biodegradable containers (Da Ros et al., 2020).

Several studies have shown the role of physio-activators, such as plant growth-promoting bacteria (PGPB), and synthetic hormones, such as plant growth regulators (PGRs), in the increase of the growth, development, and germination abilities over a wide range of terrestrial plants (Russo and Berlyn, 1990; Crunkilton et al., 1994; Swaminathaan and Srinivasan, 1996; Ortíz-Castro et al., 2009; Small and Degenhardt, 2018; Kumari et al., 2023). These molecules promote vegetative propagation, enhancing root and leaf formation and growth (Salisbury and Ross, 1992; Crunkilton et al., 1994; Katiresan and Moorthy, 1994; Munoz, 1995; Swaminathaan and Srinivasan, 1996). Moreover, the PGPB increase plant resilience against abiotic stressors (i.e., salinity, drought) and protect plants from diseases, inducing defense systems (Adhikari et al., 2001; Bloemberg and Lugtenberg, 2001; Weyens et al., 2009; O'Callaghan, 2016; Sánchez-López et al., 2018; Rossi et al., 2021).

Only a few studies investigated the effects of PGRs on Mediterranean seagrasses, with promising results on the plants' growth (Munoz, 1995; Balestri and Bertini, 2003; Balestri and Lardicci, 2006; Balestri et al., 2011), but the effects of PGRs and PGPBs have never been investigated for enhancing the restoration efficacy on Mediterranean seagrasses (Loquès et al., 1990; Munoz, 1995), particularly for those interventions requiring *ex-situ* maintenance or growth and reproduction. The use of plant promoters could indeed increase the restoration effectiveness (Cebrian et al., 2021; Smith et al., 2023). The present study aims

to test the effects of PGRs and PGPB on the survival and growth of *C. nodosa*. To avoid any impact on natural populations we explored their potential to produce new shoots and roots from fragmented plants that could represent a potentially important source of plants for restoration interventions (Campbell, 2002).

2 Materials and equipment

2.1 The species

C. nodosa is a pioneer seagrass (Marín-Guirao et al., 2016), forming dense meadows in shallow waters across the Mediterranean Sea and the Northeast Atlantic, including the Canary Islands (Reyes et al., 1995; Pavón-Salas et al., 2000; Alberto et al., 2008; Cunha and Araújo, 2009). This dioecious species is characterized by horizontal rhizomes, which at each node bring a short vertical rhizome ending dorsally with a leaf tuft of 3–4 leaves, and ventrally with irregularly branched roots. The leaves have a ribbon shape and feature 7–9 parallel ribs, and a rounded and obtuse apex (Rodríguez-Prieto et al., 2013). For its role in ecosystem structuring, *C. nodosa* is considered the second most important seagrass species in the Mediterranean Sea, after *P. ocenica*. It shows a wide environmental tolerance: along the sandy coasts, it grows in shallow and sheltered areas, in clear waters, also beyond the deep limit of *P. oceanica*, but also on dead *matte* of *P. oceanica* (Rodríguez-Prieto et al., 2013).

2.2 Samples' collection

During October and November 2023, two samplings were conducted at Torrette site (near Ancona city, North-western Adriatic Sea; 43°36'36"N, 13°27'30"E; Figures 1A, B). In this site, between the coastline and the breakwaters, there is a rock pool formed by artificial reefs, hosting a meadow of *C. nodosa* (ca. 1 hectare wide) at about 0.5 m depth on muddy substrate.

During the two samplings, a total of 15 and 40 fragments were collected, respectively, stranded, or manually collected by hand from plants. Since *C. nodosa* is under conservationist attention, the minimum number of fragments has been collected to run the experiments. For each sampling, the fragments were transported (in transportable aerated tanks, with seawater collected *in situ*) to the Aquarium Facility of the Department of Life and Environmental Science (Polytechnic University of Marche, Ancona; 43°58'N; 13° 51'E), located 8 km from the sampling site, for ca. 14 minutes of transport.

Once arrived, the fragments were acclimatized for one hour through a slow mixing between the seawater used for the transport and the water of the tanks (previously prepared at the same temperature and salinity). The fragments collected during the first and second sampling were used for testing the effect of PGRs and PGPB, respectively, through 2 experiments in mesocosms, running separately.

3 Methods

3.1 Maintenance in the mesocosms

For each experiment, 2 separate aquaria systems were used, each consisting of 2 tanks (volume 50 L, each): one aquarium for the treatment (2 tanks with fragments exposed to PGRs or PGPB, in the first and second experiment, respectively) and 2 used as control (2 tanks with fragments).

The LSS (Life Support System) was used to maintain the plants in the mesocosms. It consists of aquaria, a reserve in which there are three socks of 100 µm for mechanical filtration, and immersed razor clams for biological filtration. Fluorescent lamps produced 260-nm (λ) UV-C rays, sterilizing the water, damaging nucleic acids, and preventing microbes' proliferation. A Teco TK 500 cooler was used to maintain the temperature. The light intensity was generated by two light-emitting diode lamps (SilverMoon Marine 10,000 K and SilverMoon Universal 6,500 K) 40 cm above the water surface. Irradiance was measured with a Photometer of the Apogee Model MQ-500. The system ensures the maintenance of constant ambient water conditions. The photoperiod was set to a 12:12 h light: dark cycle, with an intensity of 80-100 µmol photons m^{-2} s^{-1} to simulate the environmental conditions present during sampling. Temperature, salinity, pH, and light intensity were measured at the sampling site and were set up in aquaria following Marín-Guirao et al. (2011) for the same sampling period. These parameters

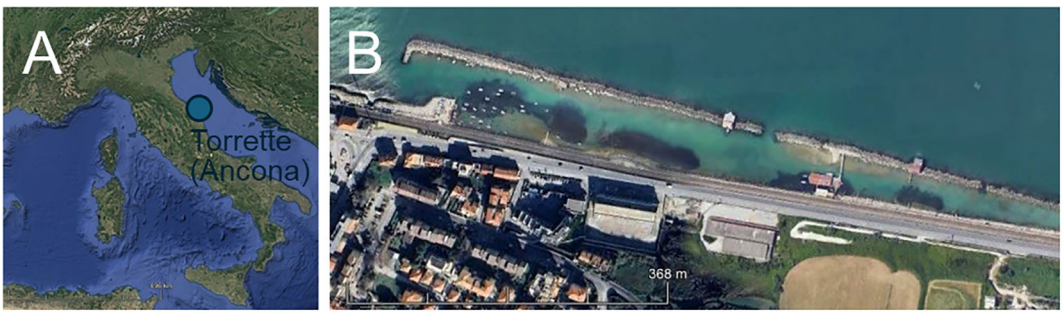

FIGURE 1
(A) Location of the study area in the Mediterranean Sea; **(B)** Detail of the study area (43°36'36"N, 13°27'30"E). Map created using the Free and Open Source QGIS.

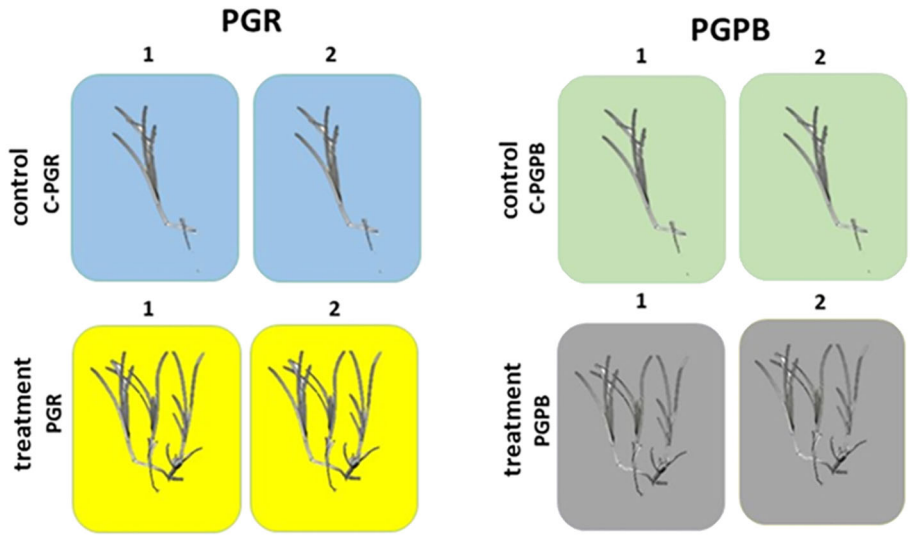

FIGURE 2
Experimental design for the PGRs and PGPB experiments. In each experiment, *C. nodosa* fragments were exposed to PGR (left panel) or PGPB (right panel) (n = 2) and compared to fragments not exposed (n = 2). Treatment = treated fragments (with PGR or PGPB, depending on the experiment); Control = fragment not exposed during each experiment (C-PGR and C-PGPB, respectively); 1 and 2 = code of the tank used.

were maintained throughout the experiments: temperature was 20 ± 1°C, salinity was 37, and pH was 8.2. Furthermore, for routine system maintenance, water loading and unloading, lights, movement pumps, a cooler, and any water leaks at the pipe joints were checked. To ensure the sterilization of the system, the socks were washed, tubs were siphoned to remove organic debris, and 20% of the seawater was exchanged every week. The replacement water was prepared using artificial salts.

3.2 Experimental design

The first experiment consisted of 4 tanks (volume 50 L, each), 2 used for the treatment with PGRs (n = 2) and 2 as control (n = 2). The tanks used as control were labelled as C-PGRs1 and C-PGRs2, containing 2 fragments each. Those used for the treatment with PGRs were labelled as PGRs1 and PGRs2, containing 6 and 5 fragments, respectively (Figure 2). All fragments were fixed to plastic nets with a small weight to maintain them on the bottom of the tanks. In the tanks PGRs1 and PGRs2 it was added one pill of Gibaifar 10 TB, containing gibberellic acid (GA3), and 80 ml of Sprintex New® L, containing alpha-naphtaleneacetic acid (NAA).

The second experiment consisted of 4 tanks (volume 50 L, each), 2 for the treatment with PGPB (n =2) and 2 as control (n = 2). In this case, tanks used as control were labelled as C-PGPB1 and C-PGPB2. Those used for treatment with PGPB were labelled as PGPB1 and PGPB2 (Figure 2). Each tank contained 10 fragments. In this case, all the fragments were fixed to jute nets with a small weight to maintain them on the bottom of the tanks. In the mesocosms PGPB1 and PGPB2, 100 ml of Microtech Triple eco was added, which contains growth-promoting bacteria and cyanobacteria.

In both experiments, all fragments were tagged, photographed, and their growth measured. The following variables were checked once a week, for 6 and 4 weeks for the first and second experiment, respectively: number of shoots, roots, and leaves, and maximum leaf length. The collection of the abovementioned data allowed us to estimate: the number of new roots, new leaves, survivorship (number of individuals showing new leaves or roots), and trend of the maximum leaf length (following Balestri and Lardicci, 2006; Balestri et al., 2011). All the variables were measured for all the individuals in each tank and reported as tanks' mean ± standard error.

3.3 Statistical analyses

To test differences in the abovementioned variables (maximum leaf length, number of new roots and leaves, and survivorship), separately for the 2 experiments, one- or two-way permutational analysis of variance (PERMANOVA) was performed, applying two experimental designs.

For the maximum leaf length, two factors of variance were considered: "time" (fixed, 2 levels: beginning and end of the experiments, corresponding to 6 and 4 weeks for the PGRs and PGPB experiment, respectively) and "treatment" (fixed, 2 levels: control and treatment, with the factor "tank" nested in "treatment").

All other variables (i.e., number of new roots and leaves, and survivorship) were considered as a single factor of variance in the "treatment" (fixed, 2 levels: control and treated, with the factor "tank" nested in "treatment") since at the beginning there were no new roots and leaves.

10.3389/fpls.2025.1507804

TABLE 1 Variables and data measured during the experiments.

			max leaf legth (cm)		n. new roots/ind		n. new leaves/ind		survivorship (n.ind with new roots/leaves)	survivorship (n. new roots or leaves/ind)	
			avg	se	avg	se	avg	se	%	avg	se
PGRs	Ctrl	beginning	34.9	3.1	na		na		na	na	
		after 6 weeks	11.8	1.0	0.4	0.1	1.0	0.8	100	1.4	0.9
	Treat	beginning	32.1	1.7	na		na		na	na	
		after 6 weeks	12.9	4.2	0.5	0.3	0.4	0.2	100	0.9	0.5
PGPB	Ctl	beginning	20.6	5.0	na		na		na	na	
		after 4 weeks	17.3	4.9	0.0	0.0	0.02	0.01	25.0	0.04	0.01
	Treat	beginning	16.3	2.7	na		na		na	na	
		after 4 weeks	10.4	1.9	0.1	0.0	0.1	0.0	90.0	0.2	0.1

Data are reported as mean ± standard error, calculated based on the means values for each tank.

Before PERMANOVA, PERMDISP tests were carried out to test the dispersion among groups: "time x treatment(tank)" for max leaf length or "treatment(tank)" for new roots, new leaves, and survivorship. When PERMDISP was significant, the data were fourth root transformed before PERMANOVA.

Statistical analyses were performed by using the software package PRIMER7 (Clarke and Gorley, 2015).

4 Results

All the data are reported in Table 1.

The results of the PERMDISP testing for dispersion among groups for PGRs and PGPB experiments are reported in Tables 2A, B, respectively. The results of the PERMANOVA analyses testing for the effect of treatment and time or only treatment, depending on the variable, on all the considered response variables, for PGRs and PGPB experiments, are reported in Tables 3A, B, respectively.

4.1 PGRs treatment

Maximum leaf length - A significant effect of time was observed on the maximum leaf length (Table 2A). The maximum leaf length was significantly lower at the end of the experiment only in control fragments. However, the values were similar in the controls and treated fragments in the PGRs experiment, both at the beginning and the end of the experiment (i.e., after 6 weeks, Figure 3).

Formation of new roots and new leaves– The formation of new roots and new leaves was observed at the end of the experiment (after 6 weeks), both in control and treated fragments. However, no significant differences were observed between control and treated fragments, for both variables (Table 2A; Figures 4A, B). A significant effect of the factor tank was observed for new roots' formation.

Survivorship – At the end of the experiment, in control and treated experimental units, the 100% of individuals showed survivorship (measured as new leaves or roots). However, no significant difference was observed comparing control and treated fragments (Table 2A; Figure 5). A significant effect of the factor "tank" was observed.

4.2 PGPB treatment

Maximum leaf length – A significant effect of time and time x treatment was observed on the maximum leaf length (Table 2B; Figure 3). No significant differences were observed between the control and treated fragments.

TABLE 2 Output of the PERDISP conducted after PGRs (A) and PGPB (B) experiments, on all variables, testing for the dispersion among groups: "treatment(tank) x time" for max leaf length or "treatment(tank)" for new roots, new leaves, and survivorship.

		Max leaf length	New roots	New leaves	Survivorship
A)	PGRs	F: 2,4834 df1: 7 df2: 22	F: 1,4753 df1: 3 df2: 11	F: 1,7814 df1: 3 df2: 11	F: 4,8668 df1: 3 df2: 11
		P: 0.071	P: 0.253	P: 0.267	P: 0,084*
B)	PGPB	F: 1,8131 df1: 7 df2: 72	F: 1,5004 df1: 3 df2: 36	F: 0,96122 df1: 3 df2: 36	F: 0,23953 df1: 3 df2: 36
		P: 0.083	P: 0.222*	P: 0.427*	P: 0.863*

*data fourth root transformed.
df, degree of freedom; F, F statistic; P, p value.

10.3389/fpls.2025.1507804

TABLE 3 Output of PERMANOVA conducted after PGRs (A) and PGPB (B) experiments, testing for differences between treatment (tanks) and times (for the max leaf length) or treatment (tanks) (for new root, new leaves, and survivorship).

			Source	df	MS	F	P
A)	PGRs	Max leaf length	Time	1	2617.20	23.20	<0.05
			Treatment	1	4.00	0.07	ns
			Tank (Treatment)	2	33.90	0.22	ns
			Time x Treatment	1	22.95	0.20	ns
			Time x Tank (Treatment)	2	102.21	0.67	ns
			Residual	22.0	151.55		
		New roots	Treatment	1	9.84	1.09	ns
			Tank (Treatment)	2	11.07	7.03	<0.05
			Residual	11	1.58		
		New leaves*	Treatment	1	0.01	0.02	ns
			Tank (Treatment)	2	0.42	1.48	ns
			Residual	11	0.28		
		Survivorship*	Treatment	1	0.10	0.36	ns
			Tank (Treatment)	2	0.35	23.70	<0.01
			Residual	11	0.01		
B)	PGPB	Max leaf length	Time	1	146.07	305.83	<0.01
			Treatment	1	504.51	5.15	ns
			Tank (Treatment)	2	97.95	1.21	ns
			Time x Treatment	1	51.04	106.86	<0.05
			Time x Tank (Treatment)	2	0.48	0.01	ns
			Residual	72	80.96		
		New roots*	Treatment	1	1.25	16.27	<0.05
			Tank (Treatment)	2	0.08	0.29	ns
			Residual	36	0.27		
		New leaves*	Treatment	1	3.88	14.85	<0.05
			Tank (Treatment)	2	0.26	1.29	ns
			Residual	36	0.20		
		Survivorship*	Treatment	1	6.07	65.61	<0.05
			Tank (Treatment)	2	0.09	0.44	ns
			Residual	36	0.21		

*data fourth root transformed.
Source, source of variance; df, degree of freedom; MS, means of squares; F, F statistic; P, p value.

Formation of new roots and new leaves – The formation of new roots and new leaves was observed at the end of the experiment (after 4 weeks). A significant difference was observed between control and treated fragments, with higher values observed in treated fragments, for both variables (Table 2B; Figures 4A, B).

Survivorship – Overall, in control and treatment experimental units, 25 and 90% of individuals showed survivorship (measured as new leaves or roots). A significant effect of the treatment on survivorship was observed (Table 2B), with higher values observed in treated fragments (Figure 5).

5 Discussion

Mediterranean seagrasses are crucially important species, most of which are protected by international conventions such as the

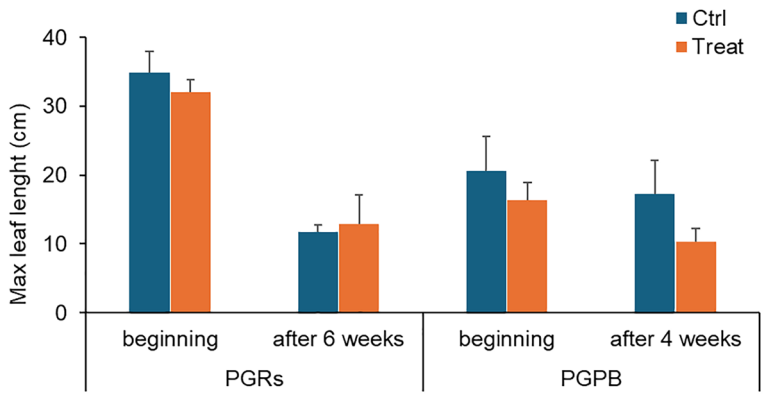

FIGURE 3
Max leaf length measured in fragments used as control (in light blue) and those exposed to PGRs or PGPB (in orange), at the beginning and after 6 and 4 weeks, respectively. Data (in cm) are reported as the average of values measured in the tanks ± standard error. Ctrl, control; Treat, treatment.

Bern Convention, the SPAMI-Barcelona Convention, and the Action Plan for the Conservation of Marine Vegetation in the Mediterranean Sea. They are also part of the Habitat Directive (Curiel et al., 2021). Due to their role in blue carbon sequestration and the coastal ecosystem functioning, marine meadows' restoration has been proposed as a tool for climate change mitigation (Orth et al., 2006; Marbà et al., 2014; United Nations Environment Agency, 2019; United Nations Environment Programme, 2019). To upscale these interventions, recent studies highlighted the importance of improving transplanting operations by reducing the cost and increasing intervention efficacy (Boudouresque et al., 2021). Moreover, the restoration intervention should be planned to avoid any possible damage to healthy populations. This can be done only by optimizing protocols, also considering phases implemented *ex situ*, and using laboratory facilities to improve the reproduction or cultivation of individuals used for the outplants or transplants at sea.

Compared to other Mediterranean species, *C. nodosa* offers the greatest chance for restoration success, due to its high tolerance to varying environmental conditions (Bellato et al., 1994; Rismondo et al., 1997; Sfriso and Ghetti, 1998). The formation of new roots allows the vegetative expansion of the plant, increasing the probability of permanent establishment of the new seagrass beds (Balestri and Lardicci, 2006). However, extreme environmental events such as storm surges, which have increased in intensity and frequency due to climate change, can cause the loss of large portions of natural seagrass meadows (Oprandi et al., 2020).

The implementation of growth-promoters has proven to be successful in stimulating the rooting capacity of seagrasses (Balestri and Bertini, 2003; Balestri and Lardicci, 2006). Our study showed that PGPB have a significantly positive effect on *C. nodosa* and its stranded fragments. This response allows more efficient use of stranded fragments of seagrasses for habitat restoration, a strategy successfully used for macroalgal forest restoration (Marletta et al., 2024). This would allow to use only some parts of the plants, avoiding using entire portion of the meadow for the restoration interventions.

The effects of these growth-promoters can depend on the molecule (PGPB or PGRs). Our results indicated survivorship (i.e., formation of new roots or leaves) both in control and treated fragments, suggesting that the cultivation conditions were optimal in the aquaria facility. However, only the PGPB growth-promoters had positive effects on the fragments' survivorship and contributed significantly to the increase in the formation of new leaves and roots in *C. nodosa*, when compared with control fragments. Therefore, the future use of growth promoters needs to be previously tested, since different promoters (i.e., different molecules) could have a different (or null) effect on the plants' growth. This is particularly important when planning a cost-effective restoration process, which includes an *ex-situ* phase. In the experiment with PGPB, the fragments had a higher survivorship when exposed to the growth-promoters (90%) than in the control ones (25%). This could be related to the ability of the plant to incorporate the PGPB through the leaves, with a process possibly catalyzed by nitrogen-fixing cyanobacteria (Kollmen and Strieth, 2022). Moreover, cyanobacteria can optimize the mineralization of organic compounds and nutrient availability (Tarquinio et al., 2019). In this regard, the potential role of microbiota for holobiont health and restoration efficacy has been recently highlighted (Corinaldesi et al., 2023).

Our study also shows that the application of growth-promoters (particularly PGPB) on the fragments increases their survival and the formation of new roots and leaves. The use of PGPB on *C. nodosa* fragments could allow the re-employment in restoration interventions, also when they are found broken or stranded along the beaches, without damaging the natural populations. This could be particularly important for restoration purposes, as already observed for macroalgae (Marletta et al., 2024). In the Mediterranean Sea, the probability of detached fragments returning back to the sea is very low, also due to the limited tide excursion, and generally, these fragments dry up on the beach (Balestri et al., 2011), but can be salvaged and used directly as a source for restoration/mitigation efforts (Balestri et al. (2011); Marletta et al., 2024) to promote habitat restoration.

The implementation of these growth-promoters, particularly PGPB, represents a yet unexplored field for marine plant research and it can offer a new way to improve seagrass health, and resilience, and increase restoration success (Tarquinio et al., 2019), reducing

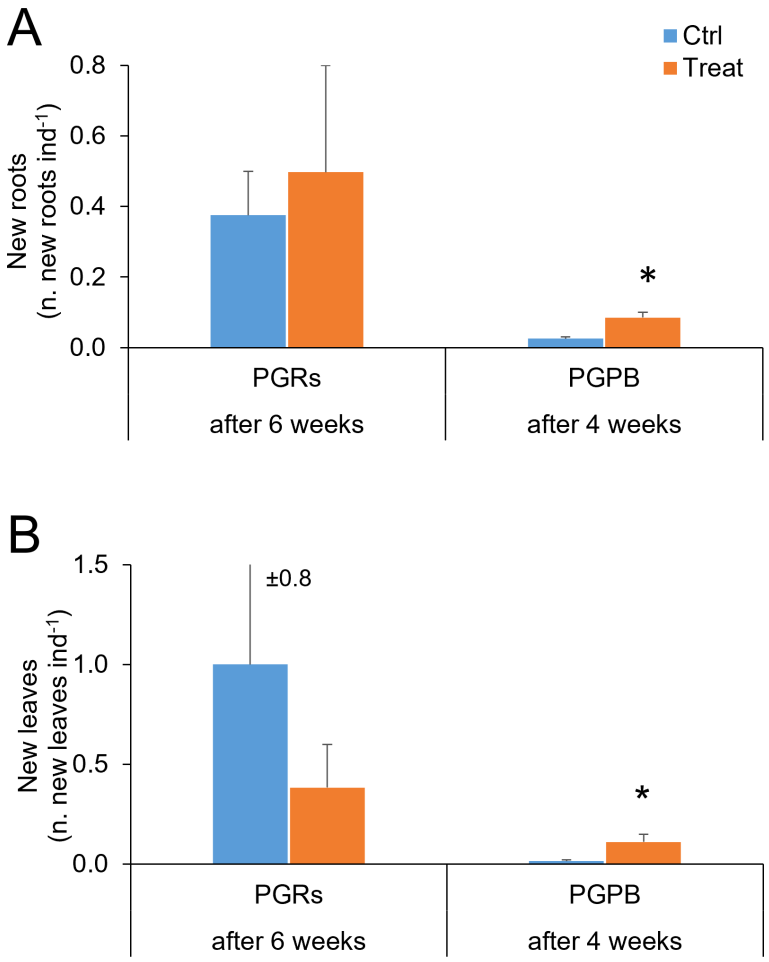

FIGURE 4
New roots **(A)** and new leaves **(B)** observed in fragments used as control (in light blue) and those exposed to PGRs or PGPB (in orange), after 6 and 4 weeks, respectively. Data (as number of new roots and leaves per fragment) are reported as the average of values measured in the tanks ± standard error. Ctrl, control; Treat, treatment; ind., individual (= fragment); *P < 0.05.

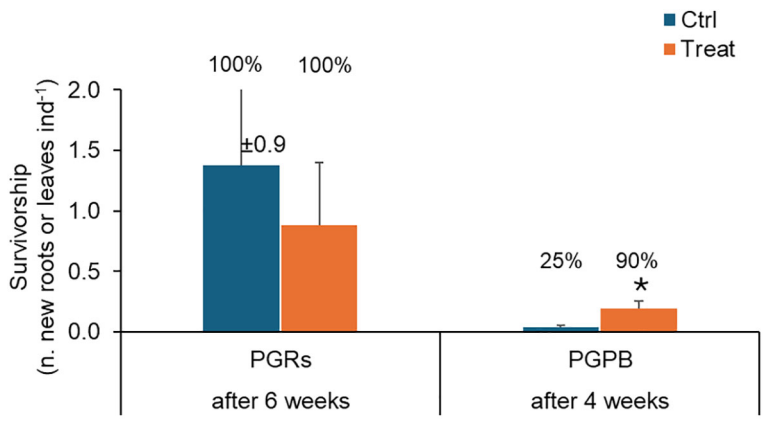

FIGURE 5
Survivorship observed in fragments used as control (in light blue) and those exposed to PGRs or PGPB (in orange), after 6 and 4 weeks, respectively. Data (as the number of new roots or leaves per fragment) are reported as the average of values measured in the tanks ± standard error. Reported are also the % of individuals developing new roots or leaves. Ctrl, control; Treat, treatment; ind., individual (= fragment); *P < 0.05.

the time and costs of plant maintenance in mesocosms and ensuring long-term transplant success (Pansini et al., 2024) speeding up the process of roots and leaves' formation (Balestri and Bertini, 2003). Nature-based solutions relying on microbiome analyses (and also through omics approaches) enable health monitoring of transplanted organisms/metacommunities and potential identification/production of probiotics/bio-promoters to stabilize unhealthy conditions of transplants (Corinaldesi et al., 2023). The use of microbes in ecosystem restoration is gaining increasing attention (Farrell et al., 2020; Watson et al., 2022). Microbe-assisted restoration has been implemented for different purposes in both terrestrial and aquatic environments (Robinson et al., 2023): plants' and animals' health (Gao et al., 2010; Contos et al., 2021; Birnbaum and Trevathan-Tackett, 2023), nutrient cycling (Garcia and Kao-Kniffin, 2018; Singh Rawat et al., 2023), drought stress tolerance (Ma et al., 2020; Sarabi and Arjmand-Ghajur, 2021), hormone production in plants and animals (Eichmann et al., 2021), climate regulation (Wu et al., 2022), pollination (Martin et al., 2022) and phytoremediation in degraded habitats (Haldar and Ghosh, 2020; Sarker et al., 2023; Agrawal et al., 2024). This study could contribute to the knowledge of new protocols for the conservation and restoration of seagrass meadows to reverse their loss and to optimize both the biodiversity and ecosystem services they provide (Possingham et al., 2015). This is an important target for the "UN Decade on Ecosystem Restoration" (Waltham et al., 2020) and the EU Biodiversity Strategy for 2030, aiming at restoring ecosystems across land and sea, especially those with considerable value in terms of goods and services such as seagrasses (Costanza et al., 2014; Vassallo et al., 2013).

Recent scientific advancements indicate that marine habitat restoration is feasible and should be upscaled, but it is constrained by: 1) the high costs when compared with terrestrial restoration and 2) the potential impact on source populations. This is particularly critical for habitat-forming species, a key targets of marine ecosystem restoration. Due to their successful application on terrestrial plants, growth promoters can be useful to enhance the recovery also of marine plants. In particular, we suggest the use of growth promoters in stranded plants, which would otherwise be lost. This phenomenon is expected to become more frequent as a consequence of climate change, or due to the increasing occurrence of storms. The use of the plant promoters tested here could make stranded organisms an important resource of viable material to be used in transplanting interventions. The set up and implementation of restoration methodologies are particularly important in the framework of the Nature Restoration Regulation recently approved by the European Union, which has binding restoration targets also for marine habitats (at least 30% of the EU's land and sea areas by 2030, 60% by 2040 and 90% by 2050).

Data availability statement

The original contributions presented in the study are included in the article/supplementary material. Further inquiries can be directed to the corresponding author.

Author contributions

GM: Data curation, Formal analysis, Investigation, Methodology, Writing – original draft, Writing – review & editing. DS: Data curation, Investigation, Methodology, Writing – review & editing. RD: Conceptualization, Funding acquisition, Resources, Supervision, Writing – review & editing. SB: Conceptualization, Data curation, Formal analysis, Investigation, Methodology, Project administration, Supervision, Validation, Writing – original draft, Writing – review & editing, Resources.

Funding

The author(s) declare that financial support was received for the research and/or publication of this article. This study was conducted in the framework of the National Recovery and Resilience Plan (NRRP), Mission 4 Component 2 Investment 1.4-Call for tender No. 3138 of 16 December, 2021, rectified by Decree n.3175 of 18 December, 2021 of Italian Ministry of University and Research funded by the European Union-NextGenerationEU; Award Number: Project code CN_00000033, Concession Decree No. 1034 of 17 June, 2022 adopted by the Italian Ministry of University and Research, Project title "National Biodiversity Future Center-NBFC" and within the frame of the European Biodiversity Partnership: Biodiversa+ funded project entitled: "Innovative approaches FORESCUE and management of algal forests in the Mediterranean Sea FORESCUE".

Conflict of interest

The authors declare that the research was conducted in the absence of any commercial or financial relationships that could be construed as a potential conflict of interest.

The author(s) declared that they were an editorial board member of Frontiers, at the time of submission. This had no impact on the peer review process and the final decision.

Generative AI statement

The author(s) declare that no Generative AI was used in the creation of this manuscript.

Publisher's note

References

Adhikari, T. B., Joseph, C. M., Yang, G., Phillips, D. A., and Nelson, L. M. (2001). Evaluation of bacteria isolated from rice for plant growth promotion and biological control of seedling disease of rice. *Can. J. Microbiol* 47, 916–924. doi: 10.1139/w01-097

Agrawal, K., Ruhil, T., Gupta, V. K., and Verma, P. (2024). Microbial assisted multifaceted amelioration processes of heavy-metal remediation: a clean perspective toward sustainable and greener future. *Crit. Rev. Biotechnol.* 44, 429–447. doi: 10.1080/07388551.2023.2170862

Alberto, F., Massa, S., Manent, P., Diaz-Almela, E., Arnaud-Haond, S., Duarte, C. M., et al. (2008). Genetic differentiation and secondary contact zone in the seagrass *Cymodocea nodosa* across the Mediterranean-Atlantic transition zone. *J. Biogeography* 35, 1270–1294. doi: 10.1111/j.1365-2699.2007.01876.x

Balestri, E., and Bertini, S. (2003). Growth and development of *Posidonia oceanica* seedlings treated with plant growth regulators: possible implications for meadow restoration. *Aquat Bot.* 76, 291–297. doi: 10.1016/S0304-3770(03)00074-3

Balestri, E., and Cinelli, F. (2001). Isolation and cell wall regeneration of protoplasts from *Posidonia oceanica* and *Cymodocea nodosa*. *Aquat Bot.* 70, 237–242. doi: 10.1016/S0304-3770(01)00157-7

Balestri, E., and Lardicci, C. (2006). Stimulation of root formation in *Posidonia oceanica* cuttings by application of auxins (NAA and IBA). *Mar Biol.* 149, 393–400. doi: 10.1007/s00227-005-0193-0

Balestri, E., Piazzi, L., and Cinelli, F. (1998).). *In vitro* germination and seedling development of *Posidonia oceanica* (L.) Delile. *Aquat Bot.* 60, 83–93. doi: 10.1016/S0304-3770(97)00017-X

Balestri, E., Vallerini, F., and Lardicci, C. (2011). Storm-generated fragments of the seagrass *Posidonia oceanica* from beach wrack–A potential source of transplants for restoration. *Biol. Conserv* 144, 1644–1654. doi: 10.1016/j.biocon.2011.02.020

Bayraktarov, E., Saunders, M. I., Abdullah, S., Mills, M., Beher, J., Possingham, H. P., et al. (2016). The cost and feasibility of marine coastal restoration. *Ecol. Appl.* 26, 1055–1074. doi: 10.1890/15-1077

Beca-Carretero, P., Winters, G., Teichberg, M., Procaccini, G., Schneekloth, F., Zambrano, R. H., et al. (2024). Climate change and the presence of invasive species will threaten the persistence of the Mediterranean seagrass community. *Sci. Total Environ.* 910, 168675. doi: 10.1016/j.scitotenv.2023.168675

Bekkby, T., Papadopoulou, N., Fiorentino, D., McOwen, C. J., Rinde, E., Boström, C., et al. (2020). Habitat features and their influence on the restoration potential of marine habitats in Europe. *Front. Mar Sci.* 7. doi: 10.3389/fmars.2020.00184

Bellato, A., Rismondo, A., Curiel, D., and Marzocchi, M. (1994). Ritrovamento di frutti e semi in germinazione di *Cymodocea nodosa* (Ucria) Ascherson in Laguna di Venezia. *Lav Soc. Ven Sc Nat.* 20, 16.

Birnbaum, C., and Trevathan-Tackett, S. M. (2023). Aiding coastal wetland restoration via the belowground soil microbiome: an overview. *Restor. Ecol.* 31, e13824. doi: 10.1111/rec.13824

Bloemberg, G. V., and Lugtenberg, B. J. J. (2001). Molecular basis of plant growth promotion and biocontrol by rhizobacteria. *Curr. Opin. Plant Biol.* 4, 343–350. doi: 10.1016/S1369-5266(00)00183-7

Boudouresque, C. F., Bernard, G., Pergent, G., Shili, A., and Verlaque, M. (2009). Regression of Mediterranean seagrasses caused by natural processes and anthropogenic disturbances and stress: A critical review. *Bot. Mar* 52, 395–418. doi: 10.1515/BOT.2009.057

Boudouresque, C. F., Blanfuné, A., Pergent, G., and Thibaut, T. (2021).). Restoration of seagrass meadows in the mediterranean sea: A critical review of effectiveness and ethical issues. *Water* 13, 1034. doi: 10.3390/w13081034

Campbell, M. L. (2002). Getting the foundation right: a scientifically based management framework to aid in the planning and implementation of seagrass transplant efforts. *Bull. Mar Sci.* 71, 1405–1414.

Cebrian, E., Tamburello, L., Verdura, J., Guarnieri, G., Medrano, A., Linares, C., et al. (2021). A roadmap for the restoration of Mediterranean macroalgal forests. *Front. Mar Sci.* 8. doi: 10.3389/fmars.2021.709219

Clarke, K. R., and Gorley, K. N. (2015). *PRIMER v7: User manual/tutorial* (Plymouth: PRIMER-E).

Contos, P., Wood, J. L., Murphy, N. P., and Gibb, H. (2021). Rewilding with invertebrates and microbes to restore ecosystems: Present trends and future directions. *Ecol. Evol.* 11, 7187–7200. doi: 10.1002/ece3.7597

Corinaldesi, C., Bianchelli, S., Candela, M., Dell'Anno, A., Gambi, C., Rastelli, E., et al. (2023). Microbiome-assisted restoration of degraded marine habitats: a new nature-based solution? *Front. Mar Sci.* 10. doi: 10.3389/fmars.2023.1227560

Costanza, R., d'Arge, R., De Groot, R., Farber, S., Grasso, M., Hannon, B., et al. (1997). The value of the world's ecosystem services and natural capital. *Nature* 387, 253–260. doi: 10.1038/387253a0

Costanza, R., De Groot, R., Sutton, P., van der Ploeg, S., Anderson, J. S., Kubiszewski, I., et al. (2014). Changes in the global value of ecosystem services. *Glob Environ. Chang* 26, 152–158. doi: 10.1016/j.gloenvcha.2014.04.002

Crunkilton, D. D., Garret, H. E., and Pallardy, S. G. (1994). Growth and ectomycorrhizial development of northern red oak seedlings treated with IBA. *Hortic. Sci.* 29, 771–773. doi: 10.21273/HORTSCI.29.7.771

Cunha, A., and Araújo, A. (2009). New distribution limits of seagrass beds in West Africa. *J. Biogeogr* 36, 1621–1622. doi: 10.1111/j.1365-2699.2009.02135.x

Curiel, D., Kraljevíc Pavelíc, S., Kovačev, A., Miotti, C., and Rismondo, A. (2021). Marine seagrasses transplantation in confined and coastal adriatic environments: methods and results. *Water* 13, 2289. doi: 10.3390/w13162289

Danovaro, R., Nepote, E., Martire, M. L., Carugati, L., Da Ros, Z., Torsani, F., et al. (2020). Multiple declines and recoveries of Adriatic seagrass meadows over forty years of investigation. *Mar Pollut. Bull.* 161, 111804. doi: 10.1016/j.marpolbul.2020.111804

Da Ros, Z., Corinaldesi, C., Dell'Anno, A., Gambi, C., Torsani, F., and Danovaro, R. (2020). Restoration of *Cymodocea nodosa* seagrass meadows: Efficiency and ecological implications. *Restor. Ecol.* 29, e13313. doi: 10.1111/rec.13313

de los Santos, C. B., Krause-Jensen, D., Alcoverro, T., Marbà, N., Duarte, C. M., Van Katwijk, M. M., et al. (2019). Recent trend reversal for declining European seagrass meadows. *Nat. Commun.* 10, 3356. doi: 10.1038/s41467-019-11340-4

Duguma, B. (1988). *Establishment of stakes of* Gliricidia sepium *(Jacq.) Walp and Leucaena leucocephala (Lam.) De Witt* Vol. 6 (Yaounde, Cameroon: NFTA), 6–9.

Eichmann, R., Richards, L., and Schäfer, P. (2021). Hormones as go-betweens in plant microbiome assembly. *Plant J.* 105, 518–541. doi: 10.1111/tpj.15135

Farrell, H. L., Léger, A., Breed, M. F., and Gornish, E. S. (2020). Restoration, soil organisms, and soil processes: emerging approaches. *Restor. Ecol.* 28, S307–S310. doi: 10.1111/rec.13237

Gao, F. K., Dai, C. C., and Liu, X. Z. (2010). Mechanisms of fungal endophytes in plant protection against pathogens. *Afr J. Microbiol Res.* 4, 1346–1351.

Garcia, J., and Kao-Kniffin, J. (2018). Microbial group dynamics in plant rhizospheres and their implications on nutrient cycling. *Front. Microbiol* 9. doi: 10.3389/fmicb.2018.01516

Gerakaris, V., Lardi, P. I., and Issaris, Y. (2020). First record of the tropical seagrass species *Halophila decipiens* Ostenfeld in the Mediterranean Sea. *Aquat Bot.* 160, 103151. doi: 10.1016/j.aquabot.2019.103151

Haldar, S., and Ghosh, A. (2020). Microbial and plant-assisted heavy metal remediation in aquatic ecosystems: a comprehensive review. *3 Biotech.* 10, 205. doi: 10.1007/s13205-020-02195-4

Katiresan, K., and Moorthy, P. (1994). Hormone-induced physiological responses of a tropical mangrove species. *Bot. Mar* 37, 139–141. doi: 10.1515/botm.1994.37.2.139

Kollmen, J., and Strieth, D. (2022). The beneficial effects of cyanobacterial co-culture on plant growth. *Life* 12, 223. doi: 10.3390/life12020223

Kumari, E., Kumari, S., Das, S. S., Mahapatra, M., and Sahoo, J. P. (2023). Plant growth-promoting bacteria (PGPB) for sustainable agriculture: current prospective and future challenges. *AgroEnviron Sustain* 1, 274–285. doi: 10.59983/s2023010309

Lepoint, G., Vangeluwe, D., Eisinger, M., Paster, M., van Treeck, P., Bouquegneau, J. M., et al. (2002). Nitrogen dynamics in Posidonia oceanica cuttings: implications for transplantation experiments. *Mar Poll Bull.* 48, 465–470. doi: 10.1016/j.marpolbul.2003.08.023

Litsi-Mizan, V., Efthymiadis, P. T., Gerakaris, V., Serrano, O., Tsapakis, M., and Apostolaki, E. T. (2023). Decline of seagrass (*Posidonia oceanica*) production over two decades in the face of warming of the Eastern Mediterranean Sea. *New Phytol.* 239, 2126–2137. doi: 10.1111/nph.19084

Loquès, F., Caye, G., and Meinesz, A. (1990). Axenic culture of selected tissue of *Posidonia oceanica*. *Aquat Bot.* 37, 171–188. doi: 10.1016/0304-3770(90)90090-8

Ma, Y., Dias, M. C., and Freitas, H. (2020). Drought and salinity stress responses and microbe-induced tolerance in plants. *Front. Plant Sci.* 11. doi: 10.3389/fpls.2020.591911

Marbà, N., Díaz-Almela, E., and Duarte, C. M. (2014). Mediterranean seagrass (*Posidonia oceanica*) loss between 1842 and 2009. *Biol. Conserv* 176, 183–190. doi: 10.1016/j.biocon.2014.05.024

Marín-Guirao, L., Ruiz, J. M., Dattolo, E., Garcia-Munoz, R., and Procaccini, G. (2016). Physiological and molecular evidence of differential short-term heat tolerance in Mediterranean seagrasses. *Sci. Rep.* 6, 28615. doi: 10.1038/srep28615

Marín-Guirao, L., Sandoval-Gil, J. M., Ruíz, J. M., and Sánchez-Lizaso, J. L. (2011). Photosynthesis, growth and survival of the Mediterranean seagrass Posidonia oceanica in response to simulated salinity increases in a laboratory mesocosm system. *Estuar Coast Shelf Sci.* 92, 286–296. doi: 10.1016/j.ecss.2011.01.003

Marletta, G., Sacco, D., Danovaro, R., and Bianchelli, S. (2024). Stranded seaweeds (*Gongolaria barbata*): an opportunity for macroalgal forest restoration. *Restor. Ecol.* 32, e14134. doi: 10.1111/rec.14134

Martin, V. N., Schaeffer, R. N., and Fukami, T. (2022). Potential effects of nectar microbes on pollinator health. *Philos. Trans. R Soc. B* 377, 20210155. doi: 10.1098/rstb.2021.0155

Munoz, J. T. (1995). Effects of some plant growth regulators on the growth of the seagrass *Cymodocea nodosa* (Ucria) Ascherson. *Aquat Bot.* 51, 311–318. doi: 10.1016/0304-3770(95)00481-E

O'Callaghan, M. (2016). Microbial inoculation of seed for improved crop performance: issues and opportunities. *Appl. Microbiol Biotechnol.* 100, 5729–5746. doi: 10.1007/s00253-016-7590-9

Oprandi, A., Mucerino, L., de Leo, F., Bianchi, C. N., Morri, C., Azzola, A., et al. (2020). Effects of a severe storm on seagrass meadows. *Sci. Total Environ.* 748, 1–13. doi: 10.1016/j.scitotenv.2020.141373

Orth, R. J., Carruthers, T. J. B., Dennison, W. C., Duarte, C. M., Fourqurean, J. W., Heck, K. L., et al. (2006). A global crisis for seagrass ecosystems. *Biosci* 56, 987–996. doi: 10.1641/0006-3568(2006)56[987:AGCFSE]2.0.CO;2

Ortíz-Castro, R., Contreras-Cornejo, H. A., Macías-Rodríguez, L., and López-Bucio, J. (2009). The role of microbial signals in plant growth and development. *Plant Signal Behav.* 4, 701–712. doi: 10.4161/psb.4.8.9047

Paling, E. I., Fonseca, M., Van Katwijk, M. M., and Van Keulen, M. (2009). "Seagrass restoration," in *Coastal wetlands: an integrated ecosystem approach*. Eds. G. Perillo, E. Wolanski, D. Cahoon and M. Brinson (Elsevier, Amsterdam, The Netherlands).

Pansini, A., Deroma, M., Guala, I., Monnier, B., Pergent-Martini, C., Piazzi, L., et al. (2024). The resilience of transplanted seagrass traits encourages detection of restoration success. *J. Environ. Manage* 357, 120744. doi: 10.1016/j.jenvman.2024.120744

Pavón-Salas, N., Herrera, R., Hernández-Guerra, A., and Haroun, R. (2000). Distribution pattern of seagrasses in the Canary Islands (Central-East Atlantic Ocean). *J. Coast Res.* 16, 329–335.

Pergent, G., Bazairi, H., Bianchi, C. N., Boudouresque, C. F., Buia, M. C., Calvo, S., et al. (2014). Climate change and Mediterranean seagrass meadows: a synopsis for environmental managers. *Mediterr Mar Sci.* 15, 462–473. doi: 10.12681/mms.621

Pergent, G., Boudouresque, C. F., Dumay, O., Pergent-Martini, C., and Wyllie-Echeverria, S. (2008). Competition between the invasive macrophyte *Caulerpa taxifolia* and the seagrass *Posidonia oceanica*: contrasting strategies. *BMC Ecol.* 8, 1–13. doi: 10.1186/1472-6785-8-20

Possingham, H. P., Bode, M., and Klein, C. J. (2015). Optimal conservation outcomes require both restoration and protection. *PloS Biol.* 13, 1–16. doi: 10.1371/journal.pbio.1002052

Reyes, J., Sansón, M., and Afonso-Carrillo, J. (1995). Distribution and reproductive phenology of the seagrass *Cymodocea nodosa* (Ucria) Ascherson in the Canary Islands. *Aquat Bot.* 50, 171–180. doi: 10.1016/0304-3770(95)00451-5

Rismondo, A., Curiel, D., Marzocchi, M., and Scattolin, M. (1997). Seasonal pattern of *Cymodocea nodosa* biomass and production in the lagoon of Venice. *Aquat Bot.* 58, 55–64. doi: 10.1016/S0304-3770(96)01116-3

Robinson, J. M., Hodgson, R., Krauss, S. L., Liddicoat, C., Malik, A. A., Martin, B. C., et al. (2023). Opportunities and challenges for microbiomics in ecosystem restoration. *Trends Ecol. Evol.* 38, 1189–1202. doi: 10.1016/j.tree.2023.07.009

Rodríguez-Prieto, C., Ballesteros, E., Boisset, F., and Afonso Carrilo, J. (2013). *Guía de las macroalgas y fanerógamas marinas del Mediterráneo Occidental* (Barcelona, Spain: Ediciones Omega).

Rossi, M., Borromeo, I., Capo, C., Glick, B. R., Del Gallo, M., Pietrini, F., et al. (2021). PGPB improve photosynthetic activity and tolerance to oxidative stress in *brassica napus* grown on salinized soils. *Appl. Sci.* 11, 11442. doi: 10.3390/app112311442

Ruiz, J. M., Boudouresque, C. F., and Enríquez, S. (2009). Mediterranean seagrasses. *Bot. Mar* 52, 369–382. doi: 10.1515/BOT.2009.058

Russo, R. O., and Berlyn, G. P. (1990). The use of organic biostimulants to help low input sustainable agriculture. *J. Sustain. Agric.* 1, 19–42. doi: 10.1300/J064v01n02_04

Salisbury, F. B., and Ross, C. W. (1992). *Plant Physiology* (Belmont: Wadsworth).

Sánchez-López, A. S., Pintelon, I., Stevens, V., Imperato, V., Timmermans, J. P., González-Chávez, C., et al. (2018). Seed endophyte microbiome of Crotalaria pumila unpeeled: identification of plant-beneficial methylobacteria. *Int. J. Mol. Sci.* 19, 291. doi: 10.3390/ijms19010291

Sarabi, V., and Arjmand-Ghajur, E. (2021). Exogenous plant growth regulators/plant growth promoting bacteria roles in mitigating water-deficit stress on chicory (*Cichorium pumilum* Jacq.) at a physiological level. *Agric. Water Manag* 245, 106439. doi: 10.1016/j.agwat.2020.106439

Sarker, A., Al Masud, M. A., Deepo, D. M., Das, K., Nandi, R., Ansary, M. W. R., et al. (2023). Biological and green remediation of heavy metal contaminated water and soils: A state-of-the-art review. *Chemosphere* 332, 138861. doi: 10.1016/j.chemosphere.2023.138861

Sfriso, A., and Ghetti, P. F. (1998). Seasonal variation in the biomass, morphometric parameters and production of rhizophytes in the lagoon of Venice. *Aquat Bot.* 61, 207–223. doi: 10.1016/S0304-3770(98)00064-3

Shili, A., Ben Maiz, N., Boudouresque, C. F., and Trabelsi, E. B. (2007). Abrupt changes in *Potamogeton* and *Ruppia* beds in a Mediterranean lagoon. *Aquat Bot.* 87, 181–188. doi: 10.1016/j.aquabot.2007.03.010

Sinclair, E. A., Sherman, C. D. H., Statton, J., Copeland, C., Matthews, A., Waycott, M., et al. (2021). Advances in approaches to seagrass restoration in Australia. *Ecol. Manag Restor.* 22, 10–21. doi: 10.1111/emr.12452

Singh Rawat, V., Kaur, J., Bhagwat, S., Arora Pandit, M., and Dogra Rawat, C. (2023). Deploying microbes as drivers and indicators in ecological restoration. *Restor. Ecol.* 31, e13688. doi: 10.1111/rec.13688

Small, C. C., and Degenhardt, D. (2018). Plant growth regulators for enhancing revegetation success in reclamation: A review. *Ecol. Eng* 118, 43–51. doi: 10.1016/j.ecoleng.2018.04.010

Smith, C. J., Verdura, J., Papadopoulou, N., Fraschetti, S., Cebrian, E., Fabbrizzi, E., et al. (2023). A decision-support framework for the restoration of *Cystoseira* sensu lato forests. *Front. Mar Sci.* 10. doi: 10.3389/fmars.2023.1159262

Stipcich, P., Marín-Guirao, L., Pansini, A., Pinna, F., Procaccini, G., Pusceddu, A., et al. (2022). Effects of current and future summer marine heat waves on *Posidonia oceanica*: plant origin matters? *Front. Clim* 4. doi: 10.3389/fclim.2022.844831

Swaminathaan, C., and Srinivasan, V. M. (1996). Seedling invigoration through plant growth substances in teak (Tectona grandis). *J. Trop. For Sci.* 8, 310–316.

Swamy, S. L., Puri, S., and Singh, A. K. (2002). Effect of auxins (IBA and NAA) and season on rooting of juvenile and mature hardwood cuttings of *Robinia pseudoacacia* and *Grewia optiva*. *New For* 23, 143–157. doi: 10.1023/A:1015653131706

Tarquinio, F., Hyndes, G. A., Laverock, B., Koenders, A., and Säwström, C. (2019). The seagrass holobiont: understanding seagrass-bacteria interactions and their role in seagrass ecosystem functioning. *FEMS Microbiol Lett.* 366, fnz057. doi: 10.1093/femsle/fnz057

United Nations Environment Agency (2019). "Resolution adopted by the general Assembly on 1 March 2019 73/284," in *United Nations Decade on Ecosystem Restoration, (2021-2030)*. New York, NY, USA.

United Nations Environment Programme (2019). *A new deal for nature – restore the degraded planet*. Available online at: https://www.unep.org/resources/policy-and-strategy/new-deal-nature (Accessed 18 June 2024).

Vassallo, P., Paoli, C., Rovere, A., Montefalcone, M., Morri, C., and Bianchi, C. N. (2013). The value of the seagrass *Posidonia oceanica*: a natural capital assessment. *Mar Pollut. Bull.* 75, 157–167. doi: 10.1016/j.marpolbul.2013.07.044

Waltham, N. J., Elliott, M., Lee, S. Y., Lovelock, C., Duarte, C. M., Buelow, C., et al. (2020). UN decade on ecosystem restoration 2021–2030—what chance for success in restoring coastal ecosystems? *Front. Mar Sci.* 7. doi: 10.3389/fmars.2020.00071

Watson, C. D., Gardner, M. G., Hodgson, R. J., Liddicoat, C., Peddle, S. D., and Breed, M. F. (2022). Global meta-analysis shows progress towards recovery of soil microbiota following revegetation. *Biol. Conserv* 272, 109592. doi: 10.1016/j.biocon.2022.109592

Waycott, M., Duarte, C. M., Carruthers, T. J., Orth, R. J., Dennison, W. C., Olyarnik, S., et al. (2009). Accelerating loss of seagrasses across the globe threatens coastal ecosystems. *Proc. Natl. Acad. Sci. U.S.A.* 106, 12377–12381. doi: 10.1073/pnas.090562010

Weyens, N., van der Lelie, D., Taghavi, S., Newman, L., and Vangronsveld, J. (2009). Exploiting plant–microbe partnerships to improve biomass production and remediation. *Trends Biotechnol.* 27, 591–598. doi: 10.1016/j.tibtech.2009.07.006

Winters, G., Beer, S., Willette, D. A., Viana, I. G., Chiquillo, K. L., Beca-Carretero, P., et al. (2020). The tropical seagrass *Halophila stipulacea*: Reviewing what we know from its native and invasive habitats, alongside identifying knowledge gaps. *Front. Mar Sci.* 7. doi: 10.3389/fmars.2020.00300

Wu, L., Zhang, Y., Guo, X., Ning, D., Zhou, X., Feng, J., et al. (2022). Reduction of microbial diversity in grassland soil is driven by long-term climate warming. *Nat. Microbiol* 7, 1054–1062. doi: 10.1038/s41564-022-01147-3

frontiers | Frontiers in Plant Science

TYPE Opinion
PUBLISHED 14 August 2025
DOI 10.3389/fpls.2025.1607207

OPEN ACCESS

EDITED BY
Yang Yu,
Beijing Forestry University, China

REVIEWED BY
Hua Liu,
Hebei University, China

*CORRESPONDENCE
Zhijie Zhang
zhangzj@caep.org.cn

RECEIVED 07 April 2025
ACCEPTED 30 June 2025
PUBLISHED 14 August 2025

CITATION
Zha X and Zhang Z (2025) Opinionated views on biophysical and social constraints on agroforestry system.
Front. Plant Sci. 16:1607207.
doi: 10.3389/fpls.2025.1607207

Opinionated views on biophysical and social constraints on agroforestry system

Xinjie Zha[1] and Zhijie Zhang[2*]

[1]Xi'an University of Finance and Economics, Xi'an, China, [2]Institute of Strategic Planning, Chinese Academy of Environmental Planning, Beijing, China

KEYWORDS

agroforestry, biophysical constraints, climate change, resource competition, ecosystem services

Introduction

Agroforestry is a collective concept that integrates indigenous, traditional and modern land-use systems combining tree cultivation with agricultural crop production and/or animal husbandry, including alley cropping, windbreaks, and silvopasture (Eichhorn et al., 2006; Terasaki Hart et al., 2023). By the late 1970s, growing awareness of the environmental and social consequences of intensified agricultural systems following the Green Revolution led to the rising recognition of agroforestry as a viable nature-based solution (NbS) and a sustainable alternative to conventional monoculture farming. Agroforestry systems enhance resource efficiency by strategically integrating species with complementary ecological niches, optimizing spatial, temporal, and physical resource use. This strategy boosts productivity in both food (e.g., cereals, vegetables and woody crops) and non-food outputs, such as timber, bioenergy, and other biomass-based materials (Dalemans et al., 2019). Furthermore, agroforestry enhances carbon sequestration or protects carbon storage on agricultural lands, with a cost-effective mitigation potential estimated between 0.12 Pg C yr^{-1} (Griscom et al., 2017) and 0.31 Pg C yr^{-1} (Roe et al., 2021). This potential estimated is comparable to other key strategies, such as reforestation (0.27 Pg C yr^{-1}) and reducing deforestation (0.49 Pg C yr^{-1}).

The overarching advantage of agroforestry lies in its multifunctionality: enhance biodiversity, mitigates climate change, reduces land degradation, improve soil health and strengthen food security and dietary diversity, while supporting sustainable livelihoods (Torralba et al., 2016; Beillouin et al., 2021). Although the ecological performance still lagged behind that of natural forest [11% lower biodiversity and 37% lower ecosystem services sourced from De Beenhouwer et al. (2013)], yet substantially higher than conventional monoculture agriculture. A meta-analysis synthesizing 365 comparisons (Torralba et al., 2016) demonstrated a significant positive effect of agroforestry on ecosystem services supply, including food production (+17.3%), soil fertility (+26.1%), biodiversity (+29.7%), and erosion control (+223%). Among agroforestry types, silvopastoral systems showed a lower mean effect size (0.324) is less than silvoarable (0.772). It is highlighted as one of the most effective options to address the multiple

environmental issues and social crisis (IPCC, 2019). Currently, about 43% of agricultural land under some variation of agroforestry approaches (Zomer et al., 2016), and approximately 1.8 billion people directly or indirectly depend on agroforestry products and services for their livelihood (ICRAF, 2006). The adoption of agroforestry remains uneven across regions: India alone manages approximately 28 Mha under agroforestry systems (Food and Agriculture Organization of the United Nations (FAO), 2021), while the EU has around 15 Mha, primarily in the form of Mediterranean wood-pasture landscapes (den Herder et al., 2016). This number is expected to rise, as agroforestry continues to receive policy incentives and supportive subsides from various agriculture- and forestry-related frameworks, such as the Common Agricultural Policy (CAP) by the European Union (EU), the Farm Bill by the United States, and AFR100 (African Forest Landscape Restoration Initiative). For example, EU's CAP offers farmers €60–120/ha/year for maintaining tree–crop systems and €100–350/ha/year for ongoing management, with some programs covering up to 100% of establishment costs. In the Amazon region, agroforestry projects promote coffee intercropped with native tree species or diverse tree mixtures, aiming to support smallholder livelihoods while conserving forests. The EverGreen Agriculture Partnership advances the systematic integration of trees into agricultural landscapes across sub-Saharan Africa, with a particular emphasis on nitrogen-fixing species to restore soil fertility and boost agricultural productivity. However, despite its potential benefits, the widespread adoption and expansion of agroforestry systems remain hindered by several biophysical and social constraints, necessitating systematically summarized and targeted interventions to fully unlock the benefits of agroforestry (Figure 1).

Biophysical constraints on agroforestry

Biophysical constraints refer to the inherent physical and biological limitations of natural systems that may affect the feasibility, effectiveness (ecosystem service and productive functions), or long-term sustainability of agroforestry systems. While artificial inputs and management interventions can often overcome these barriers, adoption ultimately hinges on whether the practice is cost-effective—both economically and ecologically. Similar to all living organisms, the biological components of agroforestry systems—including annual and perennial plants, as well as livestock—will be increasingly exposed to rising temperatures, elevated atmospheric CO_2 levels, and shifting precipitation patterns (Burke et al., 2009). Climate change-driven shifts in temperature and precipitation patterns (e.g., extreme droughts, irregular rainfall, seasonal droughts) can alter the growth (e.g., flowering, pollination, and even plant mortality) and suitability of tree species and crops cultivated in agroforestry, but highly depend on emission scenarios and geographic location (Odeny et al., 2019; Ivezić et al., 2021; Lima et al., 2022). Elevated temperatures increase evapotranspiration, resulting in soil moisture loss and plant heat stress. Many agroforestry species exhibit thermal thresholds, beyond which photosynthetic efficiency declines, flowering phenology shifts, fruit set and crop yield decreases (Guillot et al., 2019). Furthermore. niche modeling predictions indicate that, under various scenarios of future climate change, the suitable habitat for 135 tree species traditionally cultivated in Brazilian agroforestry systems is projected to decline by 22.3% to 56.3% (Lima et al., 2022). Similarly, in Tanzania, different agroforestry systems (e.g., *Albizia gummifera*, *Persea americana* and *Mangifera indica*) are expected to exhibit varying movement responses (upslope or downslope migration) to climate change (Odeny et al., 2019).

The competition between trees and crops for resources of space, water, sunlight and soil nutrition is critical determinant constraining agroforestry productivity and monetary revenue (Swieter et al., 2022). In water-limited and arid environments, trees and crops often compete for limited water resources and thus reduce yields. Such competition is particularly pronounced when deep-rooted trees extract water from underground reserves, potentially depleting groundwater supplies and exacerbating water

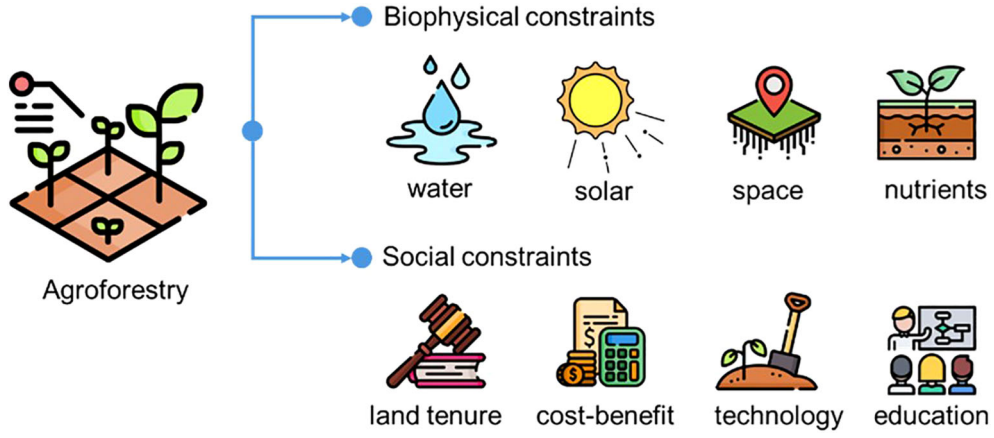

FIGURE 1
Biophysical and social constraints on agroforestry system. Icons sourced from Flaticon (www.flaticon.com).

scarcity. Tree shading can positively impact crop yield by modifying the microclimate, reducing evapotranspiration, and facilitating hydraulic lift—where plant roots transfer water from moist to drier soil layers, enhancing soil moisture retention (Bayala and Prieto, 2019). However, factors such as tree height, canopy density, and orientation regulate the extent of solar radiation reaching the cropped area throughout the day (Schmidt et al., 2019). It is produced in high-latitude regions, where the growing season is already shortened by limited daylight hours, and the lower angle of sunlight further restricts light penetration (van der Werf et al., 2007). In silvopastoral systems, resource competition between trees, pasture, and livestock is also prominent. This includes root-level competition for water and nutrients, excessive canopy shading that suppresses pasture growth, and livestock browsing that damages young trees and hinders their establishment (Jose and Dollinger, 2019; Karki et al., 2019). Rivest et al. (2013) highlight the lack of consensus on how trees influence annual crop yields, affected by depending on tree functional groups (e.g., deciduous, evergreen oak) and rainfall conditions. Such resource competition happened in aboveground and belowground part in agroforestry systems (Zhang et al., 2013; Isaac et al., 2014). For example, nutrient competition in a walnut tree root and wheat system caused nutrient depletion, negatively affecting plant health and agricultural productivity (Zhang et al., 2013). Soil fertility management, including mulching, composting, and nitrogen-fixing tree species, is necessary to mitigate these challenges.

Integrating trees into agricultural systems can influence pest and disease dynamics in complex ways, which are context-dependent, including species composition, landscape configuration and management practices. On the one hand, agroforestry systems can also suppress pest outbreaks by enhancing habitat for natural enemies, increasing plant diversity, and disrupting pest life cycles (Pumariño et al., 2015; Gurr et al., 2017). On the other hand, the interactions of tree-crop in agroforestry systems can create microclimates that favor pest proliferation, particularly in humid environments where fungal diseases thrive. This risk is especially pronounced in monoculture tree plantations within agroforestry systems (Ambele et al., 2018), where large-scale uniform tree stands provide continuous food sources and habitat for specific pests. Staton et al. (2021) suggested that agroforestry systems are likely to suppress annual, disturbance-tolerant weeds and highly mobile specialist pests, while perennial weeds and low-mobility generalist pests may persist or even proliferate. This is largely attributed to the greater structural complexity, diverse microclimates, and extended crop cycles inherent to agroforestry, which create less favorable conditions for short-lived, disturbance-adapted species while simultaneously offering more stable habitats for perennial weeds and less mobile pests.

Social constraints on agroforestry

The primary social barriers limiting the widespread adoption of agroforestry were derived from weak policy support, financial concerns and a lack of knowledge and management capacity. Among the most critical barriers is land tenure insecurity, often proven more important than other motives for agroforestry investments (e.g., cash subsidies), particular in the Global South, where land laws and policies often fail to clearly define ownership rights for trees planted on farmland (McElwee, 2009). Many high-priority areas for restoring conventional farmland through agroforestry overlap significantly with regions characterized by weak governance and unrecognized land rights, posing a challenge to the widespread adoption of agroforestry (Rakotonarivo et al., 2023). In many regions, customary land tenure systems separate land ownership from tree ownership, necessitating alignment between the land-use strategies and interests of both land and tree owners (Folefack and Darr, 2021). The significant disparity between statutory and customary land tenure systems presents fundamental challenges to achieving the intended ecological and social benefits of restoration (McLain et al., 2021). Massive local questionnaire confirmed that farmers with insecure land tenures and agroforestry rights are less motivated to adopt agroforestry (Folefack and Darr, 2021; Jha et al., 2021).

Another major concern is the financial constraints of agroforestry systems, particularly among smallholder farmers and resource-limited communities. High upfront costs, delayed financial returns, and market uncertainties make agroforestry a risky investment. The integration of fruit or timber trees into intensively managed pastures or croplands often leads to initial reductions in crop yields or grazing capacity, resulting in short-term economic losses. Establishing an agroforestry system demands substantial investment in seedlings, fencing, irrigation, and labor, with returns delayed for years. Timber and fruit trees may take 5–20 years to reach commercial viability, creating a prolonged cash flow gap that challenges farmers dependent on annual crop cycles for subsistence. While the diversified production characteristic of agroforestry can reduce the risks associated with monoculture (England et al., 2020; Akter et al., 2022), however, market fluctuations in the value of agroforestry products—timber, fruits, nuts, and medicinal plants—remain unpredictable, complicating long-term financial planning. Some modeling studies suggest that, in the absence of subsidy mechanisms (e.g., carbon incentives for agroforestry), the returns from agroforestry systems may be not profitable than those of monoculture farming.

Countries with widespread hunger and malnutrition—particularly those in sub-Saharan Africa and large developing nations—continue to face pressing food security challenges (Chen et al., 2011). Per capita food demand is steadily increasing, and some of these countries are struggling to address severe regional undernutrition and agricultural mechanization. National agricultural policies largely favor conventional monoculture farming and intensive agricultural production, offering limited integration of agroforestry into mainstream agricultural systems and failing to provide targeted subsidies. The promotion of agroforestry in such contexts may face significant challenges related to national policy objectives. Smallholder producers, in particular, lack access to stable credit and financial support, discouraging investment in farm inputs, participation in land

markets and cash crops cultivation, and making long-term commitments agroforestry (Place, 2009). This situation contrasts with that of developed economies in Europe, North America, and Oceania, where agricultural priorities increasingly focus on precision farming and reducing the environmental footprint of food production. However, agroecological transitions in developed economies may come at the cost of increasing the agricultural footprint in other countries. For example, the implementation of the European Green Deal (EGU), which supports agroforestry, diverse agricultural landscapes and other sustainable land-use practices, could result in an expansion of agricultural land outside the EU by up to 24 Mha, associated with 758.9 Mt CO_2 emissions and substantial biodiversity loss (Zhong et al., 2024).

From the perspective of NbS, agroforestry's climate mitigation and ecosystem services' benefits are largely a public good rather than a private benefit for farmers, leading to market failure (Bettles et al., 2021). Carbon markets and other payment for ecosystem services can regulate this issue by transforming public benefits into private incentives, encouraging greater agroforestry adoption. However, the cost-benefit carbon pricing is estimated at $100/Mg CO_2, making it challenging for developing countries to set competitive carbon prices (Zeng et al., 2020). Higher-yielding cropland offers the greater per-hectare carbon sequestration potential, but the opportunity cost of agriculture can be substantial, thus requiring careful trade-offs in land-use decisions (Grass et al., 2020; Wurz et al., 2022).

Additionally, the complexity of agroforestry—requiring a deep understanding of tree-crop-livestock interactions, soil management, and market dynamics—can deter farmers from transitioning to more sustainable agroforestry practice. For example, compared to annual crops, tree crops require more complex management, have a longer return period, and pose greater challenges for mechanized production. In silvopastoral systems, careful management of tree species, height, and planting density is essential to minimize resource competition between trees and pasture, and livestock browsing on economically valuable tree species (Smith et al., 2022). Limited access to training programs, extension services, and technical support further restricts their ability to adopt and effectively implement these systems, reinforcing dependence on conventional farming methods.

Agroforestry systems located at crossroads

The future of agroforestry ultimately depends on whether individual farmers adopt and sustain agroforestry practices, which, in turn, is influenced by the performance of agroforestry systems and the ability of local decision-making environments to minimize the above-mentioned barriers. The performance of agroforestry on productivity and ecosystem services is shaped by the interactions between trees, crops, environment, management practices, and policy frameworks. Enhancing agroforestry productivity requires maximizing beneficial resource interactions (e.g., available water, land, nutrients, and sunlight) while minimizing resource competition between trees and understory crops (Zhang et al., 2013; Yang et al., 2019). This requires careful design around tree species, crop types, planting patterns (spacing and canopy cover), and management practices (e.g., mowing, fertilization, and irrigation). All of them needs targeted education initiatives, hands-on training, and knowledge-sharing networks, to equip farmers with the necessary knowledge and skills for successful agroforestry implementation. governments and non-state actors must persist in research, policy formulation, and program development to overcome key barriers and enhance enabling conditions. These efforts should focus on securing land tenure rights, expanding access to technical training and knowledge, improving credit availability and short-term financing, fostering market development, and addressing inefficiencies caused by market failures and misaligned incentives (Shyamsundar et al., 2022; Schulte et al., 2022). Decades of research have demonstrated the multifunctionality of agroforestry, highlighting its role in climate change mitigation while simultaneously enhancing agricultural livelihoods and sustainability. Beyond agroforestry, a wide range of cropland transition strategies grounded in multifunctionality or circular economy principles (e.g., agrivoltaics, aquaponics, and pollinator-friendly farming) have been increasingly proposed. Each of these approaches carries distinct advantages, such as high decarbonization potential or economic returns, as well as limitations (e.g., trade-offs with biodiversity). Realizing these transition strategies' full potential in practice requires extensive and prioritized scientific efforts to comprehensively understand the biophysical and economic constraints that shape agroforestry systems.

Author contributions

XZ: Writing – original draft, Writing – review & editing, Funding acquisition. ZZ: Writing – original draft, Formal Analysis, Funding acquisition, Writing – review & editing.

Funding

The author(s) declare financial support was received for the research and/or publication of this article. This research was supported by Science and Technology Projects of Xizang Autonomous Region, China (No. XZ202303ZY0003G; XZ202501ZY0034).

Conflict of interest

The authors declare that the research was conducted in the absence of any commercial or financial relationships that could be construed as a potential conflict of interest.

Generative AI statement

The author(s) declare that no Generative AI was used in the creation of this manuscript.

Publisher's note

References

Akter, R., Hasan, M. K., Kabir, K. H., Darr, D., and Roshni, N. A. (2022). Agroforestry systems and their impact on livelihood improvement of tribal farmers in a tropical moist deciduous forest in Bangladesh. *Trees Forests People* 9, 100315. doi: 10.1016/j.tfp.2022.100315

Ambele, F. C., Hervé, B. D., Ekesi, S., Akutse, K. S., Djuideu, C. T., Meupia, M. J., et al. (2018). Consequences of shade management on the taxonomic patterns and functional diversity of termites (Blattodea: Termitidae) in cocoa agroforestry systems. *Ecol. Evol.* 8, 11582–11595. doi: 10.1002/ece3.4607

Bayala, J., and Prieto, I. (2019). Water acquisition, sharing and redistribution by roots: applications to agroforestry systems. *Plant Soil* 453, 17–28. doi: 10.1007/s11104-019-04173-z

Beillouin, D., Ben-Ari, T., Malézieux, E., Seufert, V., and Makowski, D. (2021). Positive but variable effects of crop diversification on biodiversity and ecosystem services. *Global Change Biol.* 27, 4697–4710. doi: 10.1111/gcb.15747

Bettles, J., Battisti, D. S., Cook-Patton, S. C., Kroeger, T., Spector, J. T., Wolff, N. H., et al. (2021). Agroforestry and non-state actors: A review. *For. Policy economics* 130, 102538. doi: 10.1016/j.forpol.2021.102538

Burke, M. B., Lobell, D. B., and Guarino, L. (2009). Shifts in African crop climates by 2050, and the implications for crop improvement and genetic resources conservation. *Global Environ. Change* 19, 317–325. doi: 10.1016/j.gloenvcha.2009.04.003

Chen, X. P., Cui, Z. L., Vitousek, P. M., Cassman, K. G., Matson, P. A., Bai, J. S., et al. (2011). Integrated soil–crop system management for food security. *Proc. Natl. Acad. Sci.* 108, 6399–6404. doi: 10.1073/pnas.1101419108

Dalemans, F., Muys, B., and Maertens, M. (2019). Adoption constraints for small-scale agroforestry-based biofuel systems in India. *Ecol. Economics* 157, 27–39. doi: 10.1016/j.ecolecon.2018.10.020

De Beenhouwer, M., Aerts, R., and Honnay, O. (2013). A global meta-analysis of the biodiversity and ecosystem service benefits of coffee and cacao agroforestry. *Agriculture Ecosyst. Environ.* 175, 1–7. doi: 10.1016/j.agee.2013.05.003

den Herder, M., Moreno, G., Mosquera-Losada, M. R., Palma, J. H. N., Sidiropoulou, A., Santiago Freijanes, J. J., et al. (2016). Current extent and trends of agroforestry in the EU27 *(Deliverable Report 1.2)*. Available online at: https://www.agforward.eu/documents/D1_2_Extent_of_Agroforestry.pdf (Accessed May 1, 2025).

Eichhorn, M. P., Paris, P., Herzog, F., Incoll, L. D., Liagre, F., Mantzanas, K., et al. (2006). Silvoarable systems in Europe–past, present and future prospects. *Agroforestry Syst.* 67, 29–50. doi: 10.1007/s10457-005-1111-7

England, J. R., O'Grady, A. P., Fleming, A., Marais, Z., and Mendham, D. (2020). Trees on farms to support natural capital: an evidence-based review for grazed dairy systems. *Sci. Total Environ.* 704, 135345. doi: 10.1016/j.scitotenv.2019.135345

Folefack, A. J. J., and Darr, D. (2021). Promoting cocoa agroforestry under conditions of separated ownership of land and trees: Strengthening customary tenure institutions in Cameroon. *Land Use Policy* 108, 105524. doi: 10.1016/j.landusepol.2021.105524

Food and Agriculture Organization of the United Nations (FAO) (2021). *Restoration of degraded lands through agroforestry* (Rome: FAO).

Grass, I., Kubitza, C., Krishna, V. V., Corre, M. D., Mußhoff, O., Pütz, P., et al. (2020). Trade-offs between multifunctionality and profit in tropical smallholder landscapes. *Nat. Commun.* 11, 1186. doi: 10.1038/s41467-020-15013-5

Griscom, B. W., Adams, J., Ellis, P. W., Houghton, R. A., Lomax, G., Miteva, D. A., et al. (2017). Natural climate solutions. *Proc. Natl. Acad. Sci. U.S.A.* 114, 11645–11650. doi: 10.1073/pnas.1710465114

Guillot, E., Hinsinger, P., Dufour, L., Roy, J., and Bertrand, I. (2019). With or without trees: resistance and resilience of soil microbial communities to drought and heat stress in a Mediterranean agroforestry system. *Soil Biol. Biochem.* 129, 122–135. doi: 10.1016/j.soilbio.2018.11.011

Gurr, G. M., Wratten, S. D., Landis, D. A., and You, M. (2017). Habitat management to suppress pest populations: progress and prospects. *Annu. Rev. Entomology* 62, 91–109. doi: 10.1146/annurev-ento-031616-035050

ICRAF (2006). *Agroforestry for improved livelihoods and natural resources conservation: an agroforestry policy brief*. Available online at: https://www.worldagroforestry.org/publication/agroforestry-improved-livelihoods-and-natural-resources-conservation-agroforestry (Accessed May 1, 2025).

IPCC. (2019). "Summary for policymakers," in *Climate change and land: an IPCC special report on climate change, desertification, land degradation, sustainable land management, food security, and greenhouse gas fluxes in terrestrial ecosystems*. Eds. P. R. Shukla, J. Skea, E. Calvo Buendia, V. Masson-Delmotte, H.-O. Pörtner, D. C. Roberts, P. Zhai, R. Slade, S. Connors, R. van Diemen, M. Ferrat, E. Haughey, S. Luz, S. Neogi, M. Pathak, J. Petzold, J. Portugal Pereira, P. Vyas, E. Huntley, K. Kissick and M. Belkacemi (Geneva, Switzerland: Intergovernmental Panel on Climate Change (IPCC)).

Isaac, M. E., Anglaaere, L. C. N., Borden, K., and Adu-Bredu, S. (2014). Intraspecific root plasticity in agroforestry systems across edaphic conditions. *Agriculture Ecosyst. Environ.* 185, 16–23. doi: 10.1016/j.agee.2013.12.004

Ivezić, V., Yu, Y., and Werf, W. (2021). Crop yields in European agroforestry systems: a meta-analysis. *Front. Sustain. Food Syst.* 5, 606631. doi: 10.3389/fsufs.2021.606631

Jha, S., Kaechele, H., and Sieber, S. (2021). Factors influencing the adoption of agroforestry by smallholder farmer households in Tanzania: Case studies from Morogoro and Dodoma. *Land Use Policy* 103, 105308. doi: 10.1016/j.landusepol.2021.105308

Jose, S., and Dollinger, J. (2019). Silvopasture: a sustainable livestock production system. *Agroforest Syst.* 93, 1–9. doi: 10.1007/s10457-019-00366-8

Karki, U., Karki, Y., Khatri, R., and Tillman, A. (2019). Diurnal behavior and distribution patterns of Kiko wethers in southern-pine silvopastures during the cool-season grazing period. *Agroforestry Syst.* 93, 267–277. doi: 10.1007/s10457-018-0229-3

Lima, V. P., de Lima, R. A. F., Joner, F., et al. (2022). Climate change threatens native potential agroforestry plant species in Brazil. *Sci. Rep.* 12, 2267. doi: 10.1038/s41598-022-06234-3

McElwee, P. (2009). Reforesting "bare hills" in Vietnam: Social and environmental consequences of the 5 million hectare reforestation program. *Ambio: A J. Hum. Environ.* 38, 325–333. doi: 10.1579/08-R-520.1

McLain, R., Lawry, S., Guariguata, M. R., Reed, J., and Reed, J. (2021). Toward a tenure-responsive approach to forest landscape restoration: A proposed tenure diagnostic for assessing restoration opportunities. *Land Use Policy* 104, 103748. doi: 10.1016/j.landusepol.2018.11.053

Odeny, D., Karan-Ja, F., Mwachala, G., Pellikka, P., and Marchant, R. (2019). Impact of climate change on species distribution and carbon storage of agroforestry trees on isolated east african mountains impact of climate change on species distribution and carbon storage of agroforestry trees on isolated east african mountains. *Am. J. Clim. Change* 8, 364–386. doi: 10.4236/ajcc.2019.83020

Place, F. (2009). Land tenure and agricultural productivity in Africa: a comparative analysis of the economics literature and recent policy strategies and reforms. *World Dev.* 37, 1326–1336. doi: 10.1016/j.worlddev.2008.08.020

Pumariño, L., Sileshi, G. W., Gripenberg, S., Kaartinen, R., Barrios, E., and Muchane, M. N. (2015). Effects of agroforestry on pest, disease and weed control: A meta-analysis. *Basic Appl. Ecol.* 16, 573–582. doi: 10.1016/j.baae.2015.08.006

Rakotonarivo, O. S., Rakotoarisoa, M., Rajaonarivelo, H. M., Raharijaona, S., Jones, J. P., and Hockley, N. (2023). Resolving land tenure security is essential to deliver forest restoration. *Commun. Earth Environ.* 4, 179. doi: 10.1038/s43247-023-00847-w

Rivest, D., Paquettea, A., Moreno, G., and Messiera, C. (2013). A meta-analysis reveals mostly neutral influence of scattered trees on pasture yield along with some contrasted effects depending on functional groups and rainfall conditions. *Agric. Ecosyst. Environ.* 165, 74–79. doi: 10.1016/j.agee.2012.12.010

Roe, S., Streck, C., Beach, R., Busch, J., Chapman, M., Daioglou, V., et al. (2021). Land-based measures to mitigate climate change: potential and feasibility by country. *Glob. Change Biol.* 27, 6025–6058. doi: 10.1111/gcb.15873

Schmidt, M., Nendel, C., Funk, R., Mitchell, M. G., and Lischeid, G. (2019). Modeling yields response to shading in the field-to-forest transition zones in heterogeneous landscapes. *Agriculture* 9, 6. doi: 10.3390/agriculture9010006

Schulte, I., Eggers, J., Nielsen, J.Ø, and Fuss, S. (2022). What influences the implementation of natural climate solutions? A systematic map and review of the evidence. *Environ. Res. Lett.* 17, 013002. doi: 10.1088/1748-9326/ac4071

Shyamsundar, P., Cohen, F., Boucher, T. M., Kroeger, T., Erbaugh, J. T., Waterfield, G., et al. (2022). Scaling smallholder tree cover restoration across the tropics. *Global Environ. Change* 76, 102591. doi: 10.1016/j.gloenvcha.2022.102591

Smith, M. M., Bentrup, G., Kellerman, T., MacFarland, K., Straight, R., Ameyaw, L., et al. (2022). Silvopasture in the USA: A systematic review of natural resource professional and producer-reported benefits, challenges, and management activities. *Agriculture Ecosyst. Environ.* 326, 107818. doi: 10.1016/j.agee.2021.107818

Staton, T., Walters, R. J., Smith, J., Breeze, T. D., and Girling, R. D. (2021). Evaluating a trait-based approach to compare natural enemy and pest communities in agroforestry vs. arable systems. *Ecol. Appl.* 31, e02294. doi: 10.1002/eap.2294

Swieter, A., Langhof, M., and Lamerre, J. (2022). Competition, stress and benefits: Trees and crops in the transition zone of a temperate short rotation alley cropping agroforestry system. *J. Agron. Crop Sci.* 208, 209–224. doi: 10.1111/jac.12553

Terasaki Hart, D. E., Yeo, S., Almaraz, M., Beillouin, D., Cardinael, R., Garcia, E., et al. (2023). Priority science can accelerate agroforestry as a natural climate solution. *Nat. Clim. Change* 13, 1179–1190. doi: 10.1038/s41558-023-01810-5

Torralba, M., Fagerholm, N., Burgess, P. J., Moreno, G., and Plieninger, T. (2016). Do European agroforestry systems enhance biodiversity and ecosystem services? *A meta-analysis. Agriculture Ecosyst. Environ.* 230, 150–161. doi: 10.1016/j.agee.2016.06.002

van der Werf, W., Keesman, K., Burgess, P. J., Graves, A. R., Pilbeam, D. J., Incoll, L. D., et al. (2007). Yield-SAFE: a parameter-sparse process-based dynamic model for predicting resource capture, growth and production in agroforestry systems. *Ecol. Eng.* 29, 419–433. doi: 10.1016/j.ecoleng.2006.09.017

Wurz, A., Tscharntke, T., Martin, D. A., Osen, K., Rakotomalala, A. A., Raveloaritiana, E., et al. (2022). Win-win opportunities combining high yields with high multi-taxa biodiversity in tropical agroforestry. *Nat. Commun.* 13, 4127. doi: 10.1038/s41467-022-30866-8

Yang, T., Duan, Z. P., Zhu, Y., Gan, Y. W., Wang, B. J., Hao, X. D., et al. (2019). Effects of distance from a tree line on photosynthetic characteristics and yield of wheat in a jujube tree/wheat agroforestry system. *Agroforestry Syst.* 93, 1545–1555. doi: 10.1007/s10457-018-0267-x

Zeng, Y., Sarira, T. V., Carrasco, L. R., Chong, K. Y., Friess, D. A., Lee, J. S.H., et al. (2020). Economic and social constraints on reforestation for climate mitigation in Southeast Asia. *Nat. Clim. Change* 10, 842–844. doi: 10.1038/s41558-020-0856-3

Zhang, W., Ahanbieke, P., Wang, B. J., Xu, W. L., Li, L. H., Christie, P., et al. (2013). Root distribution and interactions in jujube tree/wheat agroforestry system. *Agroforestry Syst.* 87, 929–939. doi: 10.1007/s10457-013-9609-x

Zhong, H., Li, Y., Ding, J., Bruckner, B., Feng, K., Sun, L., et al. (2024). Global spillover effects of the European Green Deal and plausible mitigation options. *Nat. Sustain* 7, 1501–1511. doi: 10.1038/s41893-024-01428-1

Zomer, R., Neufeldt, H., Xu, J., Ahrends, A., Bossio, D., Trabucco, A., et al. (2016). Global Tree Cover and Biomass Carbon on Agricultural Land: The contribution of agroforestry to global and national carbon budgets. *Sci. Rep.* 6, 29987. doi: 10.1038/srep29987

frontiers | Frontiers in Plant Science

TYPE Original Research
PUBLISHED 19 September 2025
DOI 10.3389/fpls.2025.1668310

OPEN ACCESS

EDITED BY
Zhi-Qiang Zhang,
Yunnan University, China

REVIEWED BY
Shi-jian Yang,
Yunnan University, China
Ashley Webb,
WaterNSW, Australia

*CORRESPONDENCE
Yang Yu
theodoreyy@gmail.com

RECEIVED 17 July 2025
ACCEPTED 05 September 2025
PUBLISHED 19 September 2025

CITATION
Zhu H, Wang Z, Zhao J, Lin J, Qian S, Wang L, Yu Y and Cavalli M (2025) The hilly-gully watershed exhibits distinct deep soil moisture characteristics: a comparative study of paired watersheds in the Chinese Loess Plateau. *Front. Plant Sci.* 16:1668310. doi: 10.3389/fpls.2025.1668310

The hilly-gully watershed exhibits distinct deep soil moisture characteristics: a comparative study of paired watersheds in the Chinese Loess Plateau

Hongsheng Zhu[1,2], Zihan Wang[1,2], Jiongchang Zhao[1,2], Jiaming Lin[1], Shuo Qian[3], Liping Wang[1,2], Yang Yu[1,2]* and Marco Cavalli[4]

[1]School of Soil and Water Conservation, Beijing Forestry University, Beijing, China, [2]Jixian National Forest Ecosystem Observation and Research Station, Chinese National Ecosystem Research Network (CNERN), School of Soil and Water Conservation, Beijing Forestry University, Beijing, China, [3]College of Biological Sciences, University of Minnesota, Minneapolis, MN, United States, [4]National Research Council of Italy, Research Institute for Geo-Hydrological Protection, Padova, Italy

Deep soil moisture constitutes a critical component of hydrological processes in the Loess Plateau, playing an essential role in sustaining vegetation growth, maintaining ecosystem stability, and serving as an important indicator of regional water resource carrying capacity. However, the mechanisms by which long-term vegetation restoration influences deep soil moisture remain insufficiently understood. In this study, we selected two typical paired small watersheds–an Artificial forest watershed and a Farmland watershed-located in the Caijiachuan watershed in the hilly-gully region of the Loess Plateau in western Shanxi Province, China. Based on *in situ* measurements of soil moisture (0–500 cm) during the 2024 growing season (May-October), the vertical distribution and spatial variability of soil moisture have been systematically analyzed, and the impacts of long-term vegetation restoration on deep soil moisture content have been assessed. The results revealed significant differences between the paired watersheds. The average soil moisture content in the Farmland watershed (0.096 g/g) was significantly higher than in the Artificial forest watershed (0.070 g/g), indicating that artificially introduced vegetation has substantially reduced deep soil moisture reserves. Land use has pronouncedly influenced deep soil moisture, with farmland and native grassland exhibiting the highest moisture retention capacity, while vegetation restoration sites showed the lowest levels. Deep-rooted plantations in the Artificial forest watershed markedly intensified soil moisture deficits in the 200–500 cm layers, whereas the Farmland watershed exhibited comparatively moderate deficits. Moreover, soil moisture spatial heterogeneity was significantly greater in the Farmland watershed, while long-term vegetation restoration promoted a more homogeneous distribution of

deep soil moisture. Overall, large-scale restoration dominated by deep-rooted species exerted substantial impacts on deep soil moisture dynamics. These findings provide a scientific basis for vegetation restoration planning and watershed management in the Loess Plateau region.

KEYWORDS

soil moisture, vegetation restoration, vertical distribution, spatial variability, Loess Plateau

1 Introduction

Soil moisture constitutes a vital element of the terrestrial system, serving an integrative function in surface processes, particularly within water-limited regions. In these areas, the availability of soil moisture is regarded as the principal determinant of the land productivity and sustainability of watershed management (Gao et al., 2014). Soil moisture demonstrates significant heterogeneity in both spatial and temporal dimensions, even within small watersheds (Dymond et al., 2021; Wang et al., 2019). The characterization of soil moisture variations across diverse spatial and temporal scales is crucial for theoretical understanding and practical applications related to surface runoff and erosion, agriculture management, and ecological restoration (Chatterjee et al., 2022; de Queiroz et al., 2020; Deng et al., 2016).

Soil moisture presents different characteristics in time and space. Numerous studies indicate that soil moisture is affected by a range of environmental factors, including land use, vegetation types, topographical conditions, and soil properties (Fathololoumi et al., 2021; Xu et al., 2021; Yu et al., 2018, 2019). For example, at the hillslope scale, topographic conditions such as slope position and aspect significantly affect soil moisture distribution, with shady slopes and lower positions generally exhibit higher moisture levels due to reduced evaporation and runoff accumulation (Dong et al., 2018); at the watershed scale, land use type, soil properties, and topographical conditions are dominant factors shaping soil moisture variability, where grassland and farmland exhibit differing retention capacities due to root structure and infiltration rates (Huang et al., 2016; Shi et al., 2012); at the regional scale, climatic factors such as precipitation and evapotranspiration predominantly govern soil moisture dynamics, directly influencing moisture content, spatial variability, seasonal fluctuations, and interannual variability (Wang et al., 2012).

Although soil properties and topography tend to remain constant in the short term, land use and climate factors represent the principal dynamic variables (Montenegro and Ragab, 2012; Sharma et al., 2022). On one hand, alterations in land use can significantly disrupt the surface water balance, influencing the allocation of precipitation among evapotranspiration, runoff, and groundwater flow. This, in turn, plays a critical role in determining the distribution of soil moisture within ecosystems. On the other hand, deep soil moisture is less sensitive to short-term climatic fluctuations and land surface changes, but is more closely linked to long-term patterns of infiltration and groundwater dynamics. Studies have shown that deep-layer moisture is predominantly governed by soil texture, soil thickness, topographic wetness index, and antecedent precipitation, with vegetation root depth also contributing significantly to the vertical redistribution of water (Li et al., 2021; Yu et al., 2019). Unlike surface moisture, which responds rapidly to rainfall and evapotranspiration, deep soil moisture content reflects integrated hydrological processes over longer timescales and thus serves as a more stable indicator of ecohydrological conditions (Wang et al., 2024a, 2024).

The Loess Plateau is an environmentally sensitive area, soil loss and water erosion are the main environmental problems in this area. Since 1999, the "Grain to Green Program" has promoted introduced vegetation to combat soil erosion, vegetation restoration proving to be the most effective measure in ecological management (Bai et al., 2024; Wang et al., 2021; Yu et al., 2020). Despite significant progress in ecological engineering, large-scale revegetation has led to excessive water consumption, resulting in dried soil layers and stunted old trees, thus weakening the expected effect of afforestation in reducing water loss and improving the local environment (Mei and Ma, 2022; Yao et al., 2016; Yu et al., 2024). Deep soil moisture is difficult to replenish. A decline in soil moisture has many other consequences for local water resources. For instance, Wang et al. (2024) found that in China's monsoon loess critical zone, intensive land-use conversions since 1999 have been the predominant catalyst of deep soil moisture decline, exceeding the effects of climate change and threatening soil moisture security across the Loess Plateau. Cheng et al. (2020) reported that in the semi-arid regions of northern China, vegetation restoration has significantly improved precipitation utilization. However, it has inhibited the recharge of deep soil moisture. Jia and Shao, 2014 emphasized that vegetation type significantly affects the dynamics of deep soil moisture. In addition to the increasing potential evapotranspiration, plant water consumption has substantially degraded soil moisture conditions in the experimental plots.

Soil moisture monitoring at the watershed scale is a crucial component in understanding the interactions between water and vegetation. Recent research on small watersheds has predominantly

concentrated on slopes or individual land-use types. However, there is a paucity of studies examining the impact of vegetation restoration on deep soil moisture at the watershed scale. The implementation of paired watershed monitoring is a primary method for elucidating hydrological processes; nevertheless, few studies have systematically examined deep water dynamics paired with watersheds. In this study, a paired-site methodology has been employed to assess the variation and magnitude of soil moisture resulting from long-term vegetation restoration in the hilly-gully region of the Loess Plateau, China. The main research purposes of this study were (i) to compare the differences of soil moisture variation across layers between paired watersheds; (ii) to explore the relationship between land uses and soil moisture variability, and (iii) to examine the effects of long-term vegetation restoration on deep soil moisture distribution.

2 Materials and methods

2.1 Study area

The study area is located in the Caijiachuan watershed in the Loess Plateau (Figure 1) in the western part of Shanxi Province, China, with geographical coordinates ranging from 110°39′45″ to 110°47′45″E and 36°14′27″ to 36°18′23″N. Since afforestation began in 1990, the forest coverage rate in the watershed has exceeded 80%, resulting in the establishment of approximately 1,000 hectares of soil and water conservation forest. The tree layer is dominated by *Robinia pseudoacacia* (RP) and *Pinus tabuliformis* (PT), the shrub layer by *Rosa xanthina* (RX), and the herbaceous layer by *Festuca elata* (FE). The Artificial forest watershed and the Farmland watershed are two paired watersheds

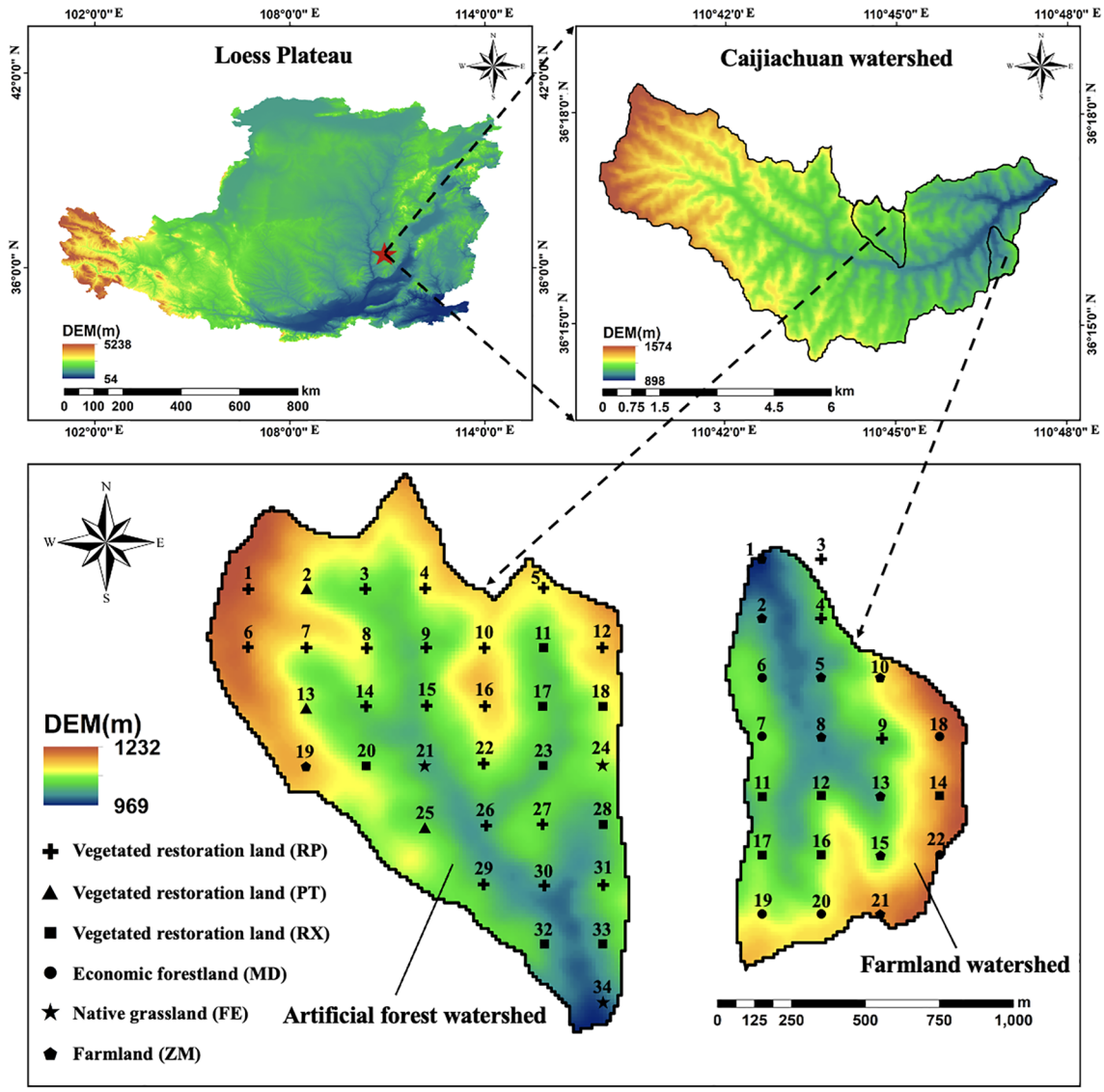

FIGURE 1
Location of the study area and experimental sites in two watersheds.

affiliated with the Caijiachuan watershed. Prior to vegetation restoration, the Artificial forest watershed was mainly farmland and shared similar land-use characteristics with the current Farmland watershed, which is geographically adjacent and thus selected as a reference (paired) watershed. Both watersheds are located in a typical loess residual plateau gully region, characterized by brown soils derived from loess parent material. The area experiences a warm-temperate continental climate, with rainfall primarily concentrated between June and September. The annual sunshine duration is approximately 2,563 hours, the average annual precipitation is 579 mm, and the average potential evapotranspiration is 1,723.9 mm. Rainfall patterns exhibit a uniform spatial distribution across the two watersheds. The Artificial forest watershed is situated in the central part of the Caijiachuan watershed, with an elevation ranging from 969 to 1,232 m and a total area of 1.52 km^2. It features high terrain in the northwest and low terrain in the southeast, with a general north-south orientation. Land use is dominated by vegetation restoration species (RP, PT, RX). In contrast, the Farmland watershed lies in the eastern part of the Caijiachuan watershed, with an elevation ranging from 915 to 1,110 m and an area of 0.76 km^2. Its terrain is high in the southeast and low in the northwest, also aligned in a north-south direction. The dominant land-use types are rain-fed farmland planted with *Zea mays* (ZM) and economic forest with *Malus domestica* (MD). The introduced vegetation types in the Caijiachuan watershed include RP, PT, and RX.

2.2 Field monitoring and experimental design

In the Artificial forest watershed and the Farmland watershed, there are different land use types. This study focused on 4 different land use types with different dominant plant species on them, which are native grassland (*Festuca elata*, FE), vegetated restoration land (*Robinia pseudoacacia*, RP; *Pinus tabuliformis*, PT; *Rosa xanthina*, RX), economic forestland (*Malus domestica*, MD), and farmland (*Zea mays*, ZM). In the Artificial Forest watershed, there were three land use types: native grassland, vegetated restoration land, and farmland, and in the Farmland watershed, there are also three land use types, which are vegetated restoration land, farmland, and economic forestland. Considering that the soil properties of the Artificial forest watershed and the Farmland watershed are generally consistent, this study, based on topographic characteristics and vegetation distribution, has established 34 experimental sites in the Artificial forest watershed: 30 of them were located within vegetated restoration land (including 19 in RP, 3 in PT, and 8 in RX), 3 of them were in native grassland (FE), and 1 of them were in farmland (ZM) (Table 1), and 22 experimental sites in the Farmland watershed: 8 of them were in vegetated restoration land (including 3 in RP and 5 in RX), 6 of them were in economic forestland (MD), and another 8 of them were in farmland (ZM) (Table 2), in August 2024 using a grid-based sampling design. At each experimental site, soil samples were collected with a soil auger to measure the gravimetric soil moisture (g/g) within the 0–500 cm soil profile. Given the pronounced topographic variability and the complex distribution of vegetation types across the Loess Plateau, the grid-based layout was adopted to enhance the spatial representativeness of the experimental sites, facilitate comparisons of soil moisture status among different land use types, and provide a robust foundation for subsequent modeling of spatial variability in deep soil moisture. During the field surveys, slope gradient, slope aspect, vegetation type, and vegetation cover were specifically documented at each experimental site. In addition, a handheld GPS device was used to measure and record the latitude, longitude, and elevation of each site.

2.3 Data collection

In the growing season of 2024 (May to October), soil moisture content in the 0–500 cm layer was measured at each experimental site. Three sampling profiles were randomly selected per site to obtain the average soil moisture content. Soil samples were collected with a 5 cm diameter auger at 10 cm intervals for the 0–100 cm layer and 20 cm intervals for the 100–500 cm layer, each profile yielded 30 samples, generating a total collection of 5040 samples across all study sites. According to previous studies conducted in the Loess Plateau (Yu et al., 2019), the annual precipitation infiltration depth generally does not exceed 200 cm, and soil moisture below this depth exhibits relatively small fluctuations and remains comparatively stable. Therefore, in this study, the 0–200 cm layer was defined as shallow soil, while the 200–500 cm layer was defined as deep soil. Samples were immediately sealed in aluminum cylinders after collection and weighed. They were then dried in an oven at 105°C until a constant weight was achieved. Soil moisture content (g/g) was calculated as the ratio of the mass lost during oven drying to the constant dry weight.

To analyze the spatial distribution of soil moisture, the Inverse Distance Weighting (IDW) method was used to interpolate soil moisture content and generate spatial distribution maps at different depths for both watersheds. ArcGIS software was employed for IDW interpolation and mapping, and its spatial analysis tools were used to perform basic statistical analyses based on the interpolated data.

2.4 Statistical analysis

The soil moisture content and profile distribution in each watershed was calculated by taking the average of all experimental sites in each soil layer. The depth-averaged gravimetric soil moisture content θ_{ij} (g/g) at each experimental site was calculated by Equation 1.

$$\theta ij = \frac{1}{i}\sum_{i=1}^{i}\theta i \quad (1)$$

where I is the number of measured strata at site j and θ_{ij} is the soil moisture content of stratum i calculated from three randomly

10.3389/fpls.2025.1668310

TABLE 1 Topographic and vegetation characteristics of monitoring plots in the Artificial forest watershed.

Land use	Vegetation type	Slope position	Elevation (m)	Slope gradient (°)	Slope aspect (°)	Sample no.
Vegetated restoration land	RP	Upper Slope	1210.13	20.24	102.53	1
		Lower Slope	1072.56	10.27	186.34	3
		Middle Slope	1126.41	25.10	253.89	4
		Middle Slope	1126.09	25.10	253.89	5
		Upper Slope	1128.54	16.61	193.57	6
		Middle Slope	1197.23	27.75	81.25	7
		Lower Slope	1121.94	36.03	161.57	8
		Lower Slope	1113.4	27.54	85.60	9
		Middle Slope	1063.21	14.62	302.47	10
		Middle Slope	1066.33	14.37	218.66	12
		Lower Slope	1107.65	29.10	72.22	14
		Lower Slope	1064.76	25.57	206.03	15
		Upper Slope	1067.77	29.50	261.87	16
		Middle Slope	1035.26	10.77	86.99	22
		Lower Slope	1072.49	28.88	22.38	26
		Middle Slope	1034.67	21.41	289.36	27
		Lower Slope	1049.71	23.41	263.37	29
		Lower Slope	1054.66	22.49	37.15	30
		Middle Slope	1020.12	27.38	169.99	31
	PT	Middle Slope	1119.27	29.39	96.12	2
		Middle Slope	1152.38	21.22	281.89	13
		Middle Slope	1097.54	16.70	216.87	25
	RX	Lower Slope	1135.44	19.00	334.18	11
		Lower Slope	1148.94	16.70	216.87	17
		Lower Slope	1063.34	20.16	60.64	18
		Middle Slope	1167.21	17.87	97.13	20
		Lower Slope	1098.18	16.56	222.27	23
		Middle Slope	1069.03	16.40	99.78	28
		Middle Slope	1068.11	18.99	305.54	32
		Middle Slope	1037.76	29.63	79.88	33
Native grassland	FE	Lower Slope	1094.72	31.53	19.03	21
		Middle Slope	1047.9	9.66	139.76	24
		Lower Slope	994.43	29.62	230.71	34
Farmland	ZM	Upper Slope	1110.06	23.31	248.20	19

FE, native grassland (*Festuca elata*); RP, PT, and RX, vegetated restoration land (*Robinia pseudoacacia*, *Pinus tabuliformis*, and *Rosa xanthina*, respectively); ZM, farmland (*Zea mays*).

10.3389/fpls.2025.1668310

TABLE 2 Topographic and vegetation characteristics of monitoring plots in the Farmland watershed.

Land use	Vegetation type	Slope position	Elevation (m)	Slope gradient (°)	Slope aspect (°)	Sample no.
Farmland	ZM	Lower Slope	917.13	7.97	278.97	1
		Lower Slope	955.02	14.20	71.57	2
		Lower Slope	961.23	17.87	299.75	5
		Lower Slope	950.96	5.11	206.57	8
		Middle Slope	1033.14	24.36	276.34	10
		Middle Slope	969.19	23.94	262.24	13
		Upper Slope	1006.23	4.85	45.00	15
		Upper Slope	1082.56	5.88	330.95	21
Economic forestland	MD	Middle Slope	984.77	30.74	70.35	6
		Middle Slope	1002.1	11.31	306.87	7
		Upper Slope	1081.54	30.22	254.06	18
		Upper Slope	1029.43	19.69	26.57	19
		Upper Slope	1030.55	19.53	338.50	20
		Upper Slope	1083.78	8.66	246.80	22
Vegetated restoration land	RP	Middle Slope	993.36	5.42	288.43	3
		Middle Slope	975.31	24.19	253.18	4
		Middle Slope	983.09	20.24	192.53	9
	RX	Lower Slope	982.83	13.52	196.93	11
		Middle Slope	995.27	28.29	318.01	12
		Upper Slope	1075.48	16.61	283.57	14
		Middle Slope	1006.59	33.10	302.47	16
		Middle Slope	1004.05	13.61	51.71	17

ZM, farmland (*Zea mays*); MD, economic forestland (*Malus domestica*); RP and RX, vegetated restoration land (*Robinia pseudoacacia* and *Rosa xanthina*, respectively).

sampled profiles. In the following analysis, gravimetric soil moisture content is calculated on a per-100-centimeter basis, with $I = 5$.

The depth-averaged gravimetric soil moisture content θ_m (g/g) for each land use type was calculated by Equation 2.

$$\theta m = \frac{1}{k}\sum_{k=1}^{k}\theta ij \tag{2}$$

where k is the number of experimental sites for each land use type.

The depth-averaged volumetric soil moisture content θ_v (%) for each land use type was calculated by Equation 3.

$$\theta v = \theta mi \times \rho bi \tag{3}$$

where ρb_i is the average soil bulk density of layer i for each land use type.

The soil moisture content depletion degree (SMCD) (%) was calculated by Equation 4.

$$SMCD = \frac{1}{k}\sum_{k=1}^{k}\frac{\theta vl - \theta vc}{\theta vl} \tag{4}$$

where θ_{vl} represents the volumetric soil moisture content of the layer i of farmland (*Zea mays*, ZM), and θ_{vc} represents the volumetric soil moisture content of the layer i under different vegetation types.

This study utilized the Inverse Distance Weighting (IDW) method within ArcGIS 10.3 to interpolate and analyze the spatial distribution of soil moisture in the Artificial Forest Watershed and the Farmland Watershed (Gao and Yang, 2023). Spatial distribution maps of soil moisture were generated using this method. IDW estimates the values of unsampled locations through a linear weighting of known sample sites, where the weights are inversely proportional to the distance between the sample and the target sites. The IDW method was calculated by Equation 5.

$$\hat{Z}(u) = \frac{\sum_{i=1}^{n}\frac{Zi}{d(u,ui)^P}}{\sum_{i=1}^{n}\frac{1}{d(u,ui)^P}} \tag{5}$$

where $\hat{Z}(u)$ is the estimated value at the unknown site u; Zi is the observed value at the known site u_i; $d(u,u_i)$ represents the

distance between the unknown site u and the known site u_i; and P is the power parameter that controls the influence of distance on the weighting (Pal and Maity, 2021).

Basic descriptive statistics, including the mean, standard deviation (SD), and coefficient of variation (CV), were calculated for each measurement. Prior to conducting the paired t-test and one-way analysis of variance (ANOVA), the Shapiro–Wilk test was applied to assess the normality of the data. Variables that did not meet the normality assumption were log-transformed before statistical analysis. A paired t-test was utilized to examine the differences in soil moisture across soil layers between the two watersheds. To assess the impact of various land use types on the overall variability of soil moisture, a one-way analysis of variance (ANOVA) was conducted. *Post hoc* multiple comparisons were executed using the Least Significant Difference (LSD) method. Microsoft Excel was employed for preliminary data organization, whereas SPSS and Origin were used for advanced statistical analysis and data visualization.

3 Results

3.1 Vertical soil moisture variation

As shown in Figure 2, a significant difference has occurred in soil moisture content between the two watersheds ($p < 0.05$). Soil moisture in the Artificial forest watershed ranged from 0.038 to 0.082 g/g, whereas in the Farmland watershed, it ranged from 0.082 to 0.130 g/g, the overall soil moisture content in the Farmland watershed is higher than that in the Artificial forest watershed. In terms of vertical distribution, the average soil moisture content in the Artificial forest watershed gradually increased with soil depth before stabilizing, whereas in the Farmland watershed, it originally decreased, then increased, and eventually stabilized. The standard deviation of soil moisture in the Farmland watershed was greater than in the Artificial forest watershed.

As shown in Figure 3, there was a significant difference ($p < 0.05$) in the average soil moisture content across different soil layers between the Artificial forest watershed and the Farmland watershed. Specifically, in the 0–100 cm soil layer, the average soil moisture content in the Farmland watershed was 0.105 g/g, which was 72.13% higher than in the Artificial forest watershed (0.061 g/g). In the 100–200 cm soil layer, soil moisture in the Farmland watershed was 0.085 g/g, 16.44% higher than in the Artificial forest watershed (0.073 g/g). In the 200–300 cm soil layer, the Farmland watershed recorded 0.092 g/g, 24.32% higher than the Artificial forest watershed (0.074 g/g). In the 300–400 cm soil layer, the moisture content in the Farmland watershed was 0.096 g/g, 29.73% higher than in the Artificial forest watershed (0.074 g/g). In the 400–500 cm soil layer, it was 0.094 g/g in the Farmland watershed, 20.51% higher than in the Artificial forest watershed (0.078 g/g). Overall, the average soil moisture content in the 0–500 cm layer in the Farmland watershed was 0.096 g/g, representing a 37.14% increase compared to the Artificial forest watershed (0.070 g/g).

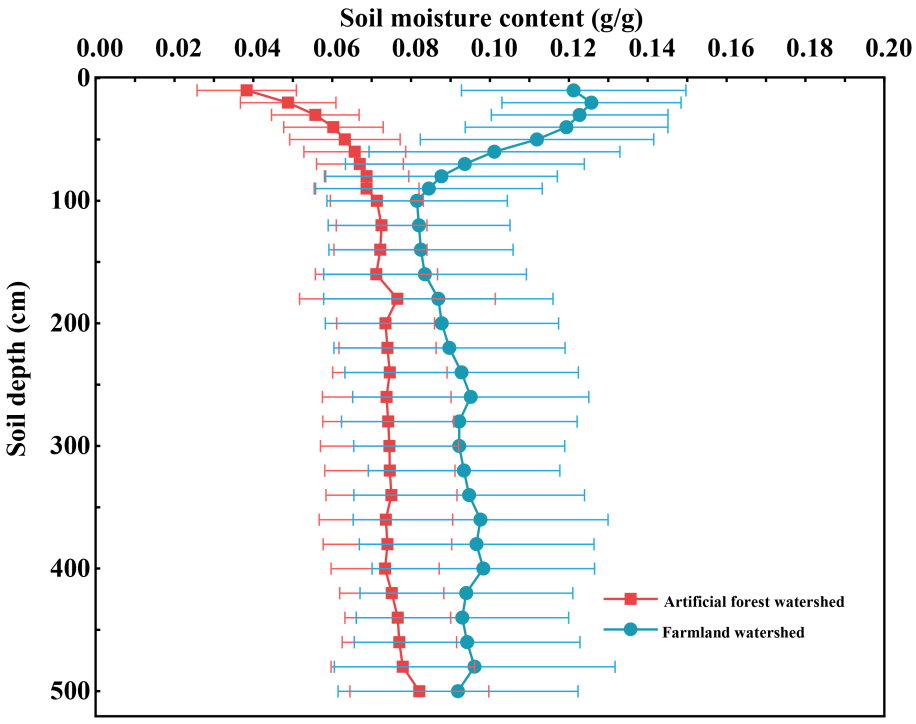

FIGURE 2
Profile distribution of the mean soil moisture content in two watersheds, the error bars indicate standard deviation.

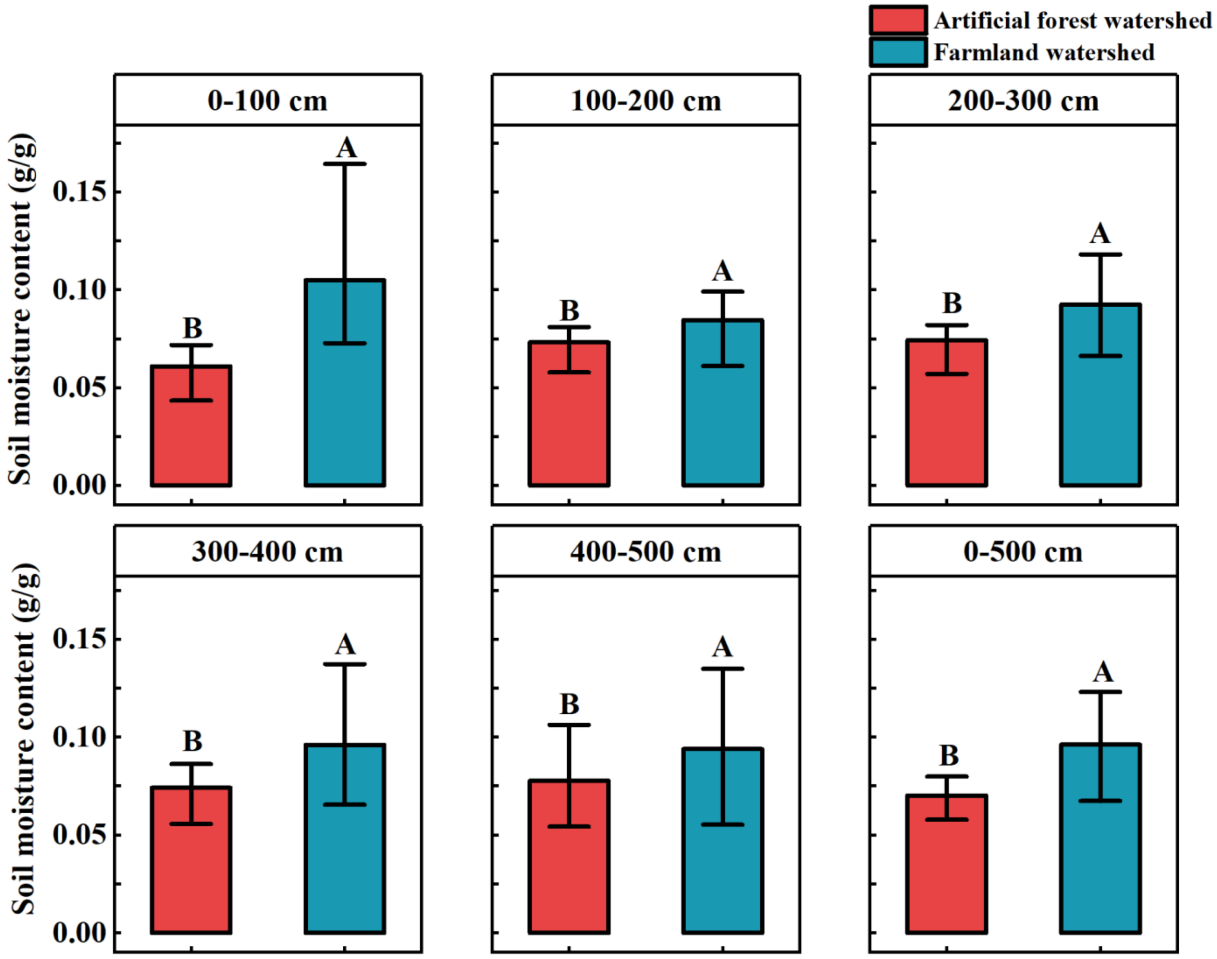

FIGURE 3
Comparison of soil moisture content of different soil layers in two watersheds, error bars indicate standard deviation, different uppercase letters above the bars indicate significant differences in soil moisture content between the two watersheds.

3.2 Soil moisture of different land use types in paired watersheds

In the two watersheds, soil moisture content was highest in farmland (ZM), followed by native grassland (FE), and lower in the vegetated restoration land (RP, PT, RX), and economic forestland (MD) (Figure 4; Table 3). After the LSD test (Table 3), the differences in soil moisture between different vegetation types in the same watershed were statistically significant ($p < 0.05$).

In the Artificial forest watershed, there was no significant difference in mean soil moisture content among RP, PT, and RX in the vegetated restoration land ($p > 0.05$), in the 0–200 cm soil layer, the mean soil moisture content was significantly higher in native grassland (FE) than in the vegetated restoration land (RP, PT, RX) and farmland (ZM) ($p < 0.05$), and in the 200–500 cm soil layer, the mean soil moisture content was significantly higher in both native grassland (FE) and farmland (ZM) than in the vegetated restoration land (RP, PT, RX) ($p < 0.05$). In the Artificial forest watershed, the average soil moisture content in the 0–500 cm soil layer of different vegetation types, in descending order, was farmland (ZM) (0.099 g/g), native grassland (FE) (0.091 g/g), vegetated restoration land (RX) (0.071 g/g), vegetated restoration land (PT) (0.070 g/g), and vegetated restoration land (RP) (0.068 g/g), with farmland (ZM) and native grassland (FE) all having significantly higher soil moisture content than vegetated restoration land (RP, PT, RX).

In contrast, in the 0–100 cm soil layer of Farmland watershed, the mean soil moisture content was significantly higher ($p < 0.05$) in farmland (ZM) and vegetated restoration land (RP) than in vegetated restoration land (RX) and economic forestland (MD), with no significant differences detected between economic forestland (MD)-vegetated restoration land (RP) pair and vegetated restoration land (RX)-economic forestland (MD) pair ($p > 0.05$), and in the 100–500 cm soil layer, the mean soil moisture content was significantly higher ($p < 0.05$) in farmland (ZM) than in vegetated restoration land (RP, RX), and economic forestland (MD). No significant differences have occurred in vegetated restoration land (RP), and statistical analysis revealed no detectable differences ($p > 0.05$) between the soil moisture of vegetated restoration land (RX) and economic forestland (MD).

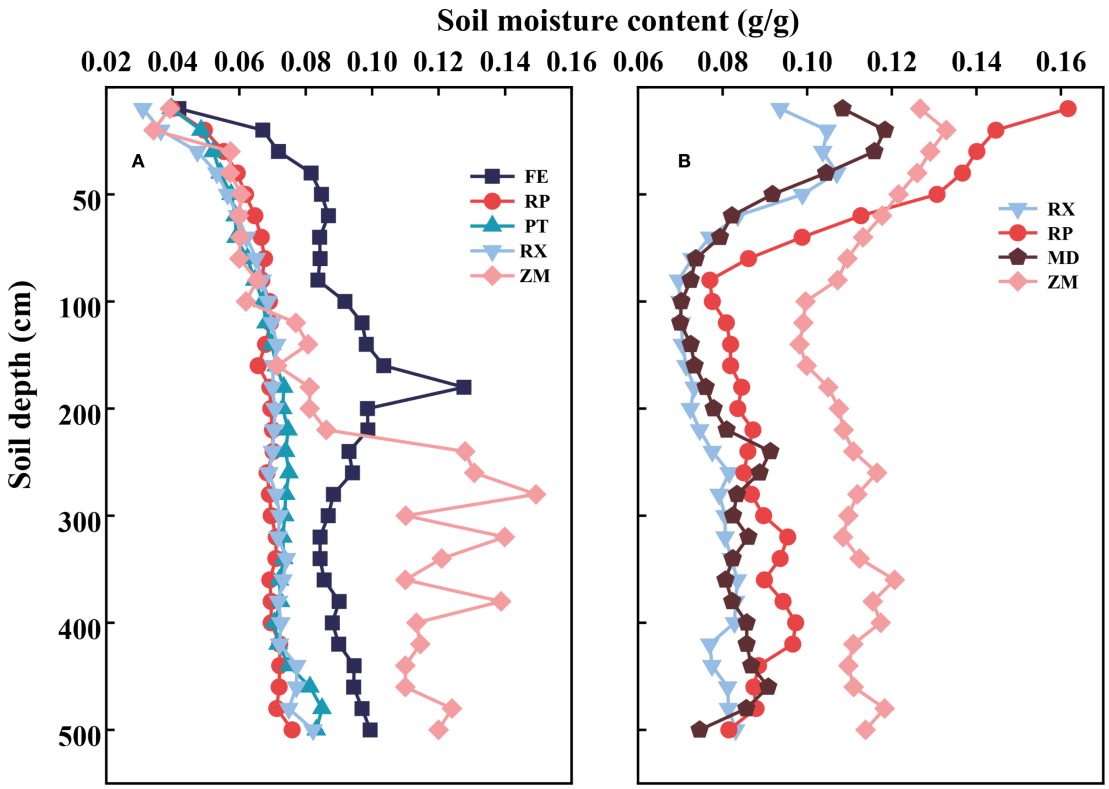

FIGURE 4
Soil moisture in different land use types in two watersheds **(A)** Artificial forest watershed and **(B)** Farmland watershed. FE, native grassland (*Festuca elata*); RP, PT, and RX, vegetated restoration land (*Robinia pseudoacacia*, *Pinus tabuliformis*, and *Rosa xanthina*, respectively); ZM, farmland (*Zea mays*); MD, economic forestland (*Malus domestica*).

In the Farmland watershed, across the 0–500 cm profile, farmland (ZM) (0.120 g/g) maintained the highest average soil moisture content, followed in decreasing order by vegetated restoration land (RP) (0.094 g/g), economic forestland (MD) (0.084 g/g), and vegetated restoration land (RX) (0.080 g/g), in which the average soil moisture content of farmland (ZM) was significantly higher than vegetated restoration land (RP) ($p < 0.05$), the average soil moisture content of vegetated restoration land (RP) were significantly higher than vegetated restoration land (RX) and economic forestland (MD) ($p < 0.05$), and there was no significant difference between vegetated restoration land (RX) and economic forestland (MD) ($p > 0.05$).

3.3 Soil moisture depletion of different land use types in paired watersheds

Compared to farmland (ZM), both Artificial forest watershed and Farmland watershed exhibited varying degrees of soil moisture deficit (SMCD), with the deficit being more severe in Artificial forest watershed (Figure 5, Table 4).

Within the Artificial forest watershed, significant differences in SMCD were observed across soil layers for the same vegetation type. In native grassland (FE), the 0–100 cm and 100–200 cm layers showed no moisture deficit, while the 200–300 cm, 300–400 cm, and 400–500 cm layers exhibited deficits of 26.68%, 36.23%, and 25.10%, respectively. Similarly, no deficit was found in the 0–100 cm layer of vegetated restoration land (RP), but the 100–200 cm, 200–300 cm, 300–400 cm, and 400–500 cm layers showed SMCDs of 17.74%, 45.16%, 47.75%, and 42.03%, respectively. SMCD values were significantly higher in the 200–500 cm layers than in the 100–200 cm layer. For vegetated restoration land (PT and RX), all soil layers exhibited moisture deficits. In vegetated restoration land (PT), SMCD values reached 42.33% in the 200–300 cm, 300–400 cm, and 400–500 cm layers, which were significantly higher than the values in the 0–100 cm (6.60%) and 100–200 cm (17.79%) layers. Similarly, vegetated restoration land (RX) showed SMCDs of 43.48%, 44.92%, and 37.89% in the 200–300 cm, 300–400 cm, and 400–500 cm layers, all significantly higher than those in the 0–100 cm (9.95%) and 100–200 cm (13.77%) layers. Additionally, SMCD varied significantly among different vegetation types within the same soil layer. The vegetated restoration land (RP, PT, RX) exhibited significantly higher SMCD values than native grassland (FE) across all layers from 0–500 cm.

Within the Farmland watershed, the soil moisture content difference (SMCD) of vegetated restoration land (RX) and economic forestland (MD) did not differ significantly among soil layers. Vegetated restoration land (RP) did not experience water deficit in the 0–100 cm soil layer; however, soil moisture depletion was observed in the 100–200 cm, 200–300 cm, 300–400 cm, and

10.3389/fpls.2025.1668310

TABLE 3 Soil moisture (g/g) of 0–500 cm soil layers in different land use types.

Land use	Soil depth (cm)	Native grassland	Vegetated restoration land			Farmland	Economic forestland
		FE	RP	PT	RX	ZM	MD
Artificial forest watershed	0–100	0.078 ± 0.016a	0.060 ± 0.010b	0.056 ± 0.009b	0.055 ± 0.014b	0.056 ± 0.011b	
	100–200	0.105 ± 0.018a	0.068 ± 0.046b	0.071 ± 0.003b	0.071 ± 0.003b	0.078 ± 0.004b	
	200–300	0.092 ± 0.005a	0.070 ± 0.005b	0.073 ± 0.001b	0.079 ± 0.006b	0.121 ± 0.024a	
	300–400	0.087 ± 0.005a	0.070 ± 0.005b	0.072 ± 0.003b	0.077 ± 0.005b	0.125 ± 0.014a	
	400–500	0.095 ± 0.006a	0.073 ± 0.004b	0.079 ± 0.006b	0.071 ± 0.013b	0.116 ± 0.006a	
	0–500	0.091 ± 0.021a	0.068 ± 0.010b	0.070 ± 0.012b	0.071 ± 0.013b	0.099 ± 0.038a	
Farmland watershed	0–100		0.117 ± 0.015a		0.088 ± 0.015b	0.118 ± 0.030a	0.092 ± 0.019b
	100–200		0.083 ± 0.010b		0.072 ± 0.010b	0.102 ± 0.036a	0.074 ± 0.009b
	200–300		0.087 ± 0.017b		0.079 ± 0.011b	0.112 ± 0.041a	0.085 ± 0.007b
	300–400		0.094 ± 0.014b		0.082 ± 0.015b	0.115 ± 0.039a	0.083 ± 0.010b
	400–500		0.088 ± 0.017b		0.080 ± 0.025b	0.113 ± 0.036a	0.085 ± 0.013b
	0–500		0.094 ± 0.021b		0.080 ± 0.012c	0.120 ± 0.017a	0.084 ± 0.014c

Different lowercase letters indicate significant differences among land use types within the same soil layer ($p < 0.05$). FE, native grassland (*Festuca elata*); RP, PT, and RX, vegetated restoration land (*Robinia pseudoacacia*, *Pinus tabuliformis*, and *Rosa xanthina*, respectively); ZM, farmland (*Zea mays*); MD, economic forestland (*Malus domestica*).

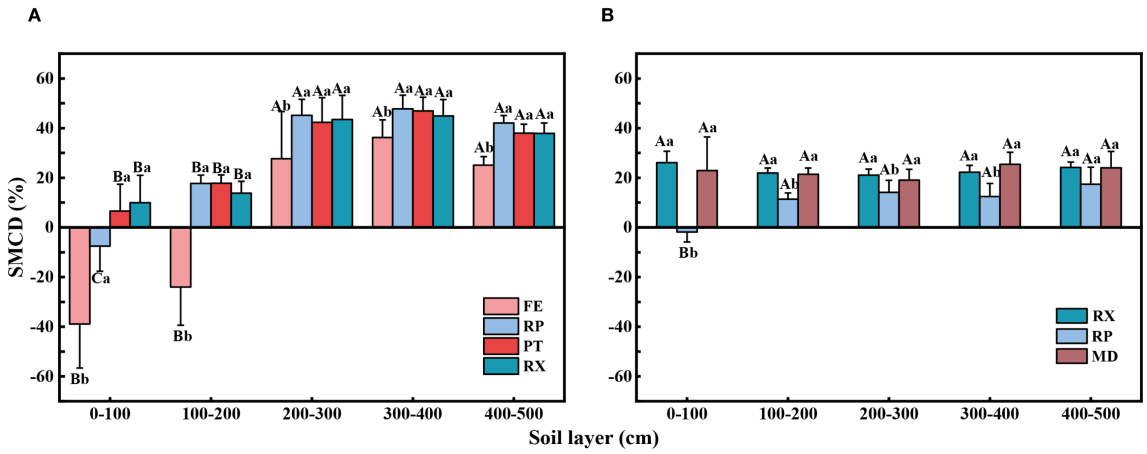

FIGURE 5
Variations in soil moisture depletion degree (SMCD) across soil layers under different land use types in two watersheds: **(A)** Artificial forest watershed and **(B)** Farmland watershed. Different lowercase and uppercase letters above the bars indicate significant differences between different land uses at the same soil depth and between the same land use at different soil depths ($p < 0.05$). FE, native grassland (*Festuca elata*); RP, PT, and RX, vegetated restoration land (*Robinia pseudoacacia*, *Pinus tabuliformis*, and *Rosa xanthina*, respectively); MD, economic forestland (*Malus domestica*).

400–500 cm layers, with SMCDs of 11.35%, 14.11%, 12.48%, and 17.39%, respectively. In addition, significant differences in SMCD were observed among different vegetation types within the same soil layer, with vegetated restoration land (RX) and economic forestland (MD) exhibiting significantly higher SMCD values than vegetated restoration land (RP) across all soil layers from 0–500 cm.

3.4 Spatial distribution of soil moisture in different depths

Figure 6 was generated with the Inverse Distance Weighting (IDW) method to characterize the spatial distribution of soil moisture in the Artificial forest watershed and the Farmland watershed. The results indicate that soil moisture distribution was closely associated with land use type, with relatively higher soil moisture in farmland (ZM) and native grassland (FE), and lower moisture levels at vegetated restoration land (RP, PT, RX). In the Farmland watershed, soil moisture showed a spatial pattern of high values in the northwest and low values in the southeast, while the Artificial forest watershed exhibited the opposite trend-lower values in the northwest and higher values in the southeast. The maximum mean soil moisture content in the 0–500 cm layer of the Artificial forest watershed occurred in native grassland (FE) (0.101 g/g at site 24), while the minimum occurred in vegetated restoration land (RP) (0.0526 g/g at site 6). In the Farmland watershed, the highest mean soil moisture was observed in farmland (ZM) (0.170 g/g at site 5), and the lowest in vegetated restoration land (RX) (0.067 g/g at site 14).

Table 5 presents the statistics of soil moisture content across different soil layers in the two watersheds. In the 0–500 cm depth range, the coefficient of variation in the Artificial forest watershed ranges from 19.98% to 25.72%, with a standard deviation of 0.013–0.017. In the Farmland watershed, the coefficient of variation ranges from 29.95% to 31.29%, and the standard deviation ranges from 0.026 to 0.031. Both the coefficient of variation and standard deviation in the Farmland watershed are higher than those in the Artificial forest watershed.

4 Discussion

4.1 Vertical distribution characteristics of soil moisture

The monitoring of deep soil moisture revealed that there were significant differences in soil moisture content between the paired watersheds (Figure 2). The Farmland watershed exhibited a markedly higher average soil moisture compared to the Artificial forest watershed. This phenomenon is consistent with the findings of Jia et al. (2017) and Liu et al. (2018), both of which indicated that, in typical vegetated restoration areas of the Loess Plateau, prolonged high-density afforestation has resulted in sustained depletion of deep soil moisture. The dynamics of soil moisture are directly influenced by precipitation, topography, and vegetation. Among these factors, precipitation constitutes a critical constraint on vegetated restoration and reconstruction in the Loess Plateau and represents one of the principal sources of soil moisture (Hou et al., 2018; Jin et al., 2018). In this study, the selected paired watersheds are adjacent to each other, with similar elevation and spatial precipitation distribution. Additionally, the Loess Plateau is characterized by deep soil layers, and soil moisture below the infiltration depth in restored vegetation areas remains relatively stable with minimal interannual fluctuations (Yang et al., 2012).

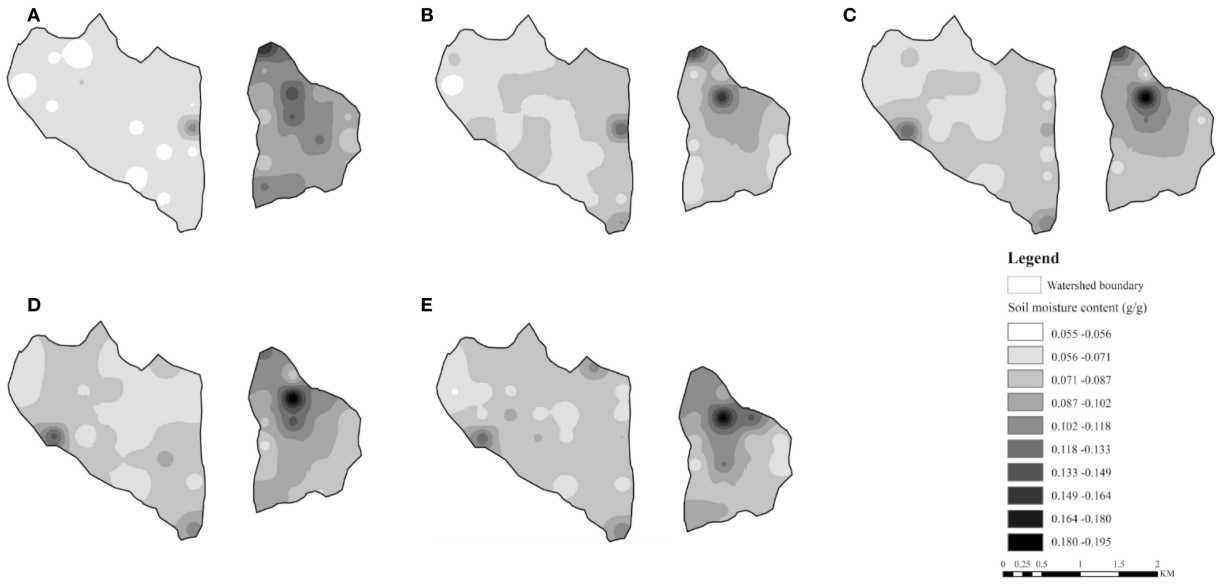

FIGURE 6
Soil moisture content interpolated by the IDW method in different soil depths. **(A)** 0–100 cm, **(B)** 100–200 cm, **(C)** 200–300 cm, **(D)** 300–400 cm, and **(E)** 400–500 cm.

TABLE 4 Soil moisture depletion degree (SMCD) of the 0–500 cm soil layers.

Land use	Soil depth (cm)	Native grassland	Vegetated restoration land			Economic forestland
		FE	RP	PT	RX	MD
Artificial forest watershed	0–500	5.22 ± 14.15b	29.03 ± 23.68a	30.32 ± 17.31a	30.00 ± 8.30a	
Farmland watershed	0–500		10.69 ± 7.38b		23.10 ± 2.01a	22.57 ± 2.46a

Different lowercase letters indicate significant differences among land use types within the same watershed ($p < 0.05$). FE, native grassland (*Festuca elata*); RP, PT, and RX, vegetated restoration land (*Robinia pseudoacacia*, *Pinus tabuliformis*, and *Rosa xanthina*, respectively); MD, economic forestland (*Malus domestica*).

Although the analysis in this study is based on monitoring data from a single growing season, short-term climatic variations have limited effects on deep soil moisture. Therefore, the primary factor responsible for the observed differences in deep soil moisture between the paired watersheds is likely the influence of vegetation roots under long-term restoration. The introduced vegetation in the Artificial forest watershed has developed extensive root systems, which, under identical rainfall conditions, exert a greater influence on soil moisture content compared to farmland and grassland (Wyatt et al., 2021). Moreover, the vegetation density in the Artificial forest watershed considerably exceeds the carrying capacity of natural precipitation, and rainfall is insufficient to meet the growth and development demands of such biomass-rich artificial plantations, thereby leading to excessive depletion of soil moisture (Jin et al., 2018). In contrast, the Farmland watershed is mainly cultivated with shallow-rooted annual crops such as ZM, which primarily consume surface soil moisture, allowing deeper moisture to be conserved.

By comparing soil moisture content across different soil depths in the two watersheds (Figure 3), it was found that the soil moisture content of the 0–100 cm layer in the Farmland watershed was 0.105 g/g, which was significantly higher than that in the Artificial forest watershed (0.061 g/g), representing a difference of 72.13%. In the 100–500 cm soil layer, however, the difference in soil moisture content narrowed to 16.44%, 24.32%, 29.73%, and 20.51%. This could be attributed to the fact that the lateral roots of the introduced vegetation species (RP, PT, RX) in the Artificial forest watershed are mainly distributed within the 0–100 cm layer, where considerable amounts of soil moisture are consumed during the growing season to sustain plant development (Cui et al., 2023; Zhou et al., 2022). Additionally, precipitation predominantly affects shallow soil moisture. Due to extensive vegetation cover in the Artificial forest watershed, canopy interception reduces surface infiltration, resulting in lower soil moisture content (O'Donnell et al., 2021; Wu et al., 2021). In the Farmland watershed, long-term cultivation practices have left crop residues and surface organic matter that help reduce bare soil exposure and minimize evaporation losses of surface soil moisture (Tuure et al., 2021). Furthermore, continuous tillage has altered the soil structure, promoted infiltration, and consequently increased soil moisture content in the 0–100 cm layer (Wang et al., 2017). The deep soil moisture content in the Artificial forest watershed remained lower than in the Farmland watershed. This may be because, under long-term vegetation restoration, plants tend to develop deeper roots to access moisture when the upper soil layers experience water stress, thereby depleting deep soil moisture and forming a dried soil layer (Tijdeman and Menzel, 2021; Wang et al., 2024).

In addition to root distribution and vegetation density, species-specific water use characteristics further elucidate the observed contrasts in deep soil moisture. Sap flow and eddy covariance studies in the Loess Plateau have shown that *Robinia pseudoacacia* (RP) exhibits annual evapotranspiration levels of approximately 480–550 mm·yr^{-1}. Due to its deep root system and high canopy transpiration demand, the overall water consumption of RP often exceeds the mean annual precipitation (Wu et al., 2021). By contrast, Zea mays (ZM) generally has an annual evapotranspiration of 350–450 mm·yr^{-1}, which is more closely aligned with regional precipitation inputs (Liu et al., 2010). This

TABLE 5 Basic statistics on soil moisture content (g/g) in two watersheds based on IDW.

Soil depth (cm)	Artificial forest watershed					Farmland watershed				
	Min g/g	Max g/g	Mean g/g	SD	CV (%)	Min g/g	Max g/g	Mean g/g	SD	CV (%)
0–100	0.043	0.109	0.061	0.013	25.72	0.073	0.164	0.105	0.031	29.95
100–200	0.045	0.132	0.073	0.016	21.74	0.061	0.161	0.085	0.026	30.66
200–300	0.057	0.131	0.074	0.015	20.71	0.066	0.191	0.092	0.029	30.99
300–400	0.056	0.136	0.074	0.016	21.41	0.065	0.192	0.096	0.028	29.55
400–500	0.054	0.126	0.078	0.016	19.98	0.055	0.185	0.094	0.029	31.29
0–500	0.053	0.101	0.070	0.017	24.29	0.067	0.171	0.096	0.030	31.25

SD, standard deviation; CV, coefficient of variation.

indicates that ZM primarily relies on seasonal rainfall, whereas RP continuously depletes deep soil moisture. These interspecific differences in water use efficiency further demonstrate the importance of considering evapotranspiration demand when selecting restoration species in water-limited regions such as the Loess Plateau.

4.2 Mechanisms driving the spatial variability of deep soil moisture

This study found that the spatial heterogeneity of soil moisture in the Farmland watershed was considerably higher than that in the Artificial forest watershed (Figure 6). Across the 0–500 cm profile, the coefficient of variation in the Farmland watershed reached 31.25%, exceeding the 24.29% observed in the Artificial forest watershed. In all soil layers, the coefficient of variation in the Farmland watershed was consistently higher, which aligns with the findings of Yang et al. (2014), who reported that the distribution of soil moisture in the Farmland watersheds is more complex compared to the Artificial forest watersheds. The primary reason for this difference lies in the contrasting land use structures between the two watersheds. The Artificial forest watershed has undergone long-term vegetation restoration, resulting in a predominantly monocultural vegetation pattern dominated by artificial forest, which leads to relatively uniform soil moisture distribution. By contrast, the Farmland watershed comprises a mosaic of farmland, economic forest, and shrubland, thereby increasing the spatial variability of soil moisture distribution. The significant differences in deep soil moisture between the two watersheds indicate that complex land use structures are associated with higher spatial heterogeneity of deep soil moisture, whereas large-scale vegetation restoration tends to enhance the spatial homogeneity of deep soil moisture.

In addition, soil and water conservation projects also play a crucial role in shaping the spatial pattern of deep soil moisture. Among the 22 experimental sites in the Farmland watershed, sites 1, 5, 8, and 13 exhibited substantially higher soil moisture than other sites. This is likely because these sites were located within check dams, which are typical soil and water conservation measures in the Farmland watersheds. Check dams promote water infiltration, reduce surface runoff, and control soil erosion, thereby contributing to increased soil moisture (Helman and Mussery, 2020; Luan et al., 2022).In the Artificial forest watershed, the highest soil moisture in the 0–200 cm layer was observed at site 24, possibly because this site was situated in native grassland (FE). FE has shallow root systems, resulting in less uptake of deep soil moisture (Ye et al., 2019). Additionally, the canopy height and biomass of FE are relatively low, leading to lower canopy interception and evaporation compared to other vegetation types. As a result, a greater proportion of precipitation infiltrates into the soil, maintaining higher soil moisture content (Jian et al., 2015). In the 200–500 cm layer, the highest soil moisture was recorded at sites 19 and 34. This may be attributed to site 19 being located in farmland (ZM), where tillage practices modify the structure of surface soil aggregates, increase soil porosity, and facilitate infiltration of rainfall, thereby accelerating the percolation of moisture into deeper soil layers. Site 34 was located at the outlet of the watershed, in a relatively low-lying terrain position. Under identical precipitation or snowmelt input conditions, water tends to accumulate along the slope and infiltrate into deep soil layers, forming a moisture convergence zone and resulting in higher deep soil moisture content (Chang et al., 2024).

4.3 Implications for vegetation restoration

In the Loess Plateau region, deep soil moisture plays a critical role in sustaining the growth and ecological functions of artificial vegetation (Figure 4). This study demonstrated that, in the Artificial forest watershed, soil moisture content across all soil layers under vegetated restoration land (RP, PT, RX) was significantly lower compared to farmland (ZM) and native grassland (FE). Specifically, the average soil moisture content (0–500 cm) in the Artificial forest watershed was significantly higher in ZM (0.099 g/g) and FE (0.091 g/g) than in RP (0.068 g/g), PT (0.070 g/g), and RX (0.071 g/g). A similar pattern was observed in the Farmland watershed, where the difference in moisture content between vegetated restoration land and farmland was also significant. In the Farmland watershed, farmland (ZM) showed the highest average moisture content in the 0–500 cm soil layer (0.120 g/g), significantly higher than RP (0.094 g/g), MD (0.080 g/g), and RX (0.080 g/g). This difference may be attributed to the annual crop (ZM), which has a shallow root system and short life cycle, consuming mainly surface soil moisture and thus conserving deeper soil moisture (Shen et al., 2014; Xiao et al., 2014). Native grassland (FE), despite having year-round coverage, also possesses relatively shallow roots that consume less deep-layer moisture, thus maintaining higher deep soil moisture levels (Zhang et al., 2024). In contrast, vegetated restoration sites (RP, PT, RX) have deeper root systems and, over prolonged restoration periods, continuously consume deep soil moisture through transpiration, resulting in a lower soil moisture content (Liu et al., 2024a).

The difference in soil moisture content between vegetated restoration sites and farmland can represent the extent of soil moisture depletion caused by vegetation restoration. Results from this study (Figure 5) indicate that the soil moisture deficit at vegetated restoration sites (RP, PT, and RX) was significantly greater than that of native grassland (FE) within the 0–500 cm soil layer in the Artificial forest watershed. Specifically, in terms of soil depth, the soil moisture content deficit (SMCD) for RP, PT, and RX in the 0–100 cm soil layer was −7.52%, 6.60%, and 9.90%, respectively, while the most severe water depletion occurred in the 300–400 cm soil layer, with deficits of 47.75%, 46.94%, and 44.90%, respectively. This pattern demonstrates that artificial vegetation significantly depleted deep soil moisture reserves, with a more pronounced depletion effect in deeper soil layers, leading to the formation of a deep, dry soil layer that gradually restricts forest growth (Zhang et al., 2018). In contrast, soil moisture depletion by artificial vegetation in the Farmland watershed did not reach such extreme levels. In the Farmland watershed, RP did not exhibit a soil moisture deficit in the 0–100 cm layer, and deeper layers showed only moderate deficits ranging from 11.35% to 17.39%. This

moderate deficit may result from the smaller scale and lower density of the RP in the Farmland watershed compared to the Artificial forest watershed, resulting in relatively lower deep soil moisture consumption (Liu et al., 2024b; Zhang et al., 2018). These findings suggest that large-scale vegetation restoration, particularly with deep-rooted species, significantly reduces deep soil moisture content, and that the depletion mechanism is closely related to the water-use characteristics of vegetation. This interpretation is consistent with Zhou et al. (2024), who emphasized that vegetation type exerts a strong influence on deep soil moisture dynamics, with deep-rooted broadleaf species contributing more to deep soil drying, whereas shallow-rooted vegetation maintains a more balanced soil moisture regime. The scarcity of deep soil moisture therefore poses a critical challenge to the sustainability of afforestation and vegetation restoration efforts in water-limited regions. Consequently, it is advisable to avoid large-scale afforestation with deep-rooted monocultures, as this practice may expedite the development of deep dry soil layers. The density of afforestation efforts should be optimized based on rigorous scientific analysis of local hydrological conditions. For existing plantations, adaptive management strategies—such as thinning to decrease stand density or replacing species—should be implemented to mitigate deep soil moisture deficits and promote the long-term sustainability of vegetation restoration efforts.

5 Conclusions

This study has systematically analyzed the vertical distribution characteristics and spatial variability of soil moisture (0–500 cm) in typical paired watersheds (Farmland watershed and Artificial forest watershed) within the Caijiachuan watershed in the hilly-gully region of the Loess Plateau in western Shanxi Province. The results demonstrated that long-term vegetation restoration substantially reduced deep soil moisture reserves. The mean soil moisture content in the Artificial forest watershed (0.070 g/g) was significantly lower than that in the Farmland watershed (0.096 g/g), indicating that artificially introduced deep-rooted vegetation markedly intensified soil moisture deficits in the 200–500 cm layers. Farmland and native grassland exhibited stronger capacities for maintaining deep soil moisture, whereas vegetation restoration sites consistently showed pronounced deep moisture depletion. In addition, the spatial heterogeneity of deep soil moisture was significantly higher in the Farmland watershed, while long-term afforestation promoted a more homogeneous spatial distribution of soil moisture content. Overall, the findings indicate that large-scale vegetation restoration dominated by deep-rooted species can lead to substantial deep soil desiccation, posing potential risks to vegetation sustainability and regional water balance. Therefore, future land-use planning and vegetation restoration efforts in the Loess hilly-gully watershed should carefully balance the trade-offs between ecological restoration and soil moisture availability, scientifically select and arrange appropriate vegetation types, and implement adaptive management strategies to ensure the long-term sustainability of ecosystem functions.

Data availability statement

The raw data supporting the conclusions of this article will be made available by the authors, without undue reservation.

Author contributions

HZ: Data curation, Validation, Visualization, Writing – original draft, Writing – review & editing. YY: Conceptualization, Investigation, Methodology, Supervision, Writing – original draft, Writing – review & editing. ZW: Resources, Validation, Visualization, Investigation, Software, Writing – review & editing. JZ: Investigation, Resources, Visualization, Writing – review & editing. JL: Investigation, Methodology, Writing – review & editing. SQ: Data curation, Investigation, Writing – review & editing. LW: Investigation, Resources, Writing – review & editing. MC: Supervision, Writing – review & editing.

Funding

The author(s) declare financial support was received for the research and/or publication of this article. This study was supported by the National Key Research and Development Program of China (No. 2023YFF1305101), the National Natural Science Foundation of China (42177310), and the Fundamental Research Funds for the Central Universities (QNTD202508).

Conflict of interest

The authors declare that the research was conducted in the absence of any commercial or financial relationships that could be construed as a potential conflict of interest.

Generative AI statement

The author(s) declare that no Generative AI was used in the creation of this manuscript.

Any alternative text (alt text) provided alongside figures in this article has been generated by Frontiers with the support of artificial intelligence and reasonable efforts have been made to ensure accuracy, including review by the authors wherever possible. If you identify any issues, please contact us.

Publisher's note

References

Bai, R., Wang, X., Li, J., Yang, F., Shangguan, Z., and Deng, L. (2024). The impact of vegetation reconstruction on soil erosion in the loess plateau. *J. Environ. Manage.* 363, 121382. doi: 10.1016/j.jenvman.2024.121382

Chang, Y., Han, L., Chen, R., Liu, Z., Li, Y., Zhao, Z., et al. (2024). Modelling of the trade-off between the deep soil moisture and vegetation restoration in the hilly area of the loess plateau, China. *J. Hydrology* 645, 132274. doi: 10.1016/j.jhydrol.2024.132274

Chatterjee, S., Desai, A. R., Zhu, J., Townsend, P. A., and Huang, J. (2022). Soil moisture as an essential component for delineating and forecasting agricultural rather than meteorological drought. *Remote Sens. Environ.* 269, 112833. doi: 10.1016/j.rse.2021.112833

Cheng, Y., Li, X., Wang, Y., Zhan, H., Yang, W., and Jiang, Q. (2020). New measures of deep soil water recharge during the vegetation restoration process in semi-arid regions of northern China. *Hydrology Earth System Sci.* 24, 5875–5890. doi: 10.5194/hess-24-5875-2020

Cui, Y., Pan, C., Ma, L., and Sun, Z. (2023). Comparing water uptake patterns of two tree species using stable isotopes on the loess plateau, China. *Hydrological Processes* 37, e15006. doi: 10.1002/hyp.15006

Deng, L., Yan, W., Zhang, Y., and Shangguan, Z. (2016). Severe depletion of soil moisture following land-use changes for ecological restoration: Evidence from northern China. *For. Ecol. Manage.* 366, 1–10. doi: 10.1016/j.foreco.2016.01.026

de Queiroz, M. G., da Silva, T. G. F., Zolnier, S., Jardim, A. M., da, R. F., de Souza, C. A. A., et al. (2020). Spatial and temporal dynamics of soil moisture for surfaces with a change in land use in the semi-arid region of Brazil. *Catena* 188, 104457. doi: 10.1016/j.catena.2020.104457

Dong, X., Lee, E., Gwak, Y., and Kim, S. (2018). Seasonal control of spatial distribution of soil moisture on a steep hillslope. *Water Sci.Technol: A J. Int. Assoc. Water pollut. Res.* 79 3, 556–565. doi: 10.2166/wcc.2018.173

Dymond, S. F., Wagenbrenner, J. W., Keppeler, E. T., and Bladon, K. D. (2021). Dynamic hillslope soil moisture in a Mediterranean montane watershed. *Water Resour. Res.* 57, e2020WR029170. doi: 10.1029/2020WR029170

Fathololoumi, S., Vaezi, A. R., Firozjaei, M. K., and Biswas, A. (2021). Quantifying the effect of surface heterogeneity on soil moisture across regions and surface characteristic. *J. Hydrology* 596, 126132. doi: 10.1016/j.jhydrol.2021.126132

Gao, X., Wu, P., Zhao, X., Wang, J., and Shi, Y. (2014). Effects of land use on soil moisture variations in a semi-arid catchment: Implications for land and agricultural water management. *Land Degradation Dev.* 25, 163–172. doi: 10.1002/ldr.1156

Gao, Y., and Yang, P. (2023). Temporal and spatial distribution of soil water repellency in grassland soils and its relation to soil moisture, hydrophobic matter, and particle size. *Sci. Total Environ.* 904, 166700. doi: 10.1016/j.scitotenv.2023.166700

Helman, D., and Mussery, A. (2020). Using landsat satellites to assess the impact of check dams built across erosive gullies on vegetation rehabilitation. *Sci. Total Environ.* 730, 138873. doi: 10.1016/j.scitotenv.2020.138873

Hou, X., Jia, Y., Han, H., and Shao, M. (2018). Response of soil moisture to single-rainfall events under three vegetation types in the gully region of the loess plateau. *Sustainability*. 10, 3793. doi: 10.3390/SU10103793

Huang, X., Shi, Z., Zhu, H., Zhang, H., Ai, L., and Yin, W. (2016). Soil moisture dynamics within soil profiles and associated environmental controls. *Catena* 136, 189–196. doi: 10.1016/J.CATENA.2015.01.014

Jia, Y.-H., and Shao, M.-A. (2014). Dynamics of deep soil moisture in response to vegetational restoration on the loess plateau of China. *J Hydrol.* 519, 523–531. doi: 10.1016/j.jhydrol.2014.07.043

Jia, X., Shao, M., Zhu, Y., and Luo, Y. (2017). Soil moisture decline due to afforestation across the loess plateau, China. *J. Hydrology* 546, 113–122. doi: 10.1016/j.jhydrol.2017.01.011

Jian, S., Zhao, C., Fang, S., and Yu, K. (2015). Effects of different vegetation restoration on soil water storage and water balance in the Chinese loess plateau. *Agric. For. Meteorology* 206, 85–96. doi: 10.1016/j.agrformet.2015.03.009

Jin, Z., Guo, L., Lin, H., Wang, Y., Yu, Y., Chu, G., et al. (2018). Soil moisture response to rainfall on the Chinese loess plateau after a long-term vegetation rehabilitation. *Hydrological Processes* 32, 1738–1754. doi: 10.1002/hyp.13143

Li, B., Li, P., Zhang, W., Ji, J., Liu, G., and Xu, M. (2021). Deep soil moisture limits the sustainable vegetation restoration in arid and semi-arid Loess Plateau. *Geoderma* 399, 115122. doi: 10.1016/j.geoderma.2021.115122

Liu, X., Cai, L., Li, M., Yan, Y., Chen, H., and Wang, F. (2024a). Why does afforestation policy lead to a drying trend in soil moisture on the loess plateau? *Sci. Total Environ.* 953, 175912. doi: 10.1016/j.scitotenv.2024.175912

Liu, X., Jiao, L., Cheng, D., Liu, J., Li, Z., Li, Z., et al. (2024b). Light thinning effectively improves forest soil water replenishment in water-limited areas: Observational evidence from *robinia pseudoacacia* plantations on the loess plateau, China. *J. Hydrology* 637, 131408. doi: 10.1016/j.jhydrol.2024.131408

Liu, Y., Li, S., Chen, F., Yang, S., and Chen, X. (2010). Soil water dynamics and water use efficiency in spring maize (*zea mays L.*) fields subjected to different water management practices on the loess plateau, China. *Agric. Water Manage.* 97, 769–775. doi: 10.1016/j.agwat.2010.01.010

Liu, Y., Miao, H., Huang, Z., Cui, Z., He, H., Zheng, J., et al. (2018). Soil water depletion patterns of artificial forest species and ages on the loess plateau (China). *For. Ecol. Manage.* 417, 137–143. doi: 10.1016/j.foreco.2018.03.005

Luan, J., Miao, P., Tian, X., Li, X., Ma, N., Xu, Z., et al. (2022). Separating the impact of check dams on runoff from climate and vegetation changes. *J. Hydrology* 614, 128565. doi: 10.1016/j.jhydrol.2022.128565

Mei, X., and Ma, L. (2022). Effect of afforestation on soil water dynamics and water uptake under different rainfall types on the loess hillslope. *Catena* 213, 106216. doi: 10.1016/j.catena.2022.106216

Montenegro, S., and Ragab, R. (2012). Impact of possible climate and land use changes in the semi arid regions: A case study from North Eastern Brazil. *J. Hydrology* 434–435, 55–68. doi: 10.1016/j.jhydrol.2012.02.036

O'Donnell, F. C., Donager, J., Sankey, T., Masek Lopez, S., and Springer, A. E. (2021). Vegetation structure controls on snow and soil moisture in restored ponderosa pine forests. *Hydrological Processes* 35, e14432. doi: 10.1002/hyp.14432

Pal, M., and Maity, R. (2021). Assimilation of remote sensing based surface soil moisture to develop a spatially varying vertical soil moisture profile database for entire Indian mainland. *J. Hydrology* 601, 126807. doi: 10.1016/j.jhydrol.2021.126807

Sharma, A., Patel, P. L., and Sharma, P. J. (2022). Influence of climate and land-use changes on the sensitivity of SWAT model parameters and water availability in a semi-arid river basin. *Catena* 215, 106298. doi: 10.1016/j.catena.2022.106298

Shen, Q., Gao, G., Fu, B., and Lü, Y. (2014). Soil water content variations and hydrological relations of the cropland-treebelt-desert land use pattern in an oasis-desert ecotone of the heihe river basin, China. *Catena* 123, 52–61. doi: 10.1016/j.catena.2014.07.002

Shi, Z., Zhu, H., Chen, J., Fang, N., and Ai, L. (2012). Spatial heterogeneity of soil moisture and its relationships with environmental factors at small catchment level. *J. Appl. Ecol.* 23 4, 889–895. doi: 10.13287/j.1001-9332.2012.0124

Tijdeman, E., and Menzel, L. (2021). The development and persistence of soil moisture stress during drought across southwestern Germany. *Hydrology Earth System Sci.* 25, 2009–2025. doi: 10.5194/hess-25-2009-2021

Tuure, J., Räsänen, M., Hautala, M., Pellikka, P., Mäkelä, P. S. A., and Alakukku, L. (2021). Plant residue mulch increases measured and modelled soil moisture content in the effective root zone of maize in semi-arid Kenya. *Soil Tillage Res.* 209, 104945. doi: 10.1016/j.still.2021.104945

Wang, L., Dalabay, N., Lu, P., and Wu, F. (2017). Effects of tillage practices and slope on runoff and erosion of soil from the loess plateau, China, subjected to simulated rainfall. *Soil Tillage Res.* 166, 147–156. doi: 10.1016/j.still.2016.09.007

Wang, Y., Gao, L., Li, J., and Peng, X. (2024a). Responses of deep soil moisture to direct rainfall and groundwater in the red soil critical zone: A four-stage pattern. *J. Hydrology* 632, 130864. doi: 10.1016/j.jhydrol.2024.130864

Wang, Y., Hu, W., Sun, H., Zhao, Y., Zhang, P., Li, Z., et al. (2024b). Soil moisture decline in China's monsoon loess critical zone: More a result of land-use conversion than climate change. *Proc. Natl. Acad. Sci.* 121, e2322127121. doi: 10.1073/pnas.2322127121

Wang, Y., Jiang, Y., Zhao, Y., Li, X., Xie, K., Yan, T., et al. (2024). Modeling the impact of long-term land use changes on deep soil hydrological processes in the loess plateau, China. *J. Hydrology* 643, 131944. doi: 10.1016/j.jhydrol.2024.131944

Wang, J., Liu, Z., Gao, J., Emanuele, L., Ren, Y., Shao, M., et al. (2021). The grain for green project eliminated the effect of soil erosion on organic carbon on China's loess plateau between 1980 and 2008. *Agric. Ecosyst. Environ.* 322, 107636. doi: 10.1016/j.agee.2021.107636

Wang, X.-Z., Jiao, F., Liu, Y.-X., Zhu, L.-T., and Lin, K. (2012). Relationships between soil moisture and environmental factors at different spatial scales. *Chinese J Ecol* 312, 319–323. doi: 10.13292/j.1000-4890.2012.0038

Wang, Y., Sun, H., and Zhao, Y. (2019). Characterizing spatial-temporal patterns and abrupt changes in deep soil moisture across an intensively managed watershed. *Geoderma* 341, 181–194. doi: 10.1016/j.geoderma.2019.01.044

Wang, S., Yang, M., Gao, X., Li, B., Cai, Y., Li, C., et al. (2024). Ecohydrological response to deep soil desiccation in a semiarid apple orchard. *Agric. For. Meteorology* 354, 110089. doi: 10.1016/j.agrformet.2024.110089

Wu, W., Li, H., Feng, H., Si, B., Chen, G., Meng, T., et al. (2021). Precipitation dominates the transpiration of both the economic forest (*malus pumila*) and ecological forest (*robinia pseudoacacia*) on the loess plateau after about 15 years of water depletion in deep soil. *Agric. For. Meteorology* 297, 108244. doi: 10.1016/j.agrformet.2020.108244

Wyatt, B. M., Ochsner, T. E., and Zou, C. B. (2021). Estimating root zone soil moisture across diverse land cover types by integrating *in-situ* and remotely sensed data. *Agric. For. Meteorology* 307, 108471. doi: 10.1016/j.agrformet.2021.108471

Xiao, L., Xue, S., Liu, G., and Zhang, C. (2014). Soil moisture variability under different land uses in the zhifanggou catchment of the loess plateau, China. *Arid Land Res. Manage.* 28, 274–290. doi: 10.1080/15324982.2013.860500

Xu, G., Huang, M., Li, P., Li, Z., and Wang, Y. (2021). Effects of land use on spatial and temporal distribution of soil moisture within profiles. *Environ. Earth Sci.* 80, 128. doi: 10.1007/s12665-021-09464-2

Yang, L., Chen, L., Wei, W., Yu, Y., and Zhang, H. (2014). Comparison of deep soil moisture in two re-vegetation watersheds in semi-arid regions. *J. Hydrology* 513, 314–321. doi: 10.1016/j.jhydrol.2014.03.049

Yang, L., Wei, W., Chen, L., and Mo, B. (2012). Response of deep soil moisture to land use and afforestation in the semi-arid loess plateau, China. *J. Hydrology* 475, 111–122. doi: 10.1016/j.jhydrol.2012.09.041

Yao, Y., Wang, X., Zeng, Z., Liu, Y., Peng, S., Zhu, Z., et al. (2016). The effect of afforestation on soil moisture content in northeastern China. *PloS One* 11, e0160776. doi: 10.1371/journal.pone.0160776

Ye, L., Fang, L., Shi, Z., Deng, L., and Tan, W. (2019). Spatio-temporal dynamics of soil moisture driven by 'grain for green' program on the loess plateau, China. *Agric. Ecosyst. Environ.* 269, 204–214. doi: 10.1016/j.agee.2018.10.006

Yu, Y., Hua, T., Chen, L., Zhang, Z., and Pereira, P. (2024). Divergent changes in vegetation greenness, productivity, and rainfall use efficiency are characteristic of ecological restoration towards high-quality development in the Yellow River basin, China. *Engineering* 34, 109–119. doi: 10.1016/j.eng.2023.07.012

Yu, B., Liu, G., Liu, Q., Huang, C., and Li, H. (2019). Effects of topographic domain and land use on spatial variability of deep soil moisture in the semi-arid loess plateau of China. *Hydrology Res.* 50, 1281–1292. doi: 10.2166/nh.2019.221

Yu, B., Liu, G., Liu, Q., Wang, X., Feng, J., and Huang, C. (2018). Soil moisture variations at different topographic domains and land use types in the semi-arid loess plateau, China. *Catena* 165, 125–132. doi: 10.1016/j.catena.2018.01.020

Yu, Y., Zhao, W., Martinez-Murillo, J. F., and Pereira, P. (2020). Loess plateau: From degradation to restoration. *Sci. Total Environ.* 738, 140206. doi: 10.1016/j.scitotenv.2020.140206

Zhang, Y., Feng, S., Wang, J., Chen, M., Wang, K., Liu, C., et al. (2024). Assessing the change in soil water deficit characteristics from grassland to forestland on the loess plateau. *Ecol. Indic.* 167, 112616. doi: 10.1016/j.ecolind.2024.112616

Zhang, Q., Jia, X., Zhao, C., and Shao, M. (2018). Revegetation with artificial plants improves topsoil hydrological properties but intensifies deep-soil drying in northern loess plateau, China. *J. Arid Land* 10, 335–346. doi: 10.1007/s40333-018-0007-0

Zhou, Z., Wang, Y., An, Z., Li, R., Xu, Y., Zhang, P., et al. (2022). Deep root information "hidden in the dark": A case study on the 21-m soil profile of *robinia pseudoacacia* in the critical zone of the chinese loess plateau. *Catena* 213, 106121. doi: 10.1016/j.catena.2022.106121

Zhou, J., Wang, Y., Li, R., He, H., Sun, H., Zhou, Z., et al. (2024). Response of deep soil water deficit to afforestation, soil depth, and precipitation gradient. *Agric. For. Meteorology* 352, 110024. doi: 10.1016/j.agrformet.2024.110024

frontiers | Frontiers in Plant Science

TYPE Original Research
PUBLISHED 11 December 2025
DOI 10.3389/fpls.2025.1695802

OPEN ACCESS

EDITED BY
Yi Han,
Jiangxi Normal University, China

REVIEWED BY
Yue Zhao,
Hubei Academy of Agricultural Sciences, China
Ao Zhou,
Shandong Agricultural University, China

*CORRESPONDENCE
Hong Wang
wanghong@hebau.edu.cn

†These authors have contributed equally to this work and share first authorship

RECEIVED 30 August 2025
REVISED 03 November 2025
ACCEPTED 10 November 2025
PUBLISHED 11 December 2025

CITATION
Zhang C, Tong S, Zhang R, Li X, Wang X-X and Wang H (2025) Intercropping with pear and cover crops as a strategy to boost soil carbon sequestration in the Taihang mountains' fragile ecosystems. *Front. Plant Sci.* 16:1695802. doi: 10.3389/fpls.2025.1695802

Intercropping with pear and cover crops as a strategy to boost soil carbon sequestration in the Taihang mountains' fragile ecosystems

Chi Zhang[1,2†], Shanshan Tong[3†], Ruifang Zhang[1,2], Xuguang Li[4], Xin-Xin Wang[5] and Hong Wang[2,3*]

[1]College of Land and Resources, Hebei Agricultural University, Baoding, China, [2]College of Resources and Environment Science, Hebei Agricultural University, Baoding, China, [3]National Research Center of Agricultural Engineering Technology in Northern Mountainous Areas, Hebei Agricultural University, Baoding, China, [4]Cultivated Land Quality Monitoring and Protection Center of Hebei Province, Shijiazhuang, China, [5]College of Horticulture, Hebei Agricultural University, Baoding, China

Introduction: Soil carbon sequestration capacity in ecologically fragile areas of the Taihang Mountains' gneiss slopes demands immediate attention. This study evaluated the synergistic effects of land-use transition (from barren hills to cropland to pear orchards) and cover crop intercropping on soil carbon storage.
Methods: Field sampling and experiments were conducted at 72 sites in Fuping County. The analysis combined multi-index assessment of soil physicochemical properties with partial least squares structural equation modeling (PLS-SEM).
Results: Land-use transition significantly increased soil carbon storage. In 8-year-old pear orchards, the organic carbon storage in the 0-20 cm soil layer reached 26.08 tC/ha, representing a 151.89% increase compared to cultivated land (10.35 tC/ha). Meanwhile, soil carbon storage in the 20-40 cm layer increased by 83.97% to 13.58 tC/ha. Under the cover cropping pattern, ryegrass in the surface 0-20 cm soil of 8-year-old orchards showed an 18.5% improvement in efficiency over natural grass. In the 20-40 cm deep soil, winter rape increased organic carbon content by 22.43% to 10.59 g/kg.
Discussion: The synergistic mechanism was attributed to increased carbon input from cover crops and root systems, optimized soil physical structure (bulk density decreased by 5.1%-8.0%, porosity increased by 2.1%-4.1%), and formation of a nutrient-carbon pool synergy. Available potassium, phosphorus, and organic carbon were significantly positively correlated. This pear orchard and cover crop intercropping system exemplifies a practical Nature-based Solutions (NbS) pathway, achieving an annual carbon sink growth rate of 4.2-5.8 tC/(ha·a). Its core mechanism lies in constructing a triple synergy of "carbon sequestration

enhancement, structural optimization, and nutrient cycling", which enhances ecosystem services multidimensionally while fostering a resilient agricultural production system. This practice provides a technical paradigm for synergizing carbon neutrality goals and ecological restoration in fragile mountainous areas.

KEYWORDS

fragile ecological zone, Taihang Mountains, pear orchard intercropping, land use, carbon stock

1 Introduction

Global warming poses a major threat to sustainable development, primarily driven by greenhouse gas emissions (Sokolov, 2021; Surya et al., 2023). As the world's largest agricultural emitter, China has committed to carbon peak by 2030 and carbon neutrality by 2060 (IEA, 2023). However, agriculture accounts for about 14% of national emissions, presenting significant mitigation challenges (Jiang and Fu, 2021; Raza et al., 2023; Xia et al., 2023). Land use transition plays a crucial role in addressing these challenges. While energy and industrial activities dominate China's emissions, land use change serves as a vital carbon sink - absorbing 1.315 billion tons of CO_2 according to national reports. Strategies like returning farmland to forest effectively enhance carbon sequestration while supporting sustainable development (Shao et al., 2019). Critically, land use transition shapes regional carbon storage by modifying ecosystems, hydrology, and soil carbon dynamics, particularly influencing soil organic carbon distribution and sequestration processes (Yang et al., 2017; Lipatov et al., 2021; Yuan et al., 2021; Wang et al., 2024).

Under intensified human activities and climate warming, ecologically fragile regions such as the Taihang Mountains are confronting ecological crises including land desertification and vegetation degradation (Fan et al., 2021). This area features shallow soil layers and high susceptibility to water erosion, while its limestone parent material accelerates soil organic matter mineralization, creating a "carbon leakage" risk. Reduced vegetation coverage intensifies surface runoff erosion, leading to physical relocation of soil carbon pools and accelerated organic carbon decomposition through aggregate destruction (Wang et al., 2022). Although the Taihang Mountains possess substantial vegetation carbon sequestration potential, current monoculture plantations limit carbon sink functionality (Tilahun et al., 2022). Our research demonstrates that implementing pear orchard intercropping systems effectively stabilizes topsoil through root systems, increases labile carbon fractions by 18.5% via litter input, and alleviates nitrogen limitation through leguminous herbs' biological nitrogen fixation, forming a dual carbon sequestration mechanism of "physical protection-biochemical regulation". The validated "pear orchard + herbaceous cover" model enhances carbon storage in typical Taihang Mountain slopes by 4.2-5.8 tC/(hm^2×a) annually, primarily through three mechanisms: extended green periods from herbs mitigating seasonal carbon sink gaps, synergistic root systems constructing carbon storage spaces, and enhanced plant diversity stimulating soil microbial carbon pumps (Sun et al., 2024). This approach provides crucial technical support for strengthening the ecological barrier functions of the Taihang Mountains within the dual carbon goals framework.

Land use transition significantly affects the rate and storage of organic carbon mineralization by impacting soil organic matter inputs, vegetation biomass, and physio-chemical properties (Economic Daily, 2020; Liu et al., 2024a). Current research utilizes field surveys (high but limited accuracy), model simulations (Yi et al., 2022), and remote sensing (focused on large-scale) (Dangulla et al., 2021; Lipatov et al., 2021), confirming significant variations in carbon storage responses across different land use methods (Totti et al., 2025). Ecologically fragile areas are particularly susceptible to degradation. Farmland contributes approximately half of agricultural carbon emissions (Liu et al., 2023), including 90% N_2O, 70% CH_4, and 20% of CO_2 emissions (Li et al., 2023a, 2023b). Optimization models can enhance the carbon sequestration potential in these regions. Farmland carbon sequestration compensates between 0.1% and 27% of annual greenhouse gas emissions (Rodrigues et al., 2021). The combined ecological protection of cultivated land and surrounding areas sequesters approximately 9.60×10^6 tons of carbon (Liu et al., 2024b), while the soil organic carbon stock in the top 0–40 cm of *Pinus tabuliformis* plantations reaches 8.7 kg/m^2 (Xu et al., 2022). In orchard systems, the expansion of pear orchards has contributed to an increase in storage capacity by 44.4 million tons, with organic carbon levels surpassing those of cultivated land (Duan et al., 2021). Converting farmland to forest has also enhanced the carbon pool (Yu et al., 2022). Cover crop management, including orchard grass and intercropping ryegrass in pear orchards, has increased the carbon pool by 21% and reduced the carbon footprint by 36.7% (Fu et al., 2023; He et al., 2023). Additionally, alfalfa cover cropping increased organic carbon by 14.3% within the 0–10 cm soil layer (Zhao et al., 2023). Meta-analyses indicate that cover planting can augment the soil carbon pool by approximately 31.1%, with a higher increase of 32.3% observed in mountainous regions compared to clear tillage systems (Li et al., 2023c).

This study involved field investigations and experiments on gneiss slopes of the Taihang Mountains to quantify the effects of intercropping cover crops in pear orchards on soil carbon storage. The research aimed to analyze the key factors driving synergistic

carbon sequestration and identify optimal management practices, providing a scientific basis for sustainable land use and carbon neutrality policies.

2 Materials and methods

2.1 Overview of the research area

The study area is located at an altitude of 302 m in the Agricultural Ecological Demonstration Park on Fuping Avenue, Baoding City, Hebei Province (115.48°E, 38.86°N) (Figure 1). Baoding City is situated on the eastern foothills of the northern Taihang Mountains. It has a temperate continental monsoon climate and is located in a warm temperate semi-humid area. Winters are characterized by cold, dry and mild snow, whereas summers are hot, humid and feature concentrated precipitation. The region experiences an average annual temperature of 12.6°C, with annual precipitation ranging from 550 to 790 mm, and a frost-free period lasting between 140 and 190 days.

The land transformation project in Fuping County commenced in 2016, involving mechanical compaction of barren hillslopes and thorough mixing with weathered surface materials to construct terraced fields with slopes of approximately 30 degrees and widths exceeding 6 meters. This process resulted in the formation of a gneiss-derived soil layer approximately 60 cm thick. On this reconstructed substrate, the cultivation of maize and pear trees facilitated the conversion of barren hillslopes into cropland and orchards. Sampling sites for this study were selected from soils representing different transformation models, specifically encompassing four types: (1) newly formed soil bare land created by mechanically crushed gneiss bedrock in 2016; (2) cultivated land developed after seven years of maize planting; (3) orchard soils where Yuluxiang pear trees had been cultivated with fertilization for 4, 6, and 8 years (corresponding to tree ages in 2024); (4) combined planting systems integrating three cover crops (ryegrass, violet cress, and winter rapeseed) with pear trees of 4, 6, and 8 planting years, respectively. For each transformation model, 12 sampling points were established, totaling 72 sample points (Figure 2).

2.2 Experimental design

2.2.1 Soil sampling sites and land use stages in the study area

In this study, soil sampling points were selected from gneiss barren hills and slopes, representing various land use stages after transformation. Specifically, samples included: (1) the original soil on barren hills and slopes; (2) newly formed soil from mechanically crushed gneiss bedrock (2016); (3) cultivated land formed after seven years of corn planting; (4) orchard soils where Yuluxiang pear trees had been planted and fertilized for 4, 6, and 8 years (corresponding to tree ages in 2024). The test crop was Yuluxiang pear, and the cover crops—ryegrass (R), violet cress (V), and winter rapeseed (W)—were supplied by the Hebei Academy of Agriculture and Forestry Sciences.

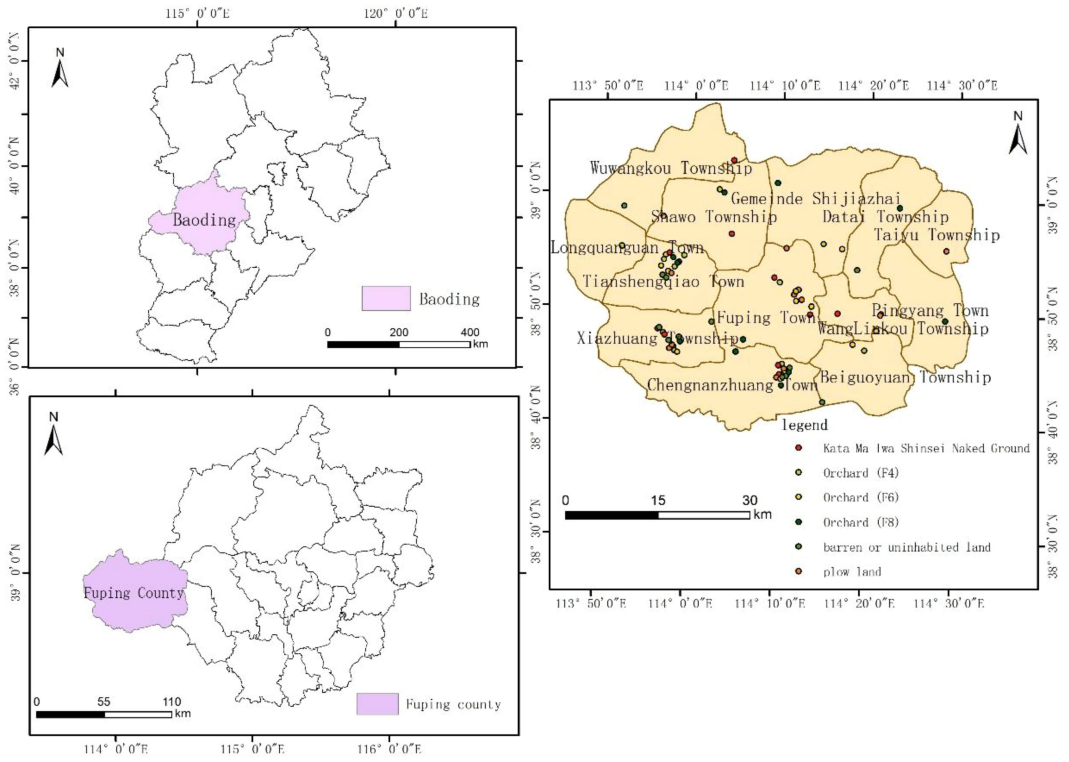

FIGURE 1
Location map of the research area.

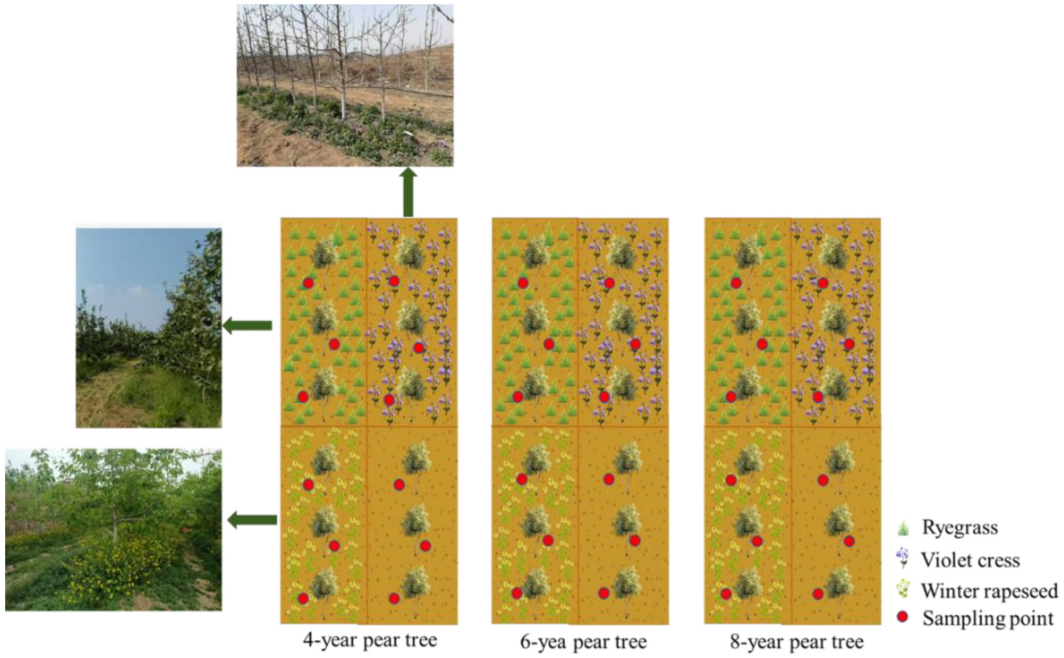

FIGURE 2
Experimental design layout diagram.

2.2.2 Delineation of ecologically fragile areas

This study was conducted in the core experimental zone of Fuping County, Baoding City, Hebei Province, specifically focusing on the Agricultural Ecological Demonstration Park along Fuping Avenue and surrounding villages implementing ecological restoration projects. The area represents a typical low mountainous and hilly region in the northern section of the eastern Taihang Mountains. Using a GIS-based spatial analysis platform, we applied a comprehensive evaluation system integrating slope gradient, soil erosion intensity, vegetation coverage, and a lithology-soil depth composite index. This multi-criteria approach, combined with field validation from 72 sampling sites, enabled precise delineation of ecologically fragile slopes. The results demonstrate that these vulnerable areas are predominantly distributed on sunny and semi-sunny slopes at elevations of 300–500 meters with gradients of 10°-25°. These locations not only constitute ecologically sensitive zones but also provide suitable site conditions for establishing and developing pear orchard ecosystems.

2.2.3 Experimental design for the impacts on soil carbon storage

Three cover crops, namely ryegrass, violet cress and winter rapeseed, were grown in a two-factor design and combined with pear trees with 4, 6 and 8 planting years, respectively. The pear trees were planted as control. A total of 12 treatments with three replicates of each were planted with 1.5 × 6 m distance and the area of each block was 54 m^2. On Apr 16, 2023, three mulching crops were planted between the rows of pear trees. Sampling of mature pear trees was conducted on Sep 2, 2024. Soil samples ranging from 0 to 40 cm were collected in layers for testing and analysis. The 0–40 cm soil profile was selected for layered sampling based on its ecological significance as the primary zone for biological activity and its demonstrated responsiveness to agricultural management interventions, providing optimal detection of carbon sequestration dynamics. Except for planting, the field management of each treatment remains consistent (Figure 2).

2.2.4 Soil measurements

To comprehensively assess soil fertility and quality, determined a number of key soil indicators were selected which are:

1. Physical and chemical properties: includes soil organic matter, pH, total salinity, soil bulk density and soil porosity;
2. Nutrient elements: total nitrogen, available phosphorus and potassium;
3. Medium elements: exchangeable calcium, magnesium and available sulfur;
4. Trace elements: involving effective iron, manganese, copper and zinc.

2.3 Research methods

2.3.1 Data acquisition

The soil sampling was carried out in accordance with the "Technical Regulations for Monitoring the Quality of Cultivated Land (NY/T1119-2012)" (National Agricultural Technology Extension and Service Center, 2012). A soil sample was collected using a 4 cm diameter spiral drill from the 0–40 cm depth, divided into two 20 cm layers. A 15-drill mixed sampling method was

implemented between the pear tree grows in each test plot. The drilled soil was mixed evenly and the excess part was removed following the four-part method and packed into zip bags. Fifteen soil samples were simultaneously collected from the adjacent bare land and mixed evenly as the control. The samples were naturally air-dried and sieved by the 20 mm and 100 mm-mesh sieves to determine the soil nutrients. In addition, a 100 cm^3 ring knife was used to collect soil to determine the soil bulk density of mature pear trees.

2.3.2 Detection methods for sample indicators

The determination methods of various soil indicators refer to the book "Soil Agrochemical Analysis" (Bao, 2000):

1. Soil Organic Matter: Determined by the oil bath heating-potassium dichromate oxidation volumetric method. Precisely 0.1 g of air-dried soil sample passed through a 0.15 mm sieve was weighed into a hard glass tube. Then, 5.00 mL of 0.8 mol/L potassium dichromate ($K_2Cr_2O_7$) standard solution and 5 mL of concentrated sulfuric acid (H_2SO_4) were added. The mixture was heated in an oil bath at 170–180 °C for 5 minutes. After cooling, the digest was transferred to a conical flask and titrated with a 0.2 mol/L ferrous sulfate ($FeSO_4$) standard solution, using o-phenanthroline as an indicator. The organic carbon content was calculated based on the amount of ferrous sulfate consumed and then multiplied by the 1.724 coefficient to obtain the organic matter content.
2. pH: Measured potentiometrically. 10.00 g of air-dried soil passed through a 2 mm sieve was placed in a 50 mL beaker. 25 mL of CO_2-free distilled water was added at a soil-to-water ratio of 1:2.5. The suspension was stirred for 1 minute and left to stand for 30 minutes. The supernatant was measured using a calibrated pH meter (Model PHSJ-4F), and the reading was recorded after stabilization, accurate to 0.01 pH unit.
3. Soil Bulk Density: Determined by the core method. A standard 100 cm^3 core cutter was vertically pressed into undisturbed soil. After removal, both ends were trimmed flat. The soil core was dried to constant weight in an oven at 105 °C for 8 h. The mass of the dried soil sample was weighed, and the bulk density (g/cm^3) was calculated based on the core cutter's volume.
4. Total Nitrogen: Determined by the Kjeldahl digestion method. 1.000 g of soil sample passed through a 0.15 mm sieve was placed in a digestion tube. 1.8 g of accelerator (a 10:1 mixture of potassium sulfate, K_2SO_4, and copper sulfate, $CuSO_4$) and 5 mL of concentrated sulfuric acid (H_2SO_4) were added. Digestion was performed at 420 °C for 2 h until the solution turned bluish-green. After cooling, distillation was carried out using a Kjeldahl nitrogen analyzer (Model K9860). The distillate was absorbed in a 2% boric acid (H_3BO_3) solution and titrated with 0.01 mol/L hydrochloric acid (HCl) standard solution, using a methyl red-bromocresol green mixed indicator for endpoint determination.
5. Available Phosphorus: Determined by sodium bicarbonate extraction-molybdenum antimony ascorbic acid colorimetry. 2.50 g of soil sample was added to 50 mL of 0.5 mol/L sodium bicarbonate ($NaHCO_3$) extraction solution (pH 8.5). The mixture was shaken for 30 minutes and then filtered. 5 mL of the filtrate was mixed with 5 mL of molybdenum-antimony-ascorbic acid color developing reagent. After developing color at room temperature for 30 minutes, the absorbance was measured at 880 nm wavelength using a UV-Vis spectrophotometer (Model UV-1800). The concentration was calculated via a standard curve.
6. Available Potassium: Determined by ammonium acetate extraction-flame photometry. 5.00 g of soil sample was added to 50 mL of 1 mol/L ammonium acetate (CH_3COONH_4) solution (pH 7.0). The mixture was shaken for 15 minutes and then filtered. The filtrate was analyzed using a flame photometer (Model FP6410) with a potassium filter at a wavelength of 768 nm. Quantification was performed using a standard curve prepared from a series of potassium standard solutions.
7. Exchangeable Calcium and Magnesium: Determined by ammonium acetate exchange-atomic absorption spectrophotometry. 10.00 g of soil sample was sequentially extracted three times using a total of 50 mL of 1 mol/L ammonium acetate (CH_3COONH_4) solution (pH 7.0). The combined filtrates were analyzed using an atomic absorption spectrophotometer (Model AA-6880). The wavelengths were set at 422.7 nm for calcium and 285.2 nm for magnesium, with deuterium lamp background correction.
8. Available Sulfur: Determined by phosphate-acetic acid extraction-barium sulfate turbidimetry. 10.00 g of soil sample was added to 50 mL of extraction solution (0.016 mol/L calcium phosphate, $Ca(H_2PO_4)_2$, + 2 mol/L acetic acid, CH_3COOH). The mixture was shaken for 1 hour and then filtered. 10 mL of the filtrate was mixed with 1 mL of stabilizer (glycerol:ethanol = 1:1) and 0.5 g of barium chloride ($BaCl_2$) crystals. After shaking for 1 minute, the turbidity was measured at 440 nm wavelength using a spectrophotometer.
9. Available Trace Elements (Fe, Mn, Cu, Zn): Determined by DTPA extraction-atomic absorption spectrophotometry. 20.00 g of soil sample was added to 40 mL of DTPA extraction solution (0.005 mol/L DTPA + 0.01 mol/L calcium chloride, $CaCl_2$ + 0.1 mol/L triethanolamine, TEA, pH 7.3). The mixture was shaken for 2 h and then filtered. The filtrate was analyzed using an atomic absorption spectrophotometer at the following wavelengths: Fe 248.3 nm, Mn 279.5 nm, Cu 324.8 nm, Zn 213.9 nm.

All determinations included blank controls and quality control using certified reference material (GSS-17). Each sample was analyzed in triplicate.

2.3.3 Data analysis

Excel 2019 and SPSS Statistics 26 software were used to organize and statistically analyze the experimental data. The effects of land use patterns, planting years, and their interactions on soil organic carbon content and carbon storage were quantitatively assessed. Correlation analysis was conducted using the Pearson correlation coefficient method. The Shapiro-Wilk test was applied to all continuous variables to assess normality. For variables meeting the normality assumption, Pearson correlation analysis was employed; For those violating normality, the more robust Spearman's rank correlation analysis was used instead. The partial least squares structural equation modeling (PLS-SEM) was constructed and analyzed using R 4.5.1 software.

3 Results

3.1 Soil chemical properties

The soil nutrient indicators of the newly formed gneiss bare land are higher than those of the original gneiss hillside soil. Specifically, organic carbon, total nitrogen, available phosphorus, potassium, exchangeable calcium, magnesium, sulfur, effective manganese and zinc in the newly formed bare land were significantly higher than hillside soil. Among them, the differences between available phosphorus and potassium are obvious. The pH values of the both soils are alkaline, but the difference were non-significant. There was no significant difference in the contents of effective iron and copper between both soil types. This data provides basic soil background information for the subsequent analysis (Table 1).

TABLE 1 Soil chemical properties.

Soil at the sampling site	Gneiss hillside soil	Gneiss is a bare ground of new soil
Organic carbon (g/kg)	3.20 ± 0.40	3.92 ± 0.89
Total nitrogen (g/kg)	0.31 ± 0.04	0.38 ± 0.03
Available phosphorus (mg/kg)	4.31 ± 0.75	13.52 ± 2.04
Available potassium (mg/kg)	46.22 ± 8.65	77.15 ± 9.84
pH	7.70 ± 0.26	7.55 ± 0.04
Exchangeable calcium (mg/kg)	726.0 ± 168.31	930.7 ± 137.89
Exchangeable magnesium (mg/kg)	179.67 ± 19.86	234.67 ± 30.57
Effective sulfur (mg/kg) Effective sulfur	22.97 ± 3.56	25.57 ± 5.11
Effective iron (mg/kg)	11.80 ± 2.57	12.33 ± 1.94
Effective manganese (mg/kg)	2.50 ± 0.26	3.60 ± 0.50
Effective copper (mg/kg)	0.60 ± 0.05	0.66 ± 0.17
Effective zinc (mg/kg)	3.20 ± 0.40	3.92 ± 0.89

3.2 Effects of different land use patterns on soil carbon sequestration capacity

Land use transition markedly impacted soil organic carbon (SOC) content and storage. In the topsoil (0–20 cm), crop land (P) had significantly higher SOC level than bare land (G), with a of 55.4% increase. Additionally, 4-year (F4), 6-year (F6), and 8-year (F8) pear orchards showed SOC increases of 80.5%, 103.6%, and 138.0%, respectively, compared to cropland. In the subsoil (20–40 cm), SOC content in the 8-year orchards was significantly higher (200.3%) than cropland. For carbon storage, topsoil carbon storage in pear orchards increased significantly by 114.7% compared to cropland. The carbon storage in these orchards was increased in F4, F6, and F8 by 296.7%, 373.4%, and 441.1%, respectively. Subsoil carbon storage also showed upward trend, with the 8-year orchards storing 418.3% more than cropland. Regarding soil layer differences: The SOC storage of the 0–20 cm topsoil in all treatments was significantly higher than 20–40 cm subsoil (Table 2). Overall, following the transition from cropland to pear orchards, SOC content and storage demonstrated a continuous and positive trend with longer cultivation duration, particularly in the topsoil. This indicates that among various land use transition models, pear orchards maximize the soil carbon sequestration capacity which enables an ideal land use pattern for optimizing regional carbon cycling and strengthening the soil carbon sink.

3.3 Effects of pear-cover crops mixed cropping on soil carbon sequestration capacity

The practical application effect of the pear-herb mixed cropping model in this region will be comprehensively evaluated. In order to provide a scientific basis for regional ecological restoration and sustainable agricultural development.

3.3.1 Soil macronutrient variations in relation to pear orchard age and cover crop

Soil nutrients in pear orchards increased significantly with stand age ($P<0.05$). In the 0–20 cm topsoil, 8-year-old orchards showed the most pronounced increases relative to 4-year-old stands: organic matter (+31.8%), available phosphorus (+59.4-64.6%), and available potassium (+76.6-92.6%). Intercropping with ryegrass and winter rapeseed further enhanced these age-related gains. Ryegrass particularly improved organic matter (+28.1%) and total nitrogen (+19.8%), whereas winter rapeseed most effectively boosted available potassium (Table 3). Although nutrient levels were generally lower in the 20–40 cm subsoil, both orchard age and cover crops still exerted significant effects ($P < 0.05$). Eight-year-old orchards exhibited increases in organic matter (+53.9-58.7%), available phosphorus (+26.2-30.8%), and available

10.3389/fpls.2025.1695802

TABLE 2 Carbon stocks in different soil layers under different land uses.

Treatment	Soil layers (cm)	Soil organic carbon (g/kg)	Soil organic carbon stocks (tC/hm^2)
G	0-20	6.16 ± 2.41aD	4.82 ± 1.09aE
	20-40	2.88 ± 0.69bC	2.62 ± 0.67aD
P	0-20	9.57 ± 0.94aC	10.35 ± 0.90aD
	20-40	5.77 ± 1.09bABC	7.38 ± 1.45bC
F4	0-20	11.12 ± 0.26aBC	19.12 ± 0.96aC
	20-40	5.62 ± 0.42bBC	9.17 ± 0.77bBC
F6	0-20	12.54 ± 0.75aAB	22.82 ± 1.34aB
	20-40	7.43 ± 0.79bAB	11.77 ± 1.11bAB
F8	0-20	14.66 ± 0.29aA	26.08 ± 0.57aA
	20-40	8.65 ± 0.16bA	13.58 ± 0.50bA

Different lowercase letters indicate statistically significant differences (P<0.05) between soil layers within the same treatment, while different uppercase letters indicate significant differences (P<0.05) among treatments within the same soil layer. Data are presented as mean ± standard deviation (n=3). G: Bare land; P: Crop land; F4: Pear-herb intercropping system (4-year trees); F6: Pear-herb intercropping system (6-year trees); F8: Pear-herb intercropping system (8-year trees).

potassium (+61.9-97.5%). Winter rapeseed was particularly effective in enhancing subsoil potassium (+54.9%), though the magnitude of phosphorus increase in the subsoil was lower than that observed in the topsoil (Table 3).

3.3.2 Impact of tree maturity and cover cropping on soil trace element composition

In 8-year-old pear orchards, exchangeable calcium and magnesium increased by 33.9%-61.6% and 24.0%-46.3% respectively, while available sulfur rose by 88.8%-128.1% compared to 4-year-old orchards. Ryegrass treatment performed optimally, achieving exchangeable calcium and magnesium levels of 2095 mg/kg and 446.33 mg/kg respectively in 8-year-old orchards, with calcium content 20.8% higher than natural fallow. Compared to nitrogen-only treatment, ryegrass intercropping enhanced exchangeable calcium and magnesium by 25.5% and 19.5% in 6-year-old orchards, and by 30.3% and 20.8% in 8-year-old orchards. In the 20–40 cm subsoil, 8-year-old orchards reached exchangeable calcium levels of 2117.67-2328.33 mg/kg (45.4%-59.9% increase), with magnesium increasing by 57.8%-81.8% and available sulfur by 148.6%-183.5%, showing the most effectiveness under winter rapeseed treatment (Table 4). Although cover crops had weaker ameliorative effects on the subsoil than on the topsoil, both ryegrass and winter rapeseed maintained relatively high nutrient levels.

3.3.3 Soil microelement fluctuations under different pear orchard ages and cover crop

Pear orchard age and cover crop management significantly enhanced trace element concentrations in the 0–20 cm topsoil (P < 0.05). Compared to 4-year-old orchards, 8-year-old orchards showed increases of 73.1%-110.0% in available Fe, 33.2%-58.6%

TABLE 3 Changes in soil macronutrients at different pear ages and cover crop treatments.

Soil traits	Year	Cover crops	0-20 (cm)	20-40 (cm)
Total porosity (%)	4	N	47.48 ± 1.95a	43.02 ± 0.63a
		R	50.37 ± 1.67a	44.84 ± 0.81a
		W	51.27 ± 1.26a	45.96 ± 0.93a
		V	50.27 ± 2a	45.71 ± 1.02a
	6	N	47.31 ± 2.89a	44.37 ± 2.08a
		R	50.26 ± 1.36a	46.06 ± 0.75a
		W	50.4 ± 1.31a	46.67 ± 1.1a
		V	50.58 ± 2.64a	46.59 ± 2.55a
	8	N	49.98 ± 1.47b	45.11 ± 1.02a
		R	52.03 ± 2.8a	46.45 ± 1.73a
		W	51.55 ± 3.85a	47.82 ± 0.33a
		V	51.33 ± 1.87a	47.15 ± 1.07a
pH	4	N	7.94 ± 0.23a	8.47 ± 0.08a
		R	7.87 ± 0.08a	7.83 ± 0.26b
		W	7.84 ± 0.27a	7.95 ± 0.22ab
		V	7.87 ± 0.17a	7.81 ± 0.08b
	6	N	8.1 ± 0.1a	8.04 ± 0.14a
		R	7.94 ± 0.26a	8.3 ± 0.07a
		W	7.74 ± 0.3a	7.98 ± 0.41a
		V	7.84 ± 0.09a	8.25 ± 0.06a
	8	N	7.93 ± 0.15a	8.15 ± 0.18a
		R	8.01 ± 0.06a	8.25 ± 0.04a
		W	7.74 ± 0.3a	8.09 ± 0.16a
		V	8.08 ± 0.09a	7.71 ± 0.34a
AK (mg/kg)	4	N	192.37 ± 6.09b	70.88 ± 7.44a
		R	225.92 ± 5.83ab	77.43 ± 7.13a
		W	233.87 ± 2.89a	90.36 ± 4.03a
		V	200.77 ± 25.06ab	87.58 ± 13.71a
	6	N	244.6 ± 7.78b	95.32 ± 10.54a
		R	286.81 ± 8.15a	117.09 ± 8.36a
		W	284.89 ± 9.3ab	119.27 ± 14.08a
		V	266.21 ± 27.56ab	105.59 ± 2.64a
	8	N	339.66 ± 5.94b	114.84 ± 3.01a
		R	389.4 ± 7.7a	133.2 ± 8.63b
		W	385.22 ± 19.59a	139.98 ± 4.52a
		V	373.97 ± 15.58ab	132.22 ± 6.76ab
AP (mg/kg)	4	N	100.83 ± 6.83a	47.45 ± 1.99a

(Continued)

10.3389/fpls.2025.1695802

TABLE 3 Continued

Soil traits	Year	Cover crops	0-20 (cm)	20-40 (cm)
		R	128.28 ± 10.76a	51.03 ± 5.72a
		W	128.46 ± 1.85a	51.75 ± 5.6a
		V	122.11 ± 10.54a	50.07 ± 2.54a
	6	N	148.9 ± 6.89b	51.78 ± 6.88a
		R	185.46 ± 3.71a	53.86 ± 3.9a
		W	183.99 ± 9.44a	56.91 ± 3.92a
		V	161.63 ± 17.64ab	53.84 ± 2.82a
	8	N	160.65 ± 10.42b	59.88 ± 1.06a
		R	201.53 ± 15.01a	61.86 ± 6.83a
		W	200.37 ± 2.76a	62.01 ± 3.89a
		V	186 ± 14.12aab	62.8 ± 6.01a
SOM (g/kg)	4	N	19.17 ± 0.45b	9.69 ± 0.72a
		R	22.75 ± 0.86a	10.66 ± 0.92a
		W	22.75 ± 0.6a	11.51 ± 1.66a
		V	21.39 ± 1.1ab	10.6 ± 1.27a
	6	N	21.61 ± 1.29b	12.81 ± 1.37a
		R	25.44 ± 1.75a	13.61 ± 0.98a
		W	25.16 ± 1.67ab	14.04 ± 0.57a
		V	24.83 ± 2.45ab	13.76 ± 1.8a
	8	N	25.27 ± 0.5b	14.91 ± 0.27b
		R	29.15 ± 0.36a	17.4 ± 1.16ab
		W	27.49 ± 0.83ab	18.26 ± 0.13a
		V	26.38 ± 0.96ab	17.67 ± 1.13ab
Total nitrogen (g/kg)	4	N	1.05 ± 0.02a	0.57 ± 0.07a
		R	1.21 ± 0.06a	0.59 ± 0.04a
		W	1.21 ± 0.03a	0.61 ± 0.05a
		V	1.16 ± 0.08a	0.59 ± 0.01a
	6	N	1.11 ± 0.02b	0.6 ± 0.01a
		R	1.29 ± 0.1a	0.63 ± 0.1a
		W	1.21 ± 0.07ab	0.64 ± 0.03a
		V	1.18 ± 0.08ab	0.62 ± 0.04a
	8	N	1.27 ± 0.02b	0.68 ± 0.07a
		R	1.45 ± 0.03a	0.78 ± 0.02a
		W	1.38 ± 0.07ab	0.77 ± 0.03a
		V	1.31 ± 0.05ab	0.74 ± 0.06a

Different lowercase letters within the same column for each soil depth and year indicate statistically significant differences among cover crop treatments ($P < 0.05$). Values sharing the same letter are not significantly different. Data are presented as mean ± standard deviation (n=3). Abbreviations for cover crop treatments: N, No cover crop (control); R, Ryegrass; W, Winter rapeseed; V, Violet cress.

TABLE 4 Changes in soil intermediate elements at different pear years and cover crop treatments.

Soil traits	Year	Cover crops	0-20 (cm)	20-40 (cm)
Exchanged Ca (mg/kg)	4	N	1296 ± 150.1a	1456.33 ± 201.75a
		R	1463 ± 85.19a	1658.33 ± 69.07a
		W	1496.67 ± 132.28a	1695.33 ± 165.41a
		V	1430 ± 223.58a	1515 ± 270.79a
	6	N	1423.33 ± 105.82b	2008.33 ± 97.2a
		R	1785.67 ± 41.53a	2197 ± 173.65a
		W	1763 ± 104.23ab	2230 ± 154.31a
		V	1614.67 ± 100.08ab	2139 ± 148.19a
	8	N	1734.67 ± 19.97b	2117.67 ± 140.28a
		R	2095 ± 162.25a	2328.33 ± 209.23a
		W	2022.33 ± 128.46ab	2328.33 ± 325.17a
		V	2004 ± 78.23ab	2139.33 ± 66.13a
Exchanged Mg (mg/kg)	4	N	305 ± 3.06a	241.67 ± 23.55a
		R	326 ± 11.36a	256.33 ± 28.29a
		W	328 ± 21.03a	251.33 ± 23.95a
		V	308 ± 19.09a	254.33 ± 27.48a
	6	N	340 ± 18.5b	303.33 ± 24.59a
		R	406.33 ± 8.65a	321.33 ± 11.17a
		W	402 ± 24.5ab	318 ± 20.01a
		V	379.67 ± 31.96ab	315.33 ± 14.33a
	8	N	378.33 ± 24.18b	381.33 ± 12.02a
		R	446.33 ± 24.63a	431.33 ± 10.71a
		W	434.67 ± 31.67ab	438.67 ± 15.9a
		V	434.67 ± 29.72ab	404.33 ± 27.03a
Effective S (mg/kg)	4	N	34.8 ± 6.98a	21.27 ± 1.68a
		R	42.37 ± 2.77a	22.9 ± 1.48a
		W	40.37 ± 3.12a	23.47 ± 1.06a
		V	39.03 ± 5.26a	22.97 ± 1.7a
	6	N	46.07 ± 0.69b	43.2 ± 2.66a
		R	60 ± 0.45a	48.27 ± 0.9a
		W	58.9 ± 5.6ab	48.5 ± 4.24a
		V	58.43 ± 5.37ab	47.7 ± 4.13a
	8	N	65.7 ± 4.57b	52.87 ± 3.77b
		H	79.37 ± 7.86a	57.17 ± 2.53ab

(Continued)

10.3389/fpls.2025.1695802

TABLE 4 Continued

Soil traits	Year	Cover crops	0-20 (cm)	20-40 (cm)
		W	77.97 ± 1.04ab	60.3 ± 0.44a
		V	76.57 ± 4.62ab	57.67 ± 1.33ab

Different lowercase letters within the same column for each soil depth and year indicate statistically significant differences among cover crop treatments ($P<0.05$). Values sharing the same letter are not significantly different. Data are presented as mean ± standard deviation (n=3). Abbreviations for cover crop treatments: N, No cover crop (control); R, Ryegrass; W, Winter rapeseed; V, Violet cress.

in Mn, 45.5%-73.3% in Cu, and 114.5%-141.8% in Zn. Ryegrass treatment notably improved Fe and Mn levels, with available Mn reaching 7.50 mg/kg, whereas winter rapeseed was most effective in enhancing Zn, achieving 8.27 mg/kg—a 12.8% increase over nitrogen-only fertilization (Table 5). Although trace element concentrations in the 20–40 cm subsoil were lower than in the topsoil, they still increased significantly with orchard age ($P < 0.05$). In 8-year-old orchards, available Fe, Mn, Cu, and Zn rose by 42.8%-54.4%, 85.3%-103.9%, 67.0%-86.4%, and 193.4%-222.6%, respectively. Winter rapeseed treatment generally maintained higher levels of most trace elements in the subsoil (Table 5).

3.3.4 Soil carbon storage variations under different pear orchard ages and cover crop

This study showed that pear orchard age and cover crop management had a significant effect on soil organic carbon content and carbon storage ($P<0.05$). Compared with natural grass fallow, ryegrass, rapeseed and violet cress treatments significantly increased soil organic carbon content and carbon storage in 0–20 cm surface soil. Compared with natural grass fallow, the organic carbon content of 4-year, 6-year and 8-year orchards increased by 18.7%, 17.6% and 15.4%, and the carbon storage increased by 24.4%, 20.3% and 18.5%, respectively. Winter rapeseed treatment was the second most effective to enhance the organic carbon content by 18.7%, 16.4% and 8.8% in 4-year, 6-year and 8-year orchards, and carbon storage by 24.1%, 17.1% and 15.0%, respectively (Table 6).

Violet cress treatment showed significant improvement in the first 6 years, with an 11.6%-14.8% increase in organic carbon, whereas, increase was only 4.4% in 8-year orchards. Although the organic carbon content and carbon storage in the 20–40 cm subsoil increased with orchard age and no significant differences were observed with the change of cover crop. It is worth noting that compared with the 4-year orchard, the 8-year orchard showed a significant increase of 31.8%-52.1% and a 36.4%-61.6% in the organic carbon content and carbon storage in the surface soil (Table 6).

3.3.5 Soil structure variations in relation to orchard age and cover crop treatments

Pear orchard age and cover crop management significantly improved the physical structure of the 0–20 cm topsoil. All cover crop treatments significantly reduced soil bulk density, with decreases of 5.1%-6.6%, 5.8%-8.0%, and 3.1%-3.8% in 4-year, 6-year, and 8-year-

TABLE 5 Changes in soil microelements at different pear years and cover crop treatments.

Soil traits	Year	Cover crops	0-20 (cm)	20-40 (cm)
Effective Fe (mg/kg)	4	N	21.53 ± 1.32b	16.6 ± 1.31a
		R	26.93 ± 1.52a	18.43 ± 0.5a
		W	23.37 ± 1.07ab	18.67 ± 2.74a
		V	23.97 ± 2.48ab	17.2 ± 1.66a
	6	N	28.93 ± 2.32b	21.8 ± 1.18a
		R	35.9 ± 0.56a	22.9 ± 1.51a
		W	34.57 ± 1.92a	23.33 ± 1.42a
		V	35.63 ± 1.51a	22.6 ± 0.98a
	8	N	37.27 ± 2.32c	23.7 ± 2.07a
		R	45.2 ± 0.5a	25.63 ± 2.09a
		W	42.7 ± 1.33ab	25.57 ± 1.27a
		V	40.33 ± 0.74bc	24.6 ± 1.94a
Effective Mn (mg/kg)	4	N	4.73 ± 0.23a	3.53 ± 0.38a
		R	5.47 ± 0.28a	3.73 ± 0.41a
		W	4.93 ± 0.44a	3.7 ± 0.38a
		V	5.47 ± 0.38a	3.67 ± 0.26a
	6	N	5.77 ± 0.24b	4.07 ± 0.15a
		R	6.87 ± 0.52a	4.43 ± 0.37a
		W	6.6 ± 0.61a	4.5 ± 0.23a
		V	6.6 ± 0.36a	4.3 ± 0.35a
	8	N	6.3 ± 0.21b	6.57 ± 0.58a
		R	7.5 ± 0.35a	6.53 ± 0.45a
		W	7.13 ± 0.5ab	7.2 ± 0.69a
		V	6.97 ± 0.47ab	6.93 ± 0.65a
Effective Cu (mg/kg)	4	N	1.01 ± 0.06a	0.88 ± 0.03a
		R	1.18 ± 0.08a	1.01 ± 0.06a
		W	1.18 ± 0.08a	1.03 ± 0.14a
		V	1.18 ± 0.08a	1.04 ± 0.11a
	6	N	1.26 ± 0.08b	1.26 ± 0.17a
		R	1.56 ± 0.16a	1.26 ± 0.11a
		W	1.58 ± 0.05a	1.35 ± 0.09a
		V	1.56 ± 0.07a	1.29 ± 0.19a
	8	N	1.47 ± 0.06b	1.47 ± 0.11a
		R	1.75 ± 0.09a	1.51 ± 0.25a
		W	1.75 ± 0.13a	1.64 ± 0.05a

(Continued)

10.3389/fpls.2025.1695802

TABLE 5 Continued

Soil traits	Year	Cover crops	0-20 (cm)	20-40 (cm)
		V	1.62 ± 0.08ab	1.57 ± 0.07a
Effective Zn (mg/kg)	4	N	3.42 ± 0.23a	1.36 ± 0.02a
		R	3.93 ± 0.16a	1.47 ± 0.05a
		W	3.79 ± 0.29a	1.48 ± 0.25a
		V	3.59 ± 0.37a	1.41 ± 0.25a
	6	N	5.22 ± 0.07b	2.7 ± 0.21a
		R	6.44 ± 0.46a	3.04 ± 0.42a
		W	6.22 ± 0.53a	3.02 ± 0.09a
		V	6.45 ± 0.3a	2.97 ± 0.08a
	8	N	7.33 ± 0.16b	3.99 ± 0.06a
		R	8.08 ± 0.46ab	4.38 ± 0.2a
		W	8.27 ± 0.28a	4.39 ± 0.29a
		V	7.92 ± 0.14ab	4.37 ± 0.25a

Different lowercase letters within the same column for each soil depth and year indicate statistically significant differences among cover crop treatments ($P<0.05$). Values sharing the same letter are not significantly different. Data are presented as mean ± standard deviation (n=3). Abbreviations for cover crop treatments: N, No cover crop (control); R, Ryegrass; W, Winter rapeseed; V, Violet cress.

old orchards, respectively. Winter rapeseed treatment reduced bulk density to 1.27 and 1.29 g/cm^3 in 4-year and 6-year-old orchards. Cover crops also significantly increased total soil porosity. In 8-year-old orchards, porosity under ryegrass, winter rapeseed, and violet cress reached 52.03%, 51.55%, and 51.33%, respectively, representing a 2.1%-4.1% increase over natural vegetation (49.98%). Soil porosity showed an increasing trend with orchard age, with ryegrass treatment achieving a 3.3% increase (Table 7). Although the physical properties of the 20–40 cm subsoil are influenced by the pear orchard age and the cover crop, the magnitude of the change is less pronounced than topsoil. Cover crop treatment, generally resulted in lower bulk density compared to natural vegetation, with the lowest value of 1.36 g/cm^3 observed in 8-year orchards under winter rapeseed. The reductions in bulk density across 4-year, 6-year, and 8-year orchards ranged from 3.4%-5.4%, 3.4%-4.1%, and 2.8%-4.9%, respectively, Porosity increased by 1.4%-4.3% under cover crops relative to natural vegetation cover, though difference were not statistically significant ($P>0.05$). Notably, the 8-year orchard with winter rape exhibited the highest porosity of 47.82%, indicating that long-term orchard cultivation may promote subsoil structure (Table 7).

3.4 Pathway analysis of pear and cover crop intercropping effects on soil carbon dynamics

A complex correlation between pH and most indicators such as available potassium, available phosphorus, total nitrogen, and organic carbon was observed (Figure 3a). It was found that available potassium was positively correlated with available phosphorus, total nitrogen, organic carbon. Organic carbon was positively correlated with trophic indexes such as exchangeable calcium, magnesium and sulfur. There was a significant negative correlation between bulk density and total porosity, as well as between bulk density and nutritional indexes such as available potassium and available phosphorus. Analysis of the topsoil layer (0–20 cm) revealed that different soil nutrients tend to enhance each other's availability and with the enhanced compactness of soil (increased bulk density) the pore space got reduced which limits nutrient supply to plants. The interplay between nutrient synergism and soil compaction results in a unique ecological dynamic that influences soil fertility in this layer (Figure 3a).

TABLE 6 Changes in soil organic carbon and carbon storage at different pear ages and cover crop treatments.

Soil traits	Year	Cover crops	0-20 (cm)	20-40 (cm)
SOC (g/kg)	4	N	11.12 ± 0.26b	5.62 ± 0.42a
		R	13.2 ± 0.5b	6.18 ± 0.53a
		W	13.2 ± 0.35a	6.68 ± 0.97a
		V	12.41 ± 0.64b	6.15 ± 0.74a
	6	N	12.54 ± 0.75b	7.43 ± 0.79a
		R	14.75 ± 1.01a	7.9 ± 0.57a
		W	14.59 ± 0.97b	8.14 ± 0.33a
		V	14.4 ± 1.42ab	7.98 ± 1.05a
	8	N	14.66 ± 0.29a	8.65 ± 0.16b
		R	16.91 ± 0.21b	10.09 ± 0.67ab
		W	15.95 ± 0.48ab	10.59 ± 0.08a
		V	15.3 ± 0.56a	10.25 ± 0.65ab
TSOC (tC/hm^2)	4	N	19.12 ± 0.96b	9.17 ± 0.77a
		R	23.79 ± 0.48a	9.73 ± 0.74a
		W	23.74 ± 0.8ab	10.36 ± 1.64a
		V	22.86 ± 2.05ab	9.57 ± 1.24a
	6	N	22.82 ± 1.34b	11.77 ± 1.11a
		R	27.45 ± 0.81a	12.19 ± 0.94a
		W	26.73 ± 2.01ab	12.4 ± 0.25a
		V	26.92 ± 2.57ab	12.04 ± 1.09a
	8	N	26.08 ± 0.57b	13.58 ± 0.29a
		R	30.9 ± 1.73a	15.48 ± 1.24a
		W	29.99 ± 2.3ab	15.81 ± 0.2a
		V	29.1 ± 1.07ab	15.51 ± 1.15a

Different lowercase letters within the same column for each soil depth and year indicate statistically significant differences among cover crop treatments ($P<0.05$). Values sharing the same letter are not significantly different. Data are presented as mean ± standard deviation (n=3). Abbreviations for cover crop treatments: N, No cover crop (control); R, Ryegrass; W, Winter rapeseed; V, Violet cress.

10.3389/fpls.2025.1695802

TABLE 7 Changes in soil physicochemical properties at different pear ages and cover crop treatments.

Soil traits	Year	Cover crops	0-20 (cm)	20-40 (cm)
Bulk density (g/cm^3)	4	N	1.36 ± 0.05a	1.48 ± 0.02a
		R	1.29 ± 0.05a	1.43 ± 0.02a
		W	1.27 ± 0.03a	1.4 ± 0.02a
		V	1.29 ± 0.05a	1.41 ± 0.03a
	6	N	1.37 ± 0.08a	1.45 ± 0.05a
		R	1.29 ± 0.04a	1.4 ± 0.02a
		W	1.29 ± 0.04a	1.39 ± 0.03a
		V	1.28 ± 0.07a	1.39 ± 0.07a
	8	N	1.3 ± 0.04a	1.43 ± 0.03a
		R	1.25 ± 0.07b	1.39 ± 0.04a
		W	1.26 ± 0.1b	1.36 ± 0.01a
		V	1.27 ± 0.05ab	1.37 ± 0.03a
Total porosity (%)	4	N	47.48 ± 1.95a	43.02 ± 0.63a
		R	50.37 ± 1.67a	44.84 ± 0.81a
		W	51.27 ± 1.26a	45.96 ± 0.93a
		V	50.27 ± 2a	45.71 ± 1.02a
	6	N	47.31 ± 2.89a	44.37 ± 2.08a
		R	50.26 ± 1.36a	46.06 ± 0.75a
		W	50.4 ± 1.31a	46.67 ± 1.1a
		V	50.58 ± 2.64a	46.59 ± 2.55a
	8	N	49.98 ± 1.47b	45.11 ± 1.02a
		R	52.03 ± 2.8a	46.45 ± 1.73a
		W	51.55 ± 3.85a	47.82 ± 0.33a
		V	51.33 ± 1.87a	47.15 ± 1.07a

Different lowercase letters within the same column for each soil depth and year indicate statistically significant differences among cover crop treatments ($P<0.05$). Values sharing the same letter are not significantly different. Data are presented as mean ± standard deviation (n=3). Abbreviations for cover crop treatments: N, No cover crop (control); R, Ryegrass; W, Winter rapeseed; V, Violet cress.

A weak correlation between pH and nutritional indicators, such as available potassium and available phosphorus was found (Figure 3b). Available potassium was positively correlated with organic carbon, exchangeable calcium, and magnesium. Organic carbon was positively correlated with structural indexes such as exchangeable magnesium and available sulfur. A significant negative correlation between bulk density and porosity, and between bulk density and nutritional indexes such as available potassium and available phosphorus was also found. The correlation between certain trace elements (e.g., available manganese, available copper) and nutritional indicators shows significant differences compared to other elements (Figure 3b).

For the 0–20 cm soil layer, the total explanatory rate of the soil layer for the mixed cropping pattern and soil physicochemical properties of pear grass was 75.3% (Figure 4a). According to the results of this PC analysis, it can be inferred that factors that contribute more to the difference of soil physical and chemical indexes are effective iron and effective zinc.

For the 20–40 cm soil layer, the total interpretation rate of different pear-grass mixed cropping patterns and soil physicochemical properties was 71.7% (Figure 4b). The PC analysis of soil layer indicated that factors that contribute more to the differences of soil physical and chemical indexes are effective zinc and effective sulfur.

Partial Least Squares Structural Equation Modeling (PLS-SEM) is a variance-based multivariate analysis method that employs iterative computations to maximize the predictive power of latent variables. This approach comprises two key components: the measurement model and the structural model, making it particularly suitable for exploratory research and analyzing complex causal mechanisms. Through evaluation metrics such as the coefficient of determination (R^2) and the significance of path coefficients, PLS-SEM can effectively quantify inter-variable relationships and assess the model's predictive performance.

This study employed partial least squares structural equation model to analyze the influence mechanism of soil chemical properties, physical properties, organic matter, organic carbon, macro elements and trace elements on carbon storage. The GOF (goodness of fit) value of reached upto 0.8002, indicating that the fit was good. The results showed that the chemical properties of the soil were positively driven by the strong significant path coefficient of 0.655 ($P<0.01$). At the same time, a significant path coefficient of 0.402 ($P<0.05$) directly promotes the accumulation of carbon storage and participates in the carbon sequestration process. Organic matter and organic carbon served as primary components, with a highly significant path coefficient of 0.930 ($P<0.001$) indicating strong support for macro elements. Additionally, a significant indirect positive effect on trace elements was observed, with a path coefficient of 0.710 ($P<0.01$). It is noteworthy that physical indicators exert a negative effect of –0.1642 on carbon storage and an inhibitory effect of –0.079 on trace elements, indicating a potential ecological risk associated with changes in the physical state. Conversely, a strong positive correlation of 0.757 ($P < 0.01$) was observed between macro elements and trace elements, emphasizing their intermediary relationship (Figure 5).

4 Discussion

4.1 Land use modification as a driver of soil carbon storage enhancement

Land-use conversion in the ecologically vulnerable Taihang Mountain region significantly enhances soil carbon sequestration capacity, exhibiting pronounced spatiotemporal heterogeneity. Through quantitative analysis of ecological restoration project data from Fuping County, this study systematically reveals the enhancement mechanism of land use transition on carbon sink capacity. Statistical analysis demonstrates that orchard ecosystems exhibit significant carbon accumulation advantages over cropland

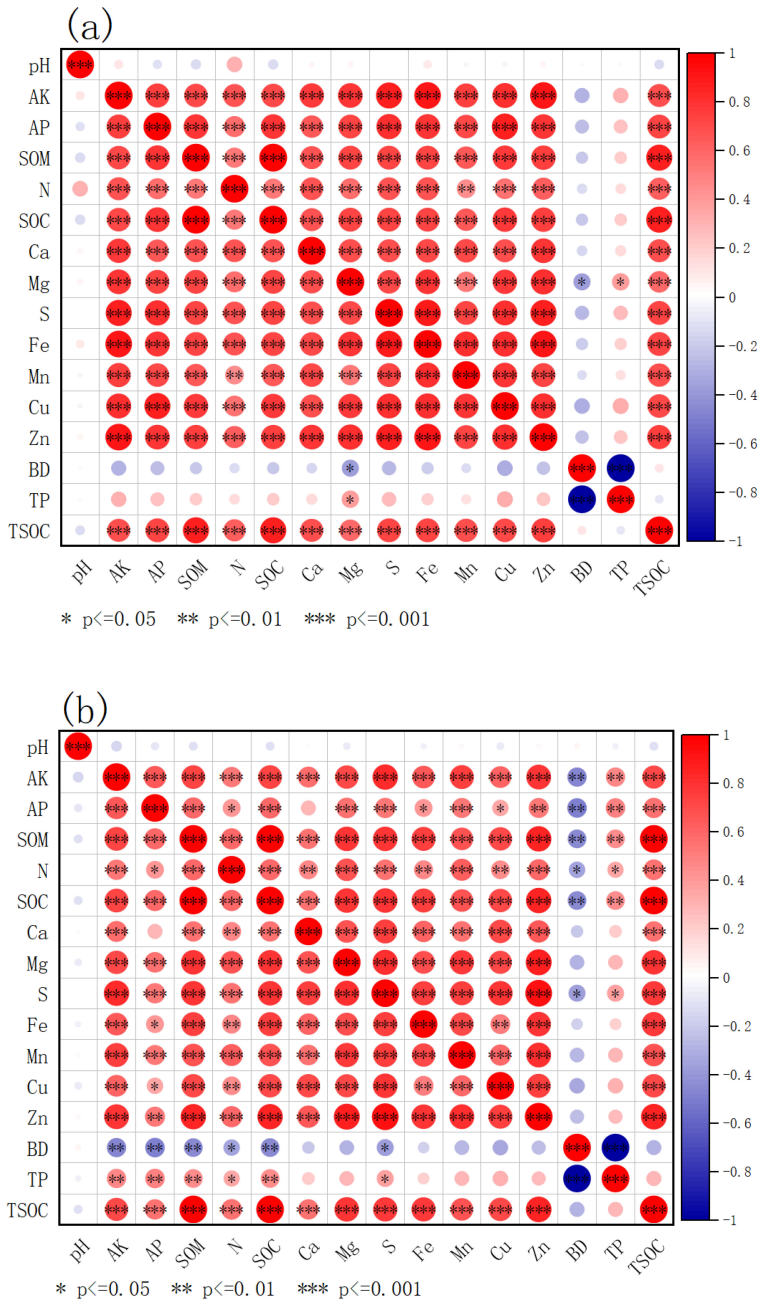

FIGURE 3
Correlation analysis diagram. **(a)** 0–20 cm surface soil; **(b)** 20–40 cm subsoil. AK, available potassium; AP, soil available phosphorus; SOM, soil organic matter; N, soil total nitrogen; SOC, soil organic carbon; pH, soil pH; Ca, exchangeable calcium; Mg, exchangeable magnesium; S, effective sulphur; Fe, effective iron; Mn, effective manganese; Cu, effective copper; Zn, effective zinc; BD, capacitance; TP, total porosity; and TSOC, soil organic carbon stocks.

systems ($P < 0.05$), with total carbon sequestration increasing by 43.4%. Dynamic monitoring of soil carbon pools shows that the soil carbon storage in 8-year-old pear orchards reaches 3.87 times that of traditional croplands, confirming the enhanced effect of perennial orchard systems on soil carbon sequestration. Efficiency evaluation further indicates that the carbon sequestration efficiency per unit area in pear orchards significantly surpasses that of cropland systems, highlighting the biological advantages of woody plant systems in carbon capture. Longitudinal comparative analysis reveals an orders-of-magnitude increase in regional carbon storage after transition compared to barren slopes and gneiss substrates ($P < 0.01$). These findings demonstrate, from four dimensions-system carbon storage, soil carbon pool capacity, carbon sequestration efficiency, and gneiss substrate transformation-the synergistic mechanism of orchard establishment in achieving carbon sink enhancement and ecological restoration in fragile ecological zones (Table 2).

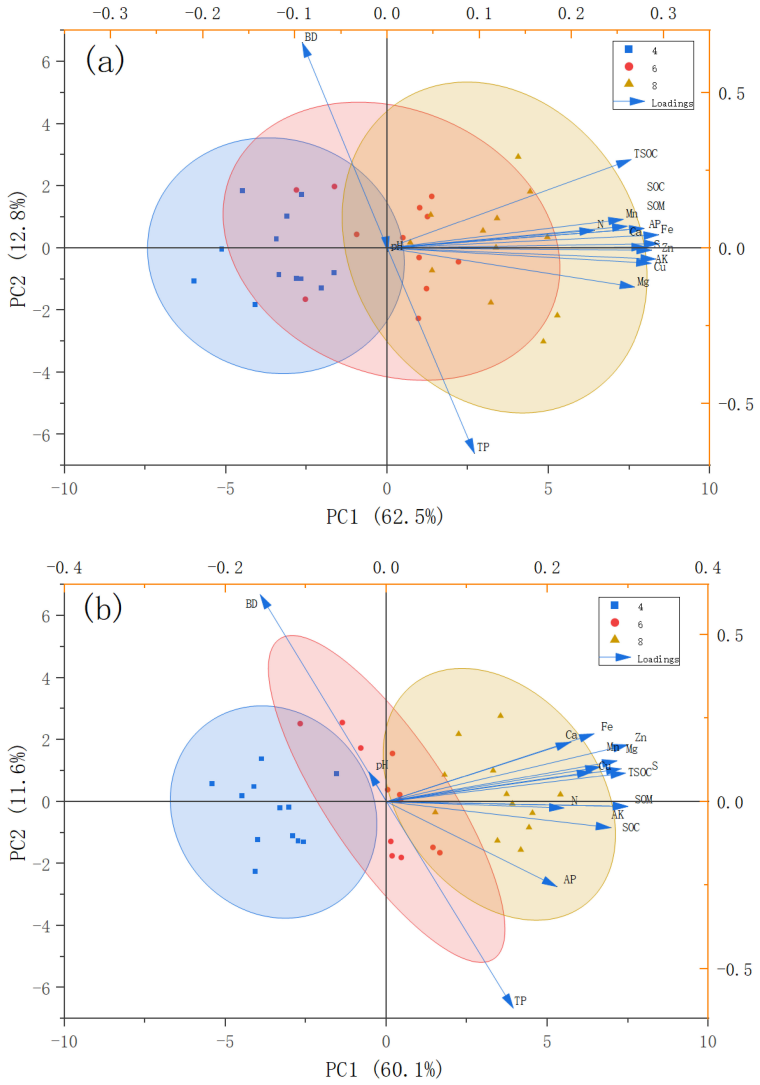

FIGURE 4
Combined PCA score and loading plot. **(a)** 0–20 cm surface soil; **(b)** 20–40 cm subsoil. AK, available potassium; AP, soil available phosphorus; SOM, soil organic matter; N, soil total nitrogen; SOC, soil organic carbon; pH, soil pH; Ca, exchangeable calcium; Mg, exchangeable magnesium; S, effective sulphur; Fe, effective iron; Mn, effective manganese; Cu, effective copper; Zn, effective zinc; BD, capacitance; TP, total porosity; and TSOC, soil organic carbon stocks. PC1 principal component 1; PC2, principal component 2.

This study systematically quantified the comprehensive effects of the "wasteland-to-orchard" model on ecosystem carbon sequestration. It organically integrated the vegetation-soil feedback mechanism proposed by Wang et al. (2024) with the canopy interception effect revealed by Tong et al. (2024), establishing a cascading feedback model of "canopy interception reducing erosion → soil environment stabilizing → litter input surging". The observed 3-fold to 5-fold increase in litter input not only verified the correlation study by Zeng et al. (2024) but is also likely a key biological factor driving the continuous accumulation of soil active organic carbon. After 8 years of transformation practice, soil organic carbon increased by 2.3-4.1 g/kg, and microbial biomass carbon rose by 58%-76%, confirming the long-term feasibility of the ecological restoration pathway proposed by Owusu et al. (2024) from a temporal perspective. However, scientific issues such as the specific responses of different tree species in the feedback cycle, the dynamics of inert carbon transformation, and the impact of extreme climates on carbon sequestration still require in-depth exploration. Future research should combine molecular biological techniques with long-term *in-situ* observations to systematically analyze the carbon cycle mechanisms in the "plant-soil-microbe" system, providing more precise theoretical support for regional ecological restoration.

4.2 Carbon input and sequestration in pear-cover crops strategy

This study systematically quantified the effects of cover crops on soil organic carbon in pear orchards, revealing a novel mechanism

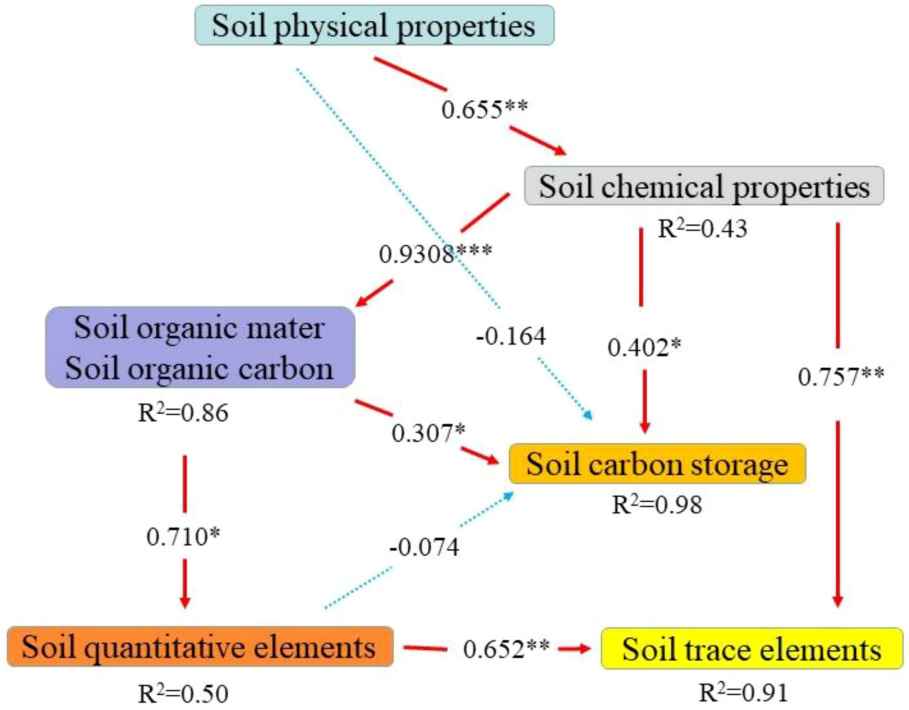

FIGURE 5
Pathway analysis of the impact of cover crop cultivation on soil carbon stocks. *, ** and *** indicate significant at $P<0.05$, $P<0.01$ and $P<0.001$ levels, respectively. AK-available potassium, AP-soil available phosphorus, SOM-soil organic matter, N-soil total nitrogen, SOC-soil organic carbon, pH-soil pH, Ca-exchangeable calcium, Mg-exchangeable magnesium, S-effective sulphur, Fe-effective iron, Mn-effective manganese, Cu-effective copper, Zn-effective zinc, BD-capacitance, TP-total porosity, and TSOC-soil organic carbon stocks. PC1 principal component 1, PC2- principal component 2. R^2-coefficient of determination; red arrows indicate a negative effect, black arrows indicate a positive effect, and the thickness of the arrow line indicates the magnitude of the path coefficients in the model. Soil physical properties (AP, AK, TN), Soil chemical properties (TP, BD), Organic matter and organic carbon (SOC, SOM), Soil trace elements (Fe, Mn, Cu, Zn), Soil quantitative elements (Ca, Mg, S), Soil carbon storage (TSOC).

through which herbaceous plants regulate the vertical distribution of soil carbon pools via root system architecture. Contrary to conventional understanding that primarily emphasizes litter input (Smith et al., 2020), we found that deep-rooted herbaceous plants (e.g., winter rapeseed) significantly enhanced soil organic carbon in the 20–40 cm deep layer (with an increase of 22.43% in 8-year-old orchards), surpassing the previous limited focus on surface carbon pools. In the unique shallow soil-bedrock abrupt-interface habitat of Fuping, deep-rooted plants successfully activated the traditionally difficult-to-utilize deep carbon pool, providing new insights into carbon cycle research in fragile ecosystems. While this study validates the theory that deep-rooted plants promote subsoil carbon sequestration (Borchard et al., 2019), it further reveals differences in carbon sequestration efficiency among herbaceous species: ryegrass demonstrated optimal performance in the surface layer (0–20 cm), with an increase of 18.51%-24.43%, whereas winter rapeseed exhibited greater advantages in deeper layers. This species-specific variability highlights the necessity of establishing a multidimensional evaluation system.

The positive correlation between tree age and carbon sequestration capacity observed in this study is consistent with findings from He et al. (2023) and Li et al. (2023a). However, it remains unclear whether this trend plateaus as trees mature and how management practices specifically regulate this mechanism. This experiment confirms that winter rapeseed exhibits better carbon sequestration performance than ryegrass in the 20–40 cm subsoil layer. This phenomenon can be reasonably explained by root architecture theory: the advantage of deep-rooted plants (e.g., winter rapeseed) over fibrous-rooted plants primarily stems from their efficient utilization of the vertical spatial niche, which is realized through two key mechanisms. On the one hand, deep root systems penetrate compacted subsoil, and during growth, root deformation and soil compression, along with the secretion of organic substances, directly promote the formation of large aggregates (Kell, 2011), providing a physical protection barrier for organic matter and thereby enhancing carbon stability. On the other hand, deep roots serve as the main pathway for transporting organic carbon into the subsoil. The root-derived carbon input, due to its complex chemical composition and the slow-decomposition environment of deeper soil layers, exhibits a longer turnover time (Rasse et al., 2005). The activation of the deep soil carbon pool observed in this study strongly supports the synergistic effect of these two mechanisms. Although the theory proposed by Lynch (1995) provides foundational support for root penetration into the subsoil, the more recent studies cited above offer more precise insights into the underlying mechanisms. Nevertheless, the relative contributions of physical protection versus biochemical pathways to carbon pool stability require further clarification using techniques such as isotope labeling.

4.3 Soil optimization and carbon storage in pear-cover crops approach

This study confirms that the pear-herb composite system significantly optimizes soil physical structure by reducing bulk density and increasing porosity, a finding that aligns with the emphasized role of plant root systems and organic matter in improving soil structure, as noted by Blanco-Canqui and Ruis (2020). More importantly, our research quantitatively reveals a negative correlation between bulk density and soil organic carbon content through structural equation modeling, thereby clarifying that physical structure optimization is a key pathway driving soil organic carbon preservation. This provides mechanistic support for the reduced carbon footprint observed in intercropping systems by Zhang et al. (2023). However, the carbon sequestration effects of improved soil structure may have certain boundaries. This study observed significant vertical heterogeneity in the improvement effects within the soil profile, primarily due to the vertical decline in herb root distribution and organic matter inputs. This new insight suggests that future assessments of carbon sequestration effects must more carefully consider the influence of soil depth. Furthermore, although the contribution of organic matter inputs to carbon sequestration is significant, its long-term stability, dynamics under varying climatic conditions, and potential saturation points remain uncertainties that require further quantification.

Several research gaps remain. For instance, how differences in root architecture and exudates among different herb species and their combinations specifically influence the formation and stability of soil aggregates warrants deeper investigation (Ogilvie et al., 2021). Additionally, when extending this pear-herb model to broader fragile ecosystems, a comprehensive assessment of its long-term ecological benefits and economic feasibility will be a critical direction for future research. Despite these uncertainties, the synergistic model of "structural improvement-carbon sequestration enhancement" established in this study provides a solid theoretical and practical foundation for enhancing ecosystem services through optimized agroforestry systems (Lal, 2018), highlighting the significant potential of soil management in addressing global change.

4.4 Nutrient-carbon interactions in pear and cover crops systems

This study elucidates the mechanism through which herbaceous intercropping systems enhance soil carbon pool stability via the dual pathways of "nutrient-driven accumulation" and "alkalinity-constrained decomposition". While this qualitative framework aligns with the functional model of cover crops proposed by Cong et al. (2015), our research provides the first quantitative evidence of the central role of soil chemical properties (R^2=0.43) in driving carbon storage, a novel finding that challenges the conventional emphasis on physical factors and offers a new perspective for understanding the carbon sink function of intercropping systems. This study reveals a dual-pathway mechanism for nutrient-carbon pool synergy: (1) In the biochemical pathway, simultaneous increases in available potassium and phosphorus alleviate microbial nutrient limitation, converting organic residues into stable microbial-derived carbon through the "microbial carbon pump" (Liang et al., 2017); (2) In the physicochemical pathway, potassium ions promote soil colloid flocculation and aggregate formation, while available phosphorus complexes with iron-aluminum oxides to jointly provide physical protection for organic carbon (Kleber et al., 2015). PLS-SEM path analysis supports this mechanism (path coefficient = 0.402), confirming that enhanced nutrient availability achieves carbon sequestration through dual pathways of "promoting transformation and inhibiting decomposition". Specifically, the observed increase in available potassium and phosphorus (17.26%-25.45%) within the intercropping system and its positive correlation with total organic carbon corroborates, from a plant nutrition-driven perspective, the findings of Fu et al. (2023) in tropical soils. More significantly, this study systematically reports, for the first time, the quantified contribution of alkaline cations (exchangeable Ca/Mg increased by 16.58%-25.46%) in suppressing carbon decomposition. This provides direct empirical support for the theory of "base environment promoting organic carbon stability" proposed by Rodrigues et al. (2021). Notably, the structural equation model revealed a negative impact of physical indicators on carbon storage. This unexpected finding suggests the potential existence of unrecognized compensatory mechanisms within the system. A significant knowledge gap remains regarding the specific pathways of the trace element network (R^2=0.91)—particularly the relative contributions and interactions of different trace elements—which constitutes a critical direction for future research. Although this study establishes a coupled chemical-physical-biogeochemical mechanism, its universality across different soil types and climatic conditions requires broader validation.

These uncertainties indicate that the complex systems theory proposed by Figueiredo et al. (2025) necessitates a more refined assessment framework. Future research should focus on: (1) the species-specific effects of different herbaceous plant combinations on alkaline cation composition; (2) the underlying mechanisms for the negative effects of physical indicators; (3) the threshold effects of the trace element network in carbon stabilization. Despite these challenges, the integrated model established in this study undoubtedly opens new avenues for enhancing ecosystem carbon sink functions through the precise management of soil chemical properties.

5 Conclusions and prospects

This study presents a typical example of Nature-based Solutions through ecological restoration practices implemented in the fragile ecological region of gneiss slopes in the Taihang Mountains. The transformation of barren slopes into pear orchards combined with herbaceous plant intercropping has successfully achieved multiple synergistic benefits, including enhanced soil carbon sequestration capacity and improved ecosystem services, embodying the core concept of "addressing climate change synergistically and enhancing

human well-being through sustainable ecosystem management". Specifically, as pear orchard stands age, soil carbon storage demonstrates a significant accumulation trend, showing notably greater carbon sequestration potential compared to traditional cropping systems. Furthermore, intercropping with deep-rooted herbaceous plants not only effectively promotes carbon storage in both surface and subsurface soil layers but also improves the physical structure and nutrient status of rocky soils through root penetration. This technical pathway of optimizing soil three-phase structure (reducing bulk density, increasing porosity) and establishing nutrient-carbon pool synergy fully demonstrates the technical characteristics of "harnessing natural processes to achieve multiple synergistic objectives".

Future research should focus on developing a pear-herb combination selection system adapted to the ecological characteristics of gneiss hilly areas. Key priorities include: analyzing the regulatory mechanisms of different herbaceous plants on soil labile and stable carbon fractions, establishing a compatibility assessment framework that integrates topographic parameters and soil factors, and investigating spatial interaction patterns between woody and herbaceous root systems. Ultimately, this will lead to optimized configurations that balance carbon sequestration effectiveness with ecological adaptability. Advancement in these research directions will provide theoretical support for precision restoration of degraded soils in ecologically fragile areas, thereby enriching the practical implications of Nature-based Solutions.

Data availability statement

The raw data supporting the conclusions of this article will be made available by the authors, without undue reservation.

Author contributions

CZ: Conceptualization, Data curation, Formal analysis, Investigation, Project administration, Resources, Writing – original draft. ST: Conceptualization, Data curation, Formal analysis, Investigation, Methodology, Writing – original draft. RZ: Project administration, Resources, Software, Writing – review & editing. XL: Software, Supervision, Validation, Visualization, Writing – review & editing. X-XW: Project administration, Resources, Software, Supervision, Validation, Visualization, Writing – review & editing. HW: Data curation, Formal analysis, Funding acquisition, Investigation, Methodology, Supervision, Validation, Visualization, Writing – review & editing.

Funding

The author(s) declare financial support was received for the research and/or publication of this article. This study was supported by the Science and Technology Project of Hebei Provincial Department of Science and Technology "Science and Technology Demonstration Base for Ecological Restoration Industry in Fuping County Degraded Rangeland".

Conflict of interest

The authors declared that this work was conducted in the absence of any commercial or financial relationships that could be construed as a potential conflict of interest.

Generative AI statement

The author(s) declare that no Generative AI was used in the creation of this manuscript.

Any alternative text (alt text) provided alongside figures in this article has been generated by Frontiers with the support of artificial intelligence and reasonable efforts have been made to ensure accuracy, including review by the authors wherever possible. If you identify any issues, please contact us.

Publisher's note

References

Bao, S. (2000). *Soil agricultural chemistry analysis* (Beijing: China Agriculture Press).

Blanco-Canqui, H., and Ruis, S. J. (2020). Cover crop impacts on soil physical properties: A review. *Soil Sci. Soc. America J.* 84, 1527–1576. doi: 10.1002/saj2.20129

Borchard, N., Bulusu, M., Meyer, N., Rodionov, A., Herawati, H., Blagodatsky, S., et al. (2019). Deep soil carbon storage in tree-dominated land use systems in tropical lowlands of Kalimantan. *Geoderma* 354, 113864. doi: 10.1016/j.geoderma.2019.07.022

Cong, W., Hoffland, E., Li, L., Six, J., Sun, J., Bao, X., et al. (2015). Intercropping enhances soil carbon and nitrogen. *Global Change Biol.* 21, 1715–1726. doi: 10.1111/gcb.12738

Dangulla, M., Manaf, L. A., Latifah, R., Firuz, M., Yacob, M. R., and Namadi, S. (2021). Exploring urban tree diversity and carbon stocks in Zaria Metropolis, North Western Nigeria. *Appl. Geogr.* 127, 102385. doi: 10.1016/j.apgeog.2021.102385

Duan, S., Sun, Z., Wang, Q., Jiang, Y., Han, C., Zhang, Y., et al. (2021). Characteristics of soil organic carbon distribution of quaternary red soils under different land use patterns. *Chin. J. Soil Sci.* 52, 1078–1084.

Economic Daily. (2020). Strive to peak carbon dioxide emissions before 2030 and achieve carbon neutrality before 2060! *Economic Daily* 42 (10), 1.

Fan, X., Yu, H., Tiando, D. S., Rong, Y., Luo, W., Eme, C., et al. (2021). Impacts of human activities on ecosystem service value in arid and semi-arid ecological regions of China. *Int. J. Environ. Res. Public Health* 18, 11121. doi: 10.3390/ijerph182111121

Figueiredo, C. C. D., Silva, L. P. D., Leite, G. G., Cabral Filho, S. L. S., Coser, T. R., Kato, E., et al. (2025). Changes in soil carbon stocks and vegetative indices in the transitional phases from degraded grassland to an agroforestry system in the Cerrado

Region, Brazil. *Commun. Soil Sci. Plant Anal.* 56, 2320–2329. doi: 10.1080/00103624.2025.2509589

Fu, H., Chen, H., Ma, Q., Chen, B., Wang, F., and Wu, L. (2023). Planting and mowing cover crops as livestock feed to synergistically optimize soil properties, economic profit, and environmental burden on pear orchards in the Yangtze River Basin. *J. Sci. Food Agric.* 103, 6680–6688. doi: 10.1002/jsfa.12763

He, Q., Liu, D. L., Wang, B., Cowie, A., Simmons, A., Waters, C., et al. (2023). Modelling interactions between cowpea cover crops and residue retention in Australian dryland cropping systems under climate change. *Agriculture Ecosyst. Environ.* 353, 108536. doi: 10.1016/j.agee.2023.108536

IEA (2023). *CO_2 Emissions in 2022* (Paris: International Energy Agency).

Jiang, L., and Fu, X.. (2021). An ammonia-hydrogen energy roadmap for carbon neutrality: opportunity and challenges in China. *Engineering* 7, 1688–1691. doi: 10.1016/j.eng.2021.11.004

Kell, D. B. (2011). Breeding crop plants with deep roots: their role in sustainable carbon, nutrient and water sequestration. *Ann. Bot.* 108, 407–418. doi: 10.1093/aob/mcr175

Kleber, M., Eusterhues, K., Keiluweit, M., Mikutta, C., Mikutta, R., and Nico, P. S. (2015). Chapter one - mineral–organic associations: formation, properties, and relevance in soil environments. *Adv. Agron.* 130, 1–140. doi: 10.1016/bs.agron.2014.10.005

Lal, R. (2018). Digging deeper: A holistic perspective of factors affecting soil organic carbon sequestration in agroecosystems. *Global Change Biol.* 24, 3285–3301. doi: 10.1111/gcb.14054

Li, L., Han, J., and Zhu, Y. (2023a). Does environmental regulation in the form of resource agglomeration decrease agricultural carbon emissions? Quasi-natural experimental on high-standard farmland construction policy. *J. Cleaner Production* 420, 138342. doi: 10.1016/j.jclepro.2023.138342

Li, W., Lin, Y., Nan, X., Wang, F., and Zhu, L. (2023c). Soil carbon and nitrogen sequestration and associated influencing factors in a sustainable cultivationsystem of fruit trees intercropped with cover crops. *Chin. J. Appl. Ecol.* 34, 471–480.

Li, M., Peng, J., Lu, Z., and Zhu, P. (2023b). Research progress on carbon sources and sinks of farmland ecosystems. *Resources Environ. Sustainability* 11, 100099. doi: 10.1016/j.resenv.2022.100099

Liang, C., Schimel, J. P., and Jastrow, J. D. (2017). The importance of anabolism in microbial control over soil carbon storage. *Nat. Microbiol.* 2, 17105. doi: 10.1038/nmicrobiol.2017.105

Lipatov, D. N., Shcheglov, A. I., Manakhov, D. V., and Brekhov, P. T. (2021). Spatial variation of organic carbon stocks in peat soils and gleyzems in the Northeast of Sakhalin Island. *Eurasian Soil Sci.* 54, 226–237. doi: 10.1134/S1064229321020083

Liu, C., Hu, S. G., Wu, S., Song, J. R., and Li, H. Y. (2024a). County-level land use carbon emissions in China: Spatiotemporal patterns and impact factors. *Sustain. Cities Soc.* 105, 105304. doi: 10.1016/j.scs.2024.105304

Liu, Y., Peng, Q., Huang, P., and Chen, D. (2024b). Estimation and multi scenario prediction of landuse carbon storagein western Sichuan plateau. *J. Soil Water Conserv.* 38, 207–219.

Liu, Z., Tian, J., Wang, K., and Lan, J. (2023). The impact of farmland circulation on the carbon footprint of agricultural cultivation in China. *Economic Anal. Policy* 78, 792–801. doi: 10.1016/j.eap.2023.04.010

Lynch, J. (1995). Root architecture and plant productivity. *Plant Physiol.* 109, 7–13. doi: 10.1104/pp.109.1.7

National Agricultural Technology Extension and Service Center. (2012). *Rules for cultivated land quality monitoring. *NY/T 1119-2012**. Ministry of Agriculture and Rural Affairs.

Ogilvie, C. M., Ashiq, W., Vasava, H. B., and Biswas, A. (2021). Quantifying root-soil interactions in cover crop systems: a review. *Agriculture* 11, 218. doi: 10.3390/agriculture11030218

Owusu, S. M., Adomako, M. O., and Qiao, H. (2024). Organic amendment in climate change mitigation: Challenges in an era of micro-and nanoplastics. *Sci. Total Environ.* 907, 168035.

Rasse, D. P., Rumpel, C., and Dignac, M.-F. (2005). Is soil carbon mostly root carbon? Mechanisms for a specific stabilisation. *Plant Soil* 269, 341–356. doi: 10.1007/s11104-004-0907-y

Raza, S., Ghasali, E., Raza, M., Chen, C., Li, B., Orooj, Y., et al. (2023). Advances in technology and utilization of natural resources for achieving carbon neutrality and a sustainable solution to neutral environment. *Environ. Res.* 220, 115135. doi: 10.1016/j.envres.2022.115135

Rodrigues, L., Hardy, B., Huyghebeart, B., Fohrafellner, J., Fornara, D., Barančíková, G., et al. (2021). Achievable agricultural soil carbon sequestration across Europe from country-specific estimates. *Global Change Biol.* 27, 6363–6380. doi: 10.1111/gcb.15897

Shao, S., Zhang, K., and Dou, J. (2019). Effects of economic agglomeration on energy saving and emission reduction:theory and empirical evidence from China. *Manage. World* 35, 36–60 + 226.

Smith, P., Soussana, J. F., Angers, D., Schipper, L., Chenu, C., Rasse, D. P., et al. (2020). How to measure, report and verify soil carbon change to realize the potential of soil carbon sequestration for atmospheric greenhouse gas removal. *Global Change Biol.* 26, 219–241. doi: 10.1111/gcb.14815

Sokolov, Y. I.. (2021). Risks of global climate change. *Issues Risk Anal* 18 (3), 32–45.

Sun, Y., Nepal, S. K., and Watanabe, T. (2024). Tourism-generated energy use characteristics and sustainability transitions. *Tourism Geographies* 26, 1111–1133. doi: 10.1080/14616688.2024.2412542

Surya, S. K., Fernandaz, C. C., Chandrasekaran, K., Thamaraiselvi, S. P., Kovilpillai, B., Srinivasan, M., et al. (2023). Farmer's perception towards mitigating climate change through adoption of soil carbon sequestration practices: a review analysis. *Int. J. Environ. Climate Change* 13, 912–926. doi: 10.9734/ijecc/2023/v13i102736

Tilahun, E., Haile, M., Gebresamuel, G., and Zeleke, G. (2022). Spatial and temporal dynamics of soil organic carbon stock and carbon sequestration affected by major land-use conversions in Northwestern highlands of Ethiopia. *Geoderma* 406, 115506. doi: 10.1016/j.geoderma.2021.115506

Tong, R., Ji, B., Wang, G. G., Lou, C., Ma, C., Zhu, N., et al. (2024). Canopy gap impacts on soil organic carbon and nutrient dynamic: a meta-analysis. *Ann. For. Sci.* 81, 12. doi: 10.1186/s13595-024-01224-z

Totti, M. C. V., Zinn, Y. L., Silva, S. H. G., Silva, B. M., Bócoli, F. A., De Faria, V. L., et al. (2025). Organic carbon stocks across various land use systems in Sandy Ultisols and Oxisols in Brazil. *Geoderma Regional* 40, e00924. doi: 10.1016/j.geodrs.2025.e00924

Wang, K., Li, X., Lyu, X., Dang, D., Dou, H., Li, M., et al. (2022). Optimizing the land use and land cover pattern to increase its contribution to carbon neutrality. *Remote Sens.* 14, 4751. doi: 10.3390/rs14194751

Wang, Y., Li, R., Yan, W., Han, X., Liu, W., and Li, Z. (2024). Variations in soil organic carbon after farmland conversion to apple orchard. *Agronomy* 14, 963. doi: 10.3390/agronomy14050963

Xia, L., Cao, L., Yang, Y., Ti, C., Liu, Y., Smith, P., et al. (2023). Integrated biochar solutions can achieve carbon-neutral staple crop production. *Nat. Food* 4, 236–246. doi: 10.1038/s43016-023-00694-0

Xu, X., Tian, Q., Sun, J., Wang, H., Wang, M., Yi, H., et al. (2022). Effects on soil carbon sink of vegetation succession in the Ziwuling area. *J. Soil Water Conserv.* 36, 159–165 + 180.

Yang, Y., Li, W., Zhu, C., Wang, Y., and Huang, X. (2017). Impact of land use/cover changes on carbon storage in a river valley in arid areas of Northwest China. *J. Arid Land* 9, 879–887. doi: 10.1007/s40333-017-0106-3

Yi, D., Ou, M. H., Guo, J., Han, Y., Yi, J. L., Ding, G. Q., et al. (2022). Progress and prospect of research on land use carbon emissions and low-carbon optimization. *Resour. Sci.* 44, 1545–1559. doi: 10.18402/resci.2022.08.02

Yu, P., Li, Y., Liu, S., Liu, J., Ding, Z., Ma, M., et al. (2022). Afforestation influences soil organic carbon and its fractions associated with aggregates in a karst region of Southwest China. *Sci. Total Environ.* 814, 152710. doi: 10.1016/j.scitotenv.2021.152710

Yuan, G., Munyampirwa, T., Mao, L., Zhang, Y., Yang, X., and Shen, Y. (2021). Effects of conservational tillage measures on soil carbonpool and stability in a winter forage-crop rotationsystem on the Loess Plateau of China. *J. Soil Water Conserv.* 35, 252–258,267.

Zeng, J., Li, X., Song, R., Xie, H., Li, X., Liu, W., et al. (2024). Mechanisms of litter input changes on soil organic carbon dynamics: a microbial carbon use efficiency-based perspective. *Sci. Total Environ.* 949, 175092. doi: 10.1016/j.scitotenv.2024.175092

Zhang, K., Zhu, C., Ma, X., Zhang, X., Yang, D., and Shao, Y. (2023). Spatiotemporal variation characteristics and dynamic persistence analysis of carbon sources/sinks in the Yellow River Basin. *Remote Sens.* 15, 323. doi: 10.3390/rs15020323

Zhao, X., Liu, S., Xu, J., Wang, Y., Guo, Z., Tang, S., et al. (2023). Effects of cover cropping on the aggregate stability of Shajiang black soil and its organic carbon fractions. *J. Agric. Resour. Environ.* 40, 1377–1387.

Frontiers in
Plant Science

Cultivates the science of plant biology and its applications

The most cited plant science journal, which advances our understanding of plant biology for sustainable food security, functional ecosystems and human health.

Discover the latest Research Topics

See more →

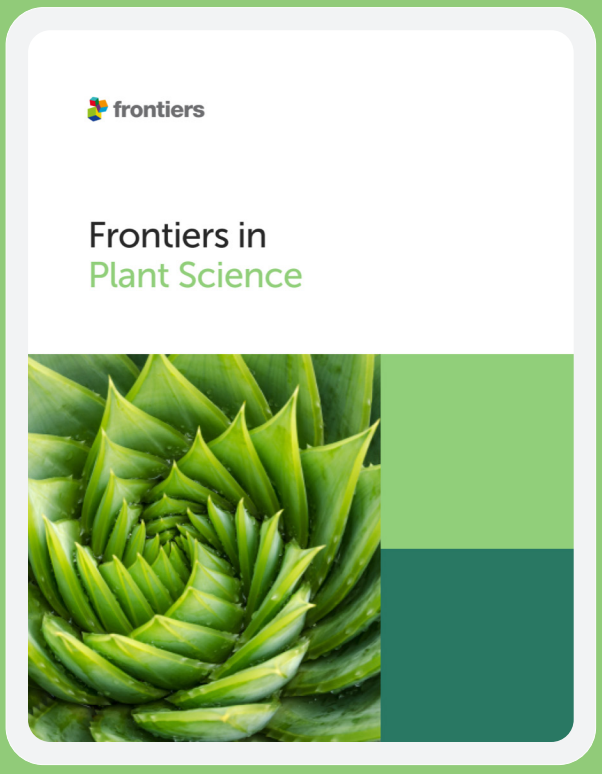

Frontiers

Avenue du Tribunal-Fédéral 34
1005 Lausanne, Switzerland
frontiersin.org

Contact us

+41 (0)21 510 17 00
frontiersin.org/about/contact